



Rodgers, Lewis Craig (2018) *Metabolic control for inflammatory cascades in monocytes in response to chronic disease stimuli*. PhD thesis.

<http://theses.gla.ac.uk/30725/>

Copyright and moral rights for this work are retained by the author

A copy can be downloaded for personal non-commercial research or study, without prior permission or charge

This work cannot be reproduced or quoted extensively from without first obtaining permission in writing from the author

The content must not be changed in any way or sold commercially in any format or medium without the formal permission of the author

When referring to this work, full bibliographic details including the author, title, awarding institution and date of the thesis must be given

Enlighten: Theses

<https://theses.gla.ac.uk/>
research-enlighten@glasgow.ac.uk

Metabolic control for inflammatory cascades in monocytes in response to chronic disease stimuli

**Lewis Craig Rodgers
BSc. (Hons)**

Thesis submitted in fulfilment of the requirements for the
degree of Doctor of Philosophy

Institute of Infection, Immunity and Inflammation
School of Life Sciences
College of Medical, Veterinary and Life Sciences

University of Glasgow

August 2018

Abstract

Tissue microenvironments within chronic inflammatory disease sites, such as the synovial compartment within rheumatoid arthritis (RA) patients contains a plethora of factors to drive immune responses. However, one specific characteristic that is commonly found at these sites is the presence of tissue hypoxia. Therefore, both resident and infiltrating immune cells need to adapt to these microenvironments in order to survive and function to promote chronic inflammation. Adaptation to hypoxia requires a level of metabolic reprogramming for this purpose. Therefore, this thesis aimed to examine what the metabolic consequences were for human monocytes that were adapting into hypoxic sites and to interrogate what role these metabolic pathways had in driving specific functions in hypoxic conditions.

Metabolomic analyses reveal that hypoxia induces metabolic alterations in human monocytes, including the decrease in abundance of carnitine metabolites, important for subsequent fatty acid oxidation (FAO), and increases in glycolytic metabolites. Furthermore, hypoxia exacerbated the release of pro-inflammatory mediators in LPS activated monocytes, such as CCL20 and IL-1 β . Manipulation of carnitine metabolites identify a role for FAO in the production of CCL20, and in the regulation of IL-1 β release. To mimic the RA synovial environment more thoroughly *in vitro*, human monocytes were cultured in cell culture medium containing RA synovial fluid (RA-SF) under hypoxic conditions. Further metabolomics analysis revealed that monocytes accumulate a number of metabolites in comparison to untreated and LPS activated cells, suggesting that monocytes may enter a stasis-like phase when challenged with RA-SF. This was reflected by low level release of pro-inflammatory mediators under these conditions. Nevertheless, media supplementation with carnitine increased CCL20 production under RA-SF treatment, highlighting FAO may have a role in CCL20 release in several inflammatory contexts.

This body of work shows that distinct metabolic pathways regulated by the extracellular environment may act in conjunction for the production of pro-inflammatory mediators in chronic inflammatory disease. This thesis highlights the influencing nature of tissue microenvironments on the functional capacity of myeloid cells by harnessing its metabolic machinery.

Table of Contents

Abstract	2
Table of Contents	3
List of Tables	6
List of Figures	7
Acknowledgement	9
Author's Declaration	11
Abbreviations.....	12
Chapter 1. Introduction.....	17
1.1 Human monocytes & macrophages.....	17
1.1.1 Monocytes	17
1.1.2 Macrophages	20
1.2 Chronic inflammatory disease	24
1.2.1 Rheumatoid arthritis	24
1.2.1.1 Introduction	24
1.2.1.2 Joint structure in rheumatoid arthritis	24
1.2.1.3 Risk factors	25
1.2.1.4 Immunopathology of rheumatoid arthritis.....	25
1.2.2 Chronic obstructive pulmonary disorder (COPD)	29
1.2.2.1 Introduction	29
1.2.2.2 Macrophages in COPD	29
1.2.2.3 Other immune cells in COPD.....	30
1.3 Hypoxia in chronic inflammatory disease	32
1.3.1 Origins of hypoxia in inflammatory tissue	32
1.3.2 Hypoxia in the rheumatoid arthritis joint	33
1.3.3 Myeloid cell adaptation to hypoxia	33
1.3.4 The impact of hypoxia on the function of myeloid cells.....	35
1.4 Pro-inflammatory mediators in chronic inflammatory disease	37
1.4.1 Introduction.....	37
1.4.2 TNF α	37
1.4.3 IL-6	38
1.4.4 IL-1 β	39
1.4.5 CCL20.....	40
1.4.6 CCL22.....	41
1.4.7 IL-8.....	41
1.5 Immunometabolism of myeloid cells	42
1.5.1 Introduction.....	42
1.5.2 Glycolysis	42
1.5.3 Tricarboxylic acid (TCA) cycle.....	45
1.5.4 Fatty acid oxidation (FAO)	48
1.5.5 Nucleotide metabolism	51
1.5.6 Amino acid metabolism	53
1.6 Aims	54
Chapter 2. Materials and Methods.....	56
2.1 Human samples, patients and controls.....	56
2.2 Primary human cell culture	56
2.2.1 Isolation of peripheral blood mononuclear cells (PBMCs)	56
2.2.2 Monocyte enrichment from PBMCs	57
2.2.3 Stimulation of human monocytes	57

2.2.4	Human alveolar macrophage (AM) isolation	58
2.2.5	Polarisation and treatment of alveolar macrophages	58
2.3	Culture of cell lines	58
2.3.1	Culture and treatment of Raji cells	58
2.3.2	Culture of Caco-2 cells	59
2.3.3	Culture of HUVECs	60
2.4	Induction of Hypoxia	60
2.4.1	Induction of 5% oxygen	60
2.4.2	Induction of 1% oxygen	61
2.5	Western Blotting	61
2.5.1	Cell lysis (RIPA buffer)	61
2.5.2	Cell lysis (Laemmli buffer)	61
2.5.3	Protein quantification	62
2.5.4	Protein denaturation	62
2.5.5	Protein gel electrophoresis	63
2.5.6	Gel transfer to PVDF membrane	63
2.5.7	Probing	64
2.5.8	Western Blot antibodies	64
2.6	Cellular assays	65
2.6.1	Wound healing scratch assay	65
2.6.2	Cellular adherence assay	65
2.6.3	MTT assay	66
2.7	Supernatant assessment	66
2.7.1	Sample harvest	66
2.7.2	Enzyme-linked immunosorbent assay (ELISA)	67
2.7.3	Meso-Scale Discovery (MSD)	68
2.7.4	Lactate assay	69
2.8	Flow cytometry (FACS)	69
2.8.1	Cell surface staining	69
2.8.2	Apoptosis assay	70
2.9	Gene expression analysis	71
2.9.1	RNA extraction	71
2.9.2	cDNA synthesis	71
2.9.3	Primer design for qPCR	72
2.9.4	Primer validation prior to qPCR	73
2.9.5	qPCR	74
2.9.6	Taqman Low Density Array (TLDA)	75
2.10	Metabolomics	75
2.10.1	Intracellular metabolite extraction of monocytes	75
2.10.2	Intracellular metabolite extraction of macrophages	76
2.10.3	Untargeted Mass Spectrometry (MS)	76
2.10.4	Data processing of untargeted MS	77
2.10.5	Targeted MS of carnitine metabolites	77
2.11	Statistical analysis	78
Chapter 3.	The impact of hypoxia on the metabolic profile on human monocytes...79	
3.1	Introduction	79
3.2	Results	82
3.2.1	Optimisation of monocyte purification and <i>in vitro</i> culturing	82
3.2.2	Confirming hypoxic adaptation	86
3.2.3	Assessing the impact of hypoxia on the metabolic profile of monocytes	91
3.3	Discussion	106

Chapter 4. Assessing the impact of hypoxia on the functional profile of monocytes.....	111
4.1 Introduction.....	111
4.2 Results.....	114
4.2.1 Functional profiling of monocytes under hypoxic conditions	114
4.2.1.1 Transcriptional analysis.....	114
4.2.1.2 Wound healing & cellular adherence.....	117
4.2.1.3 Pro-inflammatory mediator release	120
4.2.2 Metabolic manipulation of monocytes under hypoxic conditions	125
4.2.2.1 Carnitine supplementation	125
4.2.2.2 Inhibition of carnitine biosynthesis.....	128
4.2.2.3 Inhibition of carnitine shuttling	129
4.2.2.4 Glycolysis inhibition	131
4.3 Discussion.....	133
Chapter 5. Assessing the impact of the chronic inflammatory milieu on the metabolism and function of monocytes	139
5.1 Introduction.....	139
5.2 Results.....	143
5.2.1 Metabolic profiling of monocytes treated with RA-SF under normoxia or hypoxia	143
5.2.1.1 Overview of metabolic changes induced by RA-SF	143
5.2.1.2 Metabolic alterations in cellular energy metabolites	146
5.2.1.3 Carnitine metabolites	148
5.2.1.4 Urea cycle and creatinine biosynthesis.....	150
5.2.1.5 Nucleotide metabolism.....	152
5.2.2 Manipulation of carnitine metabolism in RA-SF treated monocytes	154
5.2.3 Metabolic profiling and manipulation of intracellular carnitine in end polarised alveolar macrophages	158
5.3 Discussion.....	164
Chapter 6. General discussion	171
6.1 Critical appraisal	175
6.2 Future work	176
6.3 Conclusions.....	176
Appendices	178
List of References	186

List of Tables

Table 1.1 Human monocyte subsets	18
Table 2.1 Western Blot antibodies	65
Table 2.2 ELISA kits.....	68
Table 2.3 FACS antibodies.....	70
Table 2.4 cDNA synthesis cycling.....	72
Table 2.5 Primer sequences.....	73
Table 2.6 MyTaq Red thermal cycling	74
Table 2.7 qPCR cycling conditions	74
Table 2.8 TLDA target genes.....	75
Table 3.1 Significantly altered metabolites in hypoxia (1% O ₂) compared to normoxia after 1 hour of culture	97
Table 3.2 Significantly altered metabolites in hypoxia (1% O ₂) compared to normoxia after 4 hours of culture	99

List of Figures

Figure 1.1 Ontogeny and activation of macrophages.....	22
Figure 1.2 Pathogenesis of rheumatoid arthritis.....	28
Figure 1.3 Pathogenesis of COPD.....	31
Figure 1.4 Myeloid cell adaptation to hypoxia.....	35
Figure 1.5 Glycolytic metabolism has an important role in M(LPS ± IFN γ) macrophages.....	44
Figure 1.6 The TCA cycle is broken in classically activated macrophages.....	47
Figure 1.7 The TCA cycle remains intact in M(IL-4) macrophages.....	48
Figure 1.8 Carnitine shuttling into the mitochondria.....	49
Figure 1.9 Overview of purine metabolism.....	52
Figure 3.1 Human monocyte purity analysis.....	83
Figure 3.2 Monocyte apoptosis assessment.....	85
Figure 3.3 Searching for a HIF-1 α positive control.....	87
Figure 3.4 Confirming hypoxia in monocytes.....	90
Figure 3.5 Monocytes are metabolically distinct in hypoxic conditions.....	92
Figure 3.6 The monocyte metabolome changes over time and between normoxia and hypoxia.....	94
Figure 3.7 The monocyte metabolome changes over time and between normoxia and hypoxia.....	96
Figure 3.8 Mitochondrial metabolism is altered in monocytes cultured in hypoxia (1% O $_2$) after 4 hours.....	100
Figure 3.9 Carnitine levels are also altered under 5% oxygen.....	101
Figure 3.10 Metabolites of the glycolytic pathway are altered under hypoxic (1% O $_2$) conditions.....	103
Figure 3.11 Hypoxia (1% O $_2$) alters purine metabolism in monocytes.....	105
Figure 4.1 Hypoxia induces transcriptional changes in monocytes.....	117
Figure 4.2 Hypoxia has a minimal impact on wound healing in monocytes.....	119
Figure 4.3 Hypoxia has a minimal impact on cellular adherence in monocytes	120
Figure 4.4 LPS Dose response curve of inflammatory mediators.....	121
Figure 4.5 Hypoxia has a minimal impact on the production of pro-inflammatory mediators in the short term.....	124
Figure 4.6 Time and oxygen tension influences LPS stimulated monocyte secretion of CCL20.....	124
Figure 4.7 Longer term hypoxia increases the secretion of pro-inflammatory mediators in LPS stimulated monocytes.....	125
Figure 4.8 Carnitine supplementation increases CCL20 release from monocytes.	127
Figure 4.9 Mildronate treatment has little effect on the production of inflammatory mediators in monocytes.....	128
Figure 4.10 Etomoxir (ETO) increases the release of IL-1 β from monocytes in normoxic and hypoxic conditions.....	130
Figure 4.11 2-Deoxyglucose (2-DG) inhibits pro-inflammatory cytokine production in hypoxic conditions.....	132
Figure 5.1 Metabolomics overview of monocytes unstimulated, stimulated with LPS or treated with RA-SF.....	145
Figure 5.2 Cellular energy metabolites are more abundant in RA-SF treated monocytes compared to LPS stimulated monocytes.....	147
Figure 5.3 Carnitine shuttling components are altered in monocytes cultured in RA-SF after 4 hours.....	149

Figure 5.4 Urea cycle and creatinine synthesis intermediates accumulate in monocytes stimulated with RA-SF	151
Figure 5.5 Purine metabolism is altered in monocytes cultured in RA-SF in comparison to LPS.....	153
Figure 5.6 Pyrimidine metabolism is altered in monocytes cultured in RA-SF in comparison to LPS.....	154
Figure 5.7 Assessment of pro-inflammatory mediators in RA synovial fluids	155
Figure 5.8 Exogenous carnitine increases CCL20 production in monocytes treated with RA-SF in hypoxia.....	156
Figure 5.9 Hypoxia and ETO has no effect on CCL20 & IL-6 production in RA-SF treated monocytes	158
Figure 5.10 Endogenous carnitine abundance in polarised alveolar macrophages.	160
Figure 5.11 ETO and carnitine has no impact on the production of inflammatory mediators in alveolar macrophages	163
Figure 5.12 Pre-exposure of alveolar macrophages to hypoxia reveals differences in pro-inflammatory mediator release similar to that seen in monocytes..	164
Figure 6.1 Hypoxia specific metabolism influences the release of pro-inflammatory mediators in monocytes.....	174

Acknowledgement

I would first like to thank my primary supervisor, Carl Goodyear, for his great deal of support and guidance during my PhD research. I would also like to thank my AstraZeneca supervisor, Nisha Kurian, who, despite being based out in Sweden, has dedicated a large amount of time advising me over the course of my studies. I would also like to acknowledge Iain McInnes and Mike Barrett for their input during the course of my PhD.

My PhD experience was made ever more fruitful due to a secondment period at AstraZeneca in Mölndal, Sweden. So for that, I would like to extend my thanks again to Nisha Kurian, Danen Cunoosamy and Yannick Morias who made me feel welcome on site. At home in the GLAZgo Discovery Centre, a special thanks has to go out to Amanda and Ashley for dealing with many logistical queries I had throughout. I would also like to thank John for his bioinformatics help and the rest of the research team within GLAZgo.

On the ground, I have several people to thank for helping me throughout my time in the lab. This starts from Mark and Felix who taught me a lot when I first started. Kevin for his huge help in my understanding of metabolomics and Cecilia/Aysin for FACS advice. I suppose I better thank Louise, Hussain, Simone, Heather, Shiny and Sarah as well ;).

Some of these people are collectively known as the Soodyears, who I have to pay homage to. You all have made this experience ever more enjoyable, especially on those nights involving varying levels of alcohol to get the craic and talk about something that isn't science! Thank you.

I would now like to offer a tremendous amount of thanks to my family, all of whom have given me a great deal of emotional and financial support during the course of my time at University from afar. The most prominent being my mum, Sue, although, I still don't think she really understands what I have been doing in the lab all of this time! A special thanks also goes out to my Dad, my Grandparents, Kirsty and Hilary.

Unlike my family, Louise has had the great pleasure of being with me and thoroughly enjoying/putting up with my 'banter' throughout my PhD. I would like to thank her for her love and support she has given me over these last 3 years.

Given that I am writing this on the first anniversary of his passing, I would like to end by thanking my uncle, Murray, who not only offered me a great amount of advice and mentorship during the course of my time at University, but in life. I dedicate this piece of work to you.

Author's Declaration

I declare that, unless otherwise stated, the results presented in this thesis are my own work.

Lewis Craig Rodgers

Abbreviations

2-DG	2-Deoxyglucose
ACPAs	Anti-Citrullinated Protein Antibodies
ACR	American College of Rheumatology
AM	Alveolar Macrophage
Arg-1	Arginase-1
BM	Bone Marrow
BOC	British Oxygen Company
BSA	Bovine Serum Albumin
Caco-2	Human Colorectal Adenocarcinoma Epithelial Cells
CARKL	Carbohydrate Kinase-like Protein
CCL	C-C motif chemokine ligand
CXCL	C-X-C motif chemokine ligand
CXCR	C-X-C motif chemokine receptor
CD	Cluster of Differentiation
CoCl ₂	Cobalt Chloride
COPD	Chronic Obstructive Pulmonary Disorder
CPT	Carnitine Palmitoyl Transferase
CST	Cell Signalling Technologies
DAMPs	Danger-Associated Molecular Patterns
DCs	Dendritic Cells
DMARDs	Disease Modifying anti-rheumatic drugs
DMEM	Dulbecco's Modified Eagle's Medium

DMOG	Dimethyloxalyglycine
DMSO	Dimethylsulfoxide
DNA	Deoxyribonucleic acid
DPBS	Dulbecco's Phosphate Buffered Saline
ECL	Electrochemiluminescent
EDTA	Ethylenediaminetetraacetic acid
ELISA	Enzyme-linked Immunosorbent Assay
ETO	Etomoxir
EULAR	European League Against Rheumatism
FACS	Fluorescence Activated Cell Sorting
FAO	Fatty Acid Oxidation
FAS	Fatty Acid Synthesis
FATP	Fatty Acid Transporter Protein
FBS	Fetal Bovine Serum
FLS	Fibroblast-like Synoviocyte
GAPDH	Glyceraldehyde 3-Phosphate Dehydrogenase
GM-CSF	Granulocyte-Macrophage Colony Stimulating Factor
GWAS	Genome Wide Association Studies
HEPES	4-(2-hydroxyethyl)-1-piperazineethanesulfonic acid
HIF	Hypoxia Inducible Factor
HRP	Horseradish Peroxidase
HUVECs	Human Umbilical Cord Vein Endothelial Cells
IFN	Interferon

IgG	Immunoglobulin G
IL	Interleukin
ILT4	Immunoglobulin-like Transcript 4
iNOS	inducible Nitric Oxide Synthase
JAK	Janus Kinase
LC-MS	Liquid Chromatography Mass Spectrometry
LPS	Lipopolysaccharide
LT	Life Technologies
MO	Untreated Macrophage
M(LPS + IFN γ)	Inflammatory macrophage
M(IL-4)	Anti-inflammatory Macrophage
M-CSF	Macrophage Colony Stimulating Factor
MCMV	Murine Cytomegalovirus
MHC	Major Histocompatibility Complex
MMPs	Matrix Metalloproteinases
MPS	Mononuclear Phagocyte System
MSD	Meso-Scale Discovery
MSI	Metabolomics Standards Initiative
MTT	Thiazolyl Blue Tetrazolium Bromide
NAMPT	Nicotinamide Phosphoribosyltransferase
NEAAs	Non-Essential Amino Acids
NF- κ B	Nuclear Factor Kappa Beta
NLRP3	(NOD)-like receptor protein 3

NK	Natural Killer
NO	Nitric Oxide
OXPPOS	Oxidative Phosphorylation
PAMPS	Pathogen Associated Molecular Patterns
PBMCs	Peripheral Blood Mononuclear Cells
PBS	Phosphate Buffered Saline
Pen-Strep	Penicillin-Streptomycin
PFKFB3	6-Phosphofructo-2-kinase/Fructose-2,6/Biphosphatase 3
PHD	Prolyl Hydroxylase
PKM2	pyruvate kinase Muscle Isozyme M2
PRRs	Pattern Recognition Receptors
PVDF	Polyvinylidene fluoride
QPCR	Quantitative Polymerase Chain Reaction
RA	Rheumatoid Arthritis
RA-SF	Rheumatoid Arthritis Synovial Fluid
RANKL	Receptor Activator of Nuclear Factor Kappa-B Ligand
RF	Rheumatoid Factor
RNA	Ribonucleic acid
PMA	Phorbol 12-myristate 13-acetate
ROS	Reactive Oxygen Species
RPMI	Roswell Park Memorial Institute
RT	Room Temperature
SDH	Succinate Dehydrogenase

SDS	Sodium dodecyl sulfate
SNBTS	Scottish National Blood Transfusion Service
STAT	Signal Transducers and Activators of Transcription
TCA	Tricarboxylic Acid Cycle
Th	T Helper
TGF- β	Transforming Growth Factor Beta
Tregs	T Regulatory Cells
TLR	Toll-like Receptor
TLDA	Taqman Low Density Array
TMB	Tetramethylbenzidine
TNF	Tumour Necrosis Factor
VEGF	Vascular Endothelial Growth Factor
WBCs	White Blood Cells

Chapter 1. Introduction

1.1 Human monocytes & macrophages

1.1.1 Monocytes

Blood monocytes are a circulating population of leukocytes derived from bone marrow (BM) haematopoietic precursors. In the BM, monocyte development originates from a series of differentiation steps from haematopoietic stem cells: to the common myeloid progenitor (CMP); the granulocyte-macrophage progenitor (GMP); the common macrophage and DC precursor (MDP) and then the committed monocyte progenitor (cMoP) (Geissmann et al. 2010; Hettinger et al. n.d.). Monocyte egress into the blood from the BM is thought to be governed by CCR2 dependent mechanisms (Serbina & Pamer 2006).

Human monocytes are identified by the expression of CD14 (a co-receptor for TLR4) and CD16 (an FcγRIII with low affinity for IgG). Human monocytes are typically classified into 3 separate subpopulations on the basis of cell surface expression of CD14 and CD16: Classical (CD14⁺⁺ CD16⁻); Intermediate (CD14⁺⁺ CD16⁺) and Non-classical (CD14⁺ CD16⁺⁺) (Ziegler-Heitbrock et al. 2010) (Table 1.1). This is broadly similar in mice where Classical monocytes (Ly6C^{hi}) and Non-classical monocytes (Ly6C^{lo}) monocytes have been characterised, with both populations sharing CD11b and CD115 expression (Geissmann et al. 2003; Shi & Pamer 2011). The classical and intermediate populations of monocytes are largely considered to possess pro-inflammatory roles, with the ability to infiltrate into tissues in CCR2 and/or CX3CR1 dependent mechanisms in order to contribute to immune responses and to differentiate into macrophages at the site of inflammation (Shi & Pamer 2011; Belge et al. 2002). On the other hand, non-classical monocytes are thought to have a patrolling role along the blood endothelium, whilst also possessing anti-viral capacity (Table 1.1) (Auffray et al. 2007; Cros et al. 2010). Recent *in vivo* deuterium labelling studies have shown that classical monocytes typically circulate in the blood for around 1 day, whereas intermediate and non-classical populations persist in the bloodstream for around 4 and 7 days respectively. Interestingly, during systemic inflammation, it is thought a reserve population of classical monocytes from the bone marrow can rapidly replenish the monocyte pool in the blood. (Patel et al.

2017). Despite this varying life-span, monocytes rely on macrophage colony stimulating factor (M-CSF) for their survival and maturation (Wiktor-Jedrzejczak & Gordon 1996).

	Markers	Chemokine Expression	Function
Classical	CD14 ⁺⁺ CD16 ⁻	CCR2 ^{hi} CX3CR1 ^{lo}	Pro-inflammatory & Anti-microbial
Intermediate	CD14 ⁺⁺ CD16 ⁺	CCR2 ^{lo} CX3CR1 ^{hi}	Pro-inflammatory
Non-Classical	CD14 ⁺ CD16 ⁺⁺	CCR2 ^{lo} CX3CR1 ^{hi}	Patrolling & Anti-Viral

Table 1.1 Human monocyte subsets

Migratory monocytes display a high degree of plasticity upon recruitment to tissue, and are well characterised as differentiating into tissue macrophages. However, an increasing body of evidence suggests that long-term tissue-resident macrophages are seeded from yolk sac and fetal liver precursors during embryonic development, and display properties of self-renewal to maintain the macrophage pool (**Figure 1.1**) (Schulz et al. 2012; Guilliams et al. 2013; Hoeffel et al. 2015; Hashimoto et al. 2013). This challenged the original dogma, where it was thought all mononuclear phagocytes derived from circulating monocytes (van Furth & Cohn 1968). Nevertheless, in the steady state, blood monocytes have been shown to replenish tissue resident populations in the skin and the gut (Tamoutounour et al. 2013; Bain et al. 2014).

During an inflammatory insult in the tissue, infiltration of classical monocytes provides a robust immune response. For example, CCR2 deficiency in mice has been shown to exacerbate *L. monocytogenes* bacterial infections by preventing extravasation of monocytes into the site of infection (Kurihara et al. 1997; Serbina et al. 2003). In this infection, Ly6C^{hi} monocytes (which resembles human classical monocytes) are thought to differentiate into dendritic cells (DCs) with potent production of TNF and iNOS (Serbina et al. 2003). Generally speaking, monocytes are known to phagocytose bacteria, such as *E.coli* and *S.aureus*, which is thought to be aided by their strong adherence properties (Newman & Tucci 1990; del Fresno et al. 2009). Furthermore, CCR2-deficient mice showed increased mortality when challenged with *T. gondi* infection. This is thought to

be caused by a lack of TNF and iNOS production from infiltrating monocytes (Dunay et al. 2008). In the context of murine cytomegalovirus (MCMV) infection, inflammatory monocytes are known secretors of CCL3, which is a chemokine for the recruitment of NK cells. Furthermore, stimulation of TLR2 by viral ligands promotes Type I IFN by inflammatory monocytes (Salazar-Mather et al. 1998). However, not all monocytes that enter the tissue are endowed to differentiate into macrophages. It is also thought that, at least in the steady state, monocytes recruited to the lung can acquire antigen and traffic to draining lymph nodes for subsequent presentation to naïve T cells (Jakubzick et al. 2013). This work challenges the view that only dendritic cells can present antigen to naive T cells to initiate immune responses.

Despite the well characterised role of promoting inflammation during infection, monocytes have the ability to contribute to the resolution phase of inflammation. Indeed, during skeletal muscle injury, inflammatory LyC6^{hi} monocytes can switch their phenotype to an anti-inflammatory Ly6C^{lo} phenotype with the ability to secrete transforming growth factor beta (TGF- β) to aid muscle regeneration (Arnold et al. 2007). A similar phenotypic transition has also been observed during wound repair models in the skin (Crane et al. 2014). Furthermore, monocytes are thought to express a plethora of scavenger receptors in order to clear extracellular components during the resolution phase of inflammation (Kzhyshkowska et al. 2012).

In addition to the central role of monocytes in immune responses associated with acute infection, they also have a decisive role in chronic inflammatory diseases, such as rheumatoid arthritis (RA). RA patients have been reported to have an increased proportion of CD16⁺ monocytes in the blood. Furthermore, these monocytes have an increased expression of TLR2 and appeared to reside in the synovial lining. Stimulation of these monocytes with a TLR2 ligand (e.g. lipoteichoic acid) results in increased production of TNF α , which can be augmented by addition of an anti-Fc γ RIII antibody. Suggesting a unique role for this population of monocytes when recruited to RA tissue, where TLR2 and CD16 agonists may be present (Iwahashi et al. 2004). In addition, more recent research has highlighted that classical CD14⁺⁺ CD16⁺ monocytes are increased in the peripheral blood of RA patients and appeared to promote Th17 cell

expansion *in vitro* (Rossol et al. 2012). On the other hand, the non-classical monocyte population (Ly6C^{lo}) has been shown in mouse models of rheumatoid arthritis to infiltrate and initially differentiate into inflammatory macrophages within the joint, before switching their phenotype to aid the resolution of inflammation (Misharin et al. 2014). In the murine collagen-induced arthritis model, short interfering (si)RNA against nicotinamide phosphoribosyltransferase (NAMPT) in monocytes reduced IL-6, Th17 cell number, autoantibody titres and the recruitment of monocytes, macrophages and neutrophils in the joints. Additional work illustrated that NAMPT siRNA was engulfed preferentially by classical Ly6C^{hi} monocytes, rather than Ly6C^{lo} populations. This body of work emphasises an essential role for classical monocytes in driving acute and chronic inflammatory mechanisms (Présumey et al. 2013).

1.1.2 Macrophages

Macrophages were first described as phagocytic cells by Metchnikoff at the end of the 19th century. In 1972, van Furth described the mononuclear phagocyte system, whereby all macrophages derived from circulating blood monocytes, as a lineage from haematopoietic stem cells (van Furth et al. 1972). The concept that all macrophages derived from this lineage, as discussed above, was somewhat disputed with studies suggesting tissue macrophages are long lived and have proliferative activity (Sawyer et al. 1982; Melnicoff et al. 1988). However, the original dogma was fully challenged with a range of fate mapping studies, showing that tissue macrophages such as Microglia (brain) and Langerhans cells (skin) were primarily derived from the yolk sac and fetal liver respectively in the steady state (Ginhoux et al. 2010; Hoeffel et al. 2012) (**Figure 1.1**). Similar studies then attributed this phenomenon to alveolar, kidney, pancreas, liver (Kupffer cells) and splenic red pulp macrophages (Schulz et al. 2012). In all cases, it is thought that although macrophages are seeded early during development, they are long lived cells which self-renew to maintain the macrophage pool (Jenkins et al. 2011; Hashimoto et al. 2013; Davies et al. 2011). In contrast, resident macrophages in the intestine in the steady state are independent of embryonic precursors, and instead rely on blood monocyte replenishment (Bain et al. 2014). Experimental ablation of resident tissue macrophages has shown that blood monocytes have the ability to fill an empty macrophage niche (Hashimoto et al. 2013). Therefore, inflammation may

promote the presence of macrophages of both embryonic origin and from the Mononuclear Phagocyte System (MPS) (Hettinger et al. 2013).

Despite the increasing level of research in macrophage ontogeny, their phenotype(s) are subject to widespread examination. Macrophage activation was originally defined as two categories: either classical (IFN γ stimulation) or alternative (IL-4 stimulation) (Stein et al. 1992). Thereafter, the M1-M2 axis, reflecting classical-alternative activation respectively, was coined by Mills *et al* in 2000. This was largely due to the distinct metabolism of arginine between macrophages of the C57BL/6 and Balb/c mouse strains, which favoured Th1 and Th2 responses respectively (C. D. Mills et al. 2000). Subsequent work started to appreciate that macrophages did not reside in only two separate categories of 'M1' and 'M2', and existed instead as phenotypic extremes of an activation continuum. Therefore to simplify this concept, expanded terminology such as M2a, M2b and M2c was devised (Mantovani et al. 2004; Edwards et al. 2006). The concept of a macrophage spectrum of activation was more fully established by a transcriptomic based study of macrophages stimulated in a variety of manners (Xue et al. 2014). In light of this work and the variability of reporting in macrophage terminology and culture methods in the field, a new nomenclature system was proposed (Murray et al. 2014). This recommended that for the purposes of reproducibility, the origin and differentiation of macrophages must be clearly indicated and detailed. Defining macrophages on the basis of their activator was advocated. For example, IL-4 polarised macrophages, typically characterised as 'M2', would be classified as M(IL-4) (Murray et al. 2014).

Functionally, in line with their phenotypes, macrophages display a high degree of plasticity. Classically activated M1 or M(LPS + IFN γ) macrophages are regarded as being pro-inflammatory, with the ability to secrete a variety of cytokines and chemokines, such as TNF, IL-6, IL-1 β , phagocytose pathogens upon recognition by pattern recognition receptors (PRRs) and present antigen to naïve T cells through high levels of MHC II (Mosser 2003). On the other hand, alternatively activated M2 or M(IL-4) macrophages are thought as being more anti-inflammatory. This is primarily through the production of regulatory cytokines such as IL-10. They also express a plethora of scavenger receptors to clear cellular debris and resolve inflammation (Gordon & Martinez 2010). It must be

stressed that these functions are indicative of *in vitro* generated macrophages, and therefore macrophage phenotype and function will be suitably tailored to the environment *in vivo* (Gordon et al. 2014). For example, alveolar macrophages, which reside towards the airspaces of the lung, are highly regulated by bronchial and airway epithelium by a variety of mechanisms, including IL-10, TGF- β and CD200R interactions to prevent pro-inflammatory responses to innocuous antigen such as commensal bacteria (Jiang-Shieh et al. 2010; Koning et al. 2010; Morris et al. 2003; Hussell & Bell 2014). However, they also express a variety of TLRs such as TLR-2 and TLR-4, which in turn can initiate inflammatory responses (Fernandez et al. 2004). Therefore, they are specifically tailored to maintain tolerance and to respond to specific antigen in this environment (Figure 1.1).

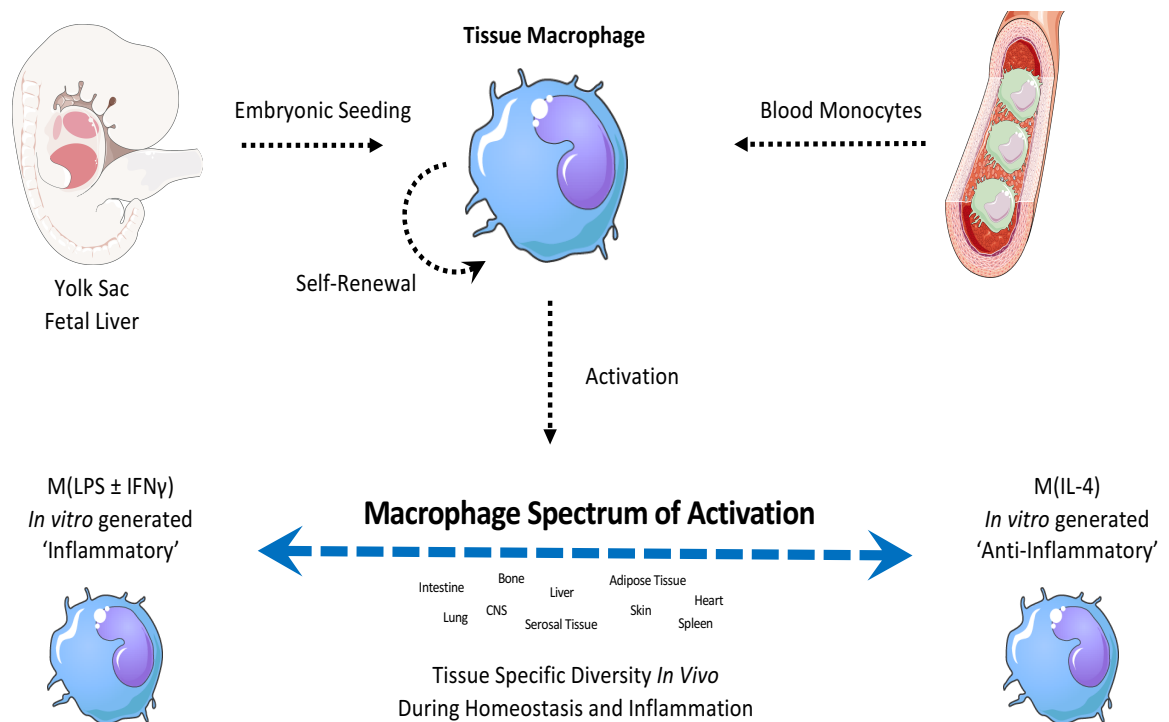


Figure 1.1 Ontogeny and activation of macrophages. Tissue resident macrophages are largely thought to be seeded from yolk sac or fetal liver precursors during embryonic development. Maintenance of the macrophage pool is thought to be carried out by self-renewal mechanisms. However, some sites, such as the intestine have been shown to be primarily derive from infiltrating blood monocytes; conforming to the original dogma of macrophage development. However, it cannot be ruled out that this is the source of macrophages in the context of acute inflammation for example. The specific tissue environment has a major role in governing the phenotype of macrophages during homeostasis and inflammation, providing the concept of a phenotypic continuum. However, common practice in laboratory *in vitro* analyses focuses on phenotypic extremes, typically M(LPS \pm IFN γ) 'inflammatory' macrophages or M(IL-4) 'anti-inflammatory' macrophages.

Despite maintaining a fine balance between tolerant and inflammatory phenotypes in the tissue, macrophages are thought to orchestrate inflammation in chronic inflammatory diseases, including COPD and RA. In patients with COPD, where cigarette smoke presents as a primary risk factor, macrophages are elevated in numbers (Barnes 2016). Cigarette smoke has been reported to activate macrophages to secrete a range of mediators, including TNF α , CXCL1, CCL2, CXCL10, ROS and a variety of MMPs and cathepsins. The ability to secrete CXCL1, CXCL10 and CCL2 in turn acts as a chemoattractant for neutrophils, T cells and monocytes respectively, which perpetuates inflammation (Russell, Thorley, et al. 2002; Barnes 2016). MMP-9 represents the most prevalent MMP produced by activated macrophages in this context, which can drive emphysema in these patients (Russell, Culpitt, et al. 2002). Overproduction of TGF- β is also associated with a fibrotic pathology. Furthermore, these macrophages display an impaired ability to phagocytose bacteria, which may explain why patients are more prone to bacterial infection (Monsó et al. 1998; Donnelly & Barnes 2012).

As with COPD, macrophages can perpetuate inflammation in patients suffering with RA. Similarly, macrophages secrete a range of pro-inflammatory mediators such as TNF α , IL-6 and IL-1 β and MMPs which can promote inflammation and tissue degradation (Kinne et al. 2007). Furthermore, other secreted cytokines, such as IL-12 and IL-23 have been shown to polarise CD4⁺ T helper cells to Th1 or Th17 states respectively, which are both thought to drive disease pathogenesis (Pène et al. 2008; Roberts et al. 2015). Unique to this environment, monocytes and macrophages have the ability to differentiate into bone degrading cells termed osteoclasts. This process called osteoclastogenesis is thought to be dependent on M-CSF and receptor activator of nuclear factor kappa- β ligand (RANKL). It is thought that within the joints of RA patients, the inflammatory environment can alter bone homeostasis to promote bone erosion (Takayanagi 2007; Tondravi et al. 1997; Kong et al. 1999).

1.2 Chronic inflammatory disease

1.2.1 Rheumatoid arthritis

1.2.1.1 Introduction

Rheumatoid arthritis is a chronic inflammatory disease where patients display immune-mediated pathology and articular destruction of the joints, typically in the hands and knees. This in turn develops into progressive disability with systemic manifestations, such as osteoporosis, cardiovascular complications and socioeconomic consequences. The condition primarily affects women with a peak onset of between 30 and 50 years of age. Treatment for the condition is largely dependent on the patient and progress of disease. Therapy typically includes painkillers, Disease Modifying anti-rheumatic drugs (DMARDs) and immunosuppressant drugs (Firestein & McInnes 2017; McInnes & Schett 2011).

1.2.1.2 Joint structure in rheumatoid arthritis

The normal joint is surrounded by a joint capsule which contains the synovium, responsible for lubrication and nutrient supply to cartilage. The synovium contains two lining layers: a sublining layer which is inhabited with fibroblasts, some immune cells and blood vessels; and a leaky intimal lining layer which primarily contains fibroblast-like and macrophage-like synoviocytes which can freely enter the synovial fluid (Smolen et al. 2018.). During RA, these layers become activated and expanded. The intimal lining layer expands due to synoviocyte activation while immune cells infiltrate the sublining layer. These cells include monocytes, macrophages, DCs, memory T cells and B cells (McInnes & Schett 2011). This results in a complex inflammatory milieu that contains inflammatory cytokines, chemokines, immune complexes and proteases to drive inflammation.

The synovial fluid is a viscous lubricant of articular cartilage which is rich in hyaluronic acid. In RA, the fluid volume accumulates and plays host to a variety of synovial membrane derived proteins, metabolites, immune complexes and immune cells such as infiltrating monocytes, T cells and B cells (Penatti et al. 2017). These are thought to include inflammatory cytokines and chemokines

such as $\text{IFN}\alpha$, $\text{TNF}\alpha$, $\text{IL-1R}\alpha$, $\text{IL-1}\beta$, IL-10 , IL-6 , CCL17 , CXCL8 and metabolites including succinate and citrulline (Hampel et al. 2013; Kim et al. 2014).

1.2.1.3 Risk factors

Whilst the exact cause of RA is largely unknown, onset of RA is thought to be dependent on a variety of risk factors, including genetics and the environment. Genetic predisposition is thought to have an important role in RA, where Genome wide association studies (GWAS) attribute immune-regulatory genes in the disease. For example, susceptibility genes such as CTLA4 and PTPN22 highlight an important role for T cell mediated inflammation in this context (Begovich et al. 2004; Kallberg et al. 2007). However, the most prominent genetic risk allele appears to be in MHC class II, with around 40% of total genetic influence (Weyand et al. 1992). This indicates that bridging both innate and adaptive arms of immunity is important for the pathology of RA.

It is thought that in addition to genetic predisposition, environmental factors have a significant role in disease onset. One of the most prominent risk factors for the development of RA is smoking. Smokers with genetic susceptibility in HLA-DRs have been reported to have enhanced risk of developing RA (Symmons et al. 1997). Moreover, smoking increases the risk of anti-citrullinated protein antibodies (ACPAs). In line with this, studies have led to the belief that pulmonary insult has promoted citrullination of proteins including fibrinogen, vimentin and collagen (Mahdi et al. 2009; van der Woude et al. 2010). The role of ACPAs in disease pathogenesis will be discussed in 1.2.1.3.

1.2.1.4 Immunopathology of rheumatoid arthritis

GWAS studies have made it quite clear that RA synovitis is governed by immune-mediated mechanisms. Furthermore, it indicates that both the innate and adaptive immune system has a role in pathogenesis. However, it is well established that a loss of tolerance has to occur in the first instance. The most well characterised mechanism for this is the presence of autoantibodies such as ACPAs or rheumatoid factor (RF), which are present in at least 80% of patients (Firestein & McInnes 2017). Interestingly, these are present before clinical onset and are thought to increase in established disease. These antibodies are known

to bind Fc receptors in the form of immune complexes on the surface of macrophages and can promote the production of TNF α . Furthermore, Fc receptor interaction on the surface of myeloid cells can induce osteoclastogenesis, which can lead to increased bone degradation (Takayanagi 2007). Despite the importance of autoantibodies in RA, they are not thought to cause disease pathogenesis in mice alone (Kuhn et al. 2006).

The innate immune system is exploited to drive pathology in RA patients, where the variety of functional mechanisms that monocytes and macrophages possess promote inflammation (1.1.1 & 1.1.2) in the synovial membrane. In addition to myeloid cells, neutrophils are also often present in the synovial fluid and can exacerbate inflammation via the production of reactive oxygen species, prostaglandins and proteases (Cascão et al. 2010). Furthermore, mast cells have been implicated in disease pathogenesis. They express a number of TLRs and Fc receptors, which upon stimulation can result in the release of cytokines such as TNF and proteases (Nigrovic & D. M. Lee 2007) (Figure 1.2).

GWAS studies, as discussed above, heavily implicate MHC class II, which suggests antigen presentation and co-stimulation of T cells may contribute to disease severity. Indeed, inflammatory arthritis chronicity is considered to be driven by pathogenic populations of Th1 and Th17 cells. Treg cells have also been shown to be present in this milieu, however, studies have reported that they are functionally impaired (Behrens et al. 2007). This may be caused by the high level of TNF α in the synovium, which has been shown to prevent Treg functionality (Nadkarni et al. 2007). T helper cells are also involved in aiding B cells to produce antibody responses, and more specifically in RA the associated autoantibodies. B cells in the RA synovium have been observed to be present in ectopic lymphoid follicles containing T cells and B cells to promote B cell differentiation and somatic hypermutation to drive a pathogenic phenotype (Seyler et al. 2005). Furthermore, the presence of B cells survival factors such as BAFF, APRIL and IL-6 supports their ability to persist in this environment (Ohata et al. 2005) (Figure 1.2).

Finally, it is important to consider the contribution of stromal tissue cells in the pathogenesis of RA. An example of this are fibroblast-like synoviocytes (FLSs). During hyperplasia in the RA synovium, the FLS population is known to be

expanded, a phenomenon thought to be dependent on the prevention of apoptosis (Korb et al. 2009). Furthermore, they characteristically release a variety of matrix metalloproteinases (MMPs) and cathepsins that can contribute to articular damage (Filer 2013). Their role in promoting bone erosion is marked by the production of RANKL, which is essential for the differentiation of osteoclasts (Shigeyama et al. 2000). In addition to promoting a loss of structural integrity in the joint, FLSs can interact with immune cells to exacerbate inflammation. For example, FLSs can support the recruitment of T cells by the production of the chemokines CCL5, CXCL12 and CX3CL1 and can present antigen to and co-stimulate T cells through expression of MHC class II and CD40 respectively. Finally, they have the ability to recruit macrophages (CCL2, CCL4, CCL5 & CCL20), neutrophils (CXCL1, CXCL5 & CXCL8) and B cells (CXCL12 & CXCL13) to the joint (Manzo et al. 2005; Koch et al. 1995; Filer 2013) (**Figure 1.2**).

Inflammatory cascades in the synovial compartment are known to enhance bone erosion. This is primarily through the bone-resorption activities of osteoclasts which can mature in response to RANKL, TNF α , IL-6 (secreted by T cells, macrophages and FLSs), and in response to autoantibodies (Schett & Gravallesse 2012; Takayanagi 2007). Together with synovial membrane inflammation and cartilage damage, bone erosion contributes heavily to the pathophysiology of RA (**Figure 1.2**).

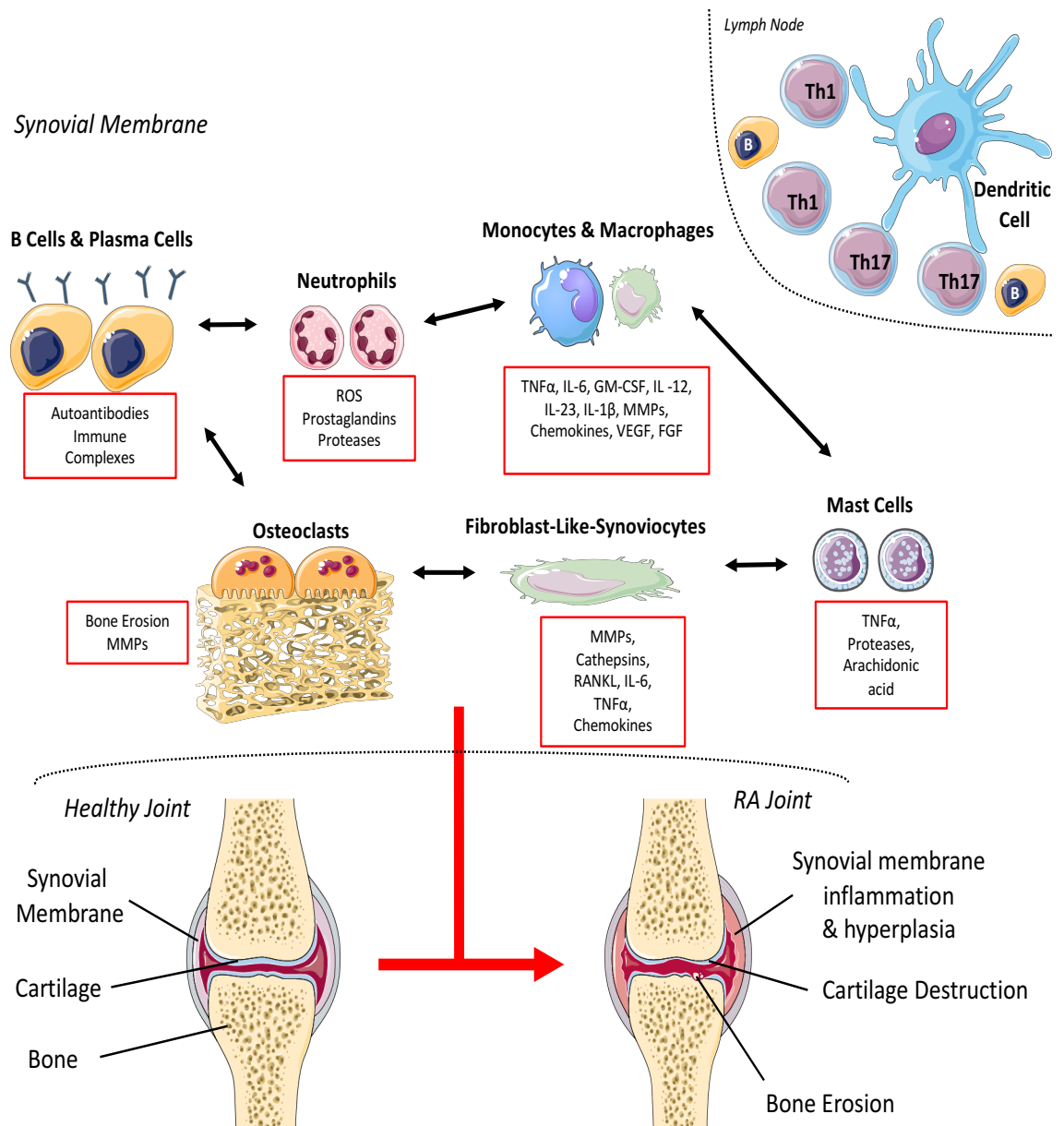


Figure 1.2 Pathogenesis of rheumatoid arthritis. Co-stimulatory interactions in the lymph node are thought to take place between dendritic cells, T cells and B cells to generate autoimmune inflammatory responses against antigens such as citrullinated self-proteins. This can lead to the production of autoantibodies (ACPAs and/or rheumatoid factor) and immune complexes. In the synovial membrane of an RA joint, infiltrating monocytes and macrophages can drive inflammation with a number of inflammatory mediators, and can promote fibrosis, articular damage through MMPs and angiogenesis via VEGF. Osteoclasts can promote bone erosion and secrete MMPs. Neutrophils and Mast cells can exacerbate inflammation and articular destruction through the production of proteases, ROS, prostaglandins and TNF α . Fibroblast-like synoviocytes produce MMPs, cathepsins and pro-inflammatory cytokines. Together, these interactions contribute to the pathology of an RA joint, which include inflammation and hyperplasia of the synovial membrane, cartilage destruction and bone erosion.

1.2.2 Chronic obstructive pulmonary disorder (COPD)

1.2.2.1 Introduction

Chronic obstructive pulmonary disorder (COPD) is a progressive inflammatory disease which causes irreversible airway obstruction of the lungs. The largest risk factor for the disease in the developed world is cigarette smoking and is thought to affect around 10% of those over 45 years of age (Lozano et al. 2012). Inflammation in COPD patients tends to be localised within the lung parenchyma and the peripheral airways. The irreversible obstruction of the airways is largely due to fibrotic mechanisms and a loss of elasticity of the parenchyma. Inflammation of the airways involves both the innate and adaptive arms of immunity, however, macrophages and neutrophils are thought to predominate. Despite the inflammatory nature of the condition, COPD patients typically lack responsiveness to steroid treatment (Barnes 2016).

1.2.2.2 Macrophages in COPD

Alveolar macrophages are well characterised as being a long lived self-renewing population of tissue resident cells derived from embryonic precursors (1.1.2) (Guilliams et al. 2013). In the lung, they reside in close contact with lung epithelial cells towards the airspace. Alveolar macrophages are important cells that assist in the maintenance of lung homeostasis. They possess an immunosuppressive phenotype, exhibit low phagocytic capacity, respiratory burst and have a decreased capacity to present antigen to T cells (Lyons et al. 1986; Hoidal et al. 1981; Hussell & Bell 2014). Combined with their ability to produce TGF- β , these mechanisms are thought to promote tolerance to innocuous antigens (Coleman et al. 2013).

Notably, these mechanisms are severely altered during COPD pathology. Fibrosis in the small airways and lack of elasticity of the lung parenchyma during COPD is largely attributed to inflammatory processes in these sites. In COPD patients, macrophage populations are significantly increased in the lungs and their numbers correlate with disease severity (Grashoff et al. 1997). Macrophages in this environment are well known to be activated when exposed to cigarette smoke. Their contribution to inflammation in COPD is marked by their ability to secrete ROS, TNF α and a variety of chemokines such as CXCL1, CXCL8 and CCL2,

which will drive recruitment of neutrophils and blood monocytes (Barnes 2016). The recruitment and subsequent differentiation of blood monocytes into macrophages is thought to be the main cause of the expansion of the macrophage pool in COPD (Traves et al. 2004). Furthermore, macrophages have been reported to recruit Th1 cells to the site of inflammation via the production of CXCL10, 11 and 12 (Grumelli et al. 2004). Exposure of macrophages to smoke also results in the secretion of a range of elastolytic enzymes such as MMPs (MMP-2,9 &12) and cathepsins, which contribute to emphysema (Russell, Thorley, et al. 2002) (**Figure 1.3**). It is thought that the production of these mediators, particularly MMP-9, is governed by the activation of NF- κ B subunits (Caramori et al. 2003). Generally speaking, macrophages are known to be phagocytic, whether that is the engulfment of bacteria during infection, or the clearance of cellular debris during resolution phases of inflammation. However, the COPD environment has been shown to impair the ability of macrophages in the lung to phagocytose bacteria and debris. This proposes a mechanism as to why COPD sufferers are prone to bacterial colonisation (found in 50% of COPD patients) and fail to resolve inflammation (Berenson et al. 2013; Hodge et al. 2003; Richens et al. 2009) (**Figure 1.3**). Subsequent studies have credited the impaired phagocytosis to defective cellular microtubular function (Donnelly & Barnes 2012). Despite the effectiveness of corticosteroids against these mechanisms *in vitro*, these findings have not been translated in patients. This is thought to be as a result of reduced Histone deacetylase 2 (HDAC2) activity induced by glucocorticoids, which would in turn prevent the transcription of inflammatory genes (Mitani et al. 2016).

1.2.2.3 Other immune cells in COPD

The other main contributor to disease pathology is through the recruitment of neutrophils. Neutrophils migrate to the lungs in response to the increased levels of Leukotriene B₄, CXCL1 and CXCL8 (Biernacki et al. 2003). In a similar manner to macrophages, activated neutrophils secrete cathepsin G, MMP-8, MMP-9 and neutrophil elastase, which cause damage to the airways and parenchyma (Vlahos et al. 2012; Barnes 2016). Furthermore, these mediators have been suggested as being activators of alveolar goblet cells to secrete mucus, which can increase airway obstruction and cause chronic bronchitis (Fahy & Dickey 2010) (**Figure**

1.3). As neutrophils are short lived in nature, the impaired ability of macrophages to engulf neutrophil cellular debris may exacerbate inflammation.

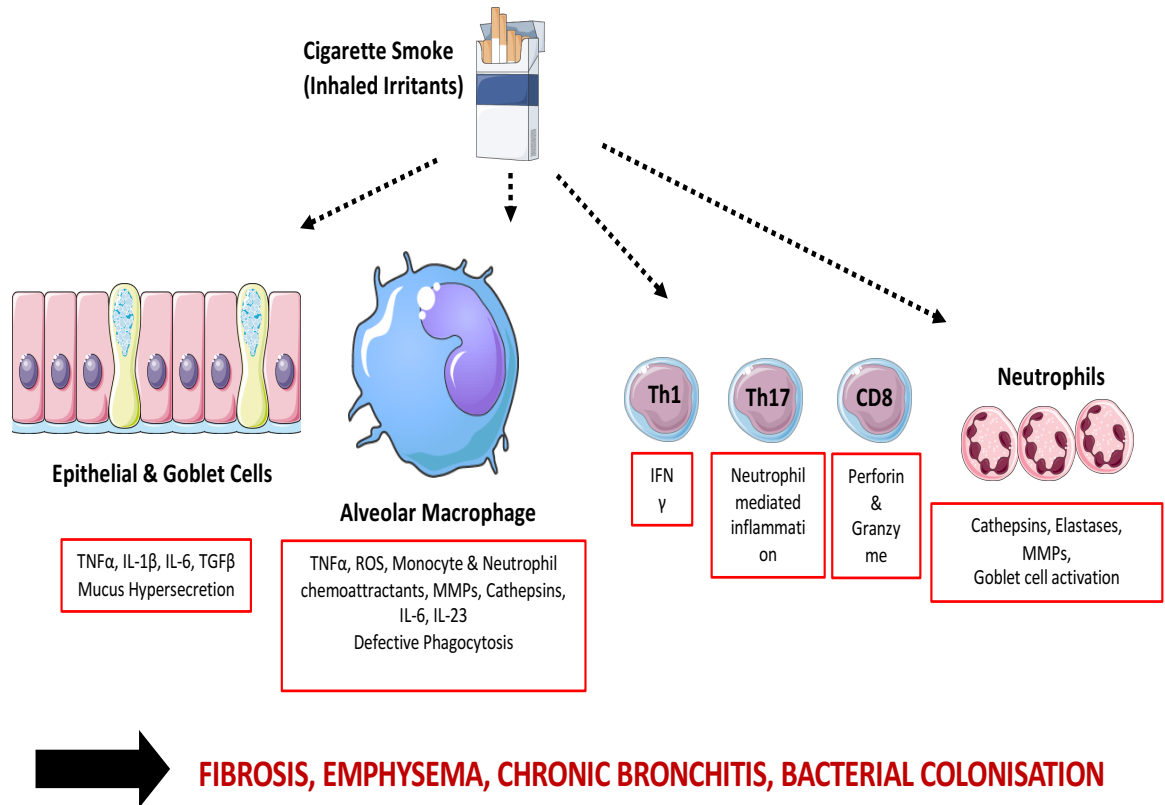


Figure 1.3 Pathogenesis of COPD. Cigarette smoke and other inhaled irritants activate a number of inflammatory and fibrotic mechanisms in the lung. One of the biggest contributors to disease pathology are macrophages which secrete a variety of cytokines and chemokines to perpetuate inflammation. Alveolar macrophages also secrete elastolytic enzymes such as MMPs and cathepsins to promote emphysema. Finally, they exhibit defective phagocytosis that leads to bacterial colonisation. Neutrophils also contribute to emphysema in a similar manner, but can induce goblet cell activation to increase mucus secretion. Cigarette smoke can also activate epithelial cells to produce pro-inflammatory cytokines, including TNF α , IL-1 β and IL-6. Furthermore, CD8 T cells can further contribute to emphysema by promoting apoptosis of pneumocytes via secreted perforin and granzyme. Finally, Th1 and Th17 cells are abundant in this disease environment, which in turn drives disease chronicity.

Despite the dominance of macrophages and neutrophils in driving the pathology of COPD, T cells are considered as having a role. Intriguingly, CD8⁺ T cells are increased in smokers with COPD compared to smokers with no symptoms (Saetta et al. 1998). Characteristically, CD8⁺ T cells can be cytolytic against epithelial cells through the action of perforin and granzyme. Alveolar macrophages dependent production of IL-6 and IL-23 could be the driving factor to promote

the increased presence of Th17 cells, which can further drive neutrophil-mediated inflammation (**Figure 1.3**).

Although not an immune cell per se, epithelial cells share some properties with immune cells in COPD. For example, when exposed to cigarette smoke, they secrete a variety of pro-inflammatory cytokines such as TNF α , IL-1 β and IL-6 to exacerbate inflammation (Gao et al. 2015) (**Figure 1.3**). Furthermore, epithelial cells can contribute to physical obstruction of the airways. Together with neutrophil-derived elastases, cigarette smoke can promote mucus hypersecretion via epithelial growth factor receptor (EGFR) stimulation on goblet cells in the epithelial layer (Shao et al. 2004).

1.3 Hypoxia in chronic inflammatory disease

1.3.1 Origins of hypoxia in inflammatory tissue

One of the most common features of many chronic inflammatory diseases, such as RA and COPD, is the presence of hypoxia within the tissue microenvironment. Hypoxia within the synovial fluid of the RA joint for example was first described in the 1970s (Lund-Olesen 1970) and is becoming more appreciated in COPD (Kent et al. 2011). Hypoxia within an inflammatory environment results when the oxygen demand exceeds the supply. In inflammation, this phenomenon is attributed to the increased infiltration and proliferation of immune cells, all of which primarily utilise oxygen for metabolic purposes for effective function. It is also thought that in the context of RA, tissue hyperplasia, synovial fluid effusion and movement of the affected joint can disrupt the capillary network and prevent blood flow to the tissue (Jawed et al. 1997). Due to this excessive demand for O₂, neovascularisation occurs. However, these structures are rather dysfunctional and poorly organised and hence acts as a contributing factor towards tissue hypoxia (Kennedy et al. 2010; Strehl et al. 2014). Therefore, infiltrating cells such as blood monocytes are met with an environmental challenge upon recruitment to the inflammatory tissue. It is well accepted that for continued survival and functionality, immune cells adapt quickly to hypoxic microenvironments, and this is primarily through the expression of the transcription factor hypoxia inducible factor 1 alpha (HIF-1 α) (Semenza & G. L.

Wang 1992). This master regulator has been reported to regulate a variety of processes, including cell metabolism, angiogenesis, migration and inflammatory cascades (Semenza 2009).

1.3.2 Hypoxia in the rheumatoid arthritis joint

Hypoxia was first described in the rheumatoid joint in the 1970s by measuring pO_2 in the synovial fluid of RA patients in comparison to OA patients (Lund-Olesen 1970). More recent work however has identified that the median pO_2 in the joint is 3.2% with a range between 0.46-7% (Fearon et al. 2016). Hypoxia in the rheumatoid environment correlates with synovial inflammation *in vivo* (Ng et al. 2010). This is in contrast to other tissues during homeostasis. For example, alveoli have been reported to have a concentration pO_2 of 13.5% while arterial blood is thought to be around 9.5%. These concentrations diffuse further when oxygen reaches the tissue. For example, the brain and liver have both been measured to have a median O_2 tension of 4% (McKeown 2014). Other tissues such as the pancreas have a median O_2 tension of 7%. In diseases such as cancer, the oxygen tension is thought to reduce substantially in peripheral tissues, typically below 2% (McKeown 2014). As discussed briefly in 1.3.1, there are several causes for synovial hypoxia. Synovial inflammation is thought to activate endothelial vessels to support increased infiltration of immune cells to the synovium. This in turn assists in the expansion of the synovium which results in an increased rate of metabolic turnover and requirement for oxygen (Fearon et al. 2016). In addition, synovial hyperplasia can result in an increased distance between vessels and the cellular infiltrate, further diluting oxygen diffusion. Disrupted angiogenesis is another feature which contributes to joint hypoxia. Activated endothelial cells are thought to lose their polarity, structure and their association with the pericyte layer (Fearon et al. 2016). This can render the vessel dysfunctional in the supply of nutrients and oxygen to the joint. Therefore, infiltrating immune cells must adapt at a transcriptional and metabolic level in order survive and to drive disease pathogenesis.

1.3.3 Myeloid cell adaptation to hypoxia

Cellular adaptation to hypoxia is achieved via the stabilisation of hypoxia inducible factors (HIFs). HIFs are typically composed of heterodimers, containing an alpha

subunit regulated by oxygen, and a stable beta subunit (Semenza & G. L. Wang 1992). In normoxia, the alpha subunits are hydroxylated by prolyl hydroxylases (PHDs) and are targeted by an E3 ubiquitin (Ub) ligase complex, termed von Hippel Lindau tumour suppressor protein (pVHL). The polyubiquitinated alpha subunits are then targeted for proteasomal degradation (Berra et al. 2003) (**Figure 1.4**). In hypoxic conditions, the PHDs lose their enzymatic activity due to the lack of oxygen, which, along with α -ketoglutarate, acts as a co-substrate for their activity. This allows the stabilisation of the alpha subunits and formation of the heterodimers (Epstein et al. 2001; Ivan et al. 2001). This in turn permits the HIFs to enter the nucleus in order to carry out transcriptional regulation of target genes for the adaptation to hypoxic conditions (**Figure 1.4**). This regulatory cascade is well characterised in macrophages (Hirani et al. 2001; Fangradt et al. 2012; Staples et al. 2011). However, this is disputed in human monocytes. Although HIF-1 α is stabilised under hypoxic conditions in monocytes, it has been postulated that NF- κ B carries out the necessary transcriptional processes, as HIF-1 α appears to be absent from the nucleus (Fangradt et al. 2012) (**Figure 1.4**). More recent work however has proposed that mitochondrial complex II may regulate hypoxia adaptation processes in monocytes (Sharma et al. 2017). These studies demonstrate that the precise mechanism of monocyte adaptation to hypoxia warrants further investigation.

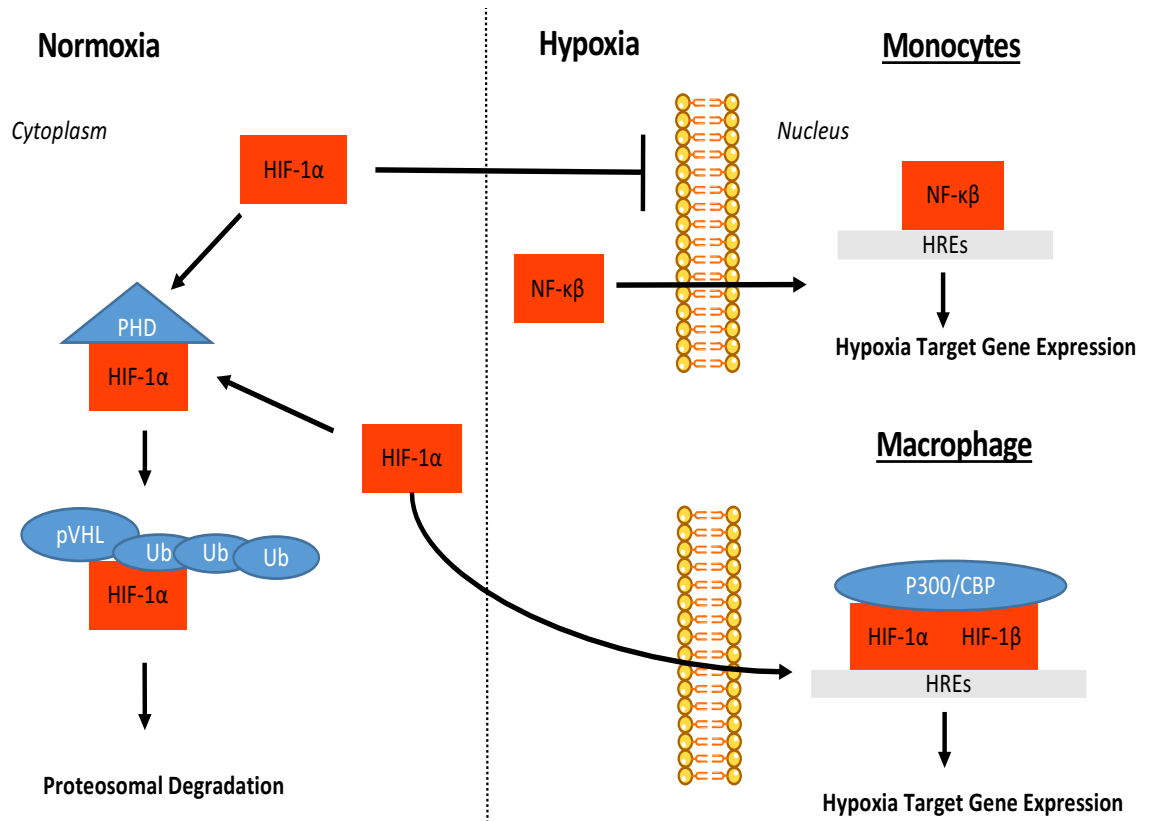


Figure 1.4 Myeloid cell adaptation to hypoxia. In normoxic conditions, HIF-1 α is hydroxylated by Proyl Hydroxylases (PHDs) and is then targeted by an E3 ubiquitin (Ub) ligase complex, termed von Hippel Lindau tumor suppressor protein (pVHL). After ubiquitination, HIF-1 α is subject to proteosomal degradation. In hypoxic conditions, HIF-1 α entry into the nucleus is thought to be blocked in monocytes, with NF- κ B postulated as carrying out gene transcription of hypoxia specific genes. In macrophages, HIF-1 α , in a complex with the constitutively active HIF-1 β , forms a complex with transcriptional coactivators including P300 and CREB-binding protein (CREB) to carry gene transcription of hypoxia responsive elements (HREs).

1.3.4 The impact of hypoxia on the function of myeloid cells

Once encountered with an environmental challenge such as hypoxia, it is thought that myeloid cells alter their functional phenotype. In an attempt to elucidate exactly how hypoxia impacts the phenotype of human monocytes, Bosco *et al* carried out a global transcriptomic study of monocytes cultured under hypoxic conditions (Bosco *et al.* 2006). This study highlighted that monocytes upregulate a number of genes associated with typical hypoxia responses, such as *VEGF* (angiogenesis), *BNIP3* (apoptosis), *GLUT-1* (glucose transport) and *HK2* (glycolytic metabolism). The authors also identified alterations in scavenger receptors (*STAB1*, *MARCO* & *MSR1*) and chemokine-related genes (*CCL15*, *CCL2*, *CCR2*). Strikingly, monocytes appeared to up-regulate *CCL20* at both the transcript and protein level in response to hypoxic

conditions, illustrating that hypoxia may act to promote the recruitment of other immune cells to the site of inflammation (Bosco et al. 2006). Subsequent studies identified CD300a as a hypoxia-inducible surface receptor that was able to regulate the expression of CCL20 and VEGF (Raggi et al. 2014). The importance of hypoxia in mediating chemotactic responses in monocytes was further marked by the up-regulation of CXCR4 receptor expression (Schioppa et al. 2003). CCL20 production has also been associated with the activation of the NF- κ B subunit, p50 (Battaglia et al. 2008). The action of this subunit supports the suggestion that NF- κ B is important for hypoxia adaptation in human monocytes (Battaglia et al. 2008; Fangradt et al. 2012) (1.3.2 & Figure 1.4). Interestingly, lower O₂ levels in the joint has been associated with increased canonical NF- κ B signalling in synovial fluids of active RA patients (Oliver et al. 2009).

In vitro hypoxia has been shown to promote an increased rate of survival in both monocytes and macrophages in a mechanism thought to be through the induction of glycolytic metabolism (Roiniotis et al. 2009). Once monocytes are recruited to the site of hypoxic inflammatory sites, they are thought to differentiate into macrophages. Studies assessing monocyte differentiation into macrophage suggests that severe hypoxia reduces phagocytosis, CD40 and CD206 expression after 5 days (Staples et al. 2011). In contrast, earlier studies report that hypoxia rather increases phagocytosis in RAW 264.7 and primary peritoneal macrophages (Anand et al. 2007). Increased VEGF production in response to hypoxia has also been observed in macrophages which suggests a pro-angiogenic phenotype under these conditions (Staples et al. 2011). Upon encountering the site of hypoxia, monocytes and macrophages together have been shown to reduce their migratory properties (L. Turner et al. 1999; Grimshaw & Balkwill 2001). Monocyte-derived macrophages also exhibit lower levels of CCL2 and increased CXCR4 in response to hypoxic conditions, suggesting severe alterations in chemotactic activities (Schioppa et al. 2003). Furthermore, macrophages are thought to modify their proteolytic capacity under hypoxic conditions by increasing MMP-7 gene expression (Burke et al. 2003). In palmitate-activated macrophages, hypoxia is thought to amplify the production of IL-6 and IL-1 β (Snodgrass et al. 2016). Taken together, this evidence suggests that hypoxia may promote pro-inflammatory properties in myeloid cells, and its presence in chronic inflammatory tissue may drive disease severity.

1.4 Pro-inflammatory mediators in chronic inflammatory disease

1.4.1 Introduction

In chronic inflammatory diseases such as RA and COPD, the affected tissue microenvironment contains a specific milieu of inflammatory cytokines and chemokines which drive disease (**Figures 1.2 & 1.3**). Monocytes and macrophages contribute to this further upon activation by a range of stimulants found in these environments. The *in vitro* studies which are relevant to chronic inflammatory disease in this thesis have implicated several of these mediators. Therefore, this section will give an overview of the mediators that were interrogated in this work.

1.4.2 TNF α

Tumour necrosis factor alpha (TNF α) is a pro-inflammatory cytokine produced by myeloid cells such as monocytes and macrophages in response to inflammatory ligands. TNF α has a number of functions to drive disease pathogenesis in RA and COPD by promoting mechanisms of cell death, survival and the activation of NF- κ B. TNF α can bind either of its two receptors, TNF receptor 1 (TNFR1) and TNFR2. Upon receptor engagement, TNFR1 binds to TNFR1-associated death domain protein (TRADD), which then recruits receptor-interacting serine/threonine-protein kinase 1 (RIPK1). The ubiquitination status of RIPK1 can determine if the signalling can promote canonical NF- κ B signalling (ubiquitinated) or cell death cascades (non-ubiquitinated) (Brenner et al. 2015). TNF α is thought to be the primary inducer of oxidative stress via reactive oxygen species. This stress can induce an inflammatory gene expression programme and can also signal for apoptosis or necrosis (Blaser et al. 2016). In the context of disease, TNF α has been shown to promote fibrosis and collagen deposition, which is of clinical importance in COPD and RA (Piguet et al. 1990). This is coupled with the induction of MMPs and TGF- β which can promote tissue remodelling (Sasaki et al. 2000; Sullivan et al. 2005). Furthermore, it is thought to have chemoattractant properties for inflammatory cells such as neutrophils and eosinophils, while promoting CCL2 release for the recruitment of other myeloid cells (Lukacs et al. 1995). Given the functional diversity of TNF α in the

exacerbation of inflammation, this has provided an attractive target for therapeutics. In light of this, a range of anti-TNF α drugs have been developed, such as monoclonal antibodies (Infliximab, Adalimumab, Golimumab and Certolizumab) and fusion proteins (Etanercept) (Rubbert-Roth et al. 2017). Generally speaking, these therapies have proven successfully in the treatment of RA. However, this has not been as efficacious in the treatment of COPD (Malaviya et al. 2017).

1.4.3 IL-6

Interleukin 6 (IL-6) is another pro-inflammatory cytokine produced by a variety of immune cells including monocytes, macrophages, T cells, B cells and even fibroblasts. IL-6 receptor binding induces an inflammatory cascade through the phosphorylation of Janus kinase (JAK) families and the recruitment of signal transducers and activators of transcription (STAT)-1 and STAT-3 (Heinrich et al. 1998). IL-6 promotes a range of immunological processes in chronic inflammatory diseases. This cytokine is involved in the recruitment of neutrophils to the site of inflammation, tissue hyperplasia and angiogenic properties (Lally et al. 2005). It can promote the survival of B cells and the differentiation of autoantibody secreting plasma cells (Diehl et al. 2008). In conjunction with IL-1 β , IL-6 has been shown to mediate the up-regulation of RANKL in fibroblast-like synoviocytes from RA patients, which contributes to the generation of osteoclasts and the subsequent bone resorption (Hashizume et al. 2008). Moreover, IL-6 has an important role in T cell immunity. For instance, IL-6 is considered as a primary factor for the differentiation of pathogenic Th17 cells and T follicular helper cells, which can mediate B cell class switching in follicles (Nurieva et al. 2009; Volpe et al. 2008). Furthermore, stimulating Treg cells with IL-6 is has been shown to inhibit FoxP3 expression in these cells, and promote Th17 cell induction through ROR γ t (Komatsu et al. 2014). This suggests that IL-6 may promote an imbalance between inflammatory and regulatory cells in chronic inflammation. IL-6 and its signalling have been the focus of several therapies for chronic inflammatory diseases. This includes the monoclonal antibody, tocilizumab, which prevents IL-6 binding to its receptor (Hunter & Jones 2015). This treatment has proved effective in the control of RA pathology, especially in combination with methotrexate (Dougados et al. 2013). JAK

inhibitors such as tofacitinib which interfere with the IL-6 signalling cascade have also been utilised for the treatment of RA (Fleischmann et al. 2012).

1.4.4 IL-1 β

IL-1 β represents another highly inflammatory cytokine which is heavily regulated in its production from monocytes, macrophages and dendritic cells. IL-1 β is originally translated into an inactive form, termed pro-IL-1 β , before being cleaved by caspase-1 to create its active form (Wilson et al. 1994; Burns et al. 2003). In order for this processing to take place, caspase protein complexes called inflammasomes are formed to activate caspase-1 from its inactive pro-caspase-1 derivative (Lamkanfi & Dixit 2014). This process is typically carried out by canonical inflammasomes such as NLRP1 and NLRP3 which leads to pyroptosis and the release of IL-1 β and IL-18 after recognition of a variety of PAMPS (Netea et al. 2015). However, monocytes are able to release IL-1 β without undergoing pyroptosis. It is thought a TLR-4 specific alternative inflammasome forms when human monocytes are stimulated with LPS to avoid pyroptosis (Gaidt et al. 2016).

Once IL-1 β has been processed and released, it has a range of pro-inflammatory functions. It is thought to be involved in the initiation of the acute phase response and induction of fever, as evident by a lack of these responses in IL-1 β deficient mice (Zheng et al. 1995). Caspase-1 deficient mice show an increased susceptibility to a variety of infections, including shigella, salmonella and influenza viruses (Suzuki et al. 2007; Raupach et al. 2006; Ichinohe et al. 2009). Furthermore, IL-1 β has been reported to be important for the development of Th17 differentiation, emphasising its inflammatory nature (Mailer et al. 2015). Stimulation of human alveolar macrophages from smokers and COPD patients with IL-1 β results in the release of IL-8, GM-CSF and MMP-9, promoting inflammation and tissue fibrosis (Culpitt et al. 2003). The release of IL-1 β from necrotic cells in hypoxic conditions is thought to have a role in the recruitment and retention of monocytes and macrophages at sites of inflammation (Rider et al. 2011).

With this range of function in mind, IL-1 β has been targeted for therapy in RA and COPD. Although few studies have been carried out in COPD, anti-IL-1R treatment to prevent IL-1 β responses have not revealed any statistical improvement in lung function of patients (Calverley et al. 2017). Similarly, anti-IL-1 β antibody treatments such as Canakinumab have not been shown to be particularly effective for the treatment of RA (Dinarello & van der Meer 2013)

1.4.5 CCL20

C-C chemokine ligand 20 (CCL20) is a chemoattractant for a variety of immune cells during homeostasis and inflammation. It is one of few ligands for its receptor, CCR6. Furthermore, it is now becoming apparent that it may have a role in other processes, such as in the development and maturation of B cells (Krzysiek et al. 2000). However, GWAS studies have identified single nucleotide polymorphisms (SNPs) in the CCR6 locus as a susceptibility gene in RA, which implicates the CCL20-CCR6 axis in disease pathogenesis (Kochi et al. 2010). Interestingly, both Th17 and Tregs show surface expression of CCR6 (Yamazaki et al. 2008). To investigate this axis inflammatory arthritis, studies in Sakaguchi mice (a murine model for autoimmune RA) revealed that CCL20 is produced by synoviocytes and Th17 cells in the joints. This suggests that in this RA model, Th17 cell recruitment is favoured over Tregs to perpetuate inflammation (Sakaguchi et al. 2003; Hirota et al. 2007). In support of this, CCL20 has been found to correlate with levels of IL-17 in human synovial fluid (Hirota et al. 2007). The increased expression of CCR6 on the surface of memory T cells in the periphery of RA patients compared to healthy controls suggests a role for the axis in the recruitment of this population as well (Liao et al. 1999; Ruth et al. 2003).

In addition, CCL20 has been reported to have a role in myeloid cell immunity. This is evident in its ability to recruit monocytes to the inflamed joint (Ruth et al. 2003). Furthermore, CCL20 is thought to activate osteoclasts which are important for bone erosion (Lisignoli et al. 2007). The production of CCL20 has been observed in neutrophils and osteoblasts in RA synovial fluid and bone tissue respectively (Pelletier et al. 2010; Lisignoli et al. 2009).

1.4.6 CCL22

CCL22 is a chemokine ligand for the receptor CCR4. It is classically produced by M(IL-4) or M2 polarised macrophages and by monocyte-derived dendritic cells, especially when stimulated with microbial PAMPs such as LPS (Godiska et al. 1997; Wu et al. 2001). CCR4 has been shown to be expressed on antigen-experienced T cells such as Th2, Th17 and Treg and on monocytes, macrophages and natural killer (NK) cells (Imai et al. 1999; Lim et al. 2008; Griffith et al. 2014). This expression profile indicates that CCL22 is a potent chemoattractant of all of these cell types to sites of inflammation. Given CCL22 production is typically associated with IL-4 macrophage stimulation and CCR4 expression of Th2 cells, suggests this inflammatory cascade has a degree of specificity for Th2-mediated immunity such as asthma (Panina-Bordignon et al. 2001). However, CCL22 has been illustrated to be present in the joints of RA patients, with CCR4 being expressed on memory T cells in these sites, indicating that this axis could also contribute to RA pathogenesis (Flytlie et al. 2010).

1.4.7 IL-8

Interleukin 8 (IL-8) is a pro-inflammatory chemoattractant produced by monocytes and macrophages when stimulated by a variety of PAMPs. IL-8 binds both CXCR1 and CXCR2, although there is thought to be a predominance for CXCR1 (D. A. Hall et al. 1999). IL-8 was first characterised as being a potent chemoattractant of neutrophils (Baggiolini et al. 1992). However it has been implicated in the recruitment of other immune cells such as monocytes, lymphocytes and eosinophils in airway inflammation (Miller et al. 1992). Upon binding to its receptor, especially CXCR1, IL-8 induces the activation of intracellular G proteins which can promote calcium efflux which trigger the degranulation of neutrophils to provide anti-microbial immunity (M. D. Turner et al. 2014). Furthermore, the mitogen activated protein kinase (MAPK) and phosphatidylinositol-3 kinase (PI3K) pathways can be activated via this chemokine to induce the expression of the adhesion molecules such as MAC-1 for efficient chemotaxis (Takami et al. 2002).

1.5 Immunometabolism of myeloid cells

1.5.1 Introduction

The field of immunometabolism, the study of intracellular metabolic control of immune responses, is a growing area of research after some seminal studies highlighted how interlinked metabolic pathways and immune regulation are. However, in the context of myeloid cells, this is by no means a new area of research. Indeed, polarised M1 and M2 macrophages were originally characterised by their distinct utilisation of arginine. M(LPS), M(IFN γ) or M1 polarised macrophages are well characterised as generating nitric oxide (NO) from arginine via inducible nitric oxide synthase (iNOS). In contrast, M(IL-4) or M2 macrophages generate ornithine via arginase-1 (Arg-1) (C. D. Mills et al. 2000). This finding epitomised how differential metabolic cascades can govern macrophage function. However, research interest in this field has only grown in more recent years.

1.5.2 Glycolysis

Glycolysis is a cytoplasmic metabolic pathway responsible for the conversion of glucose to pyruvate. This is a very inefficient mechanism of producing ATP, where only 2 ATP molecules are generated from 1 glucose molecule. Therefore, pyruvate enters the mitochondria and is converted into acetyl-CoA for the generation of more ATP through the tricarboxylic acid (TCA) cycle. In hypoxic conditions however, pyruvate is reduced to lactate as a by-product. The glycolytic pathway is illustrated in **Figure 1.5**.

Research has highlighted a number of links between glycolytic metabolites and enzymes with inflammatory cascades. For instance, studies in LPS activated murine macrophages has illustrated that glycolysis has an important role in the production of IL-1 β production, in a mechanism mediated by HIF-1 α and the accumulation of succinate (Tannahill et al. 2013) (**Figure 1.5**). Subsequent studies have shown that the glycolytic enzyme, pyruvate kinase muscle isozyme M2 (PKM2), enters a complex with HIF-1 α which in turn binds the IL-1 β promoter to increase its gene transcription (Palsson-McDermott et al. 2015). PKM2 is also thought to regulate the activation of the NLRP3 inflammasome by activating the

eukaryotic translation initiation factor 2 alpha kinase 2 (EIF2AK2) (Xie et al. 2016). Furthermore, inhibition of glycolysis is now thought to suppress macrophage migration both *in vitro* and *in vivo* in a process mediated by HIF-1 α (Semba et al. 2016). These results indicate an important role for HIF-1 α -mediated switching to glycolysis for the induction of inflammatory mechanisms in macrophages.

Upstream in the glycolytic pathway, the glycolytic activator 6-phosphofructo-2-kinase/fructose-2,6-biphosphatase 3 (PFKFB3) is thought to be an important mediator for the uptake of virally infected cells by macrophages (H. Jiang et al. 2016). In a regulatory role, glyceraldehyde 3-phosphate dehydrogenase (GAPDH) has been shown in primary human monocytes and macrophages to bind and repress TNF α mRNA translation when glycolysis is at a low state of flux. This phenomenon was reversed when glycolysis was increased or when GAPDH was knocked down, thereby increasing TNF α production (Millet et al. 2016). Other glycolytic enzymes, such as hexokinase, have also been shown to act as an innate immune receptor with the ability to activate the NLRP3 inflammasome for the production of IL-1 β and IL-18 (Wolf et al. 2016). Furthermore, cell surface expression of enolase has been observed to increase on monocytes and macrophages from RA patients. Antibodies against cell surface enolase promoted the production of TNF α , IL-1 α/β and IFN γ (Bae et al. 2012) (**Figure 1.5**).

Although the main train of thought with glycolysis is with pro-inflammatory cascades, it has been growingly associated with an immunoregulatory macrophage phenotype. For example, there has been a growing body of evidence supporting a role for glycolysis for the differentiation of M(IL-4) macrophages (Tan et al. 2015). Indeed, IL-4 induced AKT signalling has been shown to increase glucose uptake in alternatively activated macrophages for optimal IL-4 mediated gene transcription (Covarrubias et al. 2016). Separate work has suggested that the increased utilisation of glucose for M(IL-4) polarisation is mediated by the activation of the mTORC2/IRF4 pathway (S. C.-C. Huang et al. 2016). These studies highlight the complex role of the glycolytic pathway in macrophages, and how it can form the basis of pro-inflammatory and regulatory mechanisms.

In monocytes, glycolysis is considered to have a governing role in trained immunity. Trained immunity refers to the pre-programming of a cell so that has an amplified activatory profile upon re-stimulation. Studies assessing this phenomenon in a *candida albicans* trained immunity model with histone modification profiling, illustrated that trained monocytes displayed higher transcription of glycolytic genes and levels of aerobic glycolysis. The authors demonstrated that this was the result of the Warburg effect, which appeared to be mediated by an mTOR-HIF-1 α cascade (Cheng et al. 2014; Saeed et al. 2014).

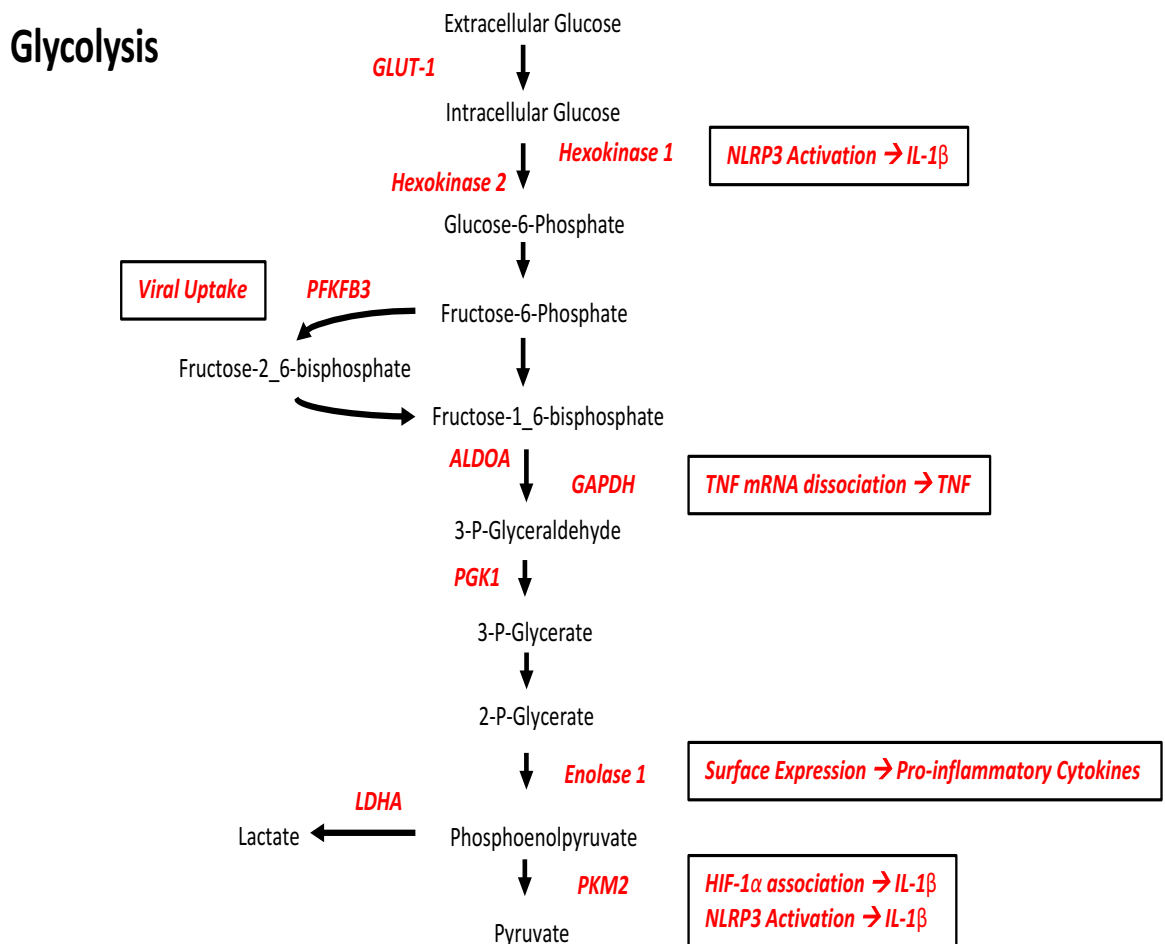


Figure 1.5 Glycolytic metabolism has an important role in M(LPS \pm IFN γ) macrophages. Schematic of glycolytic metabolism with intermediates in black and enzymes associated with immune metabolic functions in red. Boxed text describes the known immune functioning of each enzyme. Hexokinase and PKM2 are thought to promote IL-1 β production via NLRP3 inflammasome activation. PFKFB3 has been associated with viral uptake and clearance. GAPDH dissociates from TNF mRNA during high glycolytic flux, allowing its translation. Activation of cell surface enolase by antibodies promotes the release of inflammatory mediators such as TNF α , IFN γ and IL-1 α/β . Finally, PKM2 associates with HIF-1 α to promote IL-1 β release.

1.5.3 Tricarboxylic acid (TCA) cycle

The tricarboxylic acid (TCA) cycle is a vital aerobic metabolic pathway in the mitochondrial matrix for the production of ATP. This typically occurs from the oxidation of acetyl-CoA, which is generated from fatty acids, amino acids and carbohydrates (Akram 2014). The cycle and its intermediates are illustrated in **Figures 1.6 & 1.7**.

M(LPS + IFN γ) polarised macrophages exhibit a fragmented TCA cycle in comparison to their M(IL-4) counterparts, where it remains intact (Van den Bossche et al. 2017) (**Figures 1.6 & 1.7**). One of the TCA cycle breaks has been well characterised to initiate the accumulation of succinate, which has been published to enhance IL-1 β production by stabilising HIF-1 α (Tannahill et al. 2013). Inflammatory macrophages in murine models of RA have been shown to release and recycle succinate via the GPR91 receptor. Therefore, this intracellular store is thought to be as a result of both autocrine and paracrine mechanisms to perhaps act as an intracellular danger signal (Littlewood-Evans et al. 2016). Other work has noted that during LPS stimulation, macrophages show an increased mitochondrial membrane potential and mitochondrial oxidation of succinate through succinate dehydrogenase. Together, these processes are thought to induce the production of ROS and further IL-1 β . These studies highlight an important role for succinate in inflammation in macrophages (E. L. Mills et al. 2016) (**Figure 1.6**).

As well as succinate, another break point in the TCA cycle has been reported to occur during isocitrate conversion to α -ketoglutarate, which results in the accumulation of citrate in M(LPS + IFN γ) macrophages (Jha et al. 2015; O'Neill 2015) (**Figure 1.6**). Citrate accumulation has been reported to increase fatty acid synthesis which can promote the production of NO and prostaglandins (Infantino et al. 2014; Infantino et al. 2011) (**1.5.4 & Figure 1.6**). In addition to a build-up of citrate, studies have shown a reduction in the expression of the enzyme isocitrate dehydrogenase, which mediates the conversion of isocitrate to α -ketoglutarate. The same study observed an increased expression of immune-responsive gene 1 (IRG1), which mediates the cis-aconitate to itaconate reaction (Jha et al. 2015) (**Figure 1.6**). This suggests that citrate is directed for the production of itaconate in inflammatory macrophages. Itaconate has been

previously reported in macrophages to possess anti-microbial properties (Michelucci et al. 2013). Despite its anti-microbial role, itaconate has recently been shown to have anti-inflammatory properties, by possessing the ability to inhibit succinate dehydrogenase (SDH) activity and therefore regulate cellular succinate levels (Lampropoulou et al. 2016). This proposes that itaconate acts as a negative feedback to limit IL-1 β secretion through succinate. Furthermore, SDH has been recently implicated in the production of reactive oxygen species (ROS), highlighting the importance of itaconate to limit inflammatory responses in macrophages (E. L. Mills et al. 2016). Separate studies have shown that *in vivo* inhibition of SDH during bacterial insult reduces IL-1 β and increases IL-10 production from murine macrophages and thus impairs bacterial control. This work emphasises the importance of SDH in promoting inflammation (Garaude et al. 2016). Collectively, these reports highlight that TCA cycle breaks are a necessity in directing inflammatory cascades in macrophages in response to LPS + IFN γ polarising conditions.

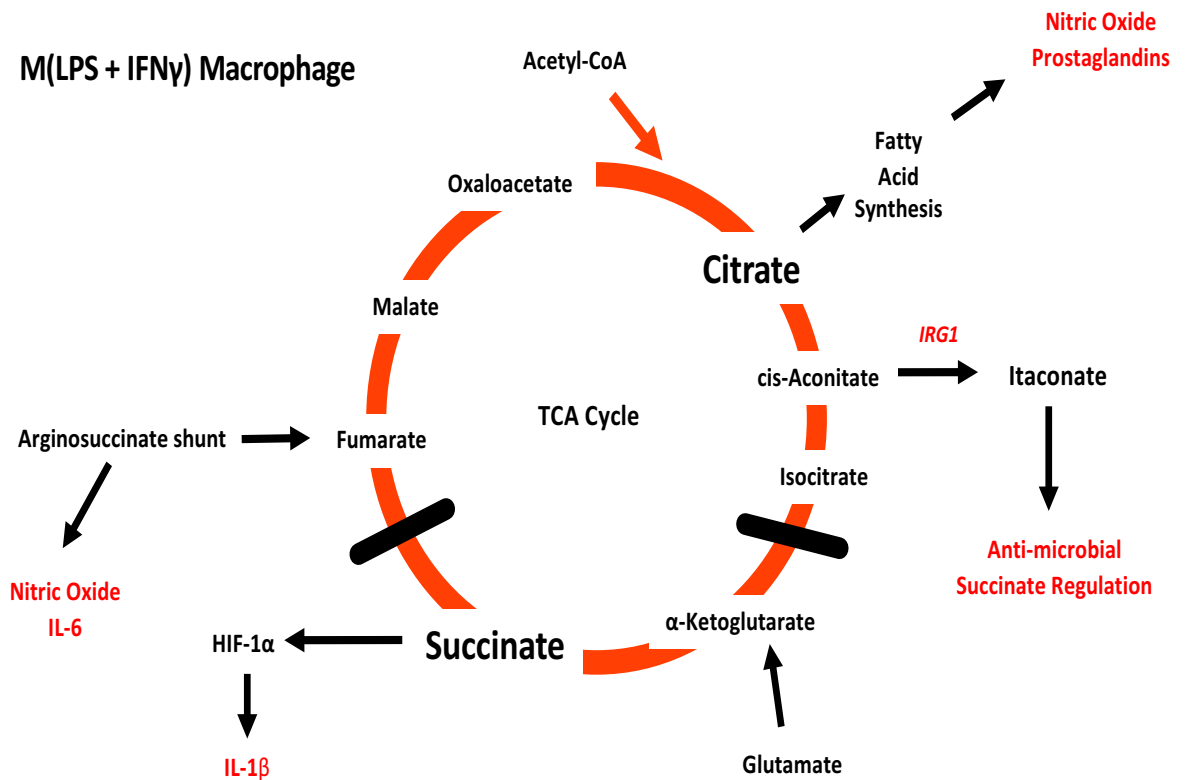


Figure 1.6 The TCA cycle is broken in classically activated macrophages. Inflammatory macrophages exhibit two breaks in the TCA Cycle. One occurs after isocitrate, which leads to citrate accumulation and the generation of Itaconate through cis-aconitate. This reaction is mediated by Immune-responsive gene 1 (IRG1). Itaconate possesses anti-microbial function and has been shown to regulate succinate levels in a regulatory manner. Furthermore, citrate accumulation has been shown to promote fatty acid synthesis for subsequent production of nitric oxide and prostaglandins. The second break occurs after succinate which promotes its build up. Its accumulation is thought to stabilise HIF-1 α for the production of IL-1 β . Glutamate and the argininosuccinate shunt are thought to replenish α -ketoglutarate and fumarate respectively. The argininosuccinate shunt is also thought to cause the production of nitric oxide and IL-6.

M(IL-4) Macrophage

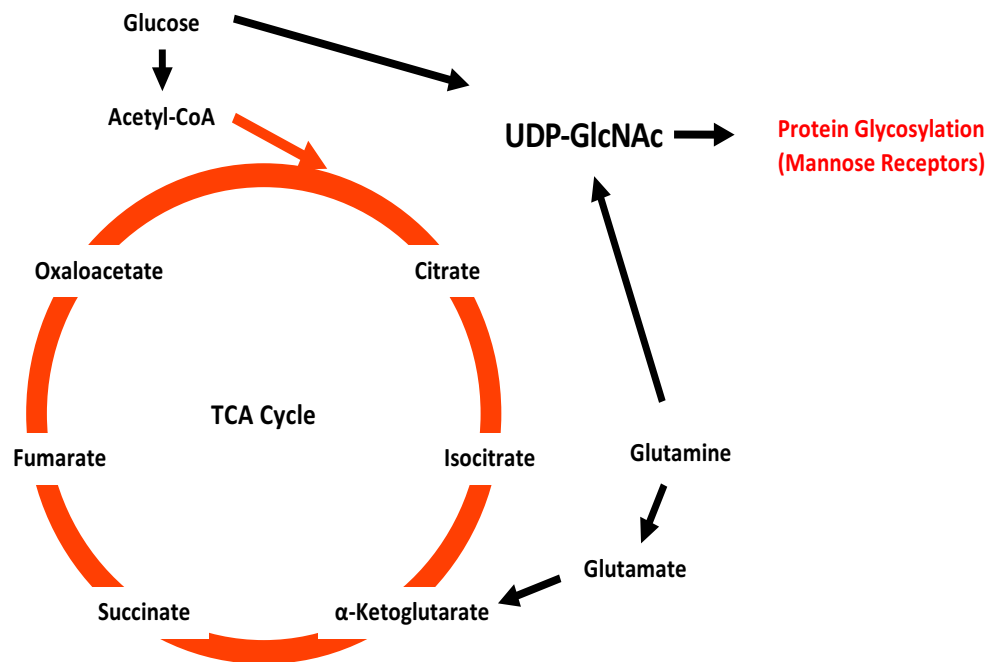


Figure 1.7 The TCA cycle remains intact in M(IL-4) macrophages. Unlike in inflammatory macrophages, IL-4 polarised macrophages display no breaks in the TCA cycle, which is replenished by glucose and glutamine. This however causes the increased utilisation of UDP-GlcNAc pathways which promotes glycosylation events, such as on scavenger receptors.

1.5.4 Fatty acid oxidation (FAO)

Fatty acid oxidation (FAO) typically refers to the process whereby fatty acids are oxidised to acetyl-CoA, which then enters the TCA cycle for the generation of ATP. Fatty acids can be intracellularly synthesised in the cytoplasm by acetyl-CoA and NADPH via the action of an enzymatic complex named fatty acid synthase. Fatty acid synthesis has been previously reported to be associated with M(LPS ± IFN γ) macrophages (Jha et al. 2015). Fatty acids can also be taken up from extracellular sources via scavenger receptors such as CD36 (Park 2014). Oxidation of fatty acids typically take place in the mitochondrial matrix. Therefore, fatty acids need to traffic from the cytoplasm. Long chain fatty acyl-CoA groups are transported by a carnitine shuttling system across the mitochondrial membrane (**Figure 1.8**) The fatty acid acyl group binds to free carnitine to form acylcarnitine by carnitine palmitoyltransferase 1 (CPT1), and is then trafficked into the inner mitochondrial membrane. The acyl group is then released into the mitochondrial matrix by CPT2 where it binds to a CoA group to

reform as an acyl-CoA (Houten & Wanders 2010). The long chain fatty acid (which varies in chain length) then undergoes a series of oxidation reactions to form acetyl-CoA.

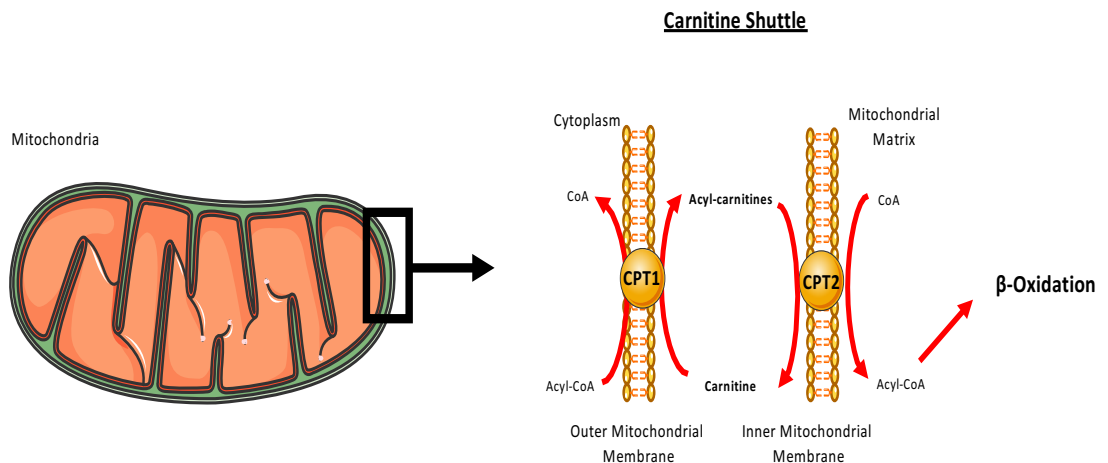


Figure 1.8 Carnitine shuttling into the mitochondria. Illustration of the mitochondrial membrane (right) within the boxed region of the whole mitochondria (left). Fatty acid acyl-CoA groups are trafficked by carnitines into the mitochondria for subsequent β -oxidation. Fatty acid acyl groups bind to free carnitine, prompting the release of CoA and the formation of acyl-carnitines. This enzymatic reaction is achieved through carnitinepalmitoyl transferase 1 (CPT1). The acyl group is then released from the carnitine and transferred to a free CoA group in the mitochondrial matrix in a mechanism mediated by CPT2. The carnitine is recycled for the trafficking of further acyl groups from the cytoplasm into the mitochondrial matrix. The acyl-CoA groups then undergo a series of oxidation reactions (β -Oxidation), and the end product, acetyl-CoA enters the TCA cycle.

The majority of research into fatty acid oxidation in myeloid cells has assessed its importance in macrophage polarisation. Initial microarray analysis attributed FAO in the polarisation of M(IL-4) or alternatively activated macrophages, which were reported to increase CD36 cell surface expression and gene expression of carnitine transferases. Furthermore, fatty acid uptake was noticeably increased under these conditions (Vats et al. 2006). More recent work identified that the fatty acids originated from triacylglycerol substrates after CD36 uptake and their lipolysis was important for the activation of M(IL-4) macrophages (S. C.-C. Huang et al. 2014). As previous studies were restricted to murine macrophages, Namgaladze and Brune tested if this was applicable to human macrophages. However, inhibition of FAO with etomoxir (ETO) appeared to have no impact on

IL-4 induced polarisation of human macrophages. IL-4 treatment itself did not appear to have any significant effect on CPT1 protein levels either (Namgaladze & Brüne 2014). Such findings promote increased debate of the translational capacity of murine studies into the human context (Seok et al. 2013; Takao & Miyakawa 2015). However, genetic ablation of CPT2 and FAO has been recently shown to have no effect on IL-4 mediated polarisation in bone marrow derived macrophages from mice (Nomura et al. 2016). Given the fact other work showed the inhibitory effect of ETO on IL-4 macrophage activation, this may suggest ETO could have off target effects. Nevertheless, increased glucose metabolism appears to have a role in M(IL-4) activation but the precise role of FAO in this process remains elusive (S. C.-C. Huang et al. 2016). A different approach assessed the role of the fatty acid transporter protein 1 (FATP1) in murine macrophages. The authors concluded that a loss of FATP1 promoted a glycolytic shift from FAO and supported a more pro-inflammatory phenotype in mouse adipose tissue macrophages, hinting at a regulatory role for fatty acid metabolism in macrophages (Johnson et al. 2016).

Given its association with regulatory M(IL-4) macrophages, the common train of thought in the field is that fatty acid metabolism is regulatory or anti-inflammatory. However, macrophage stimulation through the saturated fatty acid, palmitate, has been implicated in the production of IL-1 β release through the NLRP3 inflammasome. This suggests that its oxidation promotes an inflammatory cascade in macrophages (Wen et al. 2011). Furthermore, impairment of the utilisation of fatty acids prevents ROS production via oxidative phosphorylation and limits their bactericidal activity (C. J. Hall et al. 2013).

In somewhat contrast to the association of FAO with M(IL-4) macrophage metabolism, studies have linked fatty acid synthesis (FAS) with M(LPS) macrophage metabolism (Feingold et al. 2012; Jha et al. 2015). This also seems to be the case during M-CSF mediated differentiation of monocytes into macrophages, which exhibit increased levels of FAS and of genes associated with FAS, such as fatty acid synthase (FASN). Mechanistically, this was caused by the upregulation of sterol regulatory element-binding transcription factor 1c (SREBP1c) (Ecker et al. 2010). The role of FAS in inflammatory macrophages has

been linked to NLRP3 inflammasome activation via mitochondrial uncoupling protein 2 (UCP2) during murine sepsis (Moon et al. 2015). This work further highlights the complex nature of fatty acid metabolism and the opposing immune outcomes of fatty acid synthesis and oxidation.

1.5.5 Nucleotide metabolism

Nucleotide metabolism and their intermediates have a range of biochemical processes. For example, it forms the basis of ATP, the primary form of intracellular energy, and the precursors of DNA and RNA. Moreover, they are components of coenzymes such as CoA, NAD, and serve as intermediates in a range of biochemical pathways (Carver & Allan Walker 1995).

The role of nucleotide metabolism in immunological processes is relatively unknown in myeloid cells. However, it has been shown that purine intermediates, such as guanine, hypoxanthine and inosine are increased in LPS activated macrophages (Tannahill et al. 2013) (**Figure 1.9**). Furthermore, earlier studies indicated that adenosine may aid the metabolic switching to glycolytic metabolism in M(LPS) macrophages. Ligation of cell surface adenosine receptors such as A_{2A} and A_{2B} to adenosine on LPS activated macrophages can induce the expression of the glycolytic enzyme PFKFB3 (Ruiz-Garcia et al. 2011) (**Figure 1.9**). Despite its supposed role in promoting glycolysis, adenosine receptor signalling is thought to have a variety of anti-inflammatory functions, such as by suppressing TNF α , IL-12 and NO in monocytes and macrophages (Haskó & Pacher 2012) (**Figure 1.9**). Similar effects have been witnessed by a breakdown product of adenosine, inosine (IMP). Inosine has also been shown to reduce TNF α and in addition IL-1 production in LPS stimulated murine peritoneal macrophages (Haskó et al. 2000) (**Figure 1.9**). These studies may suggest that while nucleotides and their intermediates may promote or be indicative of an inflammatory metabolic program in macrophages, they could provide a negative feedback mechanism.

An important provider of nucleotides is the pentose phosphate pathway, which branches off the glycolytic pathway to divert intermediates for the production of nucleotides and amino acids during processes such as cell growth and proliferation. It also provides reducing equivalents of NADPH to maintain a

favourable cellular redox environment (Patra & Hay 2014). This pathway is largely thought to be upregulated in M(LPS) macrophages (Tannahill et al. 2013; Galvan-Pena & O'Neill 2014). Earlier studies illustrated that M(IL-4) macrophages upregulate expression of the sedoheptulose kinase termed carbohydrate kinase-like protein (CARKL). CARKL is thought to possess regulatory properties, as its expression switches macrophage phenotype to a more anti-inflammatory phenotype (Haschemi et al. 2012). Therefore, this pathway is likely to mediate the nucleotide pool to carry out both biochemical and perhaps immunological functions in inflammatory macrophages. However, further work is needed to fully elucidate such mechanisms.

Purine Metabolism

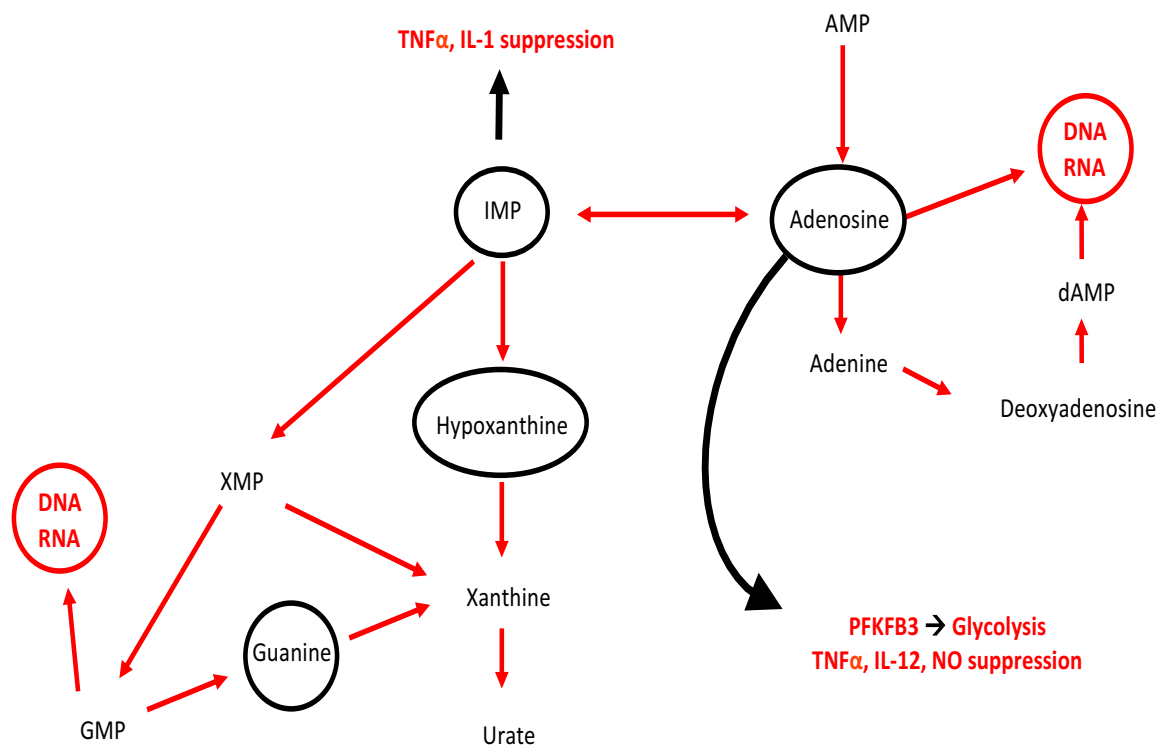


Figure 1.9 Overview of purine metabolism. Schematic of purine metabolism for the production of DNA and RNA (Red circles) or the degradation from hypoxanthine to urate. Black circled intermediates indicate those which have been published as being increased in inflammatory macrophages. Adenosine has been shown to induce the glycolytic enzyme PFKFB3 whilst also promoting suppressive effects when bound to adenosine receptors. Inosine (IMP) has been shown to have similar suppressive functions as adenosine in murine peritoneal macrophages.

1.5.6 Amino acid metabolism

Another area of immune-metabolic research is centred around the role of amino acids and their metabolism. One of the most studied amino acids in myeloid cell immunity is arginine. It has been known for a number of years that arginine is utilised differently in polarised M(LPS \pm IFN γ) and M(IL-4) macrophages. It is well characterised that M(LPS) macrophages generate NO and citrulline from arginine via iNOS. On the other hand, M(IL-4) macrophages generate ornithine through arginase activity, which implicates the urea cycle in M(IL-4) activation (C. D. Mills et al. 2000). Elsewhere in the urea cycle, arginine can be broken down for the production of creatine and creatinine. Both of which have been shown to promote a downregulation of a TLRs such as TLR-2, 3, 5 and 7 in RAW 264.7 macrophages (Leland et al. 2011). Therefore, distinct biochemical pathways from arginine can influence the inflammatory state of macrophages.

Glutamine represents another amino acid with a role in myeloid cell immunity. Early studies suggested that sufficient levels of glutamine are required for the production of both IL-1 and NO, the latter by entering into arginine metabolic pathways (Wallace & Keast 1992; Murphy & Newsholme 1998). Although this highlights a role for glutamine in inflammatory cascades in macrophages, more recent work has found that glutamine fluxes into the intact TCA cycle and uridine diphosphate N-acetylglucosamine (UDP-GlcNAc) biosynthetic pathways, which are essential for M(IL-4) macrophage activation (**Figure 1.7**). Indeed, glutamine deprivation experiments prevents CCL22 production, CD206, CD301 and Relma expression in IL-4 treated macrophages (Jha et al. 2015). In light of this work, glutamine metabolism can be argued to be associated with both inflammatory and regulatory type macrophages.

Taken together, amino acid metabolism represents one of many metabolic pathways which are interlinked with immunological cascades. The work in this thesis will aim to elucidate how an inflammatory disease microenvironment can influence immune-metabolic networks which can drive disease severity.

1.6 Aims

There is a growing body of research aimed at elucidating metabolic pathways that control of immunological cascades in monocytes and macrophages. However, the majority of studies utilise end polarised macrophages (typically M(LPS ± IFN γ) or M(IL-4)) and often in murine derived cells which have been shown to contain species differences compared to humans (Seok et al. 2013). Furthermore, experimental polarisation conditions reduce these studies relatability to chronic inflammatory disease settings in humans, such as RA and COPD.

Therefore, this thesis has set out to assess what impact the disease environment may have on the immune-metabolic functioning of monocytes in chronic inflammatory disease. Inflammatory diseases are characteristically hypoxic sites, therefore monocytes have to not only adapt to environmental pressure at a metabolic level, but carry out appropriate effector function in response to stimuli when they are recruited to the tissue. The studies addressed here will aim to carry out metabolomics analysis of monocytes cultured under hypoxic conditions and stimulated with RA synovial fluid. By conducting functional analysis of monocytes under the same conditions, the importance of altered metabolic pathways will be determined by pharmacological investigation.

This work aims to:

1. Metabolically profile monocytes cultured under short term hypoxia to identify hypoxia specific metabolic pathways.
2. Functionally profile monocytes cultured under short term hypoxia and LPS stimulation to identify functional characteristics altered in hypoxia.
3. Pharmacologically inhibit or promote altered metabolic pathways to assess their impact, if any, on monocyte functionality.
4. Analyse the metabolome, function and metabolically manipulate monocytes cultured under hypoxia and synovial fluid from an RA patient.

5. Assess if the findings from monocytes are translated into human alveolar macrophages.

Chapter 2. Materials and Methods

2.1 Human samples, patients and controls

Buffy coats from the Scottish National Blood Transfusion Service (SNBTS) and peripheral blood from healthy volunteers was used as a source of monocytes. Synovial fluid was obtained from active rheumatoid arthritis (RA) patients, which were identified from Rheumatology clinics in Glasgow Royal Infirmary and fulfilled the 2010 ACR/EULAR criteria for RA. Lung resection tissue was obtained from lobectomy procedures from the Sahlgrenska University Hospital, Gothenburg, Sweden. Tissue was derived from lung cancer, transplant or patients with Chronic Obstructive Pulmonary Disorder (COPD) with variable smoking status. All samples were obtained after written consent, with the appropriate ethical approvals in place.

2.2 Primary human cell culture

2.2.1 Isolation of peripheral blood mononuclear cells (PBMCs)

Peripheral blood mononuclear cells (PBMCs) were separated from human buffy coats provided by the SNBTS or from peripheral blood from healthy volunteers by density gradient centrifugation. Human blood from the SNBTS was diluted 1:1 in sterile DPBS (Gibco, Thermo Fisher), while peripheral blood was left undiluted. In 15ml centrifuge tubes, 8ml of blood was carefully layered on top of 3ml of Ficoll® Paque Plus (Sigma-Aldrich). This was centrifuged at 400g for 30 minutes, at room temperature (RT) with no brake. The buffy coat layer containing PBMCs was harvested into 50ml centrifuge tubes. The PBMCs were washed once in sterile DPBS at 300g for 10 minutes, with full brake, and a second time at 200g for 10 minutes to remove platelets. The cells were re-suspended in 10ml of cell separation buffer (DPBS containing 2% Fetal Bovine Serum (FBS; Invitrogen), 1mM EDTA). To count and evaluate viability, the PBMCs were assessed by trypan blue exclusion. 50µl of cells were diluted in 200µl of DPBS and 50µl of this cell suspension was mixed in 50µl of trypan blue (Sigma-Aldrich), giving a total 10x dilution. 10µl of this suspension was loaded onto a haemocytometer and viable cells were counted under light microscopy. For direct analysis, the PBMCs were re-suspended at a density of 1×10^6 /ml in RPMI 1640 (Gibco, Thermo Fisher)

containing 10% FBS, 2mM L-glutamine (Sigma-Aldrich) and 1% pen-strep (Sigma-Aldrich). For monocyte enrichment, the PBMCs were re-suspended at 5×10^7 /ml in cell separation buffer.

2.2.2 Monocyte enrichment from PBMCs

To enrich the monocyte population from the PBMCs, the EasySep monocyte enrichment kit, without CD16 depletion (StemCell Technologies), was used. It is assumed that monocytes constitute approximately 10-20% of total PBMCs. From this estimation, an appropriate volume of PBMCs (at a cell density of 5×10^7 /ml in cell separation buffer) was transferred to capped 6ml polystyrene tubes (BD Falcon). The antibody cocktail was added to the cell suspension at 50 μ l/ml and the tubes were incubated at 4°C for 10 minutes. Thereafter, magnetic beads were vortexed for 30 seconds and added to the cell suspension at 50 μ l/ml. The tubes were incubated at 4°C for 5 minutes. The tubes were topped up with cell separation buffer to a final volume of 2.5ml. The tubes were placed into an EasySep™ Magnet (StemCell Technologies) for 2.5 minutes. Afterwards, the magnet containing the tubes, was inverted into a fresh centrifuge tube to collect the negatively selected cells. 50 μ l of the negatively selected cells were added to 50 μ l of trypan blue (giving a total 2x dilution) and viable cells were counted by a haemocytometer under a light microscope. The enriched monocytes were centrifuged at 300g for 5 minutes and re-suspended at a density of 1×10^6 /ml in monocyte medium (RPMI 1640 containing 10% Human Pooled Plasma (BioWest), 2mM L-glutamine, 1% pen-strep) unless otherwise stated.

2.2.3 Stimulation of human monocytes

Human monocytes were stimulated with 10ng/ml LPS-EK ultrapure (Invivogen) unless otherwise stated. For synovial fluid experiments, monocytes were treated with media containing 5% or 10% synovial fluid from active RA patients. For metabolic manipulation, monocytes were treated with 10mM L-carnitine (Sigma-Aldrich) simultaneously with LPS or RA synovial fluid unless otherwise stated. Monocytes were pre-treated for 1 hour with etomoxir (ETO; Sigma-Aldrich) at 50 μ g/ml or 2-Deoxyglucose (2-DG; Sigma-Aldrich) at 3mM. PMA (Abcam) was used at a concentration of 10ng/ml. Dimethylxalyglycine (DMOG; Sigma-Aldrich) was used at a concentration of 100 μ M and 1mM.

2.2.4 Human alveolar macrophage (AM) isolation

Human lung tissue was transported to the laboratory at 4°C in transport medium (DMEM, 10% FBS, 2% antibiotic-antimycotic (Invitrogen), 2% non-essential amino acids (NEAAs; Invitrogen)). The tissue was placed in a large petri dish, and was flushed extensively with sterile DPBS using a 19-gauge needle. This process was repeated until no more cells were flushed out and the DPBS ran clear. The cell suspension was harvested and transferred into 50ml centrifuge tubes. The tubes were centrifuged at 300g for 10 minutes and the cells were pooled. The white blood cells (WBC) were counted using an automatic haematological analyser (Sysmex). The WBCs were re-suspended at a density 2×10^6 /ml in serum-free phenol red-free RPMI (Gibco, Thermo Fisher). The WBCs were plated in Costar® (Corning®) tissue culture treated plate, typically 500µl in 24 well plates. The cells were allowed to rest for 1 hour at 37°C to allow macrophage adherence. Non-adherent cells were gently removed by washing at least 3 times in serum-free phenol-red free RPMI. After the final wash, the cells were allowed to rest overnight in X-Vivo™ 10 media (Lonza) supplemented with 2mM L-glutamine and 1% pen-strep.

2.2.5 Polarisation and treatment of alveolar macrophages

Alveolar macrophages were polarised to an M0 (control), M(LPS ± IFNγ) (pro-inflammatory macrophage) or M(IL-4) (anti-inflammatory macrophage) phenotype. Macrophages treated with media alone (X-Vivo™ 10) are referred to as M0. Macrophages treated with 100ng/ml LPS (Sigma-Aldrich) and 20ng/ml IFNγ (Peprotech) for 24 hours are referred to as M(LPS ± IFNγ). Macrophages treated with 200ng/ml IL-4 (Peprotech) for 24 hours are referred to as M(IL-4). For metabolic manipulation, the cells were treated with L-carnitine and ETO in the same manner as in 2.2.3.

2.3 Culture of cell lines

2.3.1 Culture and treatment of Raji cells

Raji cells (Burkitt's Lymphoma; B lymphocyte cell line) were a kind gift from Mark Williams. Aliquots of Raji cells were frozen at -80°C in BAMBANKER™ solution (Wako Chemicals) in screw-capped vials at a density of 1×10^6 /ml. For

recovery, the cells were thawed in a 37°C water bath and were re-suspended in 5ml of growth media (RPMI 1640 with 10% FBS, 2mM L-glutamine and 1% pen-strep). The cells were centrifuged at 300g for 5 min and re-suspended in 15ml of fresh medium. The cells were transferred to a 75cm² tissue culture flask (Corning®) which was placed in an incubator at 37°C with 5% CO₂. The medium was changed every 2 to 3 days and the cells were sub-cultured at a 1:10 ratio when they reached a cell density of 3x10⁶/ml. To sub-culture, the cell suspension was transferred to centrifuge tubes and centrifuged at 300g for 5 minutes. The cells were re-suspended in 10ml of fresh growth medium and viable cells were counted using trypan blue (2.2.1). 3x10⁵ viable cells were transferred to a new 75cm² tissue culture flask in an upright position. For treatment of the Raji cells, cobalt chloride (CoCl₂: Sigma-Aldrich) was used at 30µg/ml and 70µg/ml.

2.3.2 Culture of Caco-2 cells

Caco-2 cells (human colorectal adenocarcinoma epithelial cells) were purchased from ATCC® (HTB-37™). The cells were cultured as per manufacturer's instructions. For recovery, the cells were thawed in the vial in a 37°C water bath and transferred to a centrifuge tube. The cells were centrifuged at 300g for 5 minutes and re-suspended in growth medium (DMEM (Gibco, Thermo Fisher) with 10% FBS, 1% Pen-Strep, 2mM L-glutamine, 1% NEAA and 15mM HEPES (pH 7.4)). The cells were counted by trypan blue exclusion under light microscopy (2.2.1) and were seeded into a 75cm² tissue culture flask at a cell density of 1x10⁴/cm² or 5x10⁴/ml. The cells were sub-cultured when they reached a confluency of approximately 80%. To sub-culture the cells, the medium was aspirated from the culture vessel and discarded. The cell monolayer was rinsed briefly with 0.25% (w/v) trypsin-EDTA solution (Sigma-Aldrich) to remove traces of serum, which contains trypsin inhibitor. 3ml of fresh 0.25% trypsin-EDTA solution was added to the monolayer, and the cells were then incubated for 5 minutes at 37°C to aid detachment from the surface. The cells were then placed under an inverted light microscope and observed until full detachment. 7ml of fresh growth medium was added to the vessel and cells were transferred to a centrifuge tube. The cells were centrifuged at 300g for 5 minutes, re-suspended in fresh growth medium and sub-cultured at a 1:6 ratio. Medium was renewed every 3-4 days. For scratch assays (2.6.1) the cells were seeded and grown to

confluence in 12 well tissue culture treated plates (Corning®). For long term storage, cells were re-suspended at a density of 1×10^6 /ml in BAMBANKER™ solution and kept at -80°C .

2.3.3 Culture of HUVECs

Human umbilical cord vein endothelial cells (HUVECs) were a kind gift from Jonathan Noonan. Aliquots of HUVECs were frozen at -80°C in BAMBANKER™ solution in screw-capped vials and were thawed in a 37°C water bath. The cells were transferred from the storage vial into a 75cm^2 tissue culture flask containing 15ml of growth medium (Endothelial cell media with SupplementMix; PromoCell). The cells were allowed to adhere overnight and the medium was changed to remove traces of BAMBANKER™ solution. The HUVECs were sub-cultured when they reached a confluency of approximately 80%. To sub-culture, the cells were detached with 0.25% trypsin-EDTA solution in the same manner as in 2.3.2. The cells were transferred to centrifuge tubes, centrifuged at 220g for 5 minutes and re-suspended in 2ml of growth medium for counting by trypan blue. The cells were inoculated into new culture vessels at a density of $5 \times 10^3/\text{cm}^2$ or 2.5×10^4 /ml. Medium was changed every 2 days and cells were not grown beyond passage 12. For long term storage, cells were re-suspended at a density of 1×10^6 /ml in BAMBANKER™ solution and kept at -80°C .

2.4 Induction of Hypoxia

2.4.1 Induction of 5% oxygen

Hypoxia was induced *in vitro* at oxygen (O_2) tensions of 5%, 2.3% and 1%. For the induction of 5% and 2.3% O_2 , a Heraeus HERA cell 150 tissue culture incubator with O_2 control (Thermo Fisher) was used. The incubator was set to 37°C , 5% CO_2 and 5% or 2.3% O_2 by using its digital control panel. To flush out and maintain low oxygen tension, the incubator was connected to a nitrogen (oxygen-free) 230 bar W sized gas cylinder purchased from the British Oxygen Company (BOC).

2.4.2 Induction of 1% oxygen

For the induction of 1% O₂, a hypoxic chamber (with its associated single-flow meter) was purchased from Billups-Rothenburg. Cell culture plates were placed inside the chamber which was clamped closed and kept airtight. The chamber was then purged with a speciality gas mixture purchased from BOC, containing 1% O₂, 5% CO₂ and N₂ balance (with an uncertainty of \pm 1% of each gas component), through an inlet port at a flow rate of 40L per minute, for 3 minutes. The inlet and outlet port was sealed closed and the chamber was placed in a standard tissue culture incubator set to 37°C.

2.5 Western Blotting

2.5.1 Cell lysis (RIPA buffer)

To generate cell lysates from monocytes for subsequent Western Blot analysis, a RIPA buffer-based lysis method was carried out. Cells were aspirated from the tissue culture well and transferred to an ice-cold microcentrifuge tube. The well was flushed with ice cold DPBS to remove any adherent cells, which was also transferred to the same tube. The tubes were centrifuged at 300g for 5 minutes to pellet the cells, which were then washed twice in ice-cold DPBS (300g for 5 minute centrifugations). Meanwhile, protease and phosphatase inhibitors (Thermo Fisher) were added to the RIPA lysis buffer (Thermo Fisher) immediately before use, at a concentration of 10 μ l/ml. After the final wash, ice-cold RIPA Buffer was added directly to the cell pellet to lyse the cells, at a concentration of 20 μ l per 1x10⁶ cells. The samples were incubated on ice with intermittent vortexing for 20 minutes. The samples were then centrifuged at 17,000g for 10 minutes to pellet cellular debris. The supernatants were stored at -80°C until Western Blot analysis.

2.5.2 Cell lysis (Laemmli buffer)

An alternative direct lysis method protocol was used to generate lysates for Western Blot analysis. The cells were harvested from the culture well and washed as described in 2.5.1. β -Mercaptoethanol (Sigma-Aldrich), which acts as a reducing agent of protein disulphide bonds, was added to 2x Laemmli Sample Buffer (Bio-Rad) to a final concentration of 5%. This sample buffer was added

directly to the cell pellet at a concentration of 20 μ l per 1x10⁶ cells. The samples were incubated on ice and vortexed intermittently for 20 minutes. When necessary, the samples were sonicated to shear DNA and reduce viscosity. The samples were then boiled at 95°C for 5 minutes to denature the proteins. The samples were subsequently stored at -80°C until Western Blot analysis.

2.5.3 Protein quantification

To ensure equal loading of protein lysates prior to Western Blotting, the RIPA buffer lysates were normalised by protein concentration. To determine the protein concentration in the samples, the Bradford assay method was used. 5x Bio-Rad protein assay (Bradford) reagent was diluted to 1x with distilled water (dH₂O). To generate the standard curve, a 1.5mg/ml BSA (Sigma-Aldrich) standard solution in 1x PBS was made. 1ml of 1x protein assay reagent was aliquoted into microcentrifuge tubes. A range of standards was prepared from a 1.5 μ g/ml lower standard to a 15 μ g/ml top standard by adding 1 μ l and 10 μ l of BSA standard solution respectively into the appropriate microcentrifuge tube. 1 μ l of sample of unknown concentration was added to a microcentrifuge tube containing 1ml of protein assay reagent. A blank sample was made by adding 1 μ l of lysis buffer to 1ml of protein assay reagent. All tubes were vortexed briefly and 200 μ l of each standard and sample was pipetted in triplicate into a 96 well plate. The absorbance was read on a Tecan Sunrise microplate reader at 595nm. The final concentration of the unknown sample was determined by using a log-parameter curve fit in Excel and taking into account the original dilution. Laemmli buffer is incompatible with the Bradford assay, due to its bromophenol blue content. The protein content of samples in Laemmli buffer was estimated by a NanoDrop™ 2000/2000c Spectrophotometer (Thermo Fisher) using the Protein 280nm method.

2.5.4 Protein denaturation

To prepare RIPA buffer lysates for denaturing before gel electrophoresis, 4x NuPAGE® LDS Sample Buffer (Thermo Fisher) was added to the samples to bring the overall concentration to 1x. The sample buffer contains lithium dodecyl sulfate, which aids the reducing agent to denature and reduce protein disulphide bonds. 10x NuPAGE™ Sample Reducing Agent (Thermo Fisher) was added to the

sample and LDS sample buffer solution to a final 1x concentration. The samples containing LDS sample buffer and reducing agent were boiled at 95 °C for 5 minutes. Lysates prepared using the direct lysis method in Laemmli buffer did not require any further denaturing step.

2.5.5 Protein gel electrophoresis

Protein gel electrophoresis was carried out using the XCell *SureLock*® Mini-Cell (Thermo Fisher) apparatus and a NuPAGE pre-cast 4-12% Bis-Tris Gel (Thermo Fisher). The gel was removed from its packaging, storage solution was rinsed off with H₂O and the tape covering the slot on the back of the gel cassette was peeled off. The apparatus was assembled as follows: pre-cast gel at the front with notch facing inwards; buffer code in centre with negative electrode slotting into the gold plate; buffer dam behind the buffer code and then the lock. 20x NuPAGE® MOPS SDS running buffer (Thermo Fisher) was diluted in dH₂O to 1x (500ml total volume needed) and was loaded into the inner chamber (between gel and buffer code) and allowed to overflow. The comb was gently removed from the gel and 10µg of sample protein (unless otherwise stated) was loaded by using elongated pipette tips into each well. 10µl of BenchMark™ Pre-stained Protein Ladder (Thermo Fisher) was added to the first well as a reference. The apparatus was connected to an electrophotometer (red to the (+) jack and black to (-) jack) and was run at 120V until the samples migrated to the bottom.

2.5.6 Gel transfer to PVDF membrane

When the electrophoresis had ended, the gel cassette was removed from the apparatus and the gel was removed from the cassette by using a gel knife. The gel was cut to size and transferred into dH₂O. Transfer of the proteins from the gel to a PVDF membrane was carried out using an iBlot® Dry Blotting System and the associated iBlot® Transfer Stack apparatus (Thermo Fisher). The bottom anode stack was inserted into the tray and the gel was placed on top of the transfer membrane. Pre-wetted filter paper (in dH₂O) was placed on top of the gel and bubbles were removed by rolling the assembly with the iBlot roller. The top cathode stack was placed on top and the assembly was rolled again. The sponge was placed into the tray in the lid of the iBlot system and the lid was closed. The proteins were transferred to the PVDF membrane using the default

programme P3 at 20V for 7 minutes. When the programme had finished, the PVDF membrane was stained briefly with Ponceau S (Sigma-Aldrich) to ensure a uniform transfer.

2.5.7 Probing

The Ponceau S stain was washed off the membrane in PBS-T (1x PBS, 0.1% Tween™ 20 (Sigma-Aldrich)) and the membrane was then blocked in blocking buffer (PBS-T, 5% non-fat dried milk (Marvel)) for 1 hour at RT. The membrane was incubated overnight at 4°C in primary antibody with rocking. When probing for HIF-1 α , the membrane was cut at 55kDa (using protein ladder as reference) so HIF-1 α (predicted weight: 120kDa) and GAPDH (predicted weight: 37kDa) housekeeping could be probed simultaneously. The primary antibody was aspirated and washed 3 times in PBS-T (10 minutes per wash). The membrane was incubated in secondary antibody for 1 hour at RT. The secondary antibody was aspirated and the membrane was washed 4 times in PBS-T. To visualise the detected bands, the membrane was incubated in WestPico or WestFemto substrate solution (to increase sensitivity; Thermo Fisher) for 3 minutes. The solution was poured off, the membranes were air-dried briefly and wrapped in cling film. The membranes were visualised by chemiluminescent detection using an Azure Biosystems c500 Western Blot imaging system.

2.5.8 Western Blot antibodies

The following antibodies were used for Western Blot analysis: Rabbit anti-human HIF-1 α primary antibody (Cell Signalling Technologies (CST)); Mouse anti-human HIF-1 α primary antibody (BD Transduction Laboratories); GAPDH XP® Rabbit primary antibody (CST); Anti-rabbit IgG, HRP-linked secondary antibody (CST); Rabbit polyclonal anti-mouse IgG HRP (Abcam) secondary antibody; Polyclonal goat anti-mouse IgG HRP (Dako). The antibodies used are noted in **Table 2.1**.

Table 2.1 Western Blot antibodies

Target	Antibody	Reactivity	Supplier	Dilution	Buffer (in PBS-T)
HIF-1 α	Primary	Human	CST	1:1000	5% BSA
HIF-1 α	Primary	Human	BD	1:750	5% Milk
GAPDH	Primary	Human	CST	1:1000	5% BSA
Rabbit-IgG	Secondary	Rabbit	CST	1:1000	5% Milk
Mouse-IgG	Secondary	Mouse	Abcam	1:2000	5% Milk
Mouse-IgG	Secondary	Mouse	Dako	1:2000	5% Milk

2.6 Cellular assays

2.6.1 Wound healing scratch assay

Wound healing (scratch) assays were performed on monolayers of Caco-2 cells and HUVECs, which were cultured as described in sections 2.3.2 and 2.3.3 respectively. Both cell types were seeded and grown to confluence in 12 well tissue culture plates (Corning®). Upon confluency, the cells were serum-starved for 24 hours by culturing in growth medium depleted in serum. The monolayers were scratched using a sterile P10 pipette tip. The monolayer was washed twice in growth medium to remove detached cells. As an alternative protocol, to obtain a more consistent area for cells to migrate, IBIDI culture inserts (2 well in μ -dish, 35mm) were used. Cells were seeded and grown to confluence in each chamber of the silicone culture insert. Using a pair of sterile tweezers, the silicone insert was removed from the surface of the dish to create a uniform, 500 μ m gap for migration. In both protocols, 2.5×10^5 human monocytes were then plated in each well or dish on top of the monolayer in monocyte medium (2.2.2). Still images (using an EVOS Cell Imaging System (Thermo Fisher)) of the scratched area were taken immediately at 0 hours and at 4 and 16 hours after culture in normoxic and hypoxic conditions. The scratched areas were drawn and measured using Image J software and the percentage wound closure was calculated, using the area measured at 0 hours as a reference.

2.6.2 Cellular adherence assay

Cellular adherence of monocytes was evaluated using crystal violet staining. Human monocytes were seeded in 96 well tissue culture plates at 2×10^5 cells/well and were cultured under normoxic or hypoxic conditions for 4 hours.

Non-adherent cells were removed by washing the wells with 200µl of 1x PBS. The cells were fixed by adding 50µl of 96% ethanol (EtOH) for 10 minutes at RT. The wells were washed twice by submersing the plates in a beaker containing dH₂O. The plates were allowed to air dry. The cells were stained with 100µl of 0.5% crystal violet (Active Motif) in 2% EtOH for 15 minutes at RT. Excess stain was washed off in dH₂O and plates were left to air dry. The stain was solubilised by adding 100µl of 1% SDS (Sigma-Aldrich) and the plates were shaken until the colour became uniform. The absorbance was read at 570nm by using a Tecan Sunrise microplate reader.

2.6.3 MTT assay

Untreated and treated monocytes were seeded in 96 well tissue culture plates at a cell density of 1×10^6 /ml, 100µl per well. Thiazoyl blue tetrazolium bromide (MTT) salt (Sigma-Aldrich) stock solution was prepared in 1x PBS at 6mg/ml. 10µl of the stock solution was added to each well, mixed briefly, and the cells were incubated at 37°C for 3 hours. During this time, metabolically active cells metabolise the salt and produce purple formazan crystals as a by-product. After incubation, the media was aspirated and the wells were left to air dry. The formazan crystals were solubilised by adding 100µl of 100% dimethylsulfoxide (DMSO; Sigma-Aldrich). The plate was placed on a shaker at RT until the crystals were fully dissolved. The absorbance was read at 550nm (650nm reference) by using a Tecan Sunrise microplate reader.

2.7 Supernatant assessment

2.7.1 Sample harvest

The cell culture supernatant was harvested to assess the levels of cytokines, chemokines and lactate secreted by cells in culture. The cell culture plates were removed from the incubator and centrifuged at 400g for 5 minutes to pellet cells and debris. The cell-free supernatant was carefully pipetted into microcentrifuge tubes or aliquoted into 96 well plates, which were wrapped in parafilm. The supernatants were stored at $\leq -20^\circ\text{C}$ until analysis.

2.7.2 Enzyme-linked immunosorbent assay (ELISA)

ELISAs were performed using manufacturer's instructions, which were specific to each kit and supplier. Suppliers used were Life Technologies (LT) and R&D Systems (R&D). All ELISAs were performed using high binding, half well, 96 well ELISA plates (Corning®) using DuoSet kits. The plates were coated overnight in capture antibody (50µl/well) diluted in 1x PBS at either 4°C (LT) or RT (R&D). The capture antibody was aspirated and the plates were washed once (LT) or 3 times (R&D) in PBS-T ELISA wash buffer (1x PBS, 0.05% Tween™ 20). The plates were blocked for 1 hour at RT to prevent non-specific antibody binding by adding 150µl/well of assay buffer (1x PBS, 5% BSA, 0.1% Tween™ 20, 0.5% ProClin™ 300 (Sigma-Aldrich)). Meanwhile, the standards were made by serial dilution and the samples were diluted as appropriate in assay buffer. In kits supplied by LT, the assay buffer was aspirated and 50µl of standards and samples were added to the plate. 25µl of detection antibody (diluted in assay buffer) was then added and the plates were left on a shaker at RT for 2 hours. In kits supplied by R&D, the assay buffer was aspirated and the plates were washed 3 times in wash buffer. 50µl of standards and samples were added and the plates were left on a shaker at RT for 2 hours. The standards and samples were aspirated, the plates washed a further 3 times and 50µl of detection antibody (diluted in assay buffer) was added. The plates were left on a shaker at RT for 2 hours. In both kits, after the incubation in detection antibody, the plates were aspirated and washed 5 times (LT) or 3 times (R&D) in wash buffer. 50µl of streptavidin-HRP (diluted in assay buffer) was added to each well and the plates were left on a shaker for 30 minutes (LT) or 20 minutes (R&D). The plates were aspirated and washed 5 times (LT) or 3 times (R&D) in wash buffer. In both kit suppliers, 50µl of tetramethylbenzidine (TMB) substrate solution (eBioscience) was added until a blue colour developed in the standards (plates were incubated in the dark). Once the standards were suitably developed to give a standard curve, 50µl of stop solution (2N sulphuric acid (H₂SO₄)) was added to each well to prevent any further development. The plates were read using a Tecan Sunrise microplate reader at 450nm (650nm reference). The data was exported to Excel and a standard curve was generated. The concentrations of the samples were calculated using the equation of the straight line. Samples which fell out-with the standard curve were re-run on the assay with an adjusted dilution. Samples

which were detected below the lowest standard were deemed non-detectable. The ELISA kits used are outlined in Table 2.2.

Table 2.2 ELISA kits

Cytokine/Chemokine	Species	Supplier	Detection Range
IL-1 β	Human	Life Technologies	31.24-2000pg/ml
IL-6	Human	Life Technologies	15.62-1000pg/ml
IL-8	Human	Life Technologies	15.62-1000pg/ml
TNF α	Human	Life Technologies	15.62-1000pg/ml
CCL20	Human	R&D Systems	15.62-1000pg/ml

2.7.3 Meso-Scale Discovery (MSD)

The following assays were used from MSD: V-PLEX Pro-inflammatory Panel 1 (human); Custom U-PLEX Pro-inflammatory Panel (IL-8, TNF α , IL-1 β , IL-6 (human)); Custom U-PLEX Chemokine Panel (CCL17, CCL22 (human)). All reagents were thawed and brought to RT. The calibrator (MSD standard) was reconstituted in Diluent 2 (Pro-inflammatory Panels) or Diluent 43 (Chemokine Panel) and serial dilutions were created for the standard curve. Samples were diluted as appropriate in Diluent 2 (Pro-inflammatory Panels) or Diluent 43 (Chemokine Panel). The calibrators and samples were added to each well (50 μ l/well) of the pre-coated MSD plates, and were shaken at RT for 2 hours. The plates were aspirated and washed 3 times in ELISA wash buffer. For pro-inflammatory panels, the detection antibody solution was created by combining 60 μ l of detection antibody of each analyte and then topping up to 3ml in Diluent 3. In the chemokine panel, the solution was topped up to 6ml in Diluent 3. 25 μ l (pro-inflammatory panel) or 50 μ l (chemokine panel) of detection antibody (conjugated to SULFO-TAG electrochemiluminescent (ECL) labels) was added to each well and the plates were incubated for 2 hours on a shaker. The detection antibody was aspirated and the plates were washed a further 3 times. 150 μ l of MSD Read Buffer T (diluted from 4x to 2x in dH₂O) was added to each well and the plates were read on either a MESO QuickPlex SQ 120 (MSD) or a MESO SECTOR S 600 (MSD) Imager. The imagers measure the light emission from the SULFO-TAG labels by passing an electrical current through the plate electrodes, giving an ECL reading. Using Discovery Workbench 4.0 (MSD) software, the ECL signals of each analyte in the samples and standards were converted to their

corresponding concentrations (pg/ml). The concentrations of the unknown samples which fell on the standard curve were extrapolated.

2.7.4 Lactate assay

Extracellular lactate concentrations were tested by using a Lactate Assay Kit (Abcam). All samples and reagents were brought to RT. Cell supernatants were diluted 1:10 in lactate assay buffer and the L-lactate standard was diluted from 100mM to 1mM in lactate assay buffer. 50µl of standards (standard curve range from 0-10 nM/well) and diluted samples were added to a 96 well plate. 50µl of the reaction mix (46µl lactate assay buffer, 2µl substrate mix, 2µl enzyme mix) was added onto the samples and standards. 50µl of a background reaction mix (48µl lactate assay buffer, 2µl substrate mix) was added to control wells. The plates were placed on a shaker and incubated at RT for ≤30 minutes for the colour reaction to occur. The absorbance was measured at 450nm by using a Tecan Sunrise microplate reader. The final OD reading was calculated by subtracting the OD from a medium alone blank and again from the background reaction mix reading. The concentration in the test sample was calculated by extrapolating the unknown sample concentration against the standard curve. The final concentration was calculated using the following equation.

$$\text{Lactate Concentration} = \left(\frac{La}{Sv} \right) * D$$

La = Lactate concentration in sample well calculated from standard curve (nmol)

Sv = Volume of sample added into the well

D = Sample dilution factor

2.8 Flow cytometry (FACS)

2.8.1 Cell surface staining

For FACS analysis, cell surface staining was performed to evaluate the cell purity of human monocytes before and after enrichment from PBMCs, as described in 2.2.2. Typically, 1×10^6 cells were transferred to 6ml polystyrene tubes. If necessary, the volume was topped up to 1ml in FACS buffer (1x DPBS, 0.5% BSA). The cells were centrifuged at 300g for 5 minutes and the supernatant was

discarded. The cell surface was stained for the following receptors to distinguish between monocytes, T cells and B cells: CD16-PE, CD3-APC, CD14-APC-Cy7, CD19-FITC. In an independent experiment, CD36 expression on the surface of monocytes was also assessed (Table 2.3). In each case, the cells were incubated for 15 minutes at 4°C in the dark. The cells were washed once in FACS buffer to remove excess stain and the supernatant was discarded. The cells were re-suspended in 250µl in FACS buffer. The samples were analysed by using an LSRII flow cytometer (BD) and the data was analysed by using FlowJo 10 software.

2.8.2 Apoptosis assay

Monocyte apoptosis levels was assessed by using the Annexin V Apoptosis Detection kit FITC (eBioscience) with propidium iodide staining solution (eBioscience). The 10x binding buffer was diluted to 1x by using dH₂O. 1x10⁶ monocytes were transferred to microcentrifuge tubes and were washed once in 1x PBS and then once in 1x binding buffer (300g for 5 minutes, discarding supernatant between each wash). The cells were re-suspended in 1x binding buffer at 1x10⁶ cells/ml. 5µl of Annexin V-FITC was added to 100µl of cell suspension, and the cells were left to incubate for 15 minutes at RT in the dark. The cells were washed in 2ml of 1x binding buffer by centrifuging at 300g for 5 minutes. The supernatant was discarded and the cells were re-suspended in 200µl of 1x binding buffer. 5µl of propidium iodide staining solution was then added to the cells, which were then analysed on a MACS QUANT (Miltenyi Biotech) flow cytometer. The data was analysed by using FlowJo 10 software.

Table 2.3 FACS antibodies

Specificity	Reactive Species	Clone	Fluorochrome	Supplier	µl/test
Annexin V	Human		FITC	eBioscience	5
CD3	Human	UCHT1	APC	BD	5
CD14	Human	M5E2	APC-Cy7	BD	5
CD16	Human	3G8	PE	BD	5
CD19	Human	HIB19	FITC	BD	5
CD36	Human	CB38	APC	BD	20
PI	Human		PI	eBioscience	5

2.9 Gene expression analysis

2.9.1 RNA extraction

RNA was extracted from monocytes using the RNeasy® Mini Kit (Qiagen). The supernatant was aspirated from each well from the tissue culture plate and the cells were lysed by adding 350µl of Buffer RLT to each well. The cells were transferred to QIAshredder columns (Qiagen), and the lysates were centrifuged through the columns at max speed for 2 minutes. 350µl of 70% EtOH was added to the lysates and the combined sample was transferred into an RNeasy spin column in a 2ml collection tube. The sample was centrifuged for 15 seconds at 8000g and the flow-through was discarded. A DNase digestion step was included in the protocol. 350µl of Buffer RW1 was added to the spin column, which was centrifuged at 8000g for 15 seconds, and flow-through discarded. Meanwhile, 10µl of DNase I stock solution (prepared by injecting 550µl of RNase-free water into the DNase I vial) was added to 70µl Buffer RDD and mixed gently. 80µl of the DNase I incubation mix was added directly to the RNeasy spin column membrane, and allowed to incubate at RT for 15 minutes. 350µl of Buffer RW1 was then added to the column and centrifuged at 8000g for 15 seconds. 500µl of Buffer RPE was added to the column and centrifuged through the column for 15 seconds at 8000g. This step was repeated, but the column was centrifuged for 2 minutes. The column was transferred to a new 2ml collection tube, and which was then centrifuged at max speed for 1 minute to dry the membrane. The spin column was transferred to a new 1.5ml microcentrifuge tube. The RNA was eluted from the column by adding 30µl of RNase-free water directly onto the membrane and centrifuging for 1 minute at 8000g. The concentration and purity (260/280) of the RNA was evaluated by a NanoDrop™ 2000/2000c Spectrophotometer.

2.9.2 cDNA synthesis

cDNA was synthesised from extracted RNA using the Affinity Script cDNA synthesis kit (Agilent Technologies). For each experiment, the concentration of RNA for each sample was normalised by diluting in RNase-free water. In 0.2ml flat capped PCR tubes (Starlab), 12.7µl of diluted RNA was added to 3µl of random primers. The tubes were centrifuged briefly to ensure all reagents were

mixed at the bottom of the tube. The samples were incubated at 65°C for 5 minutes and then cooled at 20°C for 10 minutes in a thermal cycler (Applied Biosystems 2720 thermal cycler), to allow the primers to anneal to the RNA. 4.3µl of a master mix containing: 2µl 10x AffinityScript RT Buffer; 0.8µl DNTP mix; 0.5µl RNase block ribonuclease inhibitor and 1µl AffinityScript multiple temperature RT were added to each tube and mixed briefly. The samples were returned to the thermal cycler to run the remainder of the programme, as outlined in **Table 2.4**.

Table 2.4 cDNA synthesis cycling

Temperature	Time
25°C	10 minutes
42°C	5 minutes
55°C	60 minutes
70°C	15 minutes

2.9.3 Primer design for qPCR

The forward and reverse primers (**Table 2.5**) were either obtained in-house or were designed by using PrimerBank (<http://pga.mgh.harvard.edu/primerbank/>). The primers were designed using a length of between 18-22 base pairs, a GC nucleotide content of between 40-60%, and a melting temperature (T_m) between 59-63°C. Specificity and efficiency of the primers were confirmed by using the Primer-BLAST web tool by NCBI. All primers were purchased from Integrated DNA Technologies and are listed in **Table 2.5**.

Table 2.5 Primer sequences

Gene	Forward Primer 5'-3'	Reverse Primer 5'-3'
ALDOA	ATGCCCTACCAATATCCAGCA	GCTCCCAGTGGACTCATCTG
CXCR4	ACTACACCGAGGAAATGGGCT	CCCACAATGCCAGTTAAGAAGA
GAPDH	GAACATCATCCCTGCCTCTAC	GCCAAATTCGTTGTCATACAGG
GLUT1	TCTGGCATCAACGCTGTCTTC	CGATACCGGAGCCAATGGT
HK2	TTGACCAGGAGATTGACATGGG	CAACCGCATCAGGACCTCA
LDHA	ATGGCAACTCTAAAGGATCAGC	CCAACCCCAACA ACTGTAATCT
PGK1	TGGACGTTAAAGGGAAGCGG	GCTCATAAGGACTACCGACTTGG
VEGFA	AGGGCAGAATCATCACGAAGT	AGGGTCTCGATTGGATGGCA

2.9.4 Primer validation prior to qPCR

To validate the primers, in 0.2ml PCR tubes: 0.5 μ l forward primers; 0.5 μ l reverse primers; 1 μ l cDNA; 23 μ l RNase free water and 25 μ l MyTaq™ Red Mix (Bioline) was mixed and loaded into a thermal cycler and the following programme was run (Table 2.6). The samples were run on an agarose gel. 1.8g of agarose was added to 100ml of 1x TAE Buffer (diluted from 50x TAE buffer: 242 g Tris free base, 18.61g EDTA, 57.1 ml glacial acetic acid, 1L dH₂O. 1x solution made by diluting 1:50 in dH₂O.) to make a 1.8x buffer. This was microwaved for 2 minutes, and left to cool for 5 minutes at RT. 20 μ l of ethidium bromide (Sigma-Aldrich) was added to the buffer. The buffer was loaded carefully into the gel electrophoresis tank (avoiding bubbles) and was left for 30 minutes at RT to set. The comb was removed to expose the wells for loading and the tank was topped up with approximately 1L of 1x TAE buffer. 15 μ l of sample and 15 μ l of 1kb DNA ladder (Thermo Fisher) was loaded into the appropriate wells. The electrodes were connected to the power supply and the gel was run for 1 hour at 110V. The gel was removed and the ethidium bromide staining was visualised under a UV transilluminator. Primers which were visualised at its known amplicon size (by reading against the ladder) indicated successful and specific binding of the primers, which were subsequently used for qPCR.

Table 2.6 MyTaq Red thermal cycling

Temperature	Time	Cycles
94 °C	5 minutes	1
94 °C	15 seconds	35
55 °C	30 seconds	
72 °C	30 seconds	
72 °C	10 minutes	1

2.9.5 qPCR

Gene expression was analysed by qPCR in 10µl reactions in 96 well plates (Starlabs). Each reaction contained the following: 2µl cDNA, 5µl Power SYBR™ Green master mix (Applied Biosystems); 0.1µl forward primer; 0.1µl reverse primer and 2.8µl nuclease-free water. Once loaded into the plate, the plates were sealed and centrifuged at 400g for 1 minute to ensure all contents were mixed and at the bottom of the well. The following method was used on an Applied Biosystems Step One Plus Real Time PCR System: 95 °C for 10 minutes and 40 cycles of 95 °C for 15 seconds and 60 °C for 1 minute (Table 2.7). The amplification data was exported to Excel. To analyse the data, the target genes were normalised to the housekeeping control by subtracting the C_t value of the housekeeping gene away from the C_t value of the target gene, generating the ΔC_t value. From the ΔC_t , the $2^{-\Delta C_t}$ value was calculated. Using the $2^{-\Delta\Delta C_t}$ method (Livak & Schmittgen 2001), the relative quantification of each sample compared to the experimental control was determined.

Table 2.7 qPCR cycling conditions

Temperature	Time	Cycles
95 °C	10 minutes	1
95 °C	15 seconds	40
60 °C	1 minute	

2.9.6 Taqman Low Density Array (TLDA)

The customised TLDA (Thermo Fisher) were a kind gift from Simone Kidger and the target genes are listed in **Table 2.8**. The TLDA microfluidic cards were brought to RT before use. In microcentrifuge tubes, 50µl of cDNA (from 100ng extracted RNA) was added to 50µl Taqman Universal MasterMix II, (Thermo Fisher). The samples were briefly vortexed and centrifuged to mix the contents and eliminate air bubbles. 100µl of the sample was carefully pipetted into the fill port of the microfluidic card. The microfluidic cards were loaded into Sorvall/Heraeus centrifuge buckets, and were centrifuged twice at 331g for 1 minute. The plates were sealed using a TaqMan® Array Micro Fluidic Card Sealer and the fill ports cut off. The plates were loaded into an Applied Biosystems 7900HT Sequence Detection System with the TaqMan Array Micro Fluidic Card Thermal Cycling Block installed. Using SDS2.4 software, the plates were run using the TaqMan Low Density Array cycling method. The amplification data was exported to Excel using RQ manager software, and the data was analysed using the $2^{-\Delta\Delta C_t}$ method as described in 2.9.5.

Table 2.8 TLDA target genes

CCL2	CCL22	CD36	GAPDH	MRC1	CREB1	IL8	CXCL10	CCL17	CD1C
IL6	IL12B	CSF2	CCL3	CCL4	UBC	CLEC4E	CSF2RA	TLR4	IRF5
TNF	CD1A	CD200R1	CCL20	CD209	CHI3L1	STAB1	CXCL2	CD163	CCR2

2.10 Metabolomics

2.10.1 Intracellular metabolite extraction of monocytes

All reagents and vessels were incubated on ice to bring to $\leq 4^\circ\text{C}$ before extraction. The tissue culture plates containing monocytes were immediately placed on ice, and the monocytes were aspirated and transferred to 15ml centrifuge tubes containing 13ml of ice-cold DPBS. Each well was flushed out with ice-cold DPBS to remove any more adherent cells, and the flush was transferred to the same centrifuge tube for the same well. The tubes were

centrifuged at 300g for 5 minutes at 4°C. The pellet was re-suspended in 1ml ice-cold PBS, and this was transferred to pre-cooled 1.5ml microcentrifuge tubes. The tubes were centrifuged at 300g for 5 minutes at 4°C. All of the DPBS was aspirated, and the pellet was re-suspended in 200µl ice-cold extraction solvent (chloroform:methanol:water at a 1:3:1 ratio). The tubes were incubated for 1 hour at 4°C in an Eppendorf ThermoMixer® with shaking at 1500rpm. The tubes were then centrifuged at 17,000g for 10 minutes at 4°C to pellet any cellular proteins and debris. The supernatant containing metabolites were collected into screw-capped vials and stored at -80°C until analysis. A pooled sample containing an equal volume of all samples (to a total of 200µl) was generated at this point. This sample was run during mass spectrometry analysis to assess the reproducibility of the mass spectrometer (2.10.3).

2.10.2 Intracellular metabolite extraction of macrophages

As macrophages are strongly adherent to the tissue culture plates, a modified protocol was used to extract metabolites. All reagents and vessels were incubated on ice to bring to at least $\leq 4^\circ\text{C}$ before extraction. The tissue culture plates containing macrophages were immediately placed on ice. The medium was aspirated and the cells were washed once with ice-cold DPBS. 400µl (24 well plates) or 250µl (48 well plates) of ice-cold extraction solvent was added directly onto the monolayer in the well. The plates were placed on a shaker for 1 hour at 4°C. The solvent was transferred to pre-cooled 1.5ml microcentrifuge tubes, which were incubated in a ThermoMixer with shaking at 1500rpm at 4°C for 10 minutes. The tubes were centrifuged at 17,000g for 10 minutes at 4°C to pellet any cellular proteins and debris. The supernatant containing metabolites were collected into screw-capped vials and stored at -80°C until analysis.

2.10.3 Untargeted Mass Spectrometry (MS)

Untargeted metabolomics was carried out by the metabolomics staff at the Glasgow Polyomics Facility. Hydrophilic interaction liquid chromatography (HILIC) was carried out on a Dionex UltiMate 3000 RSLC system (Thermo Fisher) using a ZIC-pHILIC column (150 mm × 4.6 mm, 5 µm column, Merck Sequant). For the MS analysis, a Thermo Orbitrap QExactive (Thermo Fisher) was operated in both positive and negative mode. The column was maintained at 30°C. The

samples were eluted with a linear gradient from 80% acetonitrile to 20% ammonium carbonate (20mM in water) over 24 minutes, at a flow rate of 0.3ml/min. Each sample was run in a random order, with a pooled sample (2.10.1) run between every 5 samples to assess for reproducibility. The MS settings were as follows: 70,000 resolution; m/z range of 70-1050; automatic gain control target of 1e6; sheath gas flow rate of 40; auxiliary gas flow rate 5; sweep gas flow rate 1; probe temperature of 150°C and capillary temperature of 320°C. For positive mode ionisation: source voltage +3.8 kV, S-Lens RF Level 30.00, S-Lens Voltage -25.00 (V), Skimmer Voltage -15.00 (V), Inject Flatopole Offset -8.00 (V), Bent Flatopole DC -6.00 (V). For negative mode ionisation: source voltage -3.8 kV. The calibration mass range was extended to cover small metabolites by inclusion of low-mass calibrants with the standard Thermo calmix masses (below m/z 138), butylamine (C₄H₁₁N₁) for positive ion electrospray ionisation (PIESI) mode (m/z 74.096426) and COF3 for negative ion electrospray ionisation (NIESI) mode (m/z 84.9906726).

2.10.4 Data processing of untargeted MS

Processing of the raw data and analysis was performed using a processing pipeline through IDEOM Excel based software. According to the metabolomics standards initiative (MSI), metabolite identifications (MSI level 1) are given when more than one feature matches an authentic standard (i.e. mass and retention time) and annotations are made when matching to a metabolite is made by mass only (MSI level 2). Included in the MS analysis was a mixture of 240 standards. These covered a range of metabolic pathways to allow metabolite identifications to be made. In the comparisons tab of the IDEOM package, the peaks were visually interrogated. Generally speaking, peaks not showing a Gaussian-type shape were rejected as a false identification, although this required some subjective judgement.

2.10.5 Targeted MS of carnitine metabolites

100µl of metabolite extract from alveolar macrophages (2.10.2) and 100µl of a calibration sample from a 6-point calibration curve (300 to 0.02nM) was added to 400µl methanol:acetonitrile containing 20µl of carnitine internal standard solution (NSK-B isotope labeled L-carnitine and acyl-carnitines in 1ml methanol;

Cambridge Isotope Laboratories, Cat. NSK-B). Liquid chromatography-mass spectrometry was performed by Lars Löfgren at AstraZeneca (Mölndal, Sweden). Liquid-chromatography was carried out by using an Acquity UPLC® BEH Amide column (1.7µm, 2.1 x 100mm; Waters, part no 186004801). Acetonitrile was used for mobile phase A. 20mM AmF + 10mM FA in 100% water was used for mobile phase B with an injection volume of 2µl. Separation was achieved in gradient mode with 0% B from 0-1min and 3-50% B from 1-5 min. The column was then washed with 50% B from 5-6 min and equilibrated at 0% B from 6.1-8.0 min before next sample was injected. Total run time was 8 minutes per sample. L-carnitine and acyl carnitines with internal standards were analysed by negative electrospray-ionisation tandem mass spectrometry (ESI-MSMS) in multiple reaction monitoring (MRM) mode using a cone voltage for ionisation of analytes of 30 (V) and a collision energy for fragmentation of the molecular ions of 20 (V) for L-Carnitine and all acyl-carnitines. All analytes were analyzed as $m/z = [M+H]$ as parent ions and the fragment $m/z = 85$. The concentration of L-carnitine and each acyl carnitine was determined from the MRM signal intensity for the analyte versus the internal standard in the sample and in the calibration samples using Masslynx 4.0 software (Waters).

2.11 Statistical analysis

Statistical analysis was carried out by using GraphPad Prism 6 software. Metabolomics data was analysed by MetaboAnalyst. All data is shown as the mean \pm standard deviation (SD) unless otherwise stated. To determine if the data was normally distributed, the Pearson/D'Agostino normality test was used. Normally distributed data were subject to parametric statistical tests. However, when the data was not normally distributed, or when the distribution could not be determined, non-parametric tests were used. The figure legends indicate which statistical test was used for each experiment. A p value of less than 0.05 was considered significant. Heatmaps were generated by John Cole by using the R statistical software package, ggplot2.

Chapter 3. The impact of hypoxia on the metabolic profile on human monocytes

3.1 Introduction

Cellular metabolism is of growing interest to the immunological community, who have recently coined the area of immunometabolism. This is a very complex system, where there are many pathways, thousands of metabolites and a very dynamic relationship between each. Nevertheless, this field has emphasised how certain metabolic pathways, their metabolites and/or enzymes can directly influence immune cell function. Some pioneering studies influenced the immunological field to think about cellular metabolism. This is particularly the case in myeloid cells, where murine M(LPS + IFN γ ; M1) and M(IL-4; M2) polarised macrophages exhibit distinct metabolic profiles and aerobic glycolysis is essential for the induction of trained immunity (Jha et al. 2015; Cheng et al. 2014; Galvan-Pena & O'Neill 2014). Although there has been increased interest in this area recently, immunometabolism has some historical relevance. Experimentally it is now well established that inflammatory 'M1' polarised macrophages and anti-inflammatory 'M2' macrophages utilise the metabolite arginine differentially. When challenged with LPS, M1 murine macrophages generate nitric oxide (NO) from arginine through inducible nitric oxide synthase (iNOS). In comparison, M2 macrophages utilise arginase-1 (Arg-1) to generate ornithine from arginine (C. D. Mills et al. 2000).

There are extensive studies investigating the importance of metabolism in myeloid cells, with an emphasis on macrophages and their polarised (M(LPS + IFN γ) or M(IL-4)) state. This use of terminology was discussed in 1.1.2. To fully characterise these distinct populations, Jha *et al* (2015) carried out a high-throughput transcriptional-metabolic screen of M(LPS + IFN γ) and M(IL-4) macrophages. Their study illustrated that M(LPS + IFN γ) macrophages displayed a fragmented TCA cycle, which was compensated by an aspartate-arginosuccinate shunt. NO and IL-6 production was inhibited when this shunt pathway was pharmacologically blocked. On the other hand, M(IL-4) macrophages had activated glutamine catabolism and UDP-GlcNAc associated pathways, responsible for glycosylation events. Indeed, inhibition of glycosylation and

glutamine starvation prevented M(IL-4) polarisation and production of CCL22 (Jha et al. 2015).

Moreover, stimulation of polarised macrophages with TLR ligands such as LPS results in altered metabolism. For example, murine M(LPS ± IFN γ) macrophages activate a glycolytic metabolic programme at the expense of mitochondrial metabolism (Rodriguez-Prados et al. 2010). This programme involves succinate, a TCA cycle intermediate, that accumulates in these cells, which in turn caused stabilised HIF-1 α protein to enhance IL-1 β release. This can be perturbed by inhibition of glycolytic metabolism with 2-Deoxyglucose (2-DG). In this context, LPS is unable to induce IL-1 β production (Tannahill et al. 2013). In juxtaposition to the glycolytic pathways in M(LPS + IFN γ), it is known that glutamine metabolism and UDP-GlcNAc synthesis are associated with M(IL-4) polarisation (Jha et al. 2015). These alternatively activated macrophages are recognised to be dependent on mitochondrial metabolism, which include fatty acid oxidation. The source of the fatty acids is thought to be from uptake from the scavenger receptor, i.e., CD36. Following uptake, it has been shown that these fatty acids undergo lipolysis by lysosomal acid lipase. These fatty acids enter the mitochondria and are subject to β -oxidation and oxidative phosphorylation to fuel M(IL-4) macrophage survival and function (S. C.-C. Huang et al. 2014). Despite all of these findings, the dependence of fatty acid oxidation on M(IL-4) polarisation has been challenged. Genetic ablation of CPT2a in mouse bone-marrow derived macrophages had no impact on M(IL-4) polarisation in this setting despite being deficient in FAO (Nomura et al. 2016). Furthermore, inhibition of FAO in human macrophages had no significant effect on M(IL-4) polarisation as well (Namgaladze & Brüne 2014).

It is important to note that the vast majority of research into myeloid metabolism has been focussed solely on M(LPS + IFN γ) or M(IL-4) polarised macrophages, and more often than not murine cells. It must be emphasised that these two populations represent extremes of a phenotypic continuum, as discussed in 1.1.2. This was highlighted by Xue *et al* (2014) with an extensive transcriptomic based study. Furthermore, environmental factors can heavily influence myeloid cell phenotype and associated function, as illustrated in tissue-resident macrophages, where the micro-environment can profoundly alter

chromatin state (Lavin et al. 2014). Given the importance of the chronic inflammatory microenvironment of diseases, such as RA and COPD, on the phenotype and function of immune cells, it is important to address if the current research of immunometabolism translates into human disease. Even before researchers considered modulating cellular metabolism to control inflammation in inflammatory diseases, drugs were already available for this purpose. For example, the disease modifying anti-rheumatic drug (DMARD) and purine metabolism inhibitor, methotrexate, was first used in low doses for the treatment for rheumatoid arthritis in the 1980s.

With this in mind, the purpose of this chapter is to deviate away from the current research, which uses experimental polarisation conditions with little focus on disease. The emphasis is therefore on human monocytes, and mimicking the initial phases of blood monocyte recruitment to a site of chronic inflammation. One of the most common features of chronic inflammation in the rheumatoid joint is hypoxia: a feature dating back to 1970 (1.3.1) (Lund-Olesen 1970). Therefore, when monocytes enter this hypoxic microenvironment, they are met with a metabolic challenge. Yet they are able to adapt to this environment and drive disease severity. The studies here will model tissue hypoxia *in vitro* to replicate this phenomenon.

The aim of this chapter was to obtain a metabolic profile of monocytes exposed to short-term hypoxia. To achieve this aim, it was important for the monocytes to be cultured appropriately for metabolic analysis. Furthermore, it was essential to confirm that hypoxia induction was reliable, and that the monocytes were adapting and surviving in low levels of oxygen. Thus, the three main aims of this chapter were:

1. Optimise a monocyte culture for metabolic assessment
2. Induce hypoxia in cells and confirm hypoxic induction by investigating HIF-1 α protein stability
3. Assess the impact of hypoxia vs normoxia on the metabolic profile of monocytes.

3.2 Results

3.2.1 Optimisation of monocyte purification and *in vitro* culturing

The primary aim of this chapter was to metabolically profile human monocytes after exposure to short term hypoxia. However, it was important to optimise the monocyte culture before this analysis. This included the assessment of monocyte purity after the enrichment protocol (2.2.2), and to analyse monocyte cell survival under hypoxic conditions and when cultured with human plasma. Culture with human plasma aimed to keep monocytes alive without inducing a macrophage differentiation programme which may have interfered with subsequent metabolic analyses (Safi et al. 2016).

The first task was to check monocyte purity after enrichment from isolated PBMCs obtained from buffy coat donors. The StemCell monocyte enrichment kit, without CD16⁺ cell depletion (2.2.2) was used because monocytes are negatively selected and are thus ‘untouched’ by tetrameric antibodies and magnetic beads. This crucially avoids any metabolic changes that may be induced by antibody and magnetic bead binding. It is also important to note that this kit isolates all three blood monocyte populations: CD14⁺⁺ CD16⁻ (classical monocytes), CD14⁺ CD16⁺⁺ (non-classical, patrolling monocytes) and CD14⁺⁺ CD16⁺ (intermediate monocytes).

To assess monocyte purity, the whole PBMC population and the negatively selected monocyte population were stained with fluorescently labelled antibodies to CD3 (T cells), CD19 (B cells) and CD14 and CD16 for monocyte populations and analysed by flow cytometry. Pre-separation analysis revealed that the PBMC population contained approximately 5% CD19⁺ B cells and 27% CD3⁺ T cells (Figure 3.1A). Following enrichment for monocytes, the CD19⁺ B cells population was depleted to below 3% and CD3⁺ T cells below 1.5% (Figure 3.1B). The PBMC population consisted of 12% CD14⁻ CD16⁺ monocytes, 4.8% CD14⁺ CD16⁺ monocytes and 37% CD14⁺ CD16⁻ monocytes (Figure 3.1C) While 46% of the total population consisted of T cells, B cells and other non-monocyte cells (Figure 3.1C). After the enrichment, the total monocyte population represented, on average, 96.3% ± 2.1% of the remaining cells (n = 4). In this representative example, the composition of the monocyte compartment was

made up of 21% CD14⁻ CD16⁺ monocytes, 11% CD14⁺ CD16⁺ monocytes and 63% CD14⁺ CD16⁻ monocytes (Figure 3.1D).

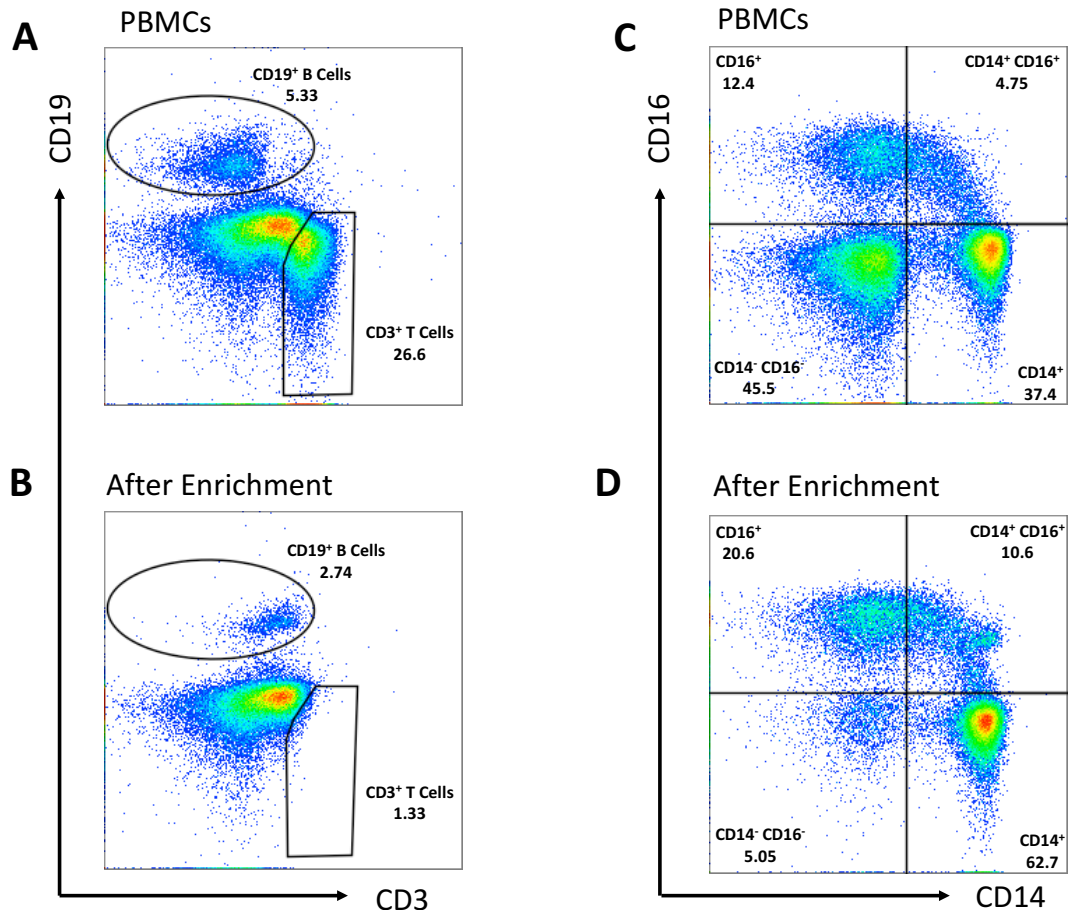


Figure 3.1 Human monocyte purity analysis. Representative example of PBMC populations before and after monocyte enrichment. Cells were selected on the basis of FSC and SSC, and ‘doublets’ were excluded. Percentage of CD3⁺ T cells and CD19⁺ B cells before [A] and after [B] enrichment for monocytes. Percentage of each monocyte population on the basis of CD14 and CD16 before [C] and after [D] enrichment for monocytes.

Based on evaluation of the enrichment protocol, $\geq 94\%$ was considered of sufficient purity to evaluate monocyte metabolism. However, prior to assessing metabolic changes in monocytes it was essential to address two further questions:

1. Does short term hypoxia initiate cell death in the monocytes?
2. Do monocytes survive when cultured with human plasma rather than M-CSF?

To check that monocytes did not undergo overt apoptosis or necrosis under (a) hypoxic conditions, (b) human plasma, (c) M-CSF, and (d) LPS stimulation, cells were evaluated for classical apoptosis/necrosis markers. To analyse cell viability, human monocytes were stained for Annexin-V and Propidium Iodide (PI), well established markers for apoptosis and cell death, and analysed by flow cytometry. The staining showed that there was very little difference in viability between culturing the cells under human plasma or M-CSF, in both normoxic and hypoxic (5% O₂) conditions, as viable cells (Annexin-V⁻ PI⁻) constituted around 83% of the total monocyte population (**Figure 3.2**). When stimulated with LPS, the percentage of viable cells did not significantly change and there appeared to be minimal impact between normoxic and hypoxic conditions and between human plasma and M-CSF (**Figure 3.2**).

These results support the concept that within the realms of this experimental setup hypoxia had very little impact on the viability of the cells. Furthermore, these results also supported the culturing of monocytes in human plasma (10% pooled human plasma in medium) rather than with M-CSF. M-CSF is classically used in the field at non-physiological concentrations to differentiate blood monocytes into macrophages, before subsequent polarisation. The decision to culture the monocytes with human plasma rather than M-CSF was to avoid capturing early metabolic changes of a differentiation programme. It was hypothesised that the metabolic profile captured in these conditions would reflect solely on hypoxia adaptation, as human plasma would maintain survival by providing physiological levels of growth factors and stimuli, without driving macrophage differentiation immediately. This method is used routinely in monocyte trained immunity models to maintain a longer-term monocyte culture (Cheng et al. 2014).

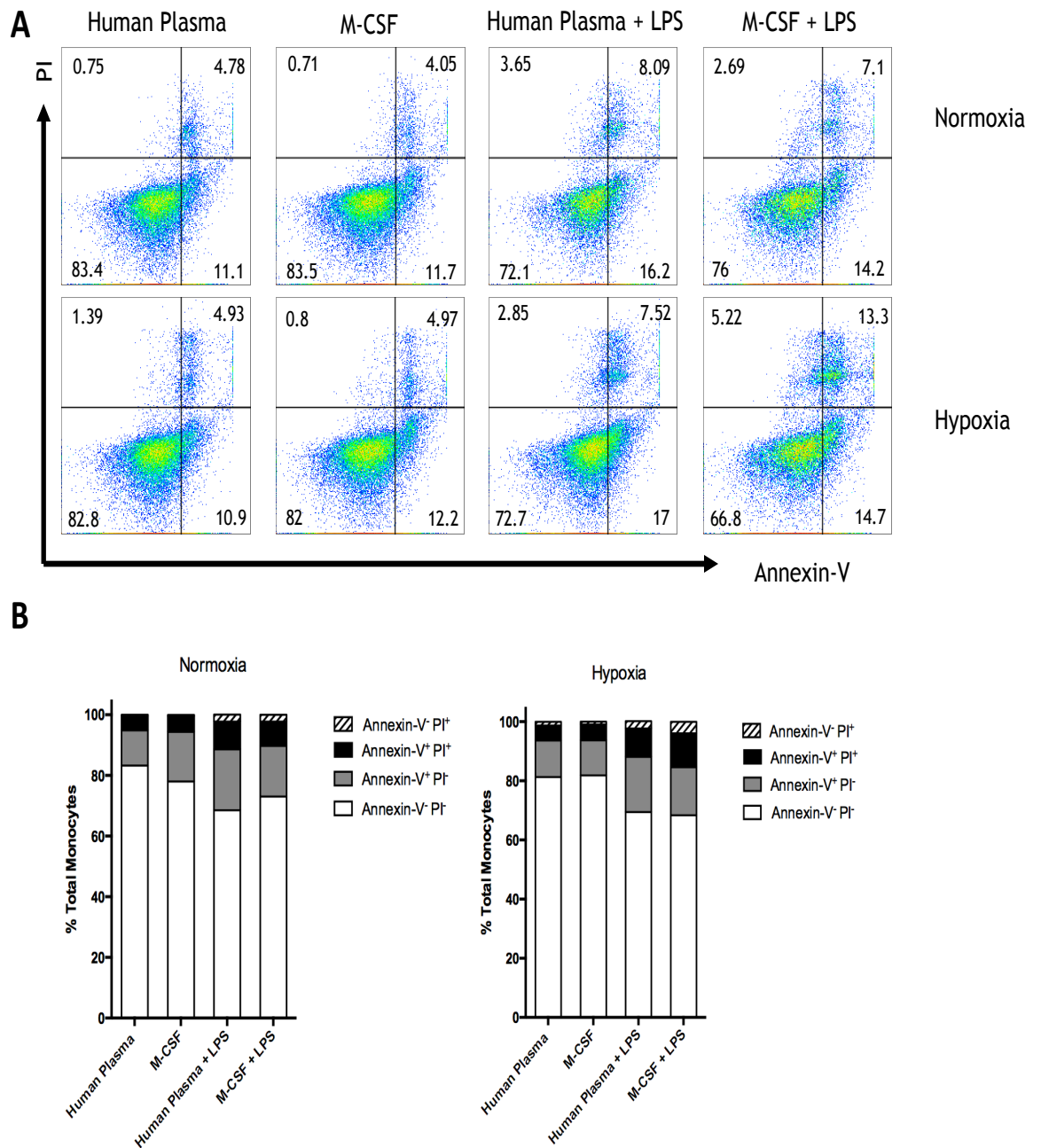


Figure 3.2 Monocyte apoptosis assessment. Representative experiment of monocytes stained for Annexin-V and Propidium Iodide (PI) after 4 hours of culture. Cells were selected based on their FSC and SSC characteristics, and 'doublets' were excluded based on FSC area vs height. **[A]** Annexin-V and PI staining of monocytes cultured in media containing 10% human plasma or 100ng/ml M-CSF \pm 100ng/ml LPS in normoxia and hypoxia (5% O₂). **[B]** Percentages of the proportion of monocytes in each state of viability when cultured under each condition. *N* = 2.

3.2.2 Confirming hypoxic adaptation

To confirm the impact of hypoxia on monocytes and demonstrate that they were adapting to this environment, HIF-1 α stability was assessed by Western Blot. Alternative methods of hypoxia induction were tested for this purpose. This included using a cell culture incubator capable of reaching 5% O₂ (Section 2.4.1) and CoCl₂, which is used to chemically induce HIF-1 α expression in cells, even in normoxic conditions (Piret et al. 2002). Firstly, monocytes were cultured in 5% O₂ for 4 hours and lysates were taken using the RIPA buffer lysis method (Section 2.5.1) for subsequent blotting. However, HIF-1 α could not be detected under these conditions. Secondly, CoCl₂ at final concentrations of 100 μ M and 1mM were used in monocytes which were cultured for 2 hours and 4 hours. Despite this, HIF-1 α could not be detected in monocytes, even when 30 μ g and 70 μ g of protein was loaded onto the gel (data not shown).

To assess if the lack of chemical induction of HIF-1 α in monocytes was specific to CoCl₂, another chemical inducer of HIF-1 α , DMOG (1mM) was utilised (Milkiewicz et al. 2004). However, this also failed to induce detectable HIF-1 α after treatment of monocytes for 2, 4 and 18 hours (data not shown).

In addition, previously published work had stimulated monocytes with LPS or PMA to induce HIF-1 α expression in monocytes as a positive control (Fangradt et al. 2012). Therefore, these stimulations were carried out in a bid to replicate this. Conversely, neither LPS (100ng/ml) nor PMA (10ng/ml) induced the protein, which is at odds with the published work.

In all the experiments described above, the loading control (GAPDH) was detectable (data not shown), which indicated that a lack of detection was specific for HIF-1 α . Taken together, this collection of results suggested that the protein extraction method using RIPA buffer may not have been suitable for HIF-1 α detection from primary human monocytes, possibly by degrading the protein.

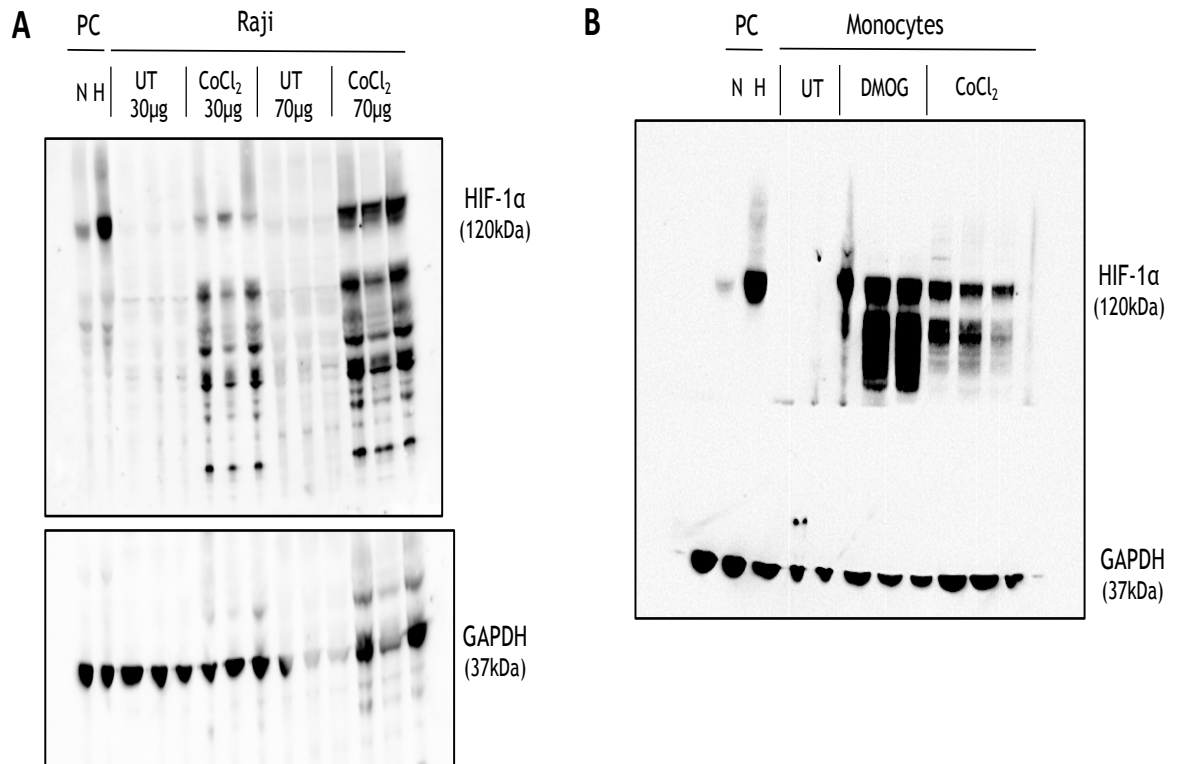


Figure 3.3 Searching for a HIF-1α positive control. [A] Raji cells (from 3 independent experiments) were either untreated (UT) or treated for 4 hours with 100μM Cobalt chloride (CoCl₂). 30μg or 70μg of whole cell protein extract was loaded for probing for HIF-1α or GAPDH (loading control). A positive control (PC) lysate from HeLa cells cultured in normoxia (N) or hypoxia (H) was also blotted. **[B]** Human monocytes were either left untreated (UT) or treated with 200μM Dimethylxaloylglycine (DMOG) or 200μM Cobalt chloride (CoCl₂) for 4 hours. A positive control (PC) lysate from HeLa cells cultured in normoxia (N) or hypoxia (H; 1% O₂) was also blotted for HIF-1α and GAPDH (loading control). *N* = 3.

To find a positive control for HIF-1α expression in non-immune cells, the Raji cell line was utilised, as they are considered to have constitutive HIF-1α expression (Kambayashi et al. 2015). The cells were either untreated in normoxia, or cultured in CoCl₂ at a final concentration at 100μM for 4 hours to chemically induce expression further. The whole cell lysates were harvested in RIPA buffer. In contrast to the published work, untreated cells did not have detectable HIF-1α protein (**Figure 3.3A**; (Kambayashi et al. 2015)). However, in this instance, CoCl₂ treated Raji cells did show HIF-1α detection, when the gel was loaded with both 30μg and 70μg of protein (**Figure 3.3A**). The positive identification of HIF-1α from CoCl₂ treated Raji cells highlighted a possible compatibility issue of RIPA buffer and HIF-1α from primary human monocytes.

In addition to preparing unstimulated and stimulated Raji samples, a HIF-1 α positive and negative control lysate from Novus Biologicals were also run on the same gel, and the target protein was detected in the positive control sample (**Figure 3.3A**). Notably, these control protein extracts were from HeLa cells cultured in normoxia (negative control) or hypoxia (positive control).

Despite the ability to detect HIF-1 α in these positive control samples, the ability to detect HIF-1 α in primary human monocytes still remained elusive. However, a previous study had examined and successfully detected HIF-1 α stability in monocytes under hypoxic conditions (Fangradt et al. 2012). It was noted that in this work, and in the Novus Biologicals control samples, that the methods used to generate cell extracts was based on direct lysis in 2x Laemmli sample buffer (Section 2.5.2), rather than RIPA lysis buffer. In addition, a primary HIF-1 α antibody from BD Transduction laboratories was used instead of an antibody from CST (**Table 2.1**).

Taking these factors into account, HIF-1 α stability was once again assessed in primary monocytes after treatment with DMOG or CoCl₂, but the cells were lysed directly in Laemmli buffer. In this experiment, the monocytes were left untreated, or were treated with 200 μ M DMOG or 200 μ M CoCl₂ for 4 hours. By probing with the BD Transduction laboratories antibody, HIF-1 α was readily detected the expected 120kDa band in the positive control sample (Novus Biologicals) and the DMOG and CoCl₂ stimulated samples (**Figure 3.2B**). This indicated that Laemmli buffer was able to maintain HIF-1 α integrity for blotting.

After optimising the detection of HIF-1 α , we also decided to further optimise the induction of hypoxia. Maintaining a hypoxic environment in a cell culture incubator used up a considerable volume of N₂ gas, which required continuous purging whereby cylinders needed constant replacement, making it impractical. Therefore, an airtight chamber which only required 3 minutes of purging before it could be sealed and maintained as hypoxic without a need for a gas source was used (Section 2.4.2). It must be noted that the airtight chamber was used at 1% O₂, while the incubator could only reach a minimum tension of 2.3%.

With increased confidence in the lysate extraction method, monocytes were cultured in normoxia and hypoxia (1% O₂) \pm LPS for 4 hours, prior to whole cell

lysate preparation in Laemmli buffer. These hypoxic conditions and sample preparation successfully allowed detection of stabilised HIF-1 α (**Figure 3.4A**). It should be noted that although stabilised levels of HIF-1 α continued to be detectable upon LPS stimulation, in the representative example one replicate had no detectable HIF-1 α , which was caused by pipetting error (**Figure 3.4A**). With this knowledge, a time-course experiment was carried out to assess how early HIF-1 α became detectable in primary monocytes. HIF-1 α was not observable after 1 or 2 hours of exposure to hypoxia, however, after 3 hours it was evident and levels increased by 4 and 5 hours (**Figure 3.4B**).

In these experiments, the monocytes were cultured in 96 well plates. In order to obtain a metabolic profile of monocytes, it was necessary to increase the number cells in each condition to enable sufficient levels of metabolites for subsequent detection. To achieve this and ensure that alterations in cell culturing conditions (i.e., increased media volume) did not alter the level of hypoxia induction, monocytes were cultured in tissue culture plates of increasing well volume. To this aim, monocytes were cultured at 4×10^6 cells/ml in 96 well plates (250 μ l), 24 well plates (500 μ l) and 12 well plates (1ml) and whole cell lysates harvested after 4 hours of hypoxia (**Figure 3.4C**). The results showed that HIF-1 α was detectable in volumes of up to 1ml in 12 well plates (**Figure 3.4C**). Based on this data and the requirements for metabolite analysis, culturing in 12 well plates was sufficient for extracting a suitable level of metabolites for metabolic profiling.

To further analyse the induction of hypoxia in primary monocytes, the level of expression of two hypoxia specific marker genes, VEGFA and CXCR4 (Fangradt et al. 2012; Raggi et al. 2014) was interrogated. Human monocytes were cultured in normoxia or hypoxia for 4 hours and the level of gene expression was analysed by qPCR. The results showed that compared to the normoxia control, monocytes cultured in hypoxic conditions upregulated both VEGFA and CXCR4 transcript (**Figure 3.4D**).

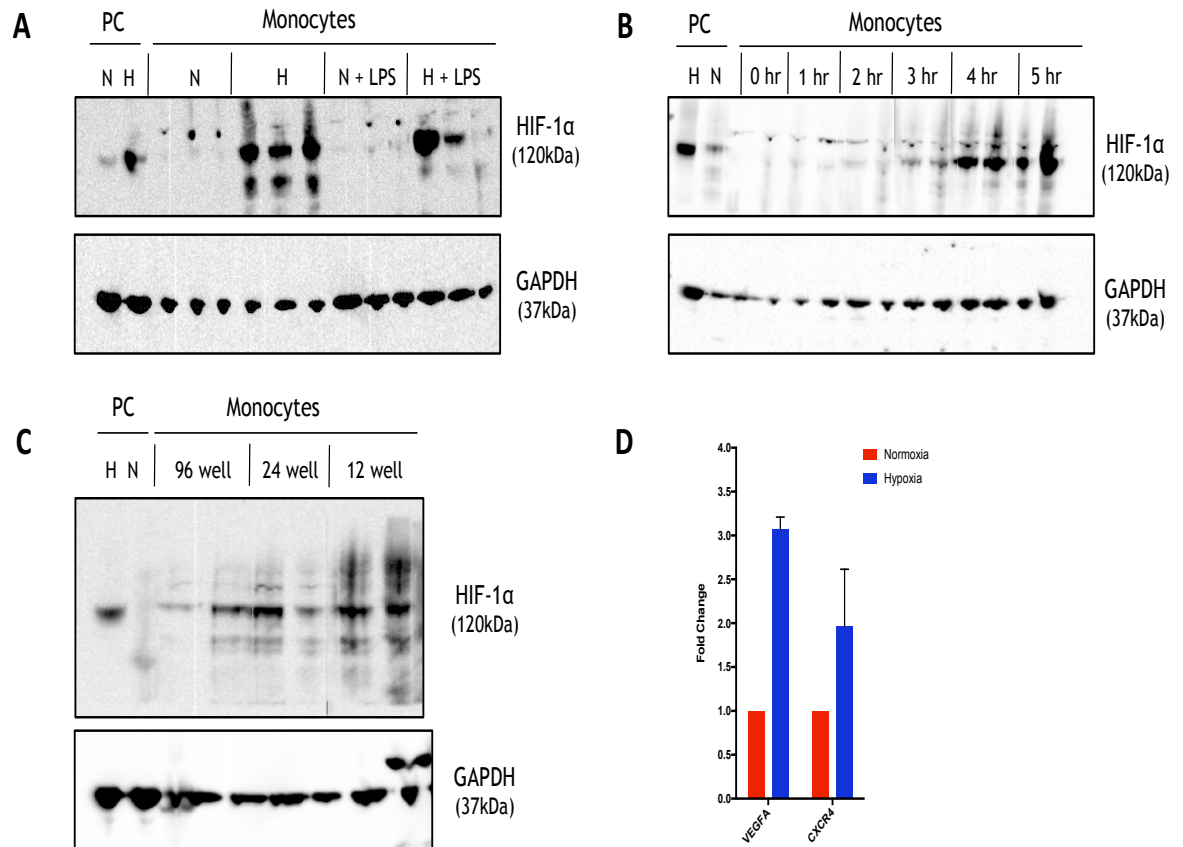


Figure 3.4 Confirming hypoxia in monocytes. [A] Monocytes were cultured in Normoxia (N) or Hypoxia (H; 1% O₂) ± 100ng/ml LPS for 4 hours. 15µl of whole cell extract protein in Laemmli buffer was blotted for HIF-1α and GAPDH (loading control). A positive control (PC) lysate from HeLa cells cultured in normoxia (N) or hypoxia (H; 1% O₂) was also probed. *N* = 3. [B] Timecourse of HIF-1α induction in monocytes from 0 hours to 5 hours of culture in hypoxia (1% O₂). A positive control (PC) lysate from HeLa cells cultured in normoxia (N) or hypoxia (H; 1% O₂) was also probed for HIF-1α and GAPDH. *N* = 2. [C] Monocytes were seeded at 4x10⁶ cells/ml in 96 well (250µl), 24 well (500µl), 12 well (1ml) and 6 well (2ml) for 4 hours in hypoxic (1% O₂) conditions. Cells were lysed directly in 20µl Laemmli buffer and were probed for HIF-1α and GAPDH (loading control). A positive control (PC) lysate from HeLa cells cultured in normoxia (N) or hypoxia (H; 1% O₂) was also blotted. *N* = 2. [D] Monocytes were cultured for 4 hours in normoxia or hypoxia (1% O₂), and the expression of the hypoxic marker genes, VEGFA and CXCR4, were assessed by qPCR. Fold change in hypoxia relative to normoxia (control) shown. Data shown as the Mean ± SD. *N* = 3.

3.2.3 Assessing the impact of hypoxia on the metabolic profile of monocytes

The results described above demonstrated that primary human monocytes tolerate culturing in human plasma, survive in hypoxic conditions, and adapt to the hypoxic environment by stabilising HIF-1 α . Thus, based on these results, the experimental setup was considered sufficient to evaluate metabolic profiling in monocytes. To achieve this and determine the global metabolic profile, an untargeted mass-spectrometry based metabolomics analysis was chosen. However, prior to acquiring the global metabolome it was deemed appropriate to initially confirm via standard assays that monocytes show metabolic changes upon hypoxic challenge. In the first instance, the general metabolic activity of the monocytes was assessed via the MTT assay (Section 2.6.3). The MTT assay evaluates the NADH-dependent reduction of thiazoyl blue tetrazolium bromide to purple formazan crystals; a surrogate of mitochondrial activity (Berridge et al. 2005). Notably, cells cultured in hypoxic conditions for 4 hours showed, on average, a $15.6\% \pm 3.1\%$ reduction in metabolic activity when compared to cells cultured in normoxia (**Figure 3.5A**). This suggested that there is altered mitochondrial dependence in hypoxia. This was not unsurprising, as glycolytic metabolism is typically associated with hypoxic conditions, especially in the tumour microenvironment (Eales et al. 2016). Therefore, to further evaluate this pathway, two methods were chosen; transcriptional changes in glycolytic genes and lactate secretion. With regard to the transcriptional changes, monocytes cultured under hypoxic conditions showed increases in several of the glycolytic genes evaluated; GLUT-1, HK2, PGK1 and LDHA (**Figure 3.5B**). Taken together this suggested that glycolytic enzymes were up-regulated, at least at transcript level, throughout all stages of the pathway (illustrated in **Figure 1.5**) in hypoxia. In agreement with this, the level of lactate secreted into the cell culture supernatant was augmented after 16 hours of exposure to hypoxic conditions (**Figure 3.5C**). However, it should be appreciated that this experiment was only performed on one healthy donor while the samples were performed in triplicate.

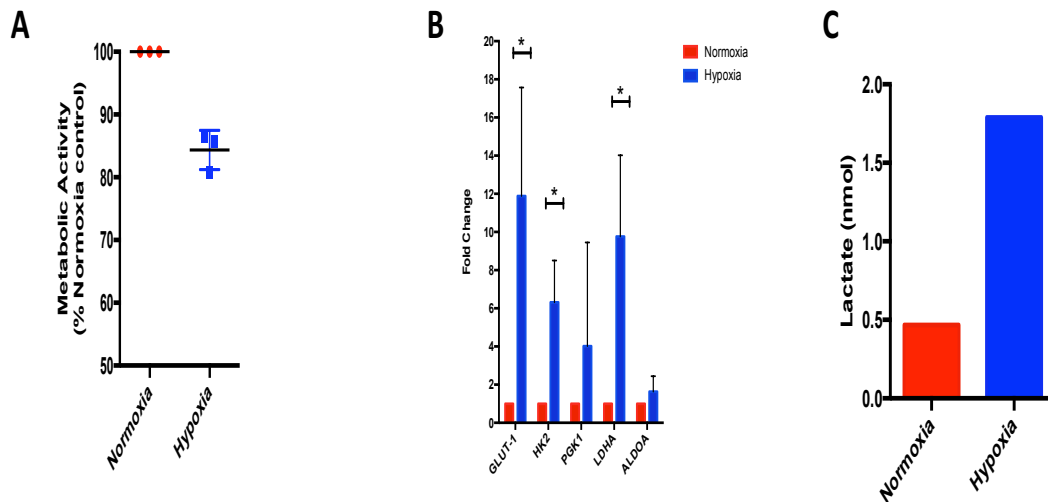


Figure 3.5 Monocytes are metabolically distinct in hypoxic conditions. [A] MTT assay of monocytes cultured normoxia or hypoxia (1% O₂) for 4 hr. *N* = 3. [B] Monocytes were cultured in normoxia or hypoxia (1% O₂) for 4 hours and the expression of genes of the glycolytic pathway were assessed by qPCR. Fold change in hypoxia relative to normoxia (control) shown. Statistically analysed by *t* Test. * *p* < 0.05. *N* = 3. [C] Monocytes were cultured in normoxia or hypoxia (1% O₂) for 16 hours and the levels of lactate secretion was assessed by lactate assay. *N* = 1. All data shown as the Mean ± SD.

Collectively, these results confirm that the monocyte response to hypoxia included the modulation of cellular metabolism, which justified evaluation of the global metabolome via mass-spectrometry. To assess the metabolome of the monocytes in normoxia and hypoxia, the intracellular metabolites were harvested at three time-points and prepared as described in Section 2.10.1. It is important to note that due to the perceived heterogeneity of human samples this dataset was based on one human donor but individual metabolic profiles are from independent wells. Thus, when interpreting these data, we have to take into account that all observations are donor specific and further work would need to be done to demonstrate that these changes are universal and have biological significance. The first extraction was immediately after plating (T₀), to obtain a baseline level of metabolites in the cells at the start of the culture. The second point of extraction was at 1 hour after exposure to normoxia or hypoxia (1% O₂). The final extraction was at 4 hours of exposure to normoxia or hypoxia (1% O₂). The metabolite extracts were then analysed at the Glasgow Polyomics Facility by liquid-chromatography mass spectrometry (Section 2.10.3).

Once the metabolites were analysed by the mass spectrometer, the data was processed through the IDEOM Excel based pipeline (Section 2.10.4; (Creek et al. 2012)). IDEOM is a macro-enabled Excel template for the automated processing of mass spectrometry raw data files into annotated metabolite lists. Subsequently, IDEOM provides a number tools for data analysis and visualisation for biological interpretation. This package offers a more simplified method for metabolite identification and the removal of noise against more complex alternatives, which use specialised statistical software (Creek et al. 2012).

As this is an untargeted analysis, there were two levels of identification of metabolites, according to the metabolomics standards initiative (MSI). The first and most confident level is by identification (mass and retention time) of a metabolite against an authentic standard, of which a standard mix is included in the analysis. If no authentic standard is included, then the metabolites (annotations) are identified on the basis of mass. After the initial automated identification of metabolites, the peaks of the identified metabolites were manually checked by interrogating the peak shape in the IDEOM package. Peaks which did not show Gaussian-like integrity (i.e. presence of shoulders and noise) were excluded from the analysis. This step is important to exclude any false identifications from the IDEOM pipeline. Metabolites which are identified as lipids were also excluded from any further analysis. This is because lipids generally elute from the column as a bolus and cannot be discriminated by retention time on this LC-MS method. Thus, the putative identification that is made by IDEOM is considered unreliable.

After data filtering (as described above), the resulting metabolites were analysed via PCA analysis to investigate the overall influence of time-point and oxygen tension. The PCA analysis demonstrated that there was a distinct separation in metabolic profile between cells at T0 and cells that have been cultured in plates for a period of time (**Figure 3.6A**). Moreover, specific analysis of the 1h and 4h samples revealed that there is also a time-dependent metabolic profile (**Figure 3.6B**), and this is independent of normoxia and hypoxia. Despite the changes cell culture has over time on the metabolic profile of the monocytes, our main interest was to interrogate the metabolic changes between normoxia and hypoxia. Therefore, the samples were examined at the 1 hour and

4 hour time-points separately (**Figures 3.6C & 3.6D**). In both cases, the metabolic profiles between normoxia and hypoxia showed some separation in the PCA, albeit with some overlap at each time-point (**Figures 3.6C & 3.6D**).

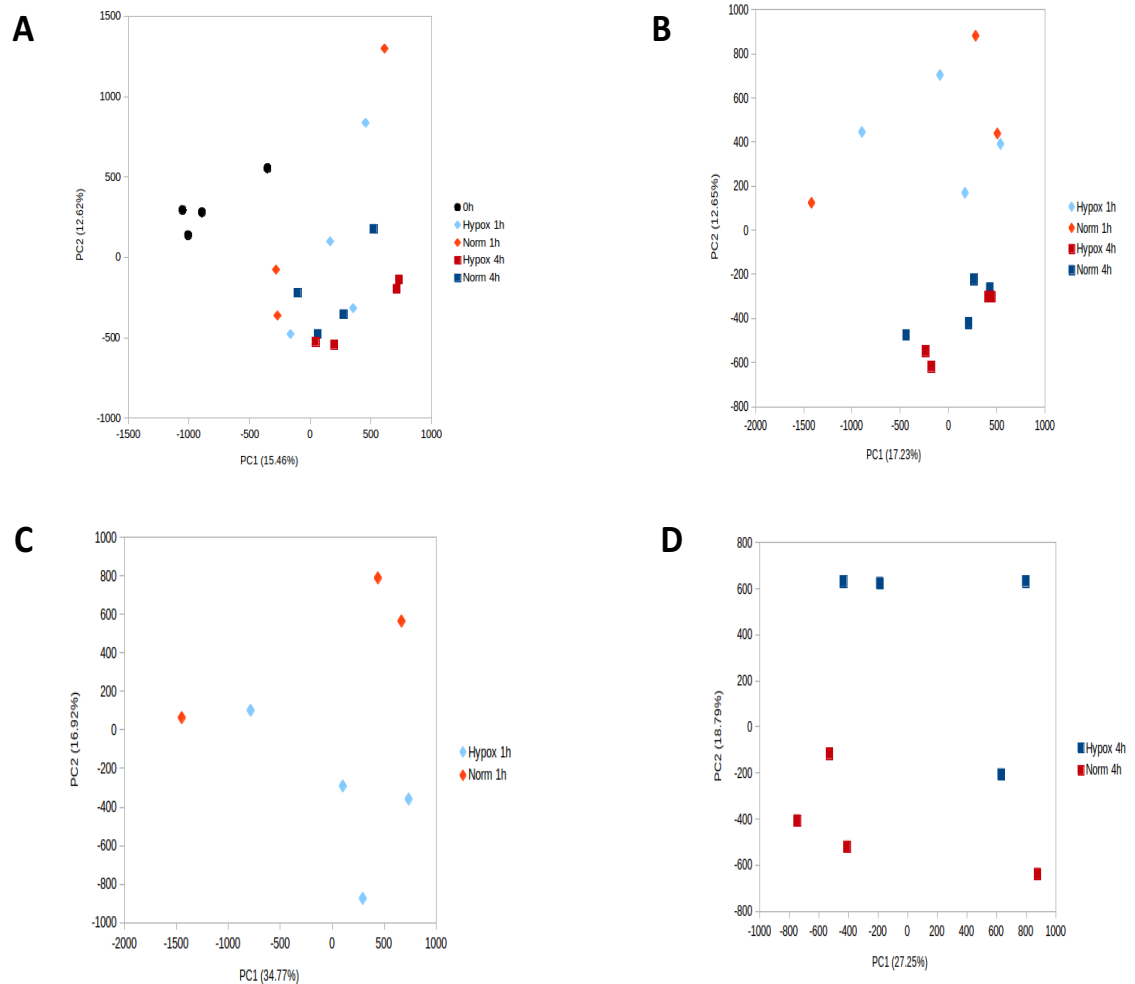


Figure 3.6 The monocyte metabolome changes over time and between normoxia and hypoxia. **[A]** PCA plot of the monocyte metabolome after extraction at 0 hours of culture, and at 1 hour and 4 hour of culture in normoxia and hypoxia (1% O₂). **[B]** PCA assessing the metabolome without the 0 hour time-point. **[C]** PCA assessing the 1 hour time-point between normoxia and hypoxia (1% O₂) only. **[D]** PCA assessing the 4 hour time-point between normoxia and hypoxia (1% O₂) only. The dataset was generated from one human donor with individual metabolic profiles from 4 independent wells.

To begin to investigate the metabolites that were contributing to this separation, heatmap analysis was performed. For this analysis, all time-points and conditions were compared to the metabolic profile obtained at T0. Visualisation of the data (**Figure 3.7A**) further illustrated the change in

metabolism between T0 and 4 hours of culture. Interestingly, the 1 hour culture appeared to have what resembled an intermediate metabolic profile between T0 and 4 hours. However, the focus of this study (as indicated above) was to evaluate the impact of hypoxia on cellular metabolism. To investigate this, the metabolic changes between normoxia and hypoxia (at 1 hour and 4 hour) was interrogated at single metabolite level by analysing the peak intensity data. At 1 hour of culture, 14 metabolites were significantly altered via hypoxia ($p < 0.05$) compared to normoxia. Thirteen of the metabolites decreased in hypoxia compared to normoxia, whilst only one had higher abundance (**Figure 3.7B & Table 3.1**). Evaluation of the 4 hour time point revealed that 33 metabolites were significantly altered in hypoxia compared to normoxia. Nineteen metabolites were of higher abundance in hypoxic conditions, while 14 metabolites were of lower abundance (**Figure 3.7B & Table 3.2**).

Interrogation of the metabolic pathways that were associated with the differentially identified metabolites at 1 hour revealed that there appeared to be a lower level of metabolites associated with mitochondrial metabolism. This included malate and fumarate, both TCA cycle intermediates, and the acylcarnitines, linoelaidylcarnitine and elaidiccarnitine all showing this tendency (**Table 3.1**). This finding suggests that hypoxia promotes immediate changes in mitochondrial processes for the adaptation to hypoxia. The loss of abundance in metabolites here implies that carnitine shuttling of fatty acids into the mitochondria (1.5.4) may be actively inhibited in hypoxic conditions. However, given that only one metabolite was increased at this time-point, the 1 hour extraction may have been too early to postulate which metabolites and associated pathways are increased to compensate for any loss of ATP produced from the mitochondria under these circumstances.

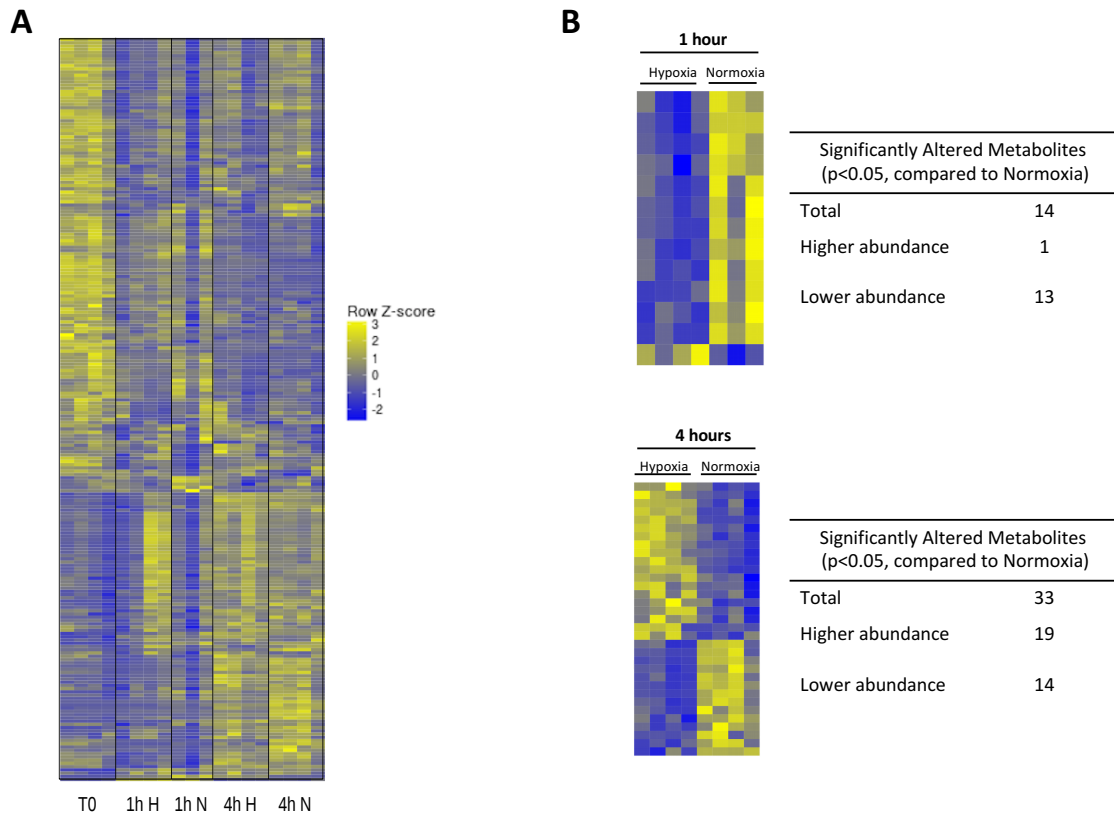


Figure 3.7 The monocyte metabolome changes over time and between normoxia and hypoxia. [A] Heatmap of all significantly altered metabolites (229 metabolites; $p \leq 0.05$) between each condition. Yellow indicates high abundance and blue indicates low abundance. T0 indicates metabolites harvested after 0 hours of culture and normoxia (N) and hypoxia (H; 1% O_2) after 1 hour (1h) and 4 hours (4h) of culture. The data at 1h and 4h was normalised to T0. [B] Heatmaps of significantly different metabolites ($p \leq 0.05$) between normoxia and hypoxia (1% O_2) only at the 1 hour and 4 hour time-points. Yellow indicates high abundance and blue indicates low abundance. The associated table lists the total number of metabolites found to be altered. The metabolites are listed in Tables 3.1 and 3.2 respectively. The dataset was generated from one human donor with individual metabolic profiles from 4 independent wells. The data was statistically analysed by t Test.

KEGG ID	Metabolite	Pathway	Standard	P value	Change
C03741	(S)-4-Amino-5-oxopentanoate			0.0011	Down
C00559	Deoxyadenosine	Purine metabolism	Yes	0.0023	Down
C00122	Fumarate	Tricarboxylic Acid Cycle	Yes	0.0024	Down
C12455	5-Aminopentanal			0.0076	Down
C00093	sn-Glycerol 3-phosphate	Glycerolipid metabolism	Yes	0.0133	Down
C09999	Aralionine A			0.0146	Down
C00149	(S)-Malate	Tricarboxylic Acid Cycle	Yes	0.0163	Down
C06771	Triethanolamine	Glycerophospholipid metabolism		0.0164	Down
No KEGG	hexanamide			0.0239	Down
C01041	Monodehydroascorbate	Ascorbate & Aldarate metabolism		0.0241	Down
No KEGG	Elaidicarnitine	Fatty Acid metabolism		0.0330	Down
C01019	6-Deoxy-L-galactose	Fructose and Mannose metabolism		0.0399	Up
No KEGG	Linoelaidylcarnitine	Fatty Acid metabolism		0.0408	Down

Table 3.1 Significantly altered metabolites in hypoxia (1% O₂) compared to normoxia after 1 hour of culture. Metabolites which do not have a KEGG ID are listed as No KEGG. The standard column indicates the metabolite that had an authentic standard during the mass spectrometry analysis. Metabolites with a P value ≤ 0.05 are listed. Change indicates whether the metabolite was increased (up) or decreased (down) in abundance in comparison to the level of abundance in normoxia.

KEGG ID	Metabolite	Pathway	Standard	P value	Change
C00262	Hypoxanthine	Purine Metabolism	Yes	0.00004	Up
C00093	sn-Glycerol 3-phosphate	Glycerolipid Metabolism	Yes	0.0001	Up
C03017	O-Propanoylcarnitine	Fatty Acid metabolism		0.0004	Down
C00118	D-Glyceraldehyde 3-phosphate	Glycolysis / PPP		0.0009	Up
No KEGG	N-(octanoyl)-L-homoserine			0.0014	Down
C00354	D-Fructose 1_6-bisphosphate	Glycolysis		0.0019	Up
C00447	D-Sedoheptulose 1_7-bisphosphate	Energy metabolism		0.0025	Up
C03901	Thiomorpholine 3-carboxylate			0.0039	Down
C00197	3-Phospho-D-glycerate	Glycolysis / PPP	Yes	0.0041	Up
C00065	L-Serine	Glycine, serine, threonine metabolism	Yes	0.0042	Up
C03771	5-Guanidino-2-oxopentanoate	Arginine & proline metabolism		0.0042	Down
C03741	(S)-4-Amino-5-oxopentanoate			0.0046	Down
C00042	Succinate	Tricarboxylic acid cycle	Yes	0.0088	Down
C00003	NAD+	Oxidative Phosphorylation		0.0095	Down
C02504	2-Isopropylmaleate	Valine, leucine and isoleucine biosynthesis		0.0121	Down
C00130	IMP	Purine Metabolism	Yes	0.0123	Up
C00670	sn-glycero-3-Phosphocholine	Glycerophospholipid metabolism	Yes	0.0134	Up
C03248	Acetylenedicarboxylate	Pyruvate Metabolism		0.0138	Down
C03824	2-Aminomuconate semialdehyde	Tryptophan metabolism		0.0143	Down
C00327	L-Citrulline	Arginine biosynthesis	Yes	0.0149	Up
No Kegg	2-Methylbutyrylcarnitine	Fatty Acid metabolism		0.0200	Down
C13050	Cyclic ADP-ribose	Calcium signalling pathway		0.0204	Down
C00668	D-Glucose 6-phosphate	Glycolysis / PPP	Yes	0.0230	Up
C00064	L-Glutamine	Amino acid & Nucleotide metabolism	Yes	0.0271	Up
C06455	Hydroxymethylphosphonate	Phosphonate metabolism		0.0288	Up
C00318	L-Carnitine	Fatty Acid metabolism	Yes	0.0297	Down
C01144	Hydroxybutyrylcarnitine	Fatty Acid metabolism		0.0347	Up
C00020	AMP	Purine metabolism		0.0434	Up
C00137	myo-Inositol	Galactose metabolism		0.0440	Up
C01092	8-Amino-7-oxononanoate	Biotin metabolism		0.0464	Down
C00077	L-Ornithine	Arginine biosynthesis	Yes	0.0481	Up

C00559	Deoxyadenosine	Purine metabolism	Yes	0.0484	Up
C00209	Oxalate	Glyoxylate and dicarboxylate metabolism		0.0490	Up

Table 3.2 Significantly altered metabolites in hypoxia (1% O₂) compared to normoxia after 4 hours of culture. Metabolites which do not have a KEGG ID are listed as No KEGG. The standard column indicates the metabolite that had an authentic standard during the mass spectrometry analysis. Metabolites with a P value ≤ 0.05 are listed. Change indicates whether the metabolite was increased (up) or decreased (down) in abundance in comparison to the level of abundance in normoxia.

Due to the increased number of metabolites altered at the 4 hour time-point under hypoxic conditions further analysis was focussed on this dataset. Based on the pathway associations (**Table 3.2**), there were three main metabolic aspects which appeared to be changed under hypoxic conditions; mitochondrial metabolism, glycolysis, and purine metabolism. These metabolic nodules contained at least four altered metabolites. Whereas the majority of the other identified pathways only contained one significantly changed metabolite (**Table 3.2**). With regard to mitochondrial metabolism (**Figure 3.8**), this dataset illustrated a reduction in cellular carnitine levels in hypoxic conditions. Carnitine can be synthesised by the methylation of the amino acid lysine or can be obtained from the diet. In its unbound form (L-carnitine), carnitine binds cytosolic fatty acid acyl groups on the outer mitochondrial membrane to form acyl-carnitines through the carnitine palmitoyltransferase I (CPTI) enzyme. The acyl-carnitine then transports the acyl group to the inner mitochondrial membrane. The acyl group is then released from the carnitine and trafficked through to the mitochondrial matrix, where it binds a fatty acid CoA to form acyl-CoA (**Figure 3.8A**). The fatty acid acyl-CoA then undergoes β -oxidation to form acetyl-CoA, which then enters the TCA cycle for the production of ATP. In this dataset, we have identified that both the unbound carnitine (L-carnitine) and a group of acyl-carnitines (O-propanoylcarnitine, hexanoylcarnitine & 2-methylbutyrylcarnitine) are substantially decreased after exposure to hypoxia (**Figure 3.8B**). Furthermore, the TCA cycle intermediate, succinate, had a lower level in extracts taken from hypoxic conditions (**Figure 3.8C**). Staying with mitochondrial metabolism, the electron carrier, NAD⁺ was also reduced in monocytes cultured in hypoxic conditions (**Figure 3.8D**). These results could have indicated that the reduction in carnitine metabolites could influence

subsequent mitochondrial activities for the generation of ATP. For example, by reducing the pool of acetyl-CoA for its consumption in the TCA cycle.

It was interesting to note that in a preliminary experiment performed in monocytes cultured in 5% O₂ for 6 hours, alterations in both free carnitine (**Figure 3.9A**) and in acyl-carnitines (**Figure 3.9B**) were observed. Supporting the findings from the dataset obtained through culturing at 1% O₂. This result was encouraging as it showed that this particular metabolic perturbation was reproducible and was identifiable during culture in a milder level of hypoxia.

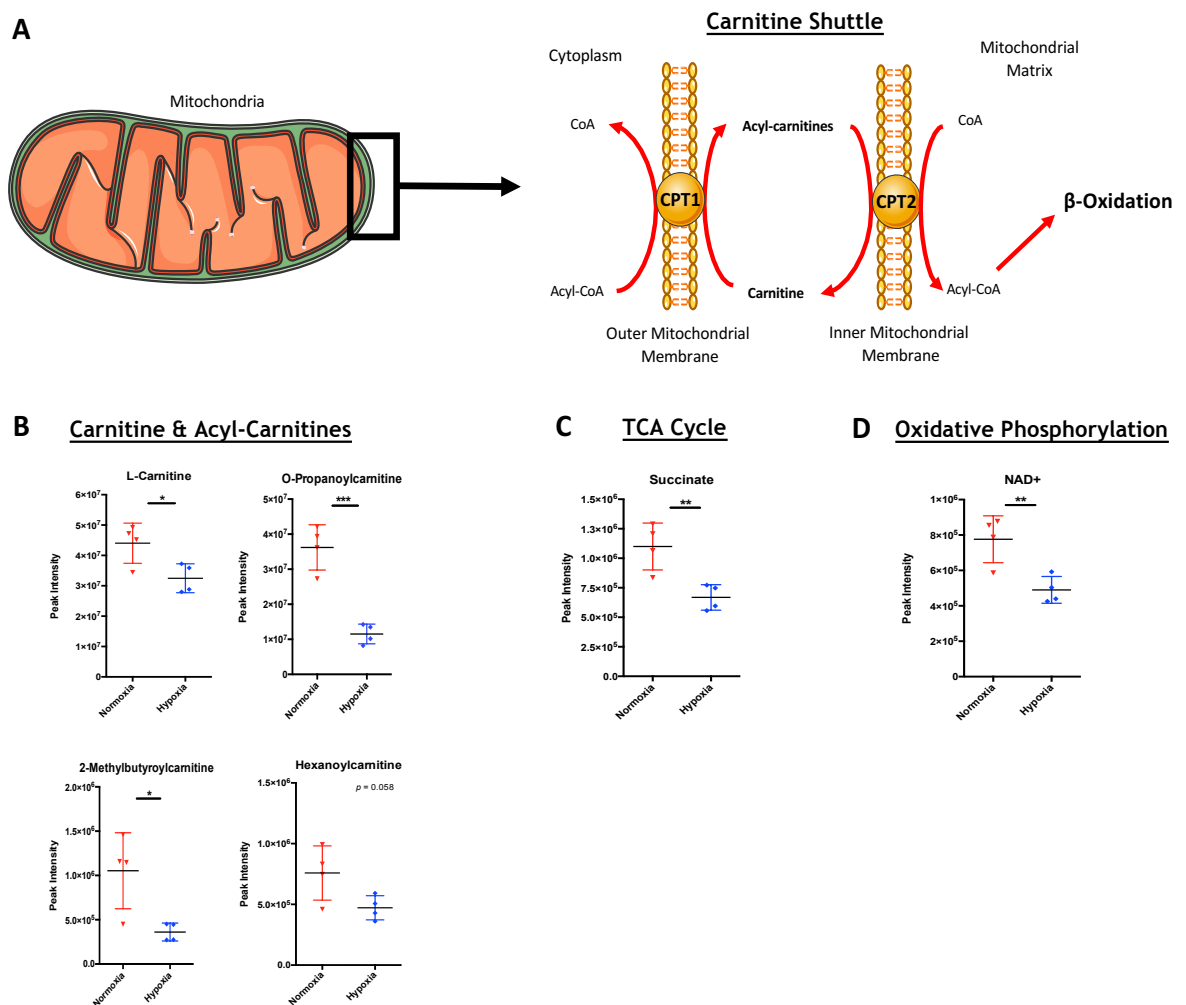


Figure 3.8 Mitochondrial metabolism is altered in monocytes cultured in hypoxia (1% O₂) after 4 hours. Graphical representation of significantly altered metabolites (from the dataset in Figure 3.7B (4 hours) and Table 3.2) associated with mitochondrial metabolism between normoxia and hypoxia (1% O₂) at 4 hours. **[A]** Diagram showing the carnitine shuttling pathway within the mitochondrial membrane (boxed area) **[B]** Alterations in carnitine metabolites associated with the shuttling pathway identified in the dataset. **[C]** Change in abundance of succinate, a TCA cycle intermediate, between normoxia and hypoxia (1% O₂). **[D]** Abundance of the electron carrier, NAD⁺, associated with mitochondrial oxidative phosphorylation. The data was generated from one human donor with individual peak intensities from 4 independent wells.

The data was statistically analysed by t Test. Line shows the Mean \pm SD. * $P \leq 0.05$, ** $p \leq 0.01$, *** $p \leq 0.001$.

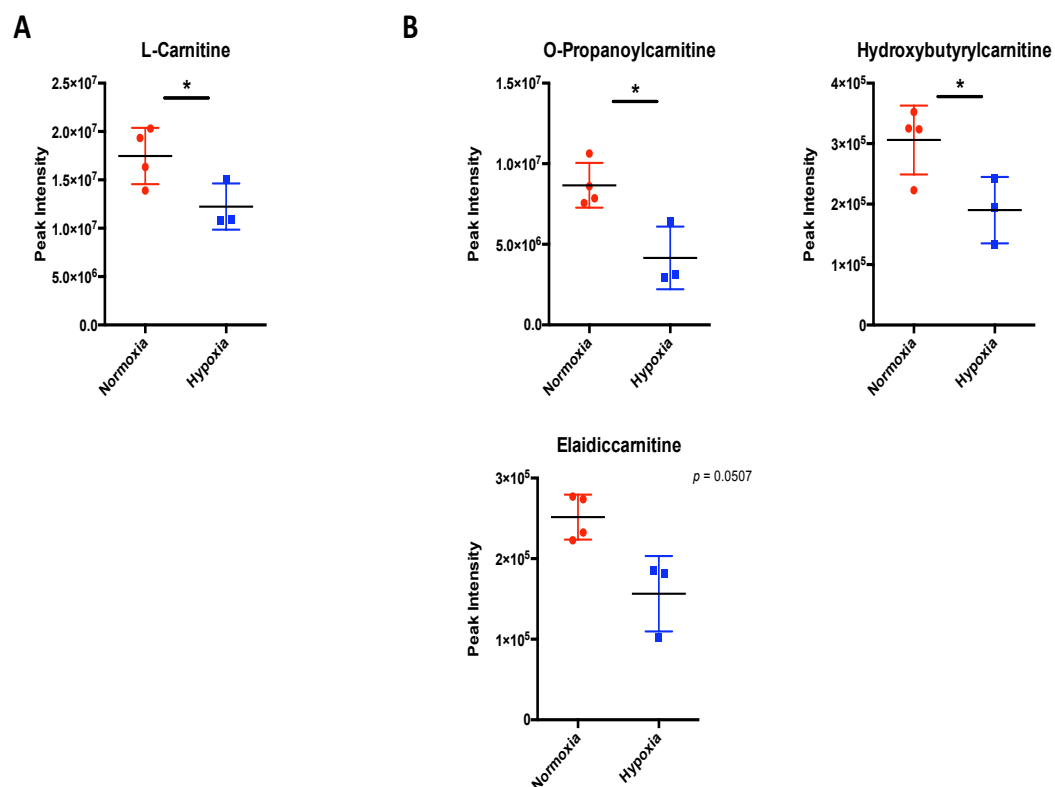


Figure 3.9 Carnitine levels are also altered under 5% oxygen. Monocytes were cultured for 6 hours under normoxia or hypoxia (5% O₂) and metabolites extracted. **[A]** Level of free L-Carnitine in normoxia and hypoxia. **[B]** Levels of altered acylcarnitines between normoxia and hypoxia. Data shown as Mean \pm SD. The dataset was generated from one human donor with individual peak intensities from independent wells. The data was statistically analysed by t Test. Line shows the Mean \pm SD. * $P \leq 0.05$.

First and foremost, these data indicated that mitochondrial metabolism is altered under hypoxic conditions. As the results showed that there was a reduction in the level of identified metabolites, one may assume that the pathway was lower in activity. However, it cannot be ruled out that the carnitine shuttle is highly active when monocytes are first exposed to hypoxia. It could be suggested that once cellular carnitine is depleted in an initial active stage, the lack of oxygen may prevent this pathway from occurring in the long term. Furthermore, as fatty acid β -oxidation, which begins from carnitine, feeds into the TCA cycle, it was encouraging to see the TCA cycle intermediate succinate, was reduced as well.

In juxtaposition to the mitochondrial metabolism pathways, the reverse effect was observed in the glycolytic metabolism, where glycolysis-associated metabolites were significantly increased (**Figure 3.10**). Notably, 4 out of 8 of the key metabolites in the glycolytic pathway (**Figure 3.10**) were putatively identified as being significantly up-regulated after 4 hours of hypoxia. In brief, there was an increase in levels of glucose 6-phosphate, fructose 1:6-bisphosphate, 3-P-Glyceraldehyde and 3-P-Glycerate (**Figure 3.10**). These results show that glycolysis may be increased in hypoxic conditions, which is in agreement with the transcriptional data in **Figure 3.5B**. As lactate is produced from pyruvate in anaerobic conditions, it was reassuring that there was an increased level of lactate production in monocytes under hypoxia (**Figure 3.5C**), illustrating that the cells are undergoing glycolysis at a higher rate than in normoxia, and in an anaerobic state. Accelerating glycolytic metabolism under hypoxic conditions may fill the void of ATP left due to the reduction in mitochondrial aspects of metabolism.

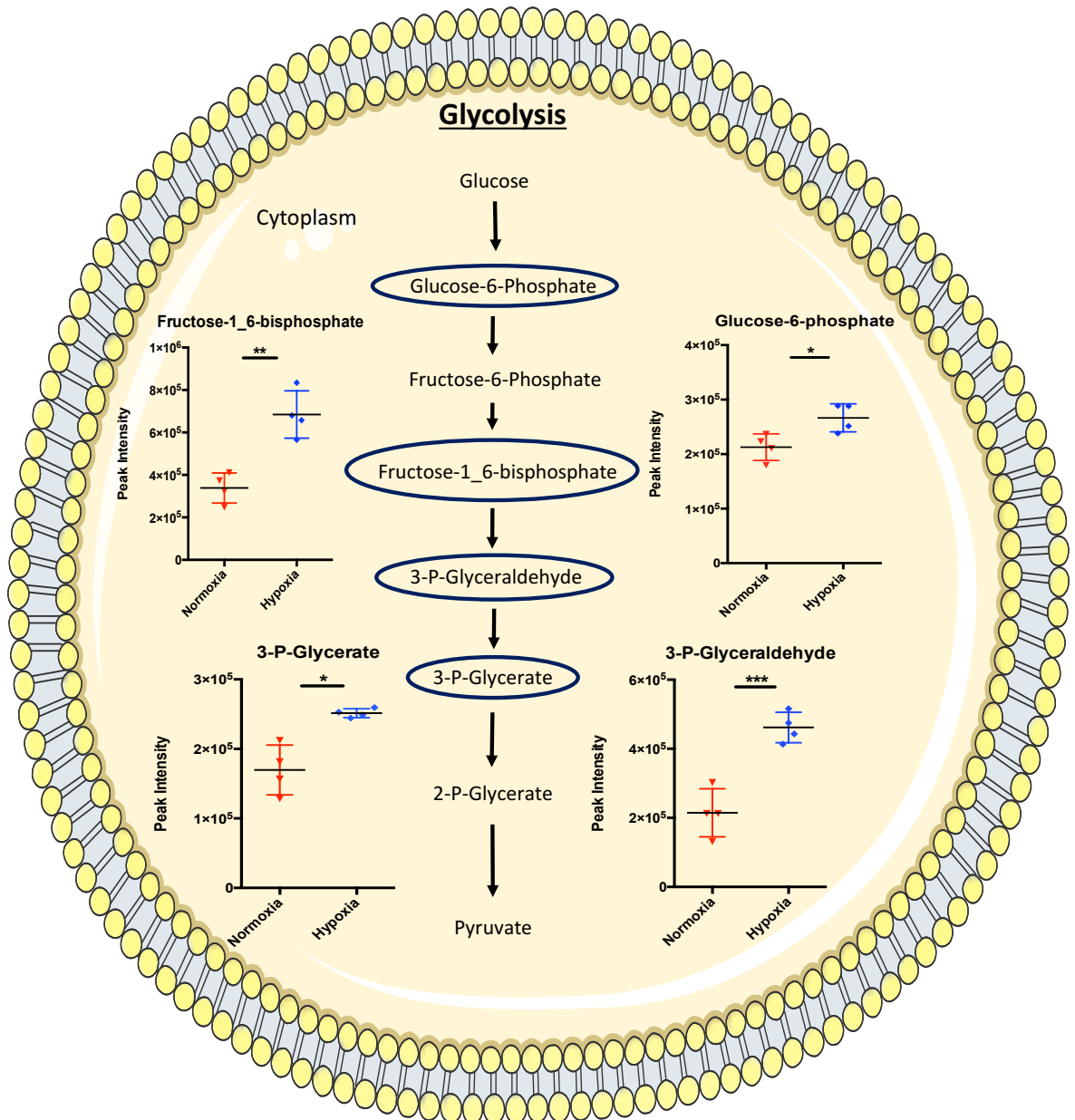


Figure 3.10 Metabolites of the glycolytic pathway are altered under hypoxic (1% O₂) conditions. Illustration showing the glycolytic pathway in the cytoplasm. Graphical representation of significantly altered (circled blue) glycolytic metabolites (from the dataset in Figure 3.7B (4 hours) and Table 3.2) between normoxia and hypoxia (1% O₂) after 4 hours. The levels of these metabolites are shown graphically. The data was generated from one human donor with individual peak intensities from 4 independent wells. The data was statistically analysed by t Test. Line shows the Mean ± SD. * $P \leq 0.05$, ** $p \leq 0.01$, *** $p \leq 0.001$.

Another pathway which was substantially altered in hypoxia compared to normoxia was the metabolism of purines. Purine nucleotides, along with pyrimidines, are classically known as the building blocks of RNA and DNA. Besides their main function to manufacture DNA and RNA, purines are also known to be components of ATP, NADH and CoA. The pathway of key intermediates of purine metabolites (**Figure 3.11**), also illustrates the metabolites (circled) that were significantly increased upon exposure to hypoxia. Notably, the metabolites IMP, AMP, deoxyadenosine and hypoxanthine were all increased in hypoxia compared to normoxia. Purine metabolism has not been covered in great depth in immunological cells, but purine synthesis has been shown to be accelerated in highly proliferative cells, such as cancer cells (Pedley & Benkovic 2017). Therefore, an active state is associated with cells that are met with high bioenergetic demands. It could be speculated that cells adapting to hypoxic conditions are met with a bioenergetic burden. These results suggest that monocytes switch from mitochondrial metabolism, which is a highly efficient process to generate ATP, to anaerobic glycolysis. Anaerobic glycolysis is a highly active process, and although is far less efficient as mechanisms such as oxidative phosphorylation, it is very rapid. Therefore, this active process may require input from purine synthesis which, as stated previously can form components of ATP itself, to compensate for the increased requirement for ATP. In addition, the adaptation process to hypoxia, possibly by HIF-1 α , to mediate this metabolic transition and the transcription and translation of hypoxia-specific genes is energy consuming and may be reliant on nucleotide synthesis.

Purine Metabolism

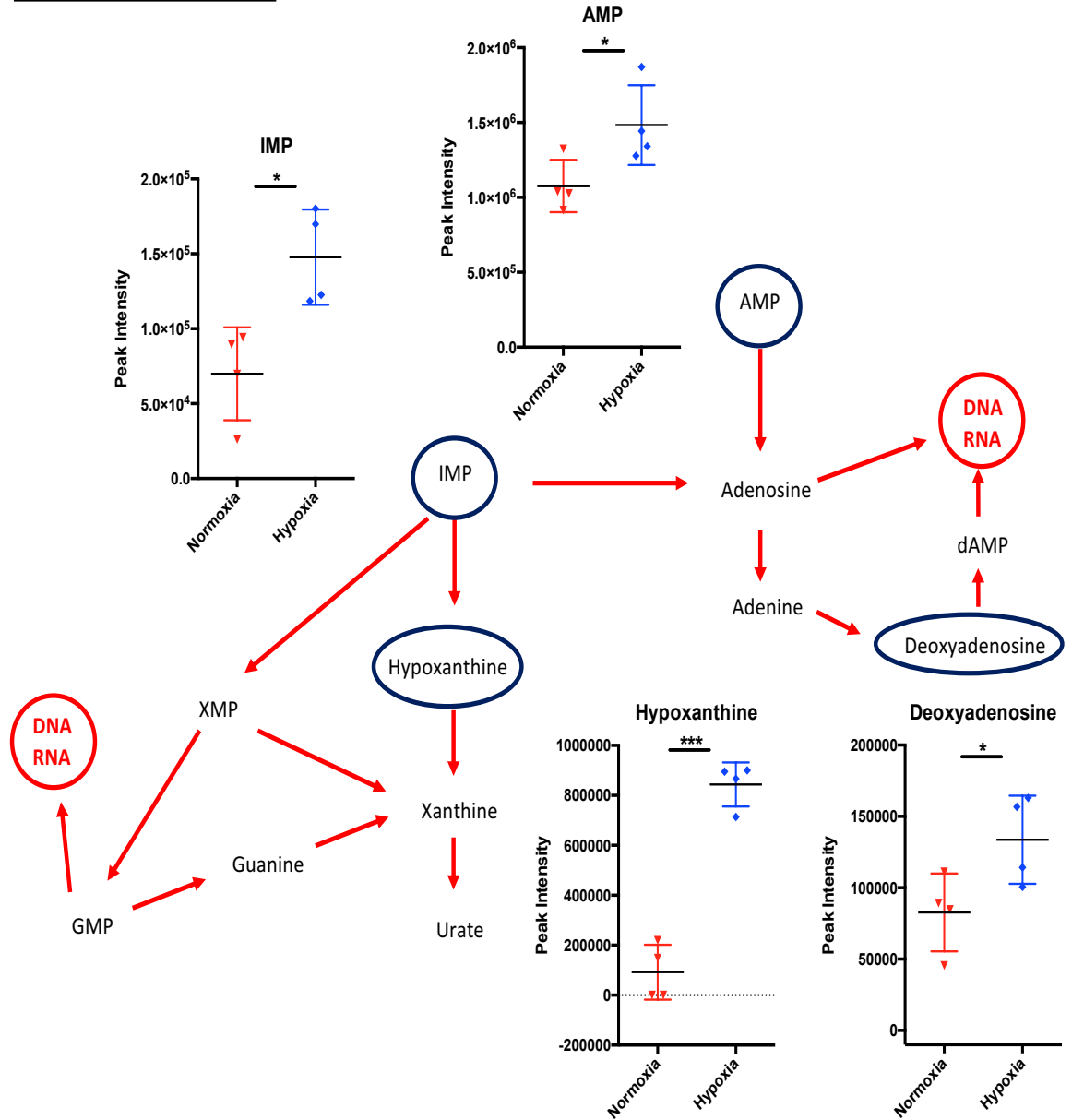


Figure 3.11 Hypoxia (1% O₂) alters purine metabolism in monocytes. Diagram showing the purine metabolic pathway for the synthesis of DNA and RNA. Graphical representation of significantly altered (circled blue) purine intermediates (from the dataset in Figure 3.7B (4 hours) and Table 3.2) between normoxia and hypoxia (1% O₂) after 4 hours. The levels of these metabolites are shown graphically. The data was generated from one human donor with individual peak intensities from 4 independent wells. The data was statistically analysed by t Test. Line shows the Mean ± SD. * $P \leq 0.05$, ** $p \leq 0.01$, *** $p \leq 0.001$.

3.3 Discussion

The presence of tissue hypoxia in chronic inflammatory diseases such as rheumatoid arthritis has been well established. In this chapter, the recruitment of human monocytes into a site of hypoxia was mimicked *in vitro* in order to obtain a metabolic profile of monocytes cultured in these conditions. Firstly, it was confirmed that monocytes were suitably enriched from the isolated PBMC population. Furthermore, hypoxia had a minimal impact on cell viability. From this point, extensive western blot analysis of HIF-1 α at protein level confirmed that the monocytes were adapting to the hypoxic environment by exhibiting stabilised expression. This work gave confidence that a reliable metabolic profile of monocytes adapting to hypoxia could be obtained. After confirming that monocytes had altered transcript levels of glycolytic genes, and secreted an increased level of lactate, a global metabolomic screen of monocytes in hypoxic conditions was conducted. The metabolomics analysis revealed substantial alterations in mitochondrial metabolism, particularly the carnitine shuttle, purine metabolism and glycolysis.

The initial aim of the chapter was to assess the effect, if any, of hypoxia on the ability of monocytes to survive in culture. The results showed that short term hypoxia did not have any detrimental effect on cell apoptosis (**Figure 3.2**). This result is in agreement with other published work (Roiniotis et al. 2009), which showed that human monocytes cultured for 3 days have rather a higher survival rate in hypoxic conditions than in normoxic conditions. In the same study, monocytes were cultured in medium containing only 10% fetal bovine serum, suggesting that M-CSF is not required under these circumstances (Roiniotis et al. 2009). This supports the use of human plasma in the work presented here, which aimed to prevent the immediate induction of macrophage differentiation (discussed in 3.2.1; (Safi et al. 2016)). The increased survival rate extended to monocyte derived macrophages in this publication, which proposes a shared survival mechanism between myeloid cells. Taken together, this reflects a previous transcriptomic study of monocytes in hypoxia, which showed increased expression of the anti-apoptotic protein, Bcl-2 (Bosco et al. 2006). It is thought that an increased level of glycolytic metabolism in myeloid cells in hypoxia acts as an anti-apoptotic mechanism to promote cell survival (Roiniotis et al. 2009). A phenomenon that is classically used in cancer cell metabolism to aid their

survival (D. Huang et al. 2014). Glycolytic metabolism was also observed in human monocytes under hypoxic conditions in this chapter, postulating that monocytes shift their cellular metabolism in hypoxia to meet their survival requirements.

With the knowledge that hypoxic conditions did not significantly impact monocyte viability, HIF-1 α stability at protein level was analysed to confirm that the monocytes were adapting to the hypoxic conditions. HIF-1 α stabilisation in this hypoxic set up occurred after only 3 hours of exposure (**Figure 3.4**).

Although monocytes do stabilise HIF-1 α in this work and in other published work (Fangradt et al. 2012), the precise role of HIF-1 α in monocytes is debatable.

Indeed, in the same study, Fangradt *et al* found that HIF-1 α , a key transcription factor for cellular adaptation to hypoxia, does not translocate to the nucleus and remains solely in the cytoplasm. The authors illustrated that in fact, NF- κ B1 translocated to the nucleus, which they claim is responsible for cellular adaptation to hypoxia. In addition, a novel adaptation process has recently been postulated, whereby mitochondrial complex II downregulation facilitates the transcriptional changes induced by hypoxia in monocytes (Sharma et al. 2017).

Interestingly, pharmacological inhibition of complex II highlights that this adaptation appears to be independent of HIF-1 α stabilisation, which is in support of the earlier work (Sharma et al. 2017; Fangradt et al. 2012). Taken together, this work illustrates that hypoxia adaptation in human monocytes may be independent of the HIF system. However, its stabilisation in hypoxic conditions in this chapter suggests a role for HIF-1 α cannot be completely ruled out. The work presented here aimed to confirm the stabilisation of HIF-1 α as a marker of hypoxia induction, however, genetic studies would be needed to establish the role, if any, of HIF-1 α in hypoxia adaptation. In support of a role for HIF-1 α , increased expression of the HIF-1 α inducible genes CXCR4 and VEGFA was observed in monocytes under hypoxic conditions (**Figure 3.4**), which is in agreement with published studies (Fangradt et al. 2012; Bosco et al. 2006).

The main aim of the chapter was to determine the metabolic impact of hypoxia on monocytes. Before carrying out mass spectrometry based metabolomics, it was found that hypoxic conditions increased the expression of genes associated with the glycolytic pathway and an increase in secretion of lactate, a by-product

of anaerobic glycolysis (**Figure 3.5**). In addition, monocytes cultured in hypoxia showed alterations in metabolic activity in the MTT assay (**Figure 3.5**). Although the MTT assay is widely used to assess proliferation and cell viability, it actually measures the rate of reduction of MTT salt by NADH oxioeductases in the mitochondria (Berridge et al. 2005). Prior to the mass spectrometry analysis, these data led to a tentative hypothesis that monocytes actively repurpose their metabolism to favour glycolytic metabolism over mitochondrial pathways.

With the culture conditions optimised, we were confident we could obtain a robust metabolic profile of monocytes in hypoxic conditions by mass spectrometry based metabolomics. This work focussed on the metabolic differences which were induced by hypoxia compared to normoxia. The most striking observation, which was detected at both 1% and 5% O₂, was the decrease in cellular carnitine and acyl-carnitines (reviewed in Section 1.5.4). This is in support of published studies showing similar alterations in fatty acid metabolism at transcriptional level when monocytes were exposed to hypoxia (Bosco et al. 2006). This finding endorses the result from the preliminary experiment with the MTT assay, showing that monocytes may be less dependent on mitochondrial metabolism under hypoxic conditions. Carnitine metabolism and fatty acid β -oxidation are typically associated with murine M(IL-4) macrophages, and appears to have a minimal role in M(LPS + IFN γ) macrophages (S. C.-C. Huang et al. 2014; Galvan-Pena & O'Neill 2014). Metabolically speaking, it appears that hypoxia induces a mitochondrial programme which reflects a more inflammatory phenotype than in normoxia. In addition, M(LPS + IFN γ) macrophages classically express NF- κ B for the production of pro-inflammatory mediators, and HIF-1 α has been linked with the production of IL-1 β after succinate accumulation (Tannahill et al. 2013). This suggests that certain intracellular events caused by inflammation and hypoxia may be interlinked. This train of thought can be applied to monocyte trained immunity, where glycolytic metabolism promotes innate-like memory responses via HIF-1 α (Cheng et al. 2014; Saeed et al. 2014). Taking this work into account, the data supports the notion that hypoxia actively limits fatty acid oxidation for the adaptation to hypoxia, which may have direct implications on cellular function, which will be interrogated in **Chapter 4**.

In contrast to the decreased reliance on mitochondrial metabolism under hypoxic conditions. The data in this chapter illustrated that there was a shift to increased glycolytic metabolism (**Figures 3.5 & 3.10**). This is in accordance with macrophages exposed to hypoxic conditions, where HIF-1 α causes a metabolic switch to glycolysis from mitochondrial metabolism (Cramer et al. 2003). This is achieved by inducing the expression of glycolytic enzymes, glucose transporters and lactate dehydrogenase (Mole et al. 2009; Semenza & G. L. Wang 1992). Oxidative phosphorylation (OXPHOS), partly fed by glycolytic pyruvate, predominates in cells in aerobic conditions for the generation of ATP. However, in hypoxia, pyruvate is metabolised to lactate by lactate dehydrogenase to prevent pyruvate supplementing the mitochondria, a process termed anaerobic glycolysis (Semenza & G. L. Wang 1992). Anaerobic glycolysis is a rapid, but very inefficient mechanism of generating ATP in comparison to OXPHOS (2 ATP per glucose). Therefore, the loss of metabolites shown in the mitochondria in the results presented in this chapter could be caused by the increase in glycolysis, fitting with the published work. This metabolic switch may provide a swift means of adaptation and survival in a hypoxic microenvironment in order to carry out effector function.

Another pathway which was altered in the metabolomics data was purine metabolism, where associated metabolites were higher in abundance in hypoxic conditions compared to normoxic conditions (**Figure 3.11**). Up-regulating purine metabolism may act as a means to supplement glycolysis and ATP production. Indeed, in LPS stimulated macrophages, activation of adenosine receptors can increase PFKFB3 activity, which in turn leads to the accumulation of fructose 2,6-bisphosphate. This can then cause increased glycolytic flux and ATP production in activated cells (Ruiz-Garcia et al. 2011). Whether this phenomenon occurs in unstimulated cells exposed to hypoxia remains to be seen, as this seemed to be dependent on Sp1 and adenosine receptor expression following TLR activation (Ruiz-Garcia et al. 2011). However, studies assessing adenosine receptor expression under hypoxic conditions could reveal if this mechanism is involved during hypoxia adaptation. Nevertheless, these results propose that purine metabolism is increased in hypoxic conditions to enhance glycolytic fluxing during metabolic switching.

In summary, this chapter illustrated how monocytes adapt to hypoxic conditions at a metabolic level. Early optimisation studies presented here ensured that the metabolic profile captured was from a pure, viable monocyte population that was readily adapting to hypoxic conditions. Metabolomics analysis revealed that monocytes appear to switch their metabolism from mitochondrial pathways, particularly fatty acid transport, to glycolysis to generate ATP. This seems to be supplemented via an increased level of purine metabolism, which may further promote glycolytic fluxing. With the knowledge that monocytes differ metabolically upon exposure to hypoxia, the next chapter will address what functional impact hypoxia may have and if this can be altered by metabolic manipulation.

Chapter 4. Assessing the impact of hypoxia on the functional profile of monocytes.

4.1 Introduction

The previous chapter illustrated the direct influence hypoxia had on monocyte metabolism. However, the impact of hypoxia on the monocyte cellular functionality was not determined. In this chapter, a number of assays were used to assess how resting and activated monocytes react at a functional level under hypoxic conditions. Furthermore, using the metabolomics insights gained from the studies in **Chapter 3**, experiments in this chapter were also aimed at addressing how altering the identified metabolic pathways could manipulate monocyte function.

As discussed in section **1.3.1**, the chronic inflammatory environment can be extremely hypoxic (Lund-Olesen 1970), and we hypothesised that this directly influences monocyte function. The literature surrounding the impact of hypoxia on monocyte function is limited. However, early studies did reveal that the chemokine receptor CXCR4 was upregulated in monocytes under hypoxic conditions (Schioppa et al. 2003); a finding which was confirmed in **Chapter 3**. Furthermore, monocytes and macrophages exhibited a reduced migratory capacity under hypoxia (L. Turner et al. 1999; Grimshaw & Balkwill 2001). Additional insights into monocyte metabolism and function were made via the global transcriptomic analysis of monocytes cultured in 1% O₂ for 16 hours (Bosco et al. 2006). This study produced supporting evidence that monocytes modulate their chemotactic activities under hypoxia, particularly by increasing their expression of CCL20; a finding which carried through to the protein level. In addition to the alteration in CCL20, this study went on to show that a monocyte's ability to scavenge was also effected by exposure to hypoxia. In brief, the investigators observed altered expression of specific scavenger receptors. Notably, both MARCO and MSR1 were upregulated while CD163 and STAB1 were down-regulated. Follow-on studies by the same group demonstrated that CCL20 induction was via NF- κ B in a CD300a-dependent pathway (Raggi et al. 2014).

Although these findings illustrated that hypoxia influences both monocyte function and cellular metabolism. There is a paucity of research that suitably describes what effect hypoxia-specific metabolism may have on cellular function in hypoxia, and whether these metabolic alterations prime the cells towards an inflammatory state. This train of thought was supported by studies which showed that hypoxia exacerbates the release of pro-inflammatory mediators from palmitate-activated macrophages by increasing JNK pathway activity (Snodgrass et al. 2016).

The metabolomics results from the previous chapter highlighted decreases in carnitine metabolites, which suggested a down-regulation of FAO in hypoxic conditions. In terms of myeloid cells, FAO has largely been considered to have a regulatory role. This was primarily due to studies suggesting that murine macrophages rely on this pathway for the induction of an M(IL-4) phenotype and the reduction of pro-inflammatory cytokines released from these cells (Vats et al. 2006). More recent work has since highlighted that FAO is favoured in murine M(IL-4) macrophages for the clearance of parasitic infections *in vivo* (S. C.-C. Huang et al. 2014). However, these findings have not been translated into the human M(IL-4) macrophages, which appear to be independent of FAO (Namgaladze & Brüne 2014; Nomura et al. 2016). Nevertheless, these studies highlight a potentially important role for FAO in the regulation of inflammation in myeloid cells. Given the altered state of carnitines in hypoxia (Section 3.2.3), the regulation of inflammatory mechanisms in monocytes may be impaired under these conditions.

Despite this body of research suggesting a regulatory role for FAO in macrophages. Studies utilising the carnitine shuttling inhibitor, etomoxir (ETO), has shown that FAO has an influence on macrophage inflammatory function as well. Indeed, it is now apparent that oxidation of the fatty acid palmitate via CPT1a can activate the NLRP3 inflammasome and promote the production of IL-1 β and IL-18 in macrophages (C. J. Hall et al. 2013; Wen et al. 2011). Furthermore, hexokinase-1 dependent glycolysis and fatty acid synthesis are known to contribute to this inflammatory cascade (Moon et al. 2015). This illustrated that metabolic pathways are not separate entities and are rather interlinked in a complex manner when influencing immune cell function. Taken

together, the studies implicated that FAO has the ability to participate in both inflammatory and anti-inflammatory mechanisms in macrophages. Therefore, the studies in this chapter will interrogate if the reduction in cellular carnitine promotes monocytes towards an inflammatory or anti-inflammatory state.

In juxtaposition to the reduction of carnitine metabolites under hypoxic conditions in **Chapter 3**, glycolytic metabolites and enzymes were up-regulated (Section 3.2.3). This led to the hypothesis that monocytes actively switch their metabolism in order to survive under these conditions (Roiniotis et al. 2009). In addition to offering survival mechanisms, glycolytic metabolism has been at the forefront of immune-metabolic literature for the control of inflammatory functions in myeloid cells. The adoption of glycolytic metabolism in macrophages was initially evident in M(LPS ± IFN γ) cells (Rodriguez-Prados et al. 2010). More recent work has since shown that inhibition of glycolysis by 2-DG prevented the production of IL-1 β in murine M(LPS) macrophages (Tannahill et al. 2013). Furthermore, it has been reported to form the molecular basis of memory responses in monocyte trained immunity models (Cheng et al. 2014; Saeed et al. 2014). In addition to glycolysis, monocyte trained immunity and macrophage IL-1 β production are thought to be mediated by HIF-1 α . Therefore, metabolic rewiring induced by hypoxia to favour glycolysis could have a significant role in exacerbating inflammatory cascades in monocytes.

The governing role of glycolysis in activated macrophages proposed that this pathway is 'pro-inflammatory'. However, other work has suggested that, like FAO, glycolysis displays regulatory properties. For example, it is now apparent that glucose uptake and metabolism is important during the activation of regulatory murine M(IL-4) macrophages (S. C.-C. Huang et al. 2016). Moreover, it has been shown that, GAPDH, when uncoupled from the glycolytic pathway, can inhibit the translation of TNF α mRNA (Millet et al. 2016).

Altogether, these studies highlight the flexible nature of both FAO and glycolysis in coordinating immune responses. The results from **Chapter 3** illustrated that the balance between these two pathways was altered under hypoxic conditions, which may affect monocyte functionality in these circumstances. As reductions in carnitine metabolites were observed (**Chapter 3**), the work in this chapter

focussed on this pathway and its manipulation to assess how it influences pro-inflammatory mechanisms in monocytes under hypoxia.

The aims of this chapter are:

1. Profile the impact of hypoxia on monocyte cellular function
2. Manipulate metabolic pathways found to be altered under hypoxia and assess how this influences monocyte function

4.2 Results

4.2.1 Functional profiling of monocytes under hypoxic conditions

4.2.1.1 Transcriptional analysis

Before any metabolic manipulation, it was important to profile monocytes functionally, to assess if the hypoxia-specific cellular metabolic profile was associated with modulation of any specific monocyte function. To achieve this, we used an array of standard functional assays. These assays have been published extensively, however, studies in this chapter were modelled on a study from Dabritz *et al* (2015), where they comprehensively characterised the function of GM-CSF stimulated monocytes. The transcriptomic profiling study from Bosco *et al* (2006) was also considered when designing a custom-made myeloid Taqman Low Density Array (TLDA) plate. The target genes are outlined in **Table 2.8** and **Figure 4.1A**.

Initial experiments evaluated the impact of short term hypoxia on the transcriptional signature of monocytes, in order to identify particular pathways that may be modified. Thus providing insight into the functional consequences of hypoxia. Monocytes were cultured in normoxia or hypoxia (1% O₂) for 4 hours. Transcriptional analysis of 3 healthy donors via the custom TLDA, revealed that the scavenger receptors CD36 and CD163 were significantly down-regulated in monocytes exposed to hypoxic conditions (**Figure 4.1A**). Which is in support of published work (Bosco *et al*. 2006). In addition to these scavenger receptors, the C-type lectin receptors MRC1, CLEC4E and CD209 were also substantially

decreased. Analysis of the chemokine/chemokine receptor transcripts evaluated in this assay revealed that CCL2, CCL22, CXCL10 and CCR2 all showed decreases in expression upon exposure to hypoxia. In juxtaposition to these down-regulated transcripts, IL-8 expression was increased upon exposure to hypoxia, although this did not reach statistical significance (**Figure 4.1A**). The up-regulation of IL-8 at transcript level in both the work presented here and by Hirani *et al* (2001) suggest a possible hypoxia-specific function of monocytes (Hirani *et al.* 2001).

To validate the transcriptional changes identified at 4 hours and investigate the kinetics of these changes, a time-course experiment was undertaken. Monocytes were cultured in normoxia or hypoxia for 2, 4, 8 and 24 hours, and samples processed for subsequent TLDA analysis. The experiment presented here was carried out in triplicate from 2 healthy donors (**Figures 4.1B, 4.1C & 4.1D**). Analysis focussed on the chemokine/chemokine receptor transcripts confirmed that both CCL20 and IL-8 were up-regulated at 4 hours (**Figure 4.1B**). Despite an initial downregulation of CCL20 (0.5-fold) at 2 hours, its expression was increased at both 4 (5-fold) and 8 hours (4.5-fold), before it decreased to a similar expression to that of normoxia at 24 hours. IL-8 was also up-regulated by 4 hours (11-fold) and the levels of this transcript were maintained over the entire 24 hours (**Figure 4.1B**). All other observed changes (*i.e.*, down-regulated CCL2, CXCL10 and CCL4) were not reproduced in this data set (**Figure 4.1B**).

Evaluation of the scavenger receptor transcript data revealed that CD36 and STAB1 were down-regulated over the 24 hour period (**Figure 4.1C**). It must be noted that the 2 and 8 hour time-points were analysed on a separate TLDA plate to the 4 and 24 hour time-points. This may reflect the fluctuations seen in CD163 expression, which could indicate a plate-specific effect in this instance (**Figure 4.1C**). The decreased level of STAB1 at 4 hours (**Figure 4.1C**) is at odds with the initial TLDA analysis shown in **Figure 4.1A**. However, the data at later time-points was in accordance with the published transcriptomic study (Bosco *et al.* 2006), which was carried out at 16 hours of hypoxic exposure. Taken together, this data proposes that prolonged hypoxia promotes a more robust reduction in expression of scavenger receptors in monocytes. Moreover, the C-type lectin receptors, CLEC4E and CD209, showed a decrease in transcript in hypoxic

conditions, especially at the 24 hour time-point (0.19 & 0.13-fold respectively). This finding was not as robust at earlier time-points, suggesting that longer-term hypoxia is required to modulate C-type lectin receptor transcript levels (**Figure 4.1D**).

One of the most consistent findings from this data, was the decreased expression of CD36 (**Figure 4.1A & 4.1C**). To determine if this decrease in transcript corresponded with a change in protein expression, the cell surface expression of CD36 on monocytes was interrogated by FACS. Monocytes were cultured in normoxia or hypoxia for 16 hours, to allow sufficient time for receptor cycling and were stained for surface CD36. No difference in surface expression between normoxia and hypoxia was observed (**Figure 4.1E**), in technical duplicates of 1 healthy donor tested.

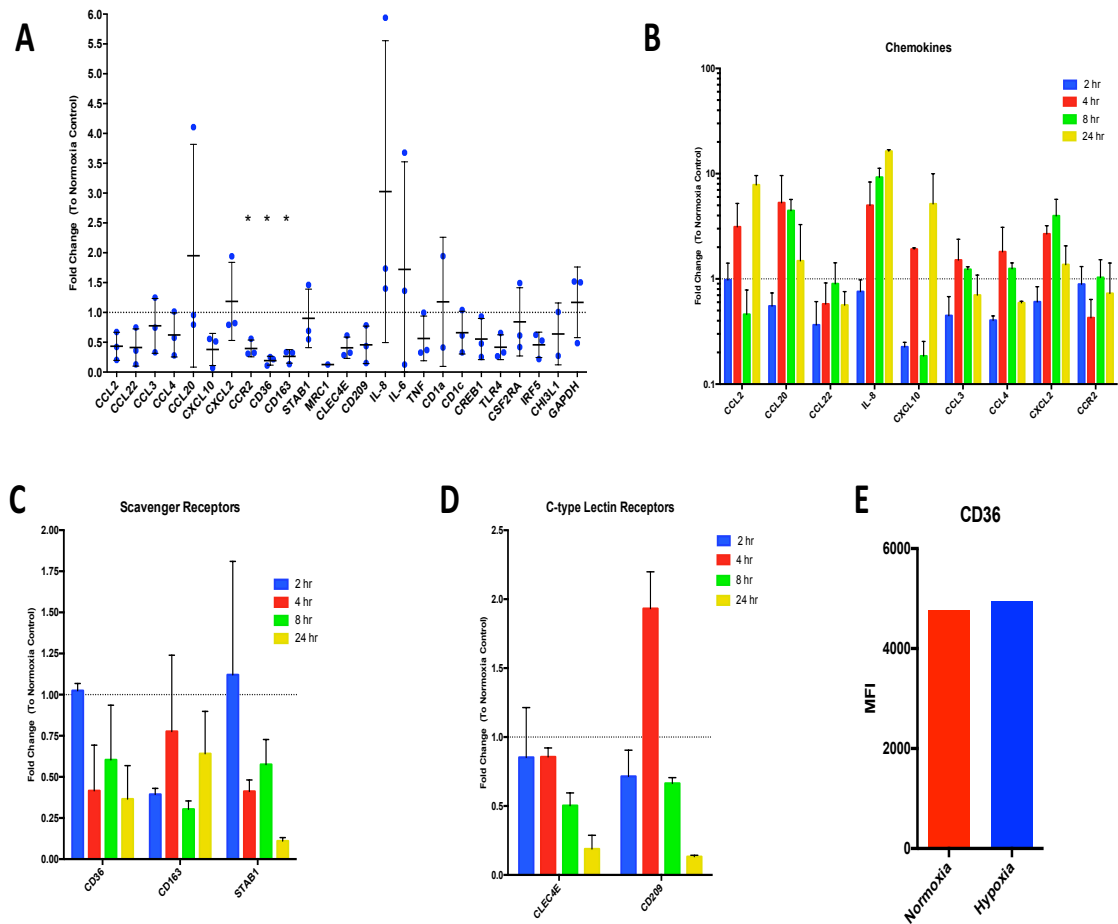


Figure 4.1 Hypoxia induces transcriptional changes in monocytes. [A] Monocytes were cultured for 4 hours in normoxia or hypoxia (1% O₂). The gene expression of indicated targets was analysed by TLDA based qPCR. Data analysed by t Test with Holm-Sidak correction. $N = 3$. * $p < 0.01$. [B-D] Monocytes were cultured for indicated times in normoxia or hypoxia (1% O₂). The gene expression of Chemokines [B], Scavenger receptors [C] and C-type lectin receptors [D] were analysed by TLDA based qPCR. The experiment was carried out in triplicate in 2 donors. [E] Monocytes were cultured for 16 hours in normoxia or hypoxia (1% O₂) and the surface expression of CD36 was analysed by FACS. The experiment was carried out in duplicate in 1 donor. All data shown as the Mean \pm SD.

4.2.1.2 Wound healing & cellular adherence

The transcript data of CD36 and STAB1 in Figure 4.1 suggested that hypoxia could alter the ability of monocytes to scavenge, a function typically associated with M(IL-4) macrophages (Mantovani et al. 2013). Another characteristic of M(IL-4) macrophages which we thought could be affected by hypoxia is the ability to aid in wound healing (Mantovani et al. 2013). Dabritz *et al* (2015) utilised a Caco-2 cell monolayer, and cultured resting or GM-CSF activated monocytes on top of a scratched monolayer and assessed wound closure. Therefore, the impact of hypoxic conditions on a monocyte's ability to close a

scratch in a wound healing assay was investigated. Initial experiments using the Caco-2 cell monolayer assay were technically compromised due to tearing and necrosis induced by the sterile pipette tip method of scratching (**Figure 4.2A**). Based on this technical issue, the type of cells and the method of cell separation was changed. In all subsequent experiments HUVECs were used and in order to limit scratch size variability, IBIDI silicone cell culture inserts were utilised. The silicone inserts are supplied in small petri dishes and contain two chambers for cell culture, separated by a silicone 'wall'. Once the HUVECs were confluent in each chamber, the silicone insert was removed to create a consistent cell free 'wound' of 500µm in length (**Figure 4.2B**). In a separate culture, monocytes were conditioned in normoxia or hypoxia for 4 hours and were then transferred onto the HUVEC monolayer. The wound was allowed to close for 16 hours in normoxia and the rate of healing was measured by light microscopy and ImageJ software. The addition of monocytes into this assay, regardless of prior exposure to normoxia or hypoxia, did not alter wound closure when compared to the control (no cell addition) (**Figure 4.2B & 4.2C**). Thus, within the realms of this experimental set up, hypoxia had no impact on the ability of monocytes to aid wound healing.

Another known function of monocytes is their ability to adhere to endothelial cells (Tso et al. 2012). Therefore, we assessed if hypoxia modulated adherence properties of monocytes. To this end, monocytes were cultured in normoxia or hypoxia for 4 hours. In addition, monocytes were treated with LPS, which has been previously shown to enhance adherence properties in these cells (Hmama et al. 1999). Non-adherent cells were washed off the plate and adhering cells were stained by crystal violet. The stain was then solubilised and read on a microplate reader to assess adherence. Both hypoxia or LPS had no impact on the capacity of monocytes to adhere in tissue culture plates in this assay compared to untreated cells in normoxia (**Figure 4.3**). Indicating that short-term hypoxia may not alter the ability of monocytes to adhere.

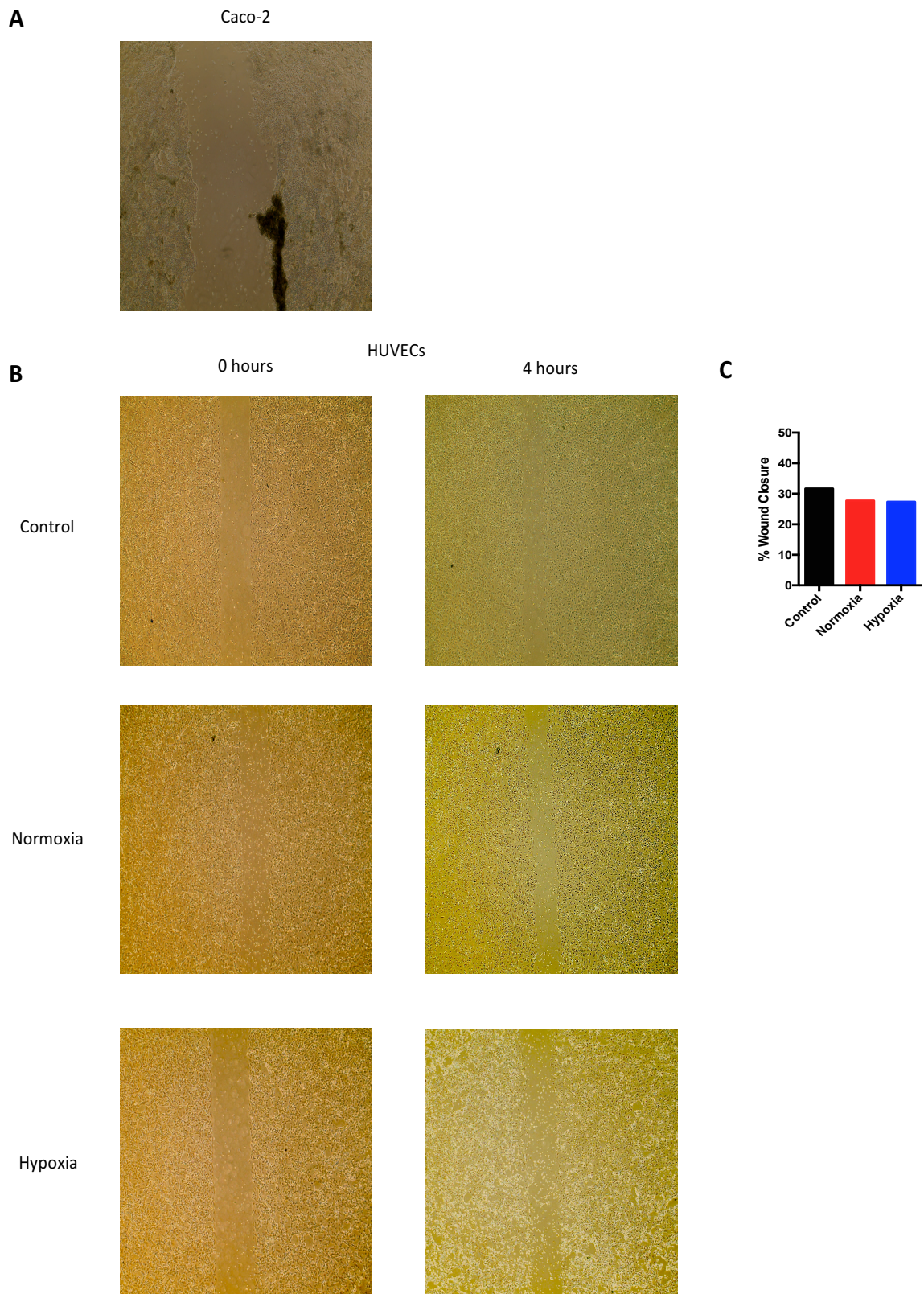


Figure 4.2 Hypoxia has a minimal impact on wound healing in monocytes. [A] Representative image of a Caco-2 cell monolayer after scratching with necrotic region (Black). **[B]** Monocytes were cultured in normoxia or hypoxia for 4 hours and were then transferred onto a HUVEC monolayer after removal of an IBIDI cell culture insert. The control refers to a monolayer with no monocytes added. The cells were then left for 16 hours to allow for wound closure in normoxic conditions. **[C]** Graphical representation of wound closure, analysed by ImageJ. Data shown as Mean. The experiment was carried out in triplicate in 1 healthy donor.

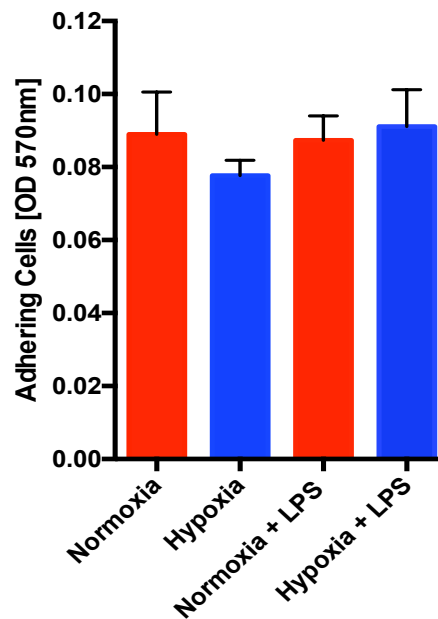


Figure 4.3 Hypoxia has a minimal impact on cellular adherence in monocytes. Monocytes were cultured in normoxia or hypoxia \pm 100ng/ml LPS for 4 hours. Adherent cells were subject to crystal violet staining, which was solubilised and analysed at 570nm. Data shown as the Mean \pm SD. The experiment was carried out in triplicates in 2 human donors.

4.2.1.3 Pro-inflammatory mediator release

The previous data highlighted that hypoxia had no observable effect at functional level in terms of scavenger receptor expression and wound healing. Therefore, we assessed the hypoxic effect on pro-inflammatory functions in monocytes. Thus, the production of pro-inflammatory mediators in unstimulated cells and in response to activation stimuli was analysed. To stimulate the cells, LPS was utilised, a classical TLR4 stimulant in human monocytes. In order to find an ideal concentration, a dose response experiment was carried out to determine the linear range of cytokine production. Monocytes were cultured in normoxia only and stimulated with various concentrations of LPS for 6 hours (**Figure 4.4**). The cell-free supernatants were analysed by IL-8 and IL-6 ELISA. The results showed that LPS at all concentrations (0.1-1000ng/ml) induced detectable levels of IL-6 and IL-8. The maximum output of IL-6 and IL-8 appeared to come when the monocytes were stimulated with 10ng/ml LPS. The

graph in **Figure 4.4** determined that the dynamic range appears to be from between 1-10ng/ml. To ensure a consistent responsiveness to LPS in individual donors, the higher concentration of 10ng/ml was used in subsequent experiments.

With a suitable concentration of LPS determined for stimulation. Monocytes were cultured in normoxia and hypoxia (5% O₂ & 1% O₂) ± LPS for 4 hours and the supernatant harvested. In cells cultured in 5% O₂, there was no significant impact on the ability of monocytes to secrete the pro-inflammatory cytokines TNF α , IL-6 and IL-1 β compared to those cultured in normoxia (**Figure 4.5A**). Despite promoting a higher level of production of mediators, LPS did not induce any differences between normoxia and hypoxia (**Figure 4.5A**). Evaluation of the 1% O₂ also showed that there was no difference between the production of IL-8 and IL-6. In contrast however, there appeared to be a reduction in the release of IL-1 β when cells were stimulated with LPS in hypoxic conditions, although this did not reach statistical significance (**Figure 4.5B**).

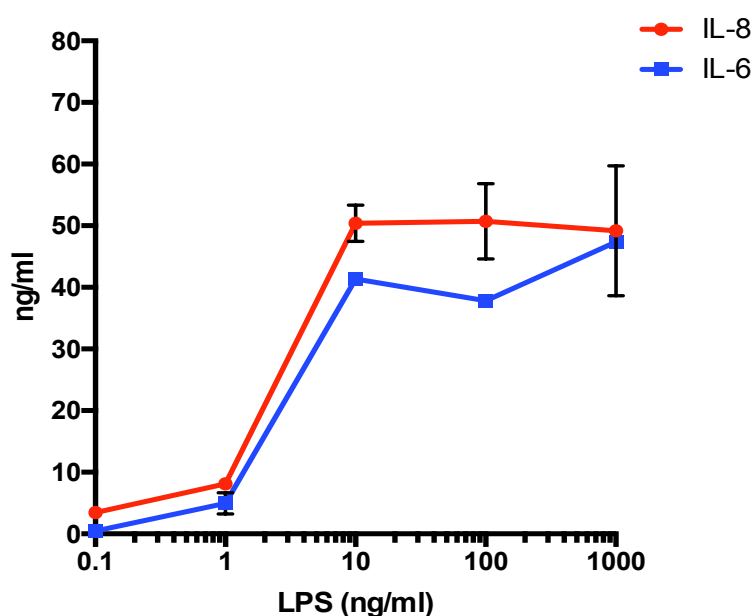


Figure 4.4 LPS Dose response curve of inflammatory mediators. Monocytes were cultured in normoxia ± LPS of varying concentrations (ng/ml) for 6 hours. Levels of IL-6 and IL-8 in harvested cell free supernatant was analysed by ELISA. Data shown as the Mean ± SD. The experiment was performed in triplicate in 2 healthy donors.

The results from **Figure 4.5** illustrated that short term hypoxia modulated IL-18 production, but not other classical mediators such as TNF α , IL-6 and IL-8. To supplement this finding, we sought to validate the key finding from Bosco *et al* (2006), where hypoxia induced CCL20 production at protein level, since, to the best of our knowledge, no other group had investigated this phenomenon. The results from **Figure 4.1** was in agreement with Bosco *et al*, as increases in CCL20 transcript level were detected in hypoxic conditions. The published work however used a 16 hour time-point and a 1% O₂ tension for the detection of CCL20 by ELISA. Thus, a time-course experiment at 5% O₂ and at a lower tension of 2.3% O₂ (achieved using the hypoxic incubator) was adopted to assess if both short term and overnight culture of hypoxia had the same effect. Thus, monocytes were cultured in normoxia or hypoxia (5% O₂ & 2.3% O₂) \pm LPS for 0, 6, 18 and 24 hours and the CCL20 release was measured by ELISA. In contrast to the published findings, hypoxia alone did not induce CCL20 production in monocytes (**Figure 4.6A & 4.6B**). Furthermore, whilst CCL20 production was induced after 6 hours of culture when the cells were stimulated with LPS, there appeared to be no hypoxic effect. Intriguingly, longer term hypoxia (18 and 24 hours) appeared to increase the production of CCL20 in 5% O₂ (**Figure 4.6A**). At 18 hours there was an increase from, on average, 312 \pm 5 pg/ml in normoxia to 406 \pm 80 pg/ml in hypoxia. This change was maintained at 24 hours, from 358 \pm 9 pg/ml in normoxia to 447 \pm 50 pg/ml (**Figure 4.6A**). In a separate experiment at 2.3% O₂, this finding was exacerbated. Indeed, at 18 hours the monocytes produced 1690 \pm 416 pg/ml of CCL20 in normoxia and 4320 \pm 991 pg/ml in hypoxia. Furthermore, monocytes secreted, on average, 2067 \pm 448 pg/ml of CCL20 in normoxia and 4867 \pm 295 pg/ml in hypoxia after 24 hours of culture (**Figure 4.6B**). Taken together, these data show that hypoxia enhances the production of CCL20 from LPS activated monocytes.

The increased level of CCL20 production in hypoxic conditions identified a hypoxia-specific function of LPS activated monocytes. To determine if this was specific only for CCL20 or was replicated in other pro-inflammatory mediators, supernatants were interrogated by Meso Scale Discovery and further ELISA analysis. In this instance, monocytes were cultured in normoxia or hypoxia (1% O₂) \pm LPS for 16 hours and the supernatant was harvested for analysis. Unstimulated cells did not produce detectable levels of the of the cytokines; IL-

1 β , IL-6 & TNF α and chemokines; CCL20 and IL-8 (except in one donor) under both normoxia or hypoxia (**Figure 4.7B**). However, in one donor (performed in triplicate), hypoxia alone did increase the production of IL-8 (**Figure 4.7A**). This is in agreement with the result at transcript level in **Figures 4.1A & 4.1B**. However, throughout the supernatant analysis in activated cells, IL-8 was detected above the dynamic range of the assay. Therefore, under these circumstances, IL-8 would have to be tested further with an adjusted dilution.

Strikingly, in monocytes stimulated with LPS, hypoxia enhanced the production of pro-inflammatory mediators. For instance, there was a significant increase of approximately 4-fold in the release of CCL20 in hypoxic conditions compared to normoxia (**Figure 4.7B**). This result, which was obtained at 1% O₂, is in agreement with the results in **Figure 4.6**, which also highlighted hypoxia-specific enhancement of CCL20 release. In addition, significant increases were observed in the secretion of IL-6 (1.7-fold increase) and IL-1 β (1.6-fold increase) in hypoxic conditions in comparison to normoxia (**Figure 4.7B**). The increase in IL-1 β in this experiment is at odds with the result in **Figure 4.5B**, which indicated a reduction in IL-1 β secretion from activated cells in hypoxic conditions. Further work is warranted to fully appreciate the kinetics of IL-1 β release in this context. However, given the links between IL-1 β and cell death pathways (at least in macrophages; (England et al. 2014)), by actively limiting IL-1 β during the initial phases of hypoxia adaptation, this could promote cell survival during this process. Moreover, TNF α production seemed to be increased under hypoxic conditions, however, this was largely a donor specific phenomenon and did not yield statistical significance (**Figure 4.7B**).

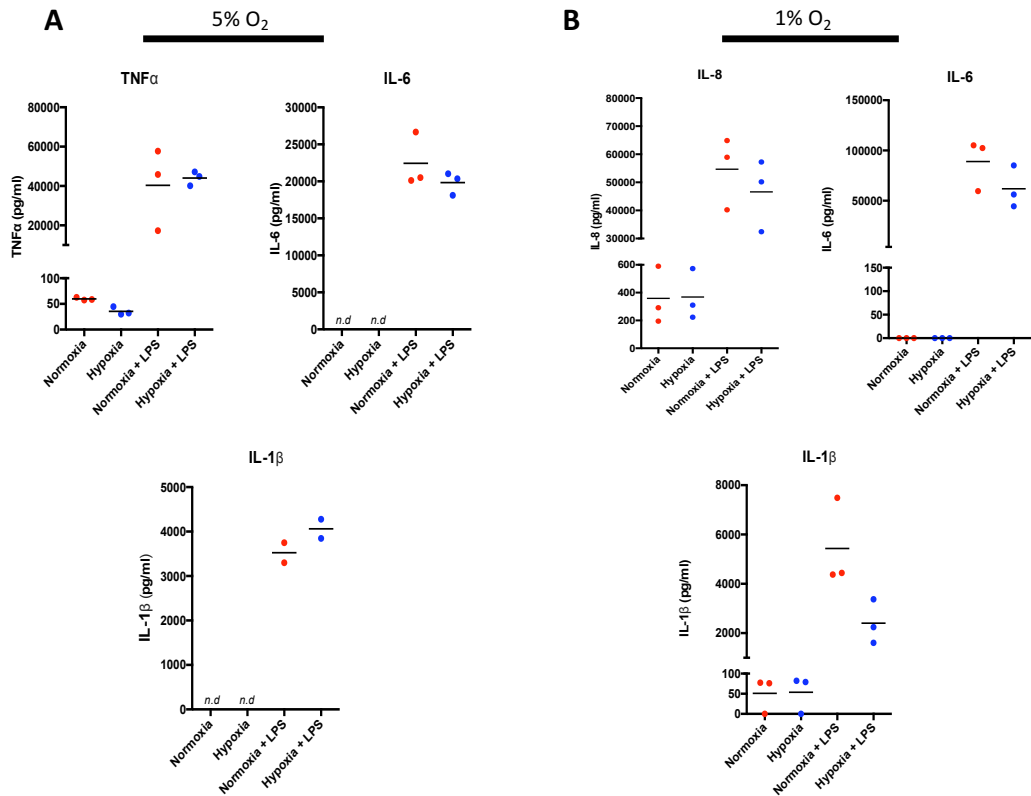


Figure 4.5 Hypoxia has a minimal impact on the production of pro-inflammatory mediators in the short term. Monocytes were cultured in normoxia or [A] 5% O₂ or [B] 1% O₂ (hypoxia) \pm LPS (10ng/ml) for 4 hours. Cell culture supernatant was harvested and assessed by ELISA for indicated mediators. Dots are indicative of separate donors with the Mean shown. $N = 3$. n.d. = non-detectable.

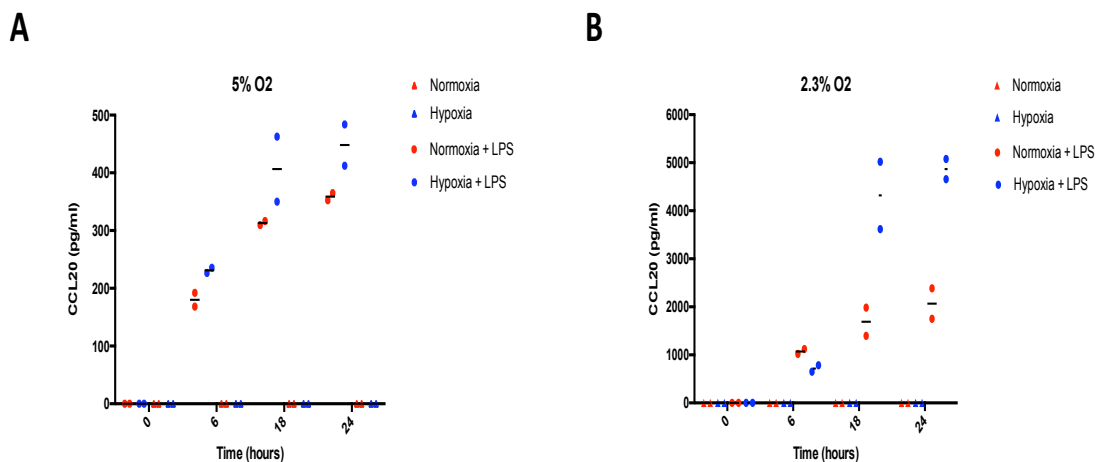


Figure 4.6 Time and oxygen tension influences LPS stimulated monocyte secretion of CCL20. Monocytes were cultured in either normoxia or [A] 5% O₂ or [B] 2.3% O₂ (hypoxia) \pm LPS (10ng/ml) for the indicated time-points. CCL20 release into the cell culture supernatant was harvested and analysed by ELISA. Dots are indicative of individual donors and the line represents the Mean. The experiments were performed in triplicate from 2 healthy donors.

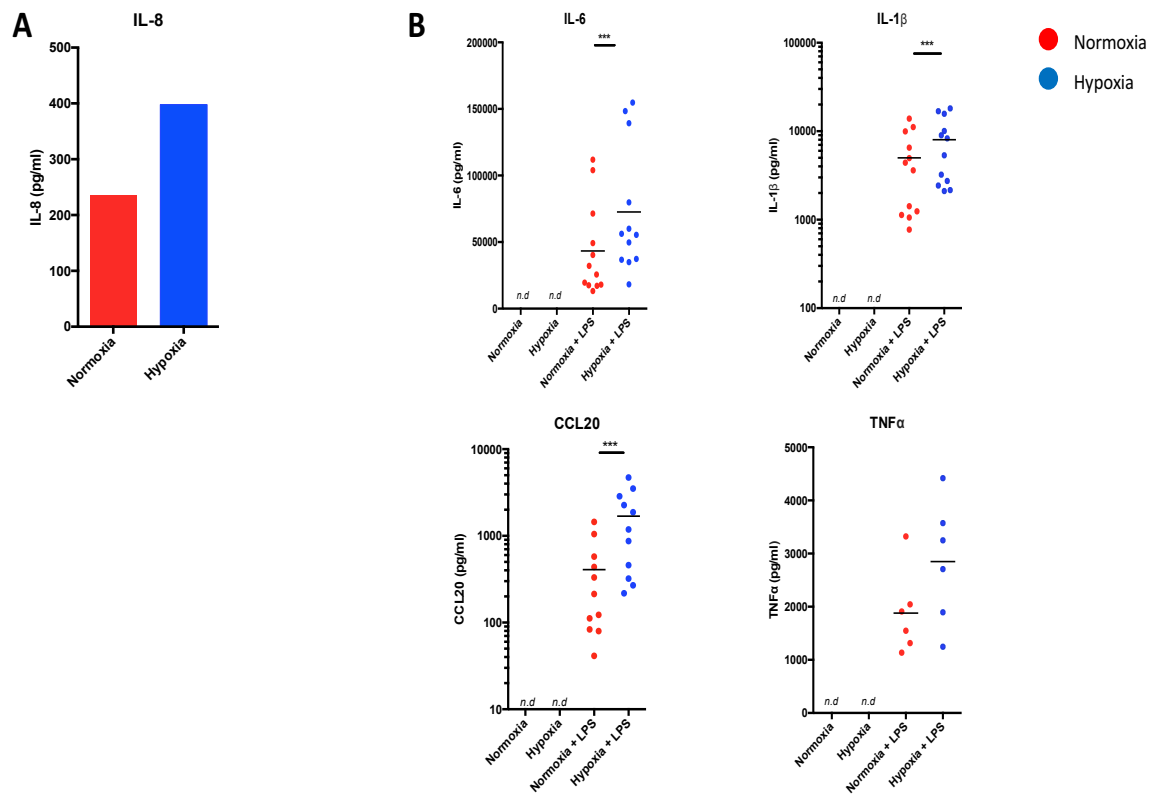


Figure 4.7 Longer term hypoxia increases the secretion of pro-inflammatory mediators in LPS stimulated monocytes. [A] Monocytes were cultured in normoxia or hypoxia (1% O₂). Cell free supernatant was harvested and assessed by MSD. *n* = 1 [B] Monocytes were cultured in normoxia or hypoxia (1% O₂) ± LPS (10ng/ml) for 16 hours. Cell free supernatant was harvested and assessed by MSD (IL-6, IL-1β & TNFα) & ELISA (CCL20). Data shown as the Mean and dots are indicative of separate healthy donors. Statistically analysed by paired t Test (IL-6 & IL-1β) or Wilcoxon rank test (CCL20 & TNFα) after D'Agostino & Pearson normality testing. *N* = 11-12. *** *p* ≤ 0.001.

4.2.2 Metabolic manipulation of monocytes under hypoxic conditions

4.2.2.1 Carnitine supplementation

Having revealed that hypoxia can have a profound effect on the ability of monocytes to produce inflammatory cytokines and chemokines upon LPS stimulation, the next step was to determine if metabolic manipulation of pathways identified in **Chapter 3** could perturb this. From the metabolomics analyses in **Chapter 3**, the carnitine shuttling and the subsequent fatty-acid β-oxidation were the most substantially altered pathways. Therefore, this pathway was targeted for modification by using standard methods such as the exogenous addition of carnitine supplements, and pharmacological inhibition via small molecules. The first method to manipulate the pathway was to supplement the

cell culture media with exogenous carnitine. With this approach, it was expected that the cells would uptake the exogenous carnitine and therefore boost fatty acid oxidation by increasing fatty acid transport into the mitochondria. This was based on the fact that carnitines were depleted in hypoxic conditions (**Figure 3.8**). Uptake of exogenous carnitine in monocytes and macrophages has been reported to occur via OCTN2 (Ingoglia et al. 2017). Earlier studies in murine macrophages had revealed that high doses (>300mM) of exogenous carnitine was toxic to these cells (Fortin et al. 2009). Therefore, in order to ensure that any changes in functionality caused by this intervention could not be attributed to cell death, a toxicity assay was performed. For this purpose, an MTT toxicity assay was utilised at a number of doses in culture with monocytes. The assay determined that concentrations above 10mM of exogenous carnitine was detrimental to the monocytes (**Figure 4.8A**). Monocytes were, therefore, cultured in the presence or absence of 10mM exogenous carnitine under both normoxia or hypoxia (1% O₂) ± LPS for 16 hours. Strikingly, the results showed that in both normoxic and hypoxic conditions, exogenous carnitine significantly increased the production of CCL20 when the cells were stimulated with LPS (**Figure 4.8B**). However, this finding did not extend to IL-1β production in LPS treated monocytes, where exogenous carnitine appeared to have no significant impact (**Figure 4.8B**).

In light of this result, the effect of a carnitine dose response on both CCL20 and IL-1β production in LPS stimulated monocytes was evaluated. Interestingly, CCL20 production was increased by exogenous carnitine in a dose dependent manner in both normoxic and hypoxic conditions, however, this only reached significance at the top concentration of 10mM (**Figure 4.8C**). In validation of the result in **Figure 4.8B**, the top dose (10mM) of carnitine had no effect on IL-1β production. Furthermore, lower doses of carnitine did not have any effect on the release of IL-1β in both normoxia and hypoxia. (**Figure 4.8C**).

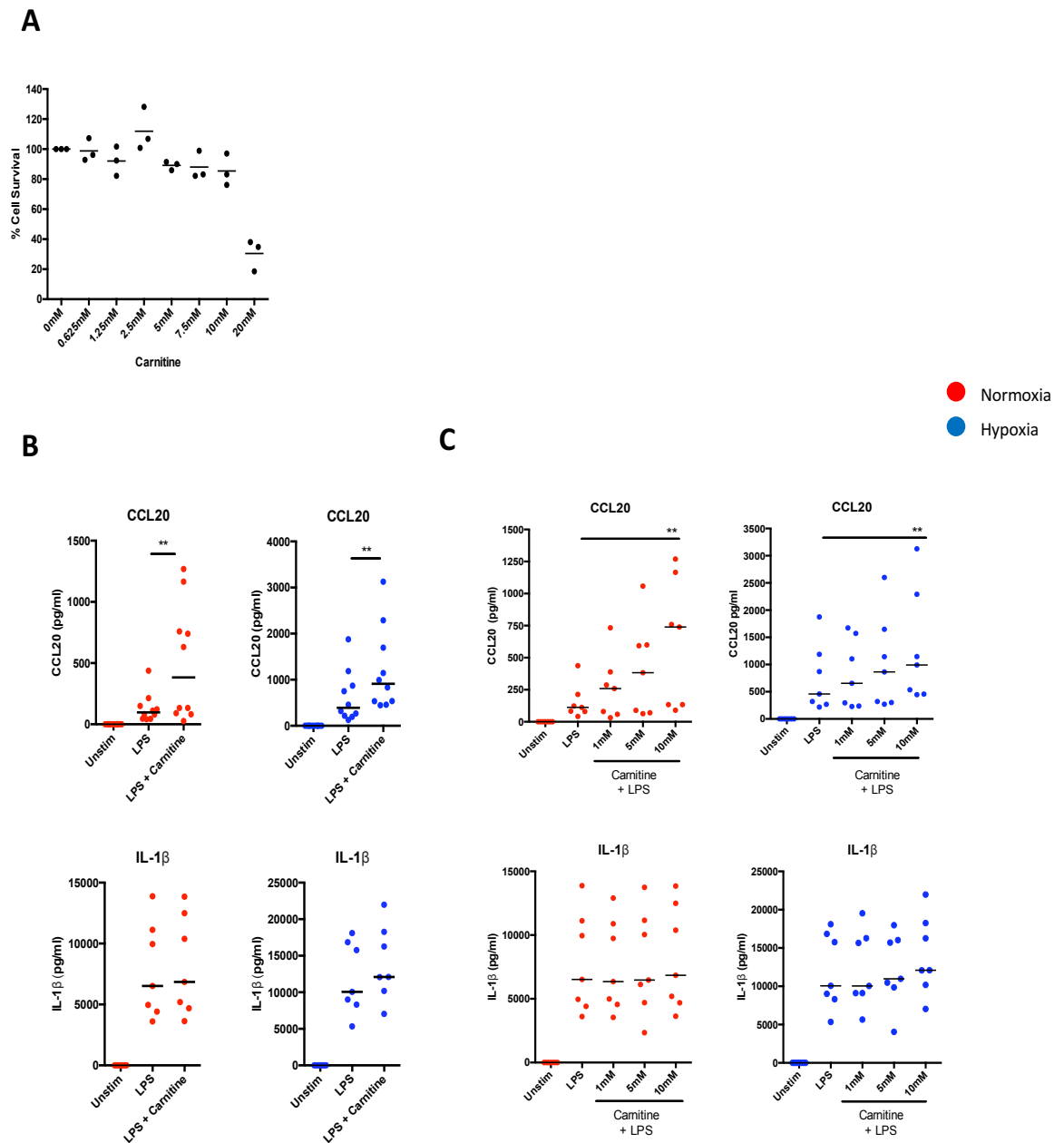


Figure 4.8 Carnitine supplementation increases CCL20 release from monocytes. [A] Monocytes were cultured in normoxia with increasing doses of carnitine (0-20mM) for 4 hours and toxicity was assessed by MTT assay. Dots indicative of separate donors and line showing the Mean. $N = 3$ **[B]** Monocytes were cultured in normoxia or hypoxia (1% O_2) \pm LPS (10ng/ml) and were supplemented with Carnitine (10mM) for 16 hours. Cell culture supernatant was assessed by CCL20 or IL-1 β ELISA. Data statistically analysed by Wilcoxon rank test. $N = 7-10$. Dots are indicative of separate donors and line illustrating the Mean. **[C]** Monocytes were cultured in normoxia or hypoxia (1% O_2) \pm LPS (10ng/ml) and were supplemented with incremental doses of Carnitine (1-10mM) for 16 hours. Cell culture supernatant was assessed by CCL20 or IL-1 β ELISA. Data statistically analysed by Friedman's test followed by Dunn's post-test compared to LPS alone as the control condition. $N = 7$. Dots are indicative of separate donors and line illustrating the Median. ** $P \leq 0.01$.

4.2.2.2 Inhibition of carnitine biosynthesis

These data support a role for fatty acid transport in the secretion of CCL20 but not IL-1 β . To assess if intracellular carnitine biosynthesis had a role in the production of CCL20, the small molecule inhibitor, Mildronate, was used. This inhibitor blocks the hydroxylation of γ -butyrobetaine by γ -butyrobetaine hydroxylase and thus prevents the biosynthesis of carnitine. Accordingly, monocytes were pre-treated with the inhibitor for 1 hour prior to being cultured in normoxia or hypoxia \pm LPS for 16 hours. The results showed that pre-treatment with Mildronate, at three separate concentrations, did not significantly alter the production of CCL20 release in normoxia or hypoxia in LPS stimulated monocytes (**Figure 4.9A**). Furthermore, pre-treatment of monocytes for 1 hour with Mildronate (50 μ M) had no effect on IL-1 β production when the cells were stimulated with LPS (**Figure 4.9A**).

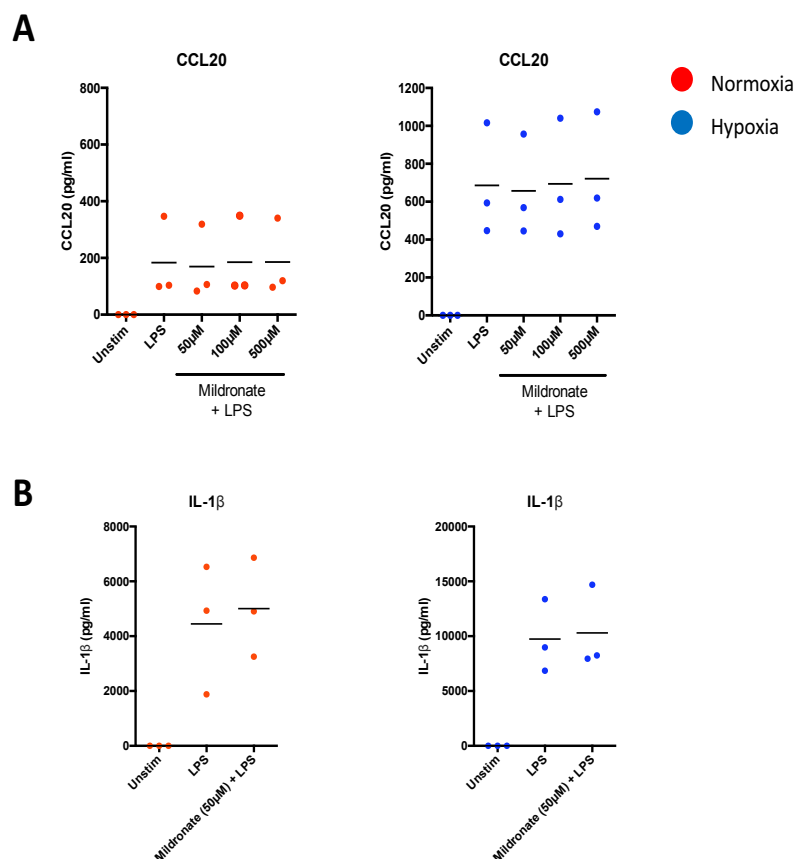


Figure 4.9 Mildronate treatment has little effect on the production of inflammatory mediators in monocytes. Monocytes were pre-treated for 1 hour with Mildronate (50-500 μ M) in normoxia. Cells were then stimulated with LPS (10ng/ml) and cultured in normoxia or hypoxia (1% O₂) for 16 hours. Cell culture supernatants were harvested assessed by CCL20 [A] or IL-1 β [B] ELISA. Dots representative of separate donors with line showing the Mean. $N = 3$.

4.2.2.3 Inhibition of carnitine shuttling

Although Mildronate acts as an inhibitor against carnitine biosynthesis, it does not inhibit the carnitine shuttle, which transports fatty acid acyl-CoA groups for β -oxidation. Therefore, an alternative inhibitor, etomoxir (ETO), which inhibits CPT-1 and subsequent fatty acid transport into the mitochondria was used. CPT-1 is located on the outer face of the inner mitochondrial membrane of the mitochondria and starts the carnitine shuttle by promoting the binding of free carnitine to fatty acid acyl groups. Monocytes were pre-treated with ETO for 1 hour, before subsequent culture in normoxia or hypoxia \pm LPS for 16 hours. In LPS stimulated monocytes under normoxia conditions, pre-treatment with ETO significantly increased the production of CCL20. In contrast, ETO had no effect on the production of CCL20 in hypoxic conditions (**Figure 4.10A**). Intriguingly, pre-treatment with ETO significantly increased the level of IL-1 β secretion in LPS stimulated cells, in both normoxia and hypoxia (**Figure 4.10B**). Taken together, the results from **Figures 4.8** and **4.10**, identify a role for the carnitine shuttle and fatty acid oxidation in the enhanced production of CCL20 and in the suppression of IL-1 β release.

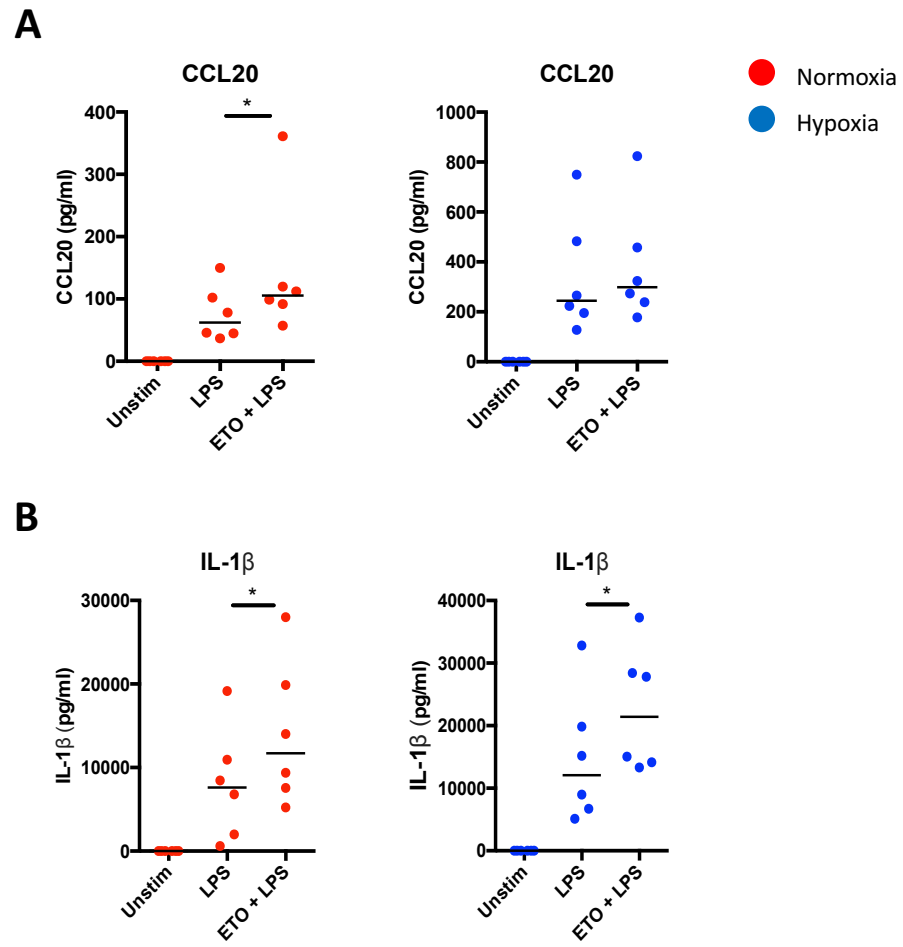


Figure 4.10 Etomoxir (ETO) increases the release of IL-1 β from monocytes in normoxic and hypoxic conditions. Monocytes were cultured in normoxia or hypoxia (1% O₂) \pm LPS (10ng/ml) for 16 hours and supernatant harvested. Cells were pre-treated with ETO (50 μ g) for 1 hour. The supernatant was analysed by ELISA for CCL20 [A] or IL-1 β [B]. Data statistically analysed by Wilcoxon rank test. Dots are indicative of separate donors with the line showing the Mean. $N = 6$. * $p \leq 0.05$.

4.2.2.4 Glycolysis inhibition

In addition to fatty acid metabolism, the metabolic data from **Chapter 3** identified glycolysis as a perturbed pathway in hypoxia. To understand the influence of this pathway on the production of pro-inflammatory mediators, monocytes were treated with the glucose analogue, 2-deoxyglucose (2-DG), which is known to inhibit glycolysis. In brief, cells which utilise glycolysis will readily uptake 2-DG into the cell via glucose transporters. After uptake, 2-DG can be phosphorylated by hexokinase to generate 2-DG-P, however, it cannot be further metabolised in the pathway. Thus, 2-DG-P will accumulate and glycolysis will become inhibited. Monocytes were therefore pre-treated for 2 hours with 10mM 2-DG and cultured in normoxia or hypoxia \pm LPS for 16 hours. The level of pro-inflammatory mediators in the supernatant were analysed by ELISA. In normoxic conditions, 2-DG had no impact on the production of IL-6, CCL20 and IL-1 β when the cells were stimulated with LPS (**Figure 4.11**). In stark contrast, pre-treatment with 2-DG dramatically decreased the secretion of IL-6, CCL20 and IL-1 β in hypoxic conditions (**Figure 4.11**). It is important to note that in this experiment, the monocytes were isolated directly from fresh blood rather than buffy coat, which may explain the lower levels of IL-1 β and CCL20 that was detected. In summation, these results suggest that, particularly in hypoxic conditions, glycolysis has a governing role in the production of pro-inflammatory mediators from LPS stimulated monocytes.

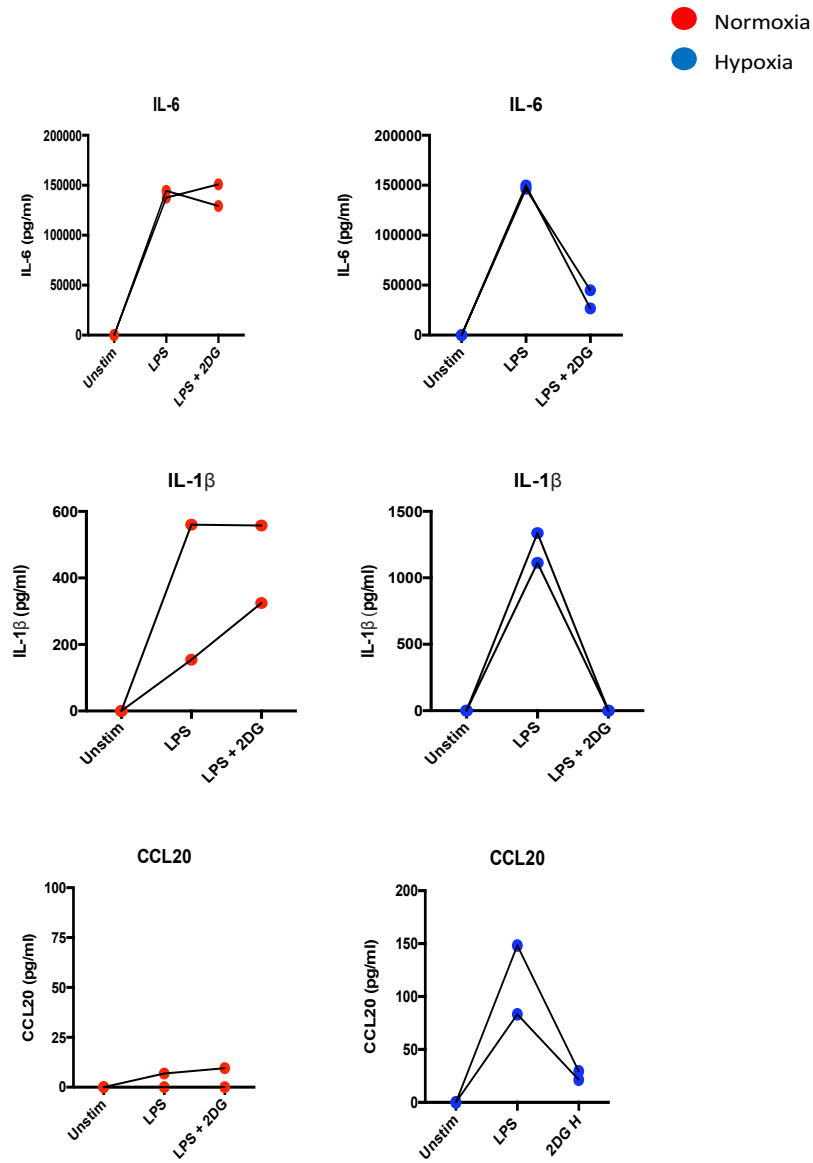


Figure 4.11 2-Deoxyglucose (2-DG) inhibits pro-inflammatory cytokine production in hypoxic conditions. Monocytes were left unstimulated, stimulated with LPS (10ng/ml) or were pre-treated for 2 hours with 2-DG (10mM) before LPS stimulation. Cells were then cultured under normoxia or hypoxia (1% O₂) for 16 hours. Cell culture supernatant was harvested and assessed for IL-6, IL-1β or CCL20 by ELISA. Dots representative of separate donors. The experiment was conducted in triplicate in 2 healthy donors.

4.3 Discussion

This chapter has utilised a number of assays with the aim of profiling how hypoxia impacts monocyte function. Transcriptomic analysis revealed that a range of transcripts, including chemokines and scavenger receptors were altered by hypoxia. However, these transcriptional changes did not fully correlate with changes at protein level. Supernatant analysis identified that hypoxia augments the production of pro-inflammatory mediator from LPS stimulated monocytes, such as CCL20 and IL-1 β . Linking this with the data produced in **Chapter 3**, it was postulated that the oxidation of fatty acids may have a role in the production of pro-inflammatory cytokines and chemokines under these conditions. Indeed, this chapter has shown that supplementation of monocytes with carnitine enhances CCL20 production in both normoxia and hypoxia. In addition, inhibition of the carnitine shuttle augmented IL-1 β production in normoxia and hypoxia, while it only increased CCL20 production in normoxic conditions. Furthermore, initial studies suggested that glycolysis also has an important role in the production of CCL20, IL-1 β and IL-6, especially under hypoxic conditions.

Little is known about the impact of hypoxia specifically on monocyte function (discussed in **1.3.3**). However, monocytes have an array of inflammatory functions, including the production of cytokines and chemokines in response to stimuli. They also retain strong adherence to extracellular matrices to carry out processes such as phagocytosis (discussed in **1.1.1** & **1.4**). In addition, monocytes possess a number of regulatory roles, such as scavenging cellular debris and aiding in wound healing processes to resolve inflammation (discussed in **1.1.1**). Therefore, a plethora of assays were utilised to assess how hypoxia alters monocyte functionality.

In the first instance, pre-designed TLDA plates were used to analyse a number of gene targets, which may have given indications of a functional phenotype. The analyses revealed that hypoxia had an impact on the expression of scavenger and C-type lectin receptors. These results also implicated changes within the chemokine network and their receptors. Likewise, a global transcriptomic analysis of monocytes under hypoxic conditions was carried out by Bosco *et al* (2006). In line with the results in this chapter, the authors identified altered

gene expression levels of scavenger receptors and chemokines/receptors. CD36 showed a lower level of gene expression in this work and the published work in hypoxia compared to normoxia. As CD36 is a scavenger receptor for fatty acid uptake, it is an important mechanism for feeding fatty acid oxidation, and therefore fits the metabolomic results from the previous chapter. CD36 is largely associated with anti-inflammatory M(IL-4) macrophages, while knockout studies suggest it is essential for murine M(IL-4) macrophage activation (S. C.-C. Huang et al. 2014). Therefore, hypoxia may promote a more inflammatory phenotype in monocytes by downregulating its expression. However, altered transcriptional expression did not translate into decreased cell surface expression. CD36 surface expression was only analysed on one donor, which may have been as a result of donor specific effects in this instance. Furthermore, this could indicate that CD36 may not be trafficked to the cell surface under these conditions. Given decreases in other scavenger receptors, such as CD163 and STAB1, were observed in this work and in the published transcriptomic study, conducting a thorough FACS examination of a number of scavenger receptors, and at a later time-point, may be more appropriate to fully determine if hypoxia reduces cell surface expression.

Monocytes display strong adherent properties to extracellular matrices *in vivo* to enhance functional properties such as phagocytosis (Newman & Tucci 1990). The results presented here illustrated that hypoxia had no impact on monocyte adherence *in vitro* (**Figure 4.3**). The experimental set up used in this work resembled that of the adherence assay used by Dabritz *et al* (2015). The authors pre-treated monocytes with GM-CSF prior to seeding into tissue culture plates and observed increased levels of adherence. The monocytes used for the experiments in this chapter were, however, seeded immediately upon exposure to normoxia and hypoxia. Therefore, a pre-exposure to hypoxia before seeding into plates may have yielded some alterations. In addition, pre-coating of wells with fibronectin was attempted in this assay to aid adherence. However, no difference was observed between normoxia and hypoxia (data not shown), indicating that hypoxia may not have any effect on cellular adherence.

These studies do not rule out the possibility of hypoxia being able to alter adherence properties *in vivo*. This may include the expression and activation of

β 2 integrins (such as CD11a-d), all of which have been reported to be expressed on human monocytes (Schittenhelm et al. 2017). Integrins are thought to contribute to the pathogenesis of RA. For example, CD11a is increased in RA and is associated with aiding transendothelial migration of monocytes to the inflamed synovium (Schittenhelm et al. 2017). Therefore, studies assessing β 2 integrin expression by flow cytometry or through the utilisation of static adhesion assays may provide increased understanding into how hypoxia may modulate monocyte adherence properties.

In addition to promoting inflammation, monocytes participate in immune regulation. The work by Dabritz *et al* found that GM-CSF activated monocytes could close a scratched monolayer of Caco-2 cells more rapidly than untreated cells. The authors suggested that GM-CSF induced characteristics in monocytes that are shared with anti-inflammatory M(IL-4) macrophages which in turn contributed to the regulation of intestinal inflammation. However, in the experiments here, scratching a monolayer of Caco-2 cells lead to cell death and tearing of the monolayer, which questioned the suitability of this cell line for the assay. This process was more reproducible when using HUVECs, however no difference was observed between normoxia and hypoxia. Likewise, with this study, the published work also observed a non-significant difference in wound closure between a monolayer without monocytes and with untreated monocytes. In summation, the results in this chapter suggest that hypoxia does not promote wound healing processes in monocytes.

In response to bacterial ligands, such as LPS, monocytes secrete an array of pro-inflammatory mediators. In a robust finding, hypoxia was shown to enhance the production of pro-inflammatory cytokines (IL-6 and IL-1 β) in response to LPS (**Figure 4.7**). Furthermore, the increases were only seen after 16 hours of culture in hypoxia, and hypoxia had no effect on secretion in resting cells. Taken together, this suggests that tissue hypoxia at inflamed sites augments inflammatory cascades. In support of this, hypoxia also enhanced the release of pro-inflammatory mediators by human macrophages in response to palmitate (Snodgrass et al. 2016). These results strengthen the argument that hypoxia may prime the cells for a more robust inflammatory response and could act as a

'danger' signal. On the other hand, bystander effects of hypoxia, such as metabolic adaptation, could enhance such responses.

In addition to the increase in cytokines, hypoxia increased the secretion of CCL20, but only in LPS stimulated monocytes (**Figure 4.7**). The results here did not fully validate published work which suggested that hypoxia increased the production of CCL20 in resting monocytes (Bosco et al. 2006). However, the enhanced secretion observed in activated cells does implicate a role for hypoxia in CCL20 release. CCL20 and its corresponding receptor, CCR6 have been associated with the pathogenesis of autoimmune diseases, such as rheumatoid arthritis (Tanida et al. 2009). Direct links have been made between CCL20 and its recruitment of CCR6⁺ Th17 cells, monocytes and in the proliferation and activation of osteoblasts and osteoclasts respectively (Hirota et al. 2007; Ruth et al. 2003; Lisignoli et al. 2009). Therefore, the hypoxic microenvironment commonly found in inflammation may prime infiltrating monocytes to secrete increased levels of CCL20 upon stimulation. This in turn could drive pathogenesis by promoting the recruitment of other immune cells. Increased cell infiltration into the inflammatory milieu could further decrease the oxygen tension via increased oxygen consumption, which may drive chronicity. On the other hand, CCR6 is also present on the surface of Treg populations, which are said to be present in the joint too (Möttönen et al. 2005). Therefore, further work is needed to establish if the CCL20:CCR6 axis has a role in the resolution of inflammation too.

To interrogate the impact of metabolic pathways for the enhanced release of pro-inflammatory mediators under hypoxia. A few approaches were undertaken to assess the effect of carnitine shuttling (and subsequently fatty acid oxidation), which was revealed to be significantly down-regulated in the metabolomics analysis in **Chapter 3**. Pre-treatment of the monocytes with Mildronate had no effect on the production of pro-inflammatory mediators upon LPS stimulation, which suggested that intracellular carnitine biosynthesis does not influence CCL20 secretion. On the other hand, inhibition of carnitine shuttling itself with etomoxir, significantly increased the production of IL-1 β (in both normoxia and hypoxia) and CCL20 (in normoxia only). Together with LPS stimulation, hypoxia may have saturated the production of CCL20, as the

inhibitor induced a significant increase only in normoxia. As etomoxir prevents fatty acid oxidation in the mitochondria, it could be speculated that in order to generate sufficient ATP under these conditions, monocytes would have a greater reliance on glycolysis. Such circumstances have been reported when cancer cells have been treated with etomoxir (Schlaepfer et al. 2015). Therefore, the increases in IL-1 β and CCL20 (normoxia only) secretion by etomoxir could be caused by increased glycolytic flux. However, subsequent metabolomic analysis would be needed to confirm this hypothesis. Nevertheless, knockdown studies of CPT1a and treatment with ETO in macrophage-differentiated THP-1 monocytic cells increased the expression of pro-inflammatory cytokines in response to palmitate at transcript level (Namgaladze et al. 2014). As well as being in support of the studies in this chapter, this highlights that FAO may have regulatory functions, by actively limiting the release of IL-1 β and CCL20 in this instance. Indeed, overexpression of CPT1a in THP-1 macrophages and RAW 264.7 macrophages attenuated inflammatory responses in response to palmitate (Namgaladze et al. 2014; Malandrino et al. 2015). Thus, metabolic switching to glycolysis may promote a more inflammatory programme in myeloid cells. The interplay between glycolysis and FAO has been studied in macrophage polarisation. Glycolysis has been typically associated with inflammatory M(LPS \pm IFN γ) macrophages while the predominant view in the field has identified FAO with anti-inflammatory M(IL-4) macrophages (Vats et al. 2006; S. C.-C. Huang et al. 2014; Rodriguez-Prados et al. 2010). Although, a growing body of evidence has now suggested that FAO may not be required for IL-4-induced polarisation in human macrophages (Namgaladze & Brüne 2014; Nomura et al. 2016).

In addition to carnitine inhibition, the promotion of fatty acid oxidation was attempted by supplementing the cells with exogenous carnitine. Carnitine supplementation increased the secretion of CCL20, but had no effect on IL-1 β release, which suggest a specific role for FAO, perhaps in conjunction with glycolysis, in CCL20 production. The lack of effect of exogenous carnitine on IL-1 β release was surprising, given that Fortin *et al* (2009) illustrated that carnitine suppressed the secretion of IL-6, IL-1 β and TNF α in murine macrophages. Furthermore, in human monocytes stimulated with LPS, carnitine reduced TNF α and IL-12 (Alesci et al. 2003). In both studies, very high doses of exogenous carnitine were used (>100mM), which were based on a lack of toxicity (by MTT

assay) in HeLa cells in concentrations of up to 400mM. When an MTT assay assessing the impact of increasing doses of carnitine was conducted human monocytes in the work presented here, toxicity was observed in concentrations above 10mM (**Figure 4.8A**), which questioned the concentrations used in the published studies. The reduction in the secretion of pro-inflammatory cytokines in the published work and the lack of effect in IL-1 β production by exogenous carnitine here was in stark contrast with the increase in the production of the chemokine, CCL20. This suggested that cytokines and chemokines could be differentially regulated at metabolic level. Indeed, alternative metabolic pathways for the control of cytokine and chemokine release has been reported before. This includes glycolysis for the control of IL-1 β release from M(LPS \pm IFN γ) macrophages and the glutamine metabolic module for CCL22 production in M(IL-4) macrophages (Tannahill et al. 2013; Jha et al. 2015). To determine if FAO is specific for CCL20 release, experiments are warranted to interrogate if exogenous carnitine (and subsequent FAO) enhances the production of other chemokines, such as IL-8.

Glycolysis is thought to have an important role in inflammatory macrophage activation (Palsson-McDermott et al. 2015; Rodriguez-Prados et al. 2010; Tannahill et al. 2013). Moreover, the metabolomics dataset from **Chapter 3** identified glycolysis as being higher in hypoxic conditions. Therefore, the impact of glycolysis on a monocyte's ability to release higher levels of pro-inflammatory cytokines and chemokines in hypoxia was analysed. Pre-treatment with 2-DG had no impact in normoxia, but strikingly, decreased CCL20, IL-1 β and IL-6 production in hypoxic conditions. Although, to increase the power of this finding, this experiment would need to be repeated as $n = 2$. A similar observation was made when 2-DG inhibited the production of IL-1 β in LPS activated macrophages (Tannahill et al. 2013). Nonetheless, these results indicated an important role for glycolysis in monocyte function, especially in hypoxia. As monocytes under hypoxic conditions reduce their mitochondrial metabolism and increase glycolysis for ATP, inhibiting glycolysis with 2-DG may cause the cells to undergo arrest or apoptosis in low oxygen. Consequently, this could have caused the reduction in inflammatory mediator release.

This chapter has illustrated that upon LPS stimulation, monocytes show enhanced production of pro-inflammatory mediators in hypoxia. This proposed that a hypoxic microenvironment can act as an extracellular danger signal which can prime monocytes for an amplified inflammatory response to stimuli. Alteration of fatty acid metabolism revealed a metabolic disconnect for the control of CCL20 and IL-1 β , where FAO may promote CCL20 production but act to limit IL-1 β release. This indicated that cytokines and chemokines could be differentially controlled at metabolic level. In all cases, glycolysis appears to have a vital role in the production of both cytokines and chemokines, especially in hypoxic conditions. The next chapter will address if these findings extend to the context of inflammatory disease, by using synovial fluid from a rheumatoid arthritis patient as a stimulus. As monocytes typically differentiate into tissue macrophages upon recruitment from the blood, the impact of metabolic pathways in end differentiated cells (alveolar macrophages) will also be interrogated.

Chapter 5. Assessing the impact of the chronic inflammatory milieu on the metabolism and function of monocytes

5.1 Introduction

The previous chapters have characterised the metabolome of monocytes cultured under hypoxia, and have identified a novel link between cellular metabolism and CCL20 production in LPS stimulated cells under these conditions. To extend these findings, studies in this chapter addressed the impact of biological stimuli associated with chronic inflammatory disease. (i.e., synovial fluid). By incorporating hypoxia and simultaneous stimulation with synovial fluid from a rheumatoid arthritis patient (RA-SF), these studies set out to mimic aspects of the chronic disease state in an *in vitro* setting. As this is a more complex stimulus, this metabolic profile was compared to the profile obtained from a comparator stimuli (LPS). Furthermore, by using human alveolar macrophages (AM) from lung resection patients, we questioned if the work from the previous chapter extended to end differentiated cells isolated directly from tissue.

RA is a complex inflammatory disease of the joints with large heterogeneity amongst patients. The RA synovial membrane is a destructive environment, characterised by an immune cell infiltrate of both the innate (such as myeloid cells) and adaptive arms (T & B cells) of immunity. Macrophages with an inflammatory phenotype are thought to play a central role in pathology, by secreting a range of inflammatory cytokines, chemokines and MMPs to drive disease. The importance of metabolic pathways in governing polarisation of inflammatory M(LPS + IFN γ) macrophages has been discussed previously (Section 1.5). Inflammatory mediators such as cytokines (TNF α , IL-6, IL-1 β) can in turn stimulate other infiltrating immune cells to promote severity. In addition to cytokines, RA synovitis is classically characterised by the presence of autoantibodies, such as ACPAs and rheumatoid factor. Autoantibodies have the ability form immune complexes that contain self-antigens such as citrullinated fibrinogen, which can in turn bind Fc γ R and potentially PRRs on macrophages to secrete TNF α (Sokolove et al. 2011). Interestingly, immune complexes can activate osteoclasts and stimulate bone degradation which in turn leads to pain and the production of IL-8 (Harre et al. 2012; Krishnamurthy et al. 2016).

In addition to humoral immune responses, T cell immunity has a vital role in perpetuating inflammation. In particular, the immuno-metabolomic set-point of T cells has been shown to be important. For instance, naïve RA T cells are thought to possess a defected glycolytic flux, where glucose was shunted into the PPP instead. This resulted in higher NADPH and ROS consumption. Thus, the increased reduction capacity had the ability to cause hyperproliferation in activated T cells, which characteristically prefer to adopt pathological Th1 or Th17 phenotypes (Yang et al. 2016)

Intracellular immune metabolism is becoming increasingly important in driving inflammatory mechanisms (discussed in Section 1.5) and therefore could have biological relevance in disease. However, there is a paucity of immune-metabolic research in myeloid cells in response to complex stimuli from chronic inflammatory disease (i.e., RA-SF). Nevertheless, studies have identified pathogenic properties in monocytes that are induced by RA-SF, such as increased CD86 expression (Chimenti et al. 2016). Furthermore, stimulation of different TLR ligands has recently been shown to induce alternative metabolic cascades,

highlighting the necessity of metabolic profiling in response to biologically relevant stimuli (Lachmandas et al. 2016; Domínguez-Andrés et al. 2017). Nonetheless, metabolomics is being increasingly utilised in clinical settings. Even though RA is a heterogeneous disease, there have been a variety of studies which aimed to metabolically profile various biological fluids from RA patients including, serum, plasma, urine and synovial fluid to identify biomarkers of disease (Kapoor et al. 2013; Kim et al. 2014; Tatar et al. 2016; M. Jiang et al. 2013). Global metabolomics revealed that synovial fluid from RA patients significantly differed from those with non-RA pathologies (Kim et al. 2014). This study identified 20 metabolites that could be potential biomarkers of RA. These included metabolites such as succinate, glutamine and citrulline (Kim et al. 2014), reassuring given citrulline's role in ACPAs.

As previously discussed (Sections 1.1.1 & 1.1.2), once recruited to the tissue during inflammation, monocytes can differentiate into macrophages. One such macrophage population are alveolar macrophages, which are long lived resident cells in the airspace of the lung tissue and reside in close proximity to airway epithelial cells and the mucus layer (Hussell & Bell 2014). In the steady state, alveolar macrophages are essential for maintaining homeostasis, by exhibiting low phagocytic capacity, respiratory burst, and are thought to be poor at presenting antigen to T cells (Lipscomb et al. 1986; Hoidal et al. 1981). Furthermore, they are active producers of TGF β that suppresses T cell activation (Coleman et al. 2013). These mechanisms are vital for providing tolerance to innocuous antigen that in turn prevents unnecessary tissue damage.

Although macrophages display immunosuppressive properties during homeostasis, they show a degree of plasticity. During acute microbial infection, AM have a number of inflammatory functions. For example, they are important in the recruitment of other inflammatory cells to the airspace (Maus et al. 2002). In addition, AM produce pro-inflammatory cytokines and ROS to drive inflammation (Losa García et al. 1999; Persoons et al. 1996). Moreover, their role in the resolution of inflammation is evident in their ability to clear apoptotic neutrophils (Cox et al. 1995)

In chronic disease, AM are thought to increase between 5 to 10 fold in those suffering with COPD. This is largely due to cigarette smoke, which presents as

the primary risk factor for COPD (Saetta et al. 1993). Cigarette smoke is known to activate AM, which prompts the release of pro-inflammatory mediators and MMPs, resulting in a milieu that can cause destruction of the lung parenchyma (Barnes et al. 2003). At a metabolic level, cigarette smoke and oxidative stress are known to disrupt glutathione metabolism in AM, which has been associated with impaired AM clearance of bacteria and apoptotic cells (Hodge et al. 2011). This is only one mechanism whereby COPD can lead to increased susceptibility to respiratory infection (Lange 2009). As AM are highly plastic cells, it has been illustrated that the COPD microenvironment can promote distinct macrophage subpopulations of which are resembling of both M(LPS + IFN γ) and M(IL-4) *in vitro* generated phenotypes (Eapen et al. 2017). M(LPS + IFN γ) macrophages promote inflammation and oxidative stress, while M(IL-4) macrophages release MMPs that are involved in lung remodelling and damage. Thus, it has been suggested that the specific ratio of these populations contributes to disease pathology (Vlahos & Bozinovski 2014).

Rheumatoid arthritis and COPD represent two chronic inflammatory diseases with a central role for myeloid cells. In the previous chapters, hypoxia, which is prominent in both diseases (Lund-Olesen 1970; Kent et al. 2011), has been shown to affect the metabolism and functionality of monocytes by altering carnitine metabolites and the production of pro-inflammatory mediators. As stated above, in this chapter the metabolic profile of monocytes cultured under normoxic and hypoxic condition and simultaneous RA-SF or LPS stimulation will be investigated. At a functional level, monocytes will be assessed for their ability to secrete CCL20 when stimulated with RA SF. In addition, by using the same methods to alter carnitine shuttling as in **Chapter 4**, the role of this pathway in CCL20 secretion will be interrogated. Finally, this chapter will begin to scrutinise the impact of hypoxia on carnitine metabolism and cellular function in AM, an end differentiated monocyte-derived cell. Therefore, the aims of this chapter are:

1. Metabolically profile monocytes when untreated or treated with RA-SF & LPS under normoxic or hypoxic conditions.
2. Assess the impact of carnitine metabolism on the ability of monocytes to release pro-inflammatory mediators in response to RA-SF.

3. Investigate carnitine metabolism at a metabolic and functional level in AM.

5.2 Results

5.2.1 Metabolic profiling of monocytes treated with RA-SF under normoxia or hypoxia

5.2.1.1 Overview of metabolic changes induced by RA-SF

The metabolic profile of monocytes under hypoxic conditions has been established already in **Chapter 3**. However, to further relate these studies to the context of inflammatory disease, monocytes were cultured in the presence of RA synovial fluid. Furthermore, the monocytes were cultured in normoxic or hypoxic conditions to mimic the hypoxic environment commonly found in the rheumatic joint. To obtain the metabolic profile, monocytes were cultured in medium containing 10% RA-SF (from one RA patient in active disease) and were exposed to normoxia or hypoxia (1% O₂) for 4 hours. The intracellular metabolites were harvested and analysed by liquid chromatography mass spectrometry. Given that RA-SF is a complex stimulus that exhibits heterogeneity amongst donors, LPS stimulation was utilised as a comparator stimulus in the metabolomic experiment.

The mass spectrometry data was processed and filtered by using the IDEOM Excel pipeline (Discussed in Sections **2.10.4** and **3.2.3**). To obtain an initial overview of the metabolic changes between each condition, the data was visualised via a heatmap (**Figure 5.1**). The processed data (N = 4) was statistically analysed by multiple paired *t* Tests with Benjamini Hochberg correction. After correction, the analysis did not reveal many significant alterations between the conditions. Therefore, the metabolites which were determined as significant ($p < 0.01$) before correction and between each condition were plotted in the heatmap.

The overall heatmap profile indicated that cell stimulation (RA-SF & LPS), rather than hypoxia, induced distinct metabolic changes in comparison to unstimulated (Unstim) cells (**Figure 5.1**). Indeed, there appeared to be a large block of

metabolites where, compared to unstimulated cells (Unstim), there was an increase in abundance of metabolites in RA-SF treated cells (Block 1; **Figure 5.1**). Furthermore, Block 2 indicated a group of metabolites that were more abundant in RA-SF treated cells when compared to both unstimulated and LPS stimulated cells. An accumulation of metabolites in RA-SF treated cells when compared to unstimulated cells was also observed in Block 3 (**Figure 5.1**). These observations suggested that RA-SF induces an accumulation of metabolites in comparison to untreated monocytes. In addition, the metabolic profile from RA-SF treated cells appeared to be divergent from LPS treated cells. Notably, hypoxia did not have a substantial impact within stimuli groups when compared to the impact of stimuli alone (**Figure 5.1**). The initial observations from the analysis are highlighted in the corresponding table, which illustrated a higher number of significantly different metabolites between treatment than oxygen tension within each treatment (**Figure 5.1**). The metabolites which are significantly altered between each condition are listed in the tables (**Sections 7.1-7.8**; highlighted metabolites indicate those which were significant after correction) in the Appendices.

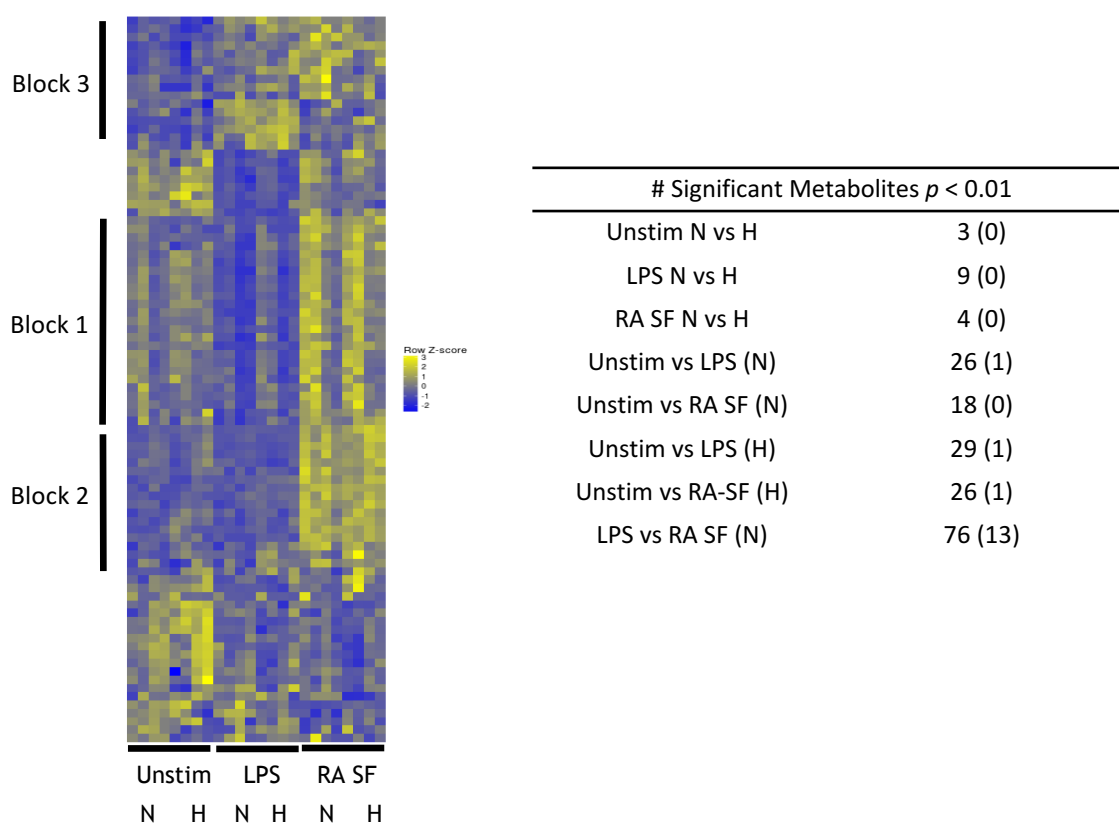


Figure 5.1 Metabolomics overview of monocytes unstimulated, stimulated with LPS or treated with RA-SF. Monocytes were left unstimulated, stimulated with LPS (10ng/ml) or were treated with RA-SF (10% in media) in normoxia (N) or hypoxia (H) for 4 hours. The intracellular metabolites were harvested and analysed by mass spectrometry. Heatmap of significantly altered metabolites ($p < 0.01$; Paired t Test) between each condition. Yellow indicates high abundance and blue indicates low abundance. $N = 4$. Associated table illustrates the number of significantly different metabolites between each comparison. Number in brackets indicates the number of significantly different metabolites after Benjamini Hochberg correction (adjusted $p < 0.05$).

5.2.1.2 Metabolic alterations in cellular energy metabolites

To investigate if certain metabolic pathways were altered by RA-SF, the metabolic profiles under each condition was evaluated at a single metabolite level. The analysis focussed on the metabolic differences between RA-SF treated and unstimulated monocytes.

One of the most predominant group of metabolites that were changed by RA-SF in comparison to both unstimulated and LPS stimulated cells, were those associated with cellular energy. The most notable was ATP; the 'energy currency' of the cell. It was apparent from the results that, at least in hypoxic conditions, RA-SF stimulation induced a significant accumulation of ATP when compared to unstimulated monocytes. In normoxia, there was an increase in abundance of ATP in RA-SF monocytes in comparison to cells stimulated with LPS (**Figure 5.2**). However, there was no difference in ADP levels between unstimulated cells and RA-SF treated cells. Interestingly, LPS stimulation substantially reduced the levels of ATP and ADP (**Figure 5.2**). These data immediately indicated that RA-SF stimulation may induce profound metabolic changes.

NAD⁺ and NADH represent the oxidised and reduced forms of NAD respectively. The analyses revealed that, in normoxia, NAD⁺ abundance was augmented in RA-SF treated monocytes when compared to untreated monocytes. This increase was also observed in comparison to LPS treated monocytes (**Figure 5.2**). These results show that RA-SF promotes the accumulation of NAD⁺. Additionally, a significant upregulation in NADH abundance in RA-SF cells was observed between unstimulated cells, but this was only identified in hypoxic conditions (**Figure 5.2**). This is in juxtaposition with LPS stimulation, which attenuated NADH abundance in comparison to untreated cells (**Figure 5.2**).

Taken together, these results suggest that RA-SF and LPS stimulations induced contrasting levels of cell metabolic activity in monocytes. Given that LPS stimulates a strong pro-inflammatory response in monocytes, they may deplete their ATP stores to meet the high bioenergetic demand. However, RA-SF monocytes appeared to have higher ATP reserves and could ultimately be less active and dependent on mitochondrial pathways, similar to that of a resting or

regulatory cell. NAD acts as an electron carrier in the mitochondria and is important for the occurrence of OXPHOS. Therefore, if this pathway is more highly utilised in RA-SF cells in comparison to LPS, it could suggest that RA-SF did not induce as strong an inflammatory response.

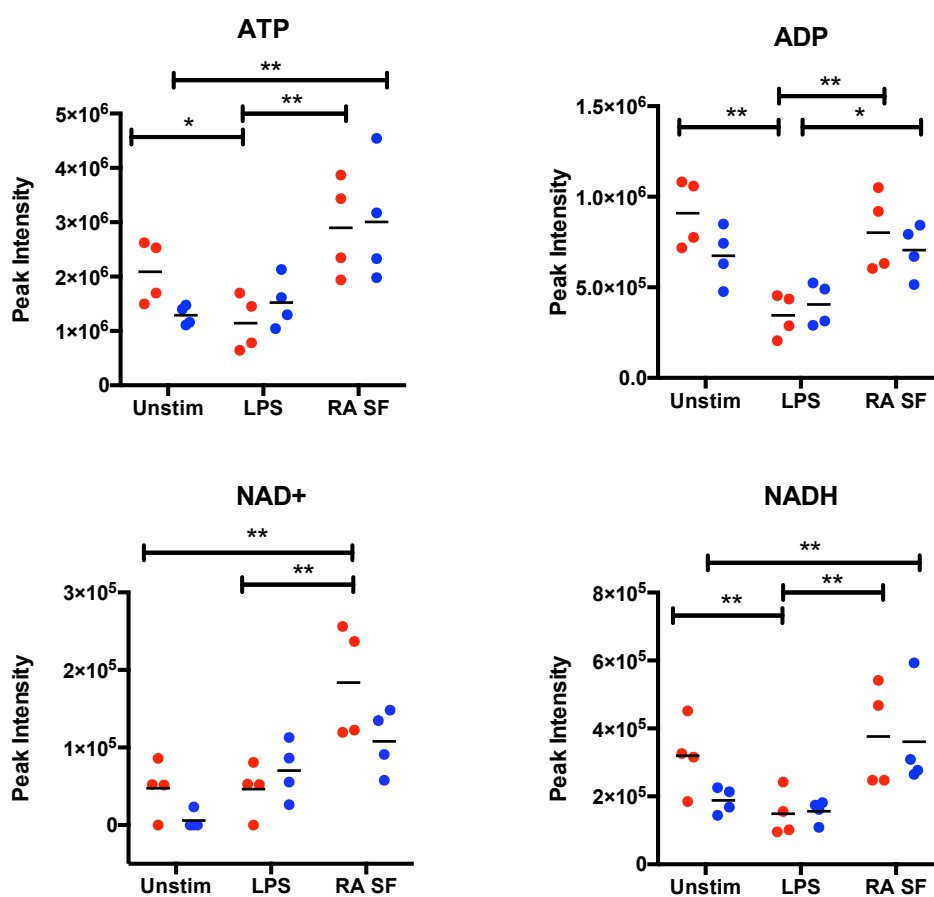


Figure 5.2 Cellular energy metabolites are more abundant in RA-SF treated monocytes compared to LPS stimulated monocytes. Mass spectrometry analysis of metabolites indicative of cellular energy metabolism which showed an accumulation in abundance between RA-SF (N) and LPS (N) treated monocytes. Dots indicative of separate donors and line showing the Mean. $N = 4$. Red dots = Normoxic conditions; Blue dots = Hypoxic conditions. Statistically analysed by two-way ANOVA with Tukey's correction. * $P \leq 0.05$, ** $p \leq 0.01$.

5.2.1.3 Carnitine metabolites

A second pathway which illustrated that RA-SF induced a distinct metabolic profile was carnitine metabolism. This pathway has been discussed in **Chapter 3**, where there was a lower level of abundance of carnitine metabolites in hypoxic conditions compared to normoxic conditions (**Chapter 3**). As in **Chapter 3**, in unstimulated cells, hypoxia appeared to decrease the abundance of unbound L-carnitine and acyl-carnitines (O-acetylcarnitine & 3-dehydroxycarnitine), although this appeared to be donor dependent (**Figure 5.3**). However, in treated cells, the hypoxic impact seen in unstimulated cells was negated (**Figure 5.3**). A more robust finding was made in O-propanoylcarnitine, where hypoxia significantly reduced its abundance in both unstimulated and RA-SF treated cells. Although these results somewhat validated the findings from **Chapter 3**, it did indicate that there is a degree of donor specificity in this observation.

In a finding that was shared between L-carnitine and O-propanoylcarnitine in normoxia, RA-SF stimulation induced an accumulation of both metabolites when compared to unstimulated cells (**Figure 5.3**). In contrast, LPS did not alter the abundance of either of these metabolites, which further emphasises the metabolic disconnect between LPS and RA-SF stimulations (**Figure 5.3**). In hypoxic conditions, RA-SF significantly increased the intracellular levels of 3-dehydroxycarnitine in comparison to unstimulated cells. However, RA-SF had no effect on the abundance of O-acetylcarnitine when these groups were evaluated (**Figure 5.3**).

Collectively, there was a higher abundance of carnitines in RA-SF stimulated cells, especially when compared to LPS stimulated cells. These data suggested that carnitine shuttling, and subsequent FAO, is utilised at a higher rate in RA-SF stimulated cells than in unstimulated and LPS stimulated cells. This metabolic observation is shared with murine M(IL-4) macrophages (S. C.-C. Huang et al. 2014), which are widely regarded as immune-regulatory. Therefore, these findings suggest that, at least in comparison to LPS, RA-SF may not induce as robust an inflammatory response from monocytes.

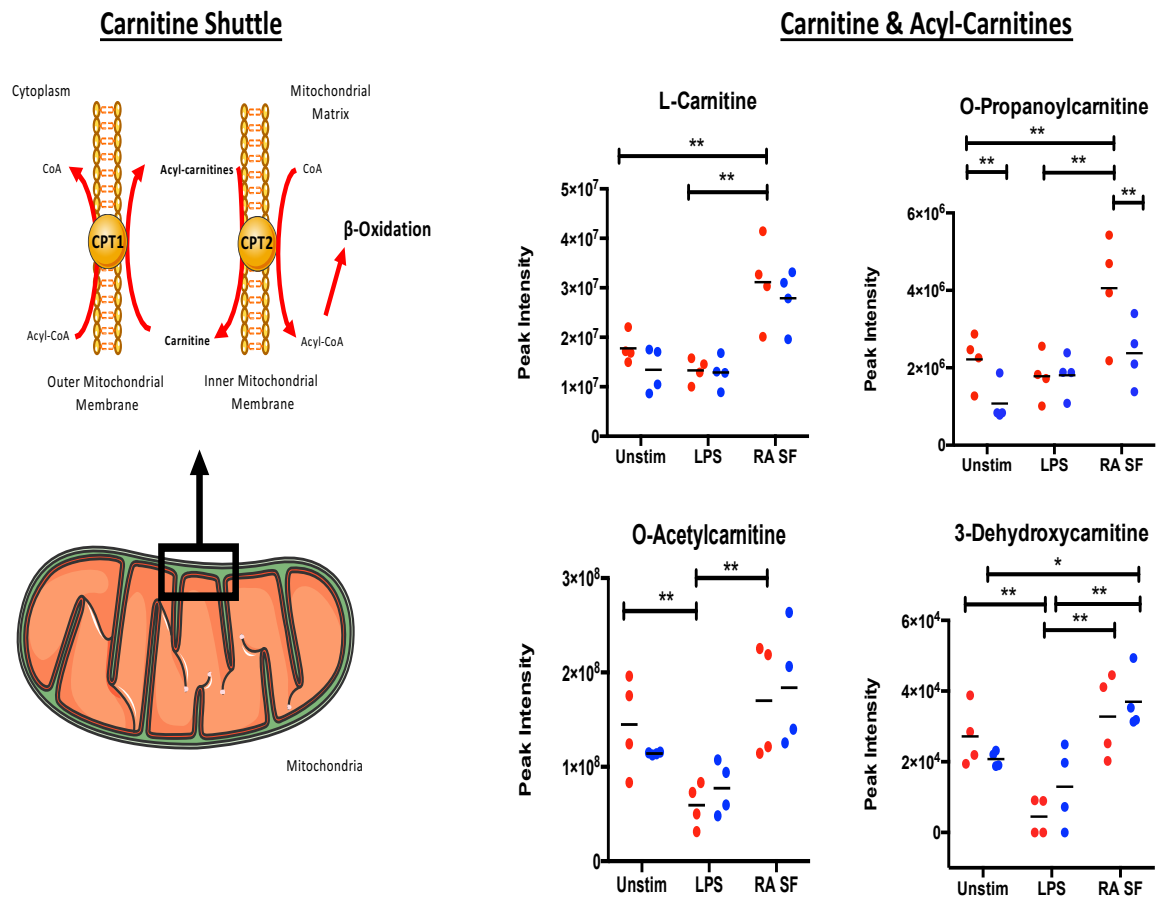


Figure 5.3 Carnitine shuttling components are altered in monocytes cultured in RA-SF after 4 hours. [A] Diagram showing the carnitine shuttling pathway in the mitochondrial membrane [B] Carnitines and acyl-carnitines which were significantly altered in RA SF in comparison to LPS in normoxia. Dots indicative of separate donors and line showing the Mean. N = 4. Red dots = Normoxic conditions; Blue dots = Hypoxic conditions. Statistically analysed by two-way ANOVA with Tukey's correction. * $P \leq 0.05$, ** $p \leq 0.01$.

5.2.1.4 Urea cycle and creatinine biosynthesis

Another pathway that showed alterations was the Urea cycle and creatinine biosynthesis (**Figure 5.4**). Notably, in addition to participating in the Urea cycle, arginine can transfer an amidino group onto glycine to generate guanidino-acetate, which is subsequently used for the synthesis of creatine and creatinine (**Figure 5.4**). Interestingly, in hypoxia, RA-SF significantly increased the abundance of glycine and guanidino-acetate when evaluated against unstimulated (**Figure 5.4**). Furthermore, RA-SF promoted a considerable build-up of creatinine in monocytes when compared to unstimulated cells in both normoxia and hypoxia. Furthermore, increased levels of creatine were also observed, but only when evaluated against LPS stimulated cells. (**Figure 5.4**). These results illustrate the RA-SF specifically enhances creatinine biosynthesis in monocytes.

Intriguingly, in comparison to unstimulated cells, RA-SF did not have any effect on the levels of l-ornithine and l-arginine. This suggests that Urea cycle activity is not altered after RA-SF treatment, but rather is repurposed for creatine and creatinine biosynthesis (**Figure 5.4**). This cycle is indicative of a more immune tolerant, less inflammatory phenotype, at least in comparison with M(LPS + IFN γ) polarised macrophages (Jha et al. 2015). Moreover, exogenous creatine and creatinine has been shown to cause a down-regulation of TLR-2, TLR-3, TLR-4 and TLR-7 in RAW 264.7 macrophages (Leland et al. 2011), supporting an anti-inflammatory role. Therefore, these results further support that concept that RA-SF promotes a more modulatory phenotype in monocytes to regulate pathological responses.

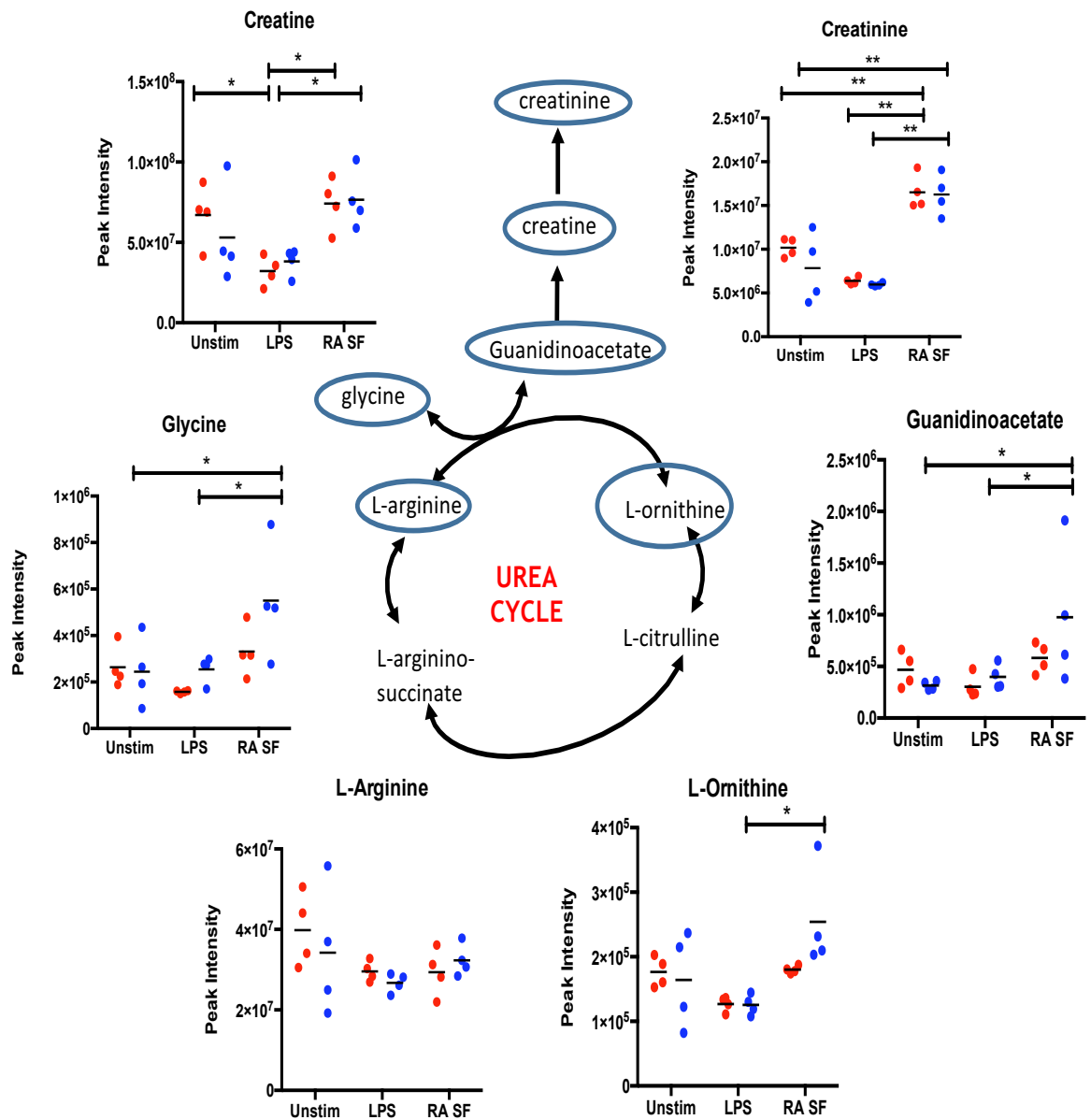


Figure 5.4 Urea cycle and creatinine synthesis intermediates accumulate in monocytes stimulated with RA-SF. Illustration of the Urea cycle with the creatinine synthesis pathway branching off. Metabolites circled in blue were identified as being significant between LPS and RA-SF in normoxia after 4 hours of culture. The levels of these metabolites are shown graphically. Dots indicative of separate donors and line showing the Mean. $N = 4$. Red dots = Normoxic conditions; Blue dots = Hypoxic conditions. Statistically analysed by two-way ANOVA with Tukey's correction. * $P \leq 0.05$, ** $p \leq 0.01$.

5.2.1.5 Nucleotide metabolism

The final group metabolites which showed significant alterations in abundance after RA-SF stimulation was found within nucleotide intermediates. In purine metabolism, RA-SF induced a significant up-regulation of the metabolites xanthine and urate when compared against unstimulated monocytes in normoxia and hypoxia (**Figure 5.5**). Additionally, RA-SF promoted a build-up of IMP and hypoxanthine when evaluated against unstimulated cells. In contrast to these results, RA-SF attenuated the levels of AMP and had no impact on the intracellular levels of adenosine (**Figure 5.5**). Intriguingly, hypoxia significantly augmented IMP abundance in unstimulated cells, which concurs with the results from Chapter 3. However, hypoxia had no significant impact on any other purine intermediates. (**Figure 5.5**). Taken together, RA-SF has a variable effect on the abundance of intermediates that are required for DNA and RNA synthesis (IMP, AMP & adenosine). However, the consistent accumulation of intermediates associated with purine breakdown (hypoxanthine, xanthine and urate) suggests that purines are actively degraded in response to RA-SF.

The pyrimidine metabolic pathway also exhibited changes after stimulation with RA-SF. Indeed, in hypoxia, RA-SF increased the accumulation of UTP when evaluated against unstimulated cells. In addition, orotate was significantly increased after RA-SF treatment in comparison to LPS stimulated cells, but only in normoxia (**Figure 5.6**). Furthermore, LPS substantially reduced the abundance of l-aspartate and UMP. However, RA-SF treated cells did not exhibit any significant alteration. (**Figure 5.6**).

In summation, the data suggests that RA-SF induces the accumulation of metabolites associated with purine nucleotide breakdown. However, no consistent observations were made in purine and pyrimidine intermediates involved in DNA and RNA synthesis. Nevertheless, the results emphasise that RA-SF induces profound metabolic changes in human monocytes.

Purine Metabolism

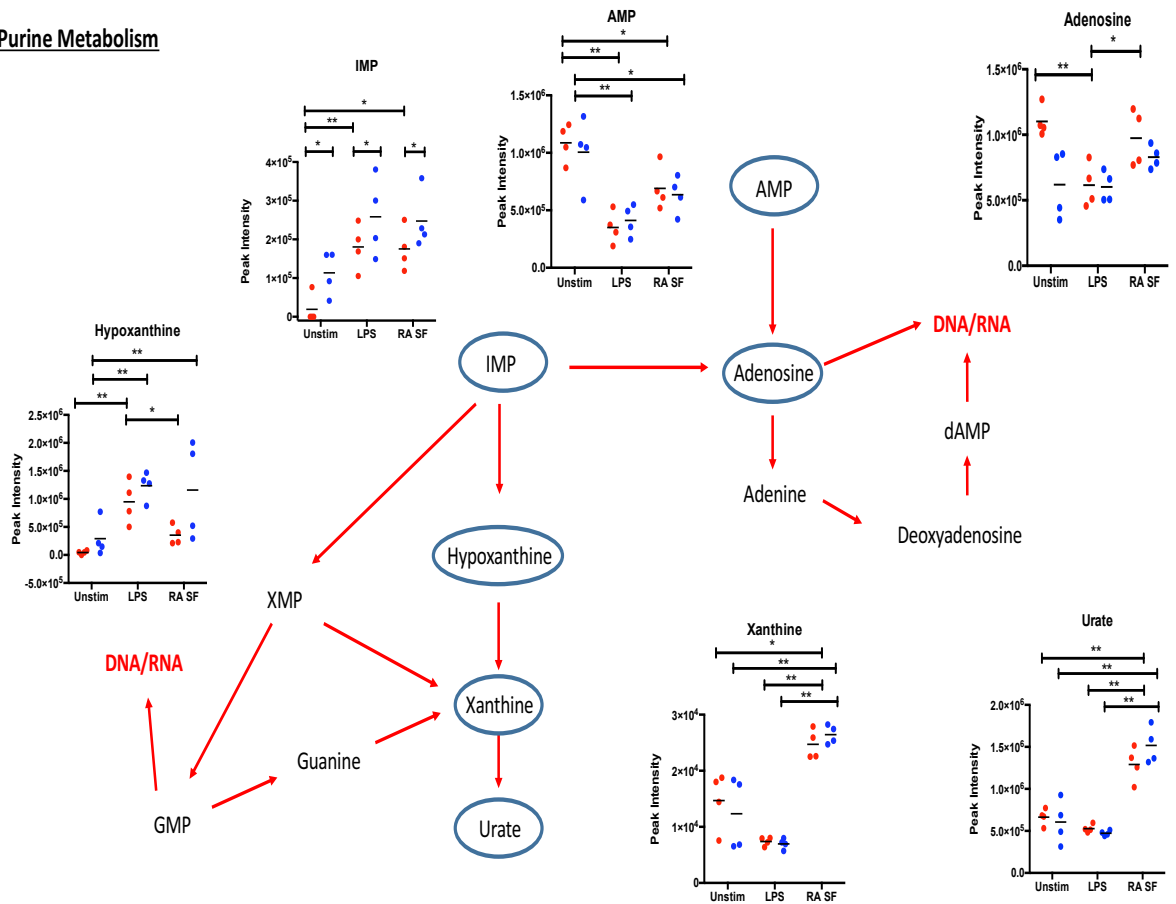


Figure 5.5 Purine metabolism is altered in monocytes cultured in RA-SF in comparison to LPS. Diagram showing the purine metabolic pathway for the synthesis of DNA and RNA. Metabolites circled blue indicate those which showed a significant difference between LPS and RA-SF in normoxia after 4 hours. The levels of these metabolites are shown graphically. Dots indicative of separate donors and line showing the Mean. $N = 4$. Red dots = Normoxic conditions; Blue dots = Hypoxic conditions. Statistically analysed by two-way ANOVA with Tukey's correction. * $P \leq 0.05$, ** $p \leq 0.01$.

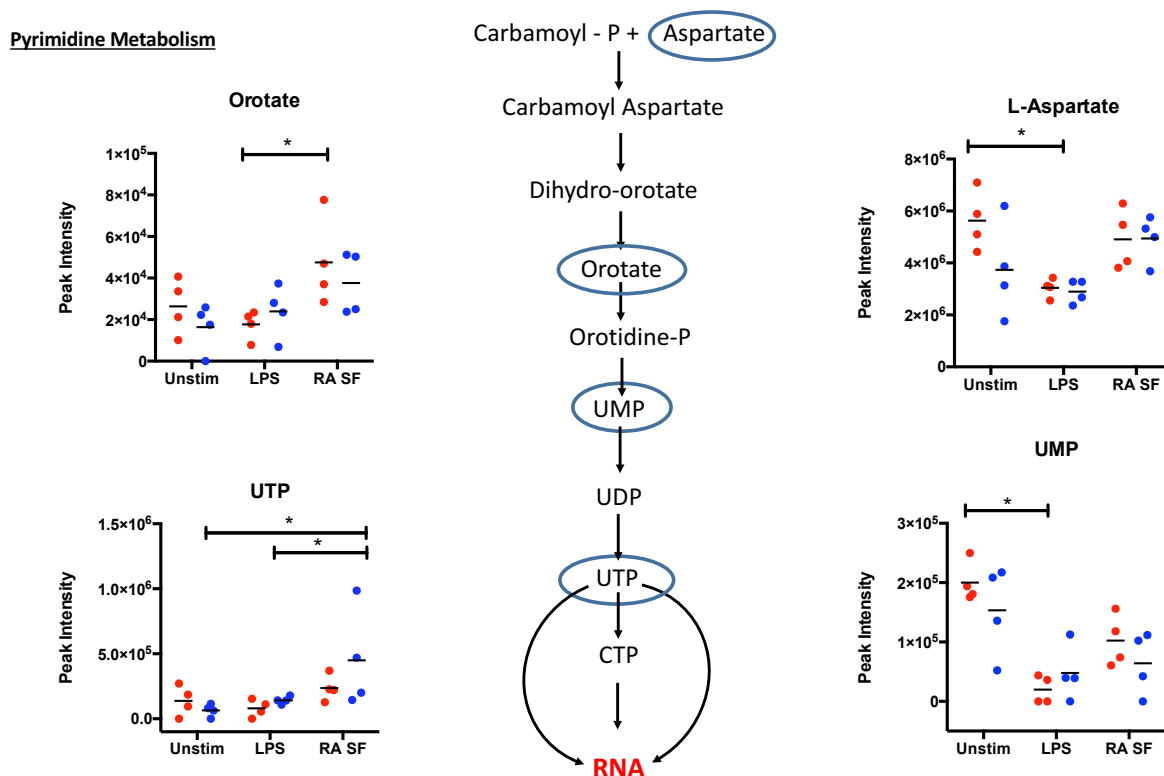


Figure 5.6 Pyrimidine metabolism is altered in monocytes cultured in RA-SF in comparison to LPS. Diagram showing the pyrimidine metabolic pathway for the production of RNA components. Metabolites circled in blue were identified as significant between LPS and RA-SF in normoxic conditions. Dots indicative of separate donors and line showing the Mean. $N = 4$. Red dots = Normoxic conditions; Blue dots = Hypoxic conditions. Statistically analysed by two-way ANOVA with Tukey's correction. * $P \leq 0.05$, ** $p \leq 0.01$.

5.2.2 Manipulation of carnitine metabolism in RA-SF treated monocytes

The metabolomics analysis illustrated that RA-SF caused an increase in abundance of metabolites belonging to several metabolic pathways, including cellular energy, carnitines, urea cycle and nucleotide metabolites. Furthermore, hypoxia had no significant influence in the metabolism of stimulated cells, and appeared to have a more potent effect at metabolite level in untreated cells. Since carnitines were altered after RA-SF stimulation (**Figure 5.3**) and in hypoxia (**Chapter 3**), the impact of carnitine metabolism on the ability of monocytes to produce pro-inflammatory cytokines in response to RA-SF was assessed. This was achieved using the same approach undertaken in **Chapter 4**.

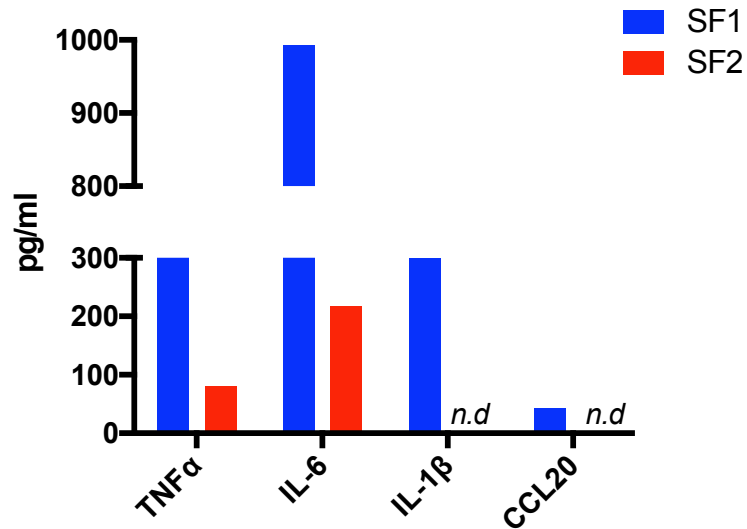


Figure 5.7 Assessment of pro-inflammatory mediators in RA synovial fluids. The levels of TNF α , IL-6, IL-1 β and CCL20 within the synovial fluids from 2 individual RA patients were tested by ELISA. The analysis was conducted in technical duplicate. Data shown as the Mean. n.d. = non-detectable.

Before any functional analysis was carried out, the levels of pro-inflammatory mediators within RA-SF from 2 separate donors (RA-SF 1 & 2; 10% in media) was determined by ELISA to obtain a baseline level of each within the cell culture. ELISA analysis revealed that RA SF 1 contained a higher level of pro-inflammatory mediators (TNF α , IL-6, IL-1 β & CCL20) than RA SF 2 (**Figure 5.7**). The difference in levels of pro-inflammatory mediators between the two RA-SFs emphasise the heterogeneity amongst samples. Therefore, the studies subsequently presented herein focussed on one RA-SF sample (RA-SF 1) across multiple healthy donor monocytes. Thus, further studies will be required to determine the generalisability of these findings to all RA-SF. In addition, RA-SF 1 did not induce the release of IL-1 β or TNF α from monocytes above the baseline, suggesting that these mediators are not produced by RA-SF in this culture system (data not shown). However, additional secretion of CCL20 and IL-6 was observed above the baseline values, hence the release of these mediators was assessed after metabolic perturbation (**Figures 5.8 & 5.9**).

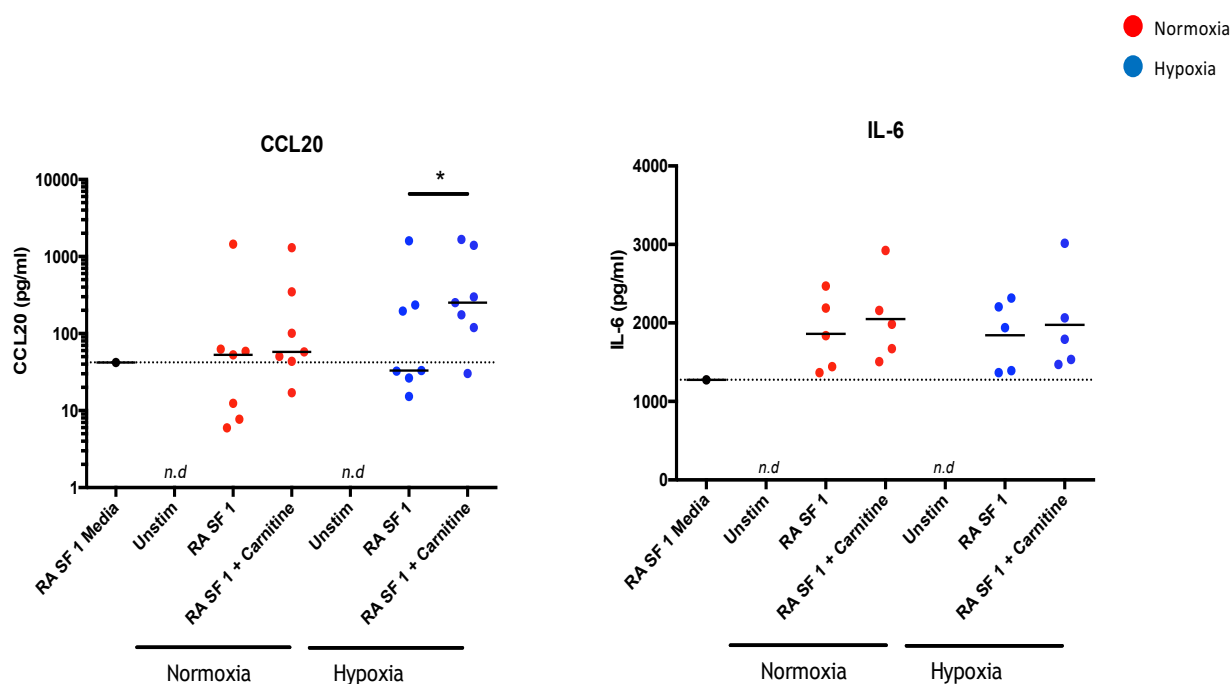


Figure 5.8 Exogenous carnitine increases CCL20 production in monocytes treated with RA-SF in hypoxia. Monocytes were left unstimulated, or were stimulated with RA SF (10% in medium) \pm 10mM exogenous carnitine in normoxia or hypoxia (1% O₂). The cells were left for 16 hours, supernatants harvested and analysed by CCL20 and IL-6 ELISA. The levels of CCL20 and IL-6 in the media containing RA-SF was analysed to give baseline levels of each (dotted line). Dots are indicative of separate healthy donors of monocytes with line showing the Mean. N = 5-7. Statistically analysed by Wilcoxon rank test. * P < 0.05. n.d. = non-detectable.

The first approach to assess the influence, if any, of carnitine metabolism on the production of pro-inflammatory mediators when stimulated with RA-SF, was to supplement monocytes with exogenous carnitine. To this aim, monocytes were stimulated with RA-SF 1 (10% in media) in normoxia or hypoxia (1% O₂) in the presence or absence of 10mM carnitine. The cells were incubated for 16 hours and the supernatant was harvested and analysed by ELISA. The results showed that RA-SF 1 induced IL-6 secretion from monocytes, as it was above the level of IL-6 in the media supplemented with RA-SF by 1.5 fold. (Figure 5.8). Notably, there was no difference between cells in normoxia or hypoxia. This is counter to what was observed after LPS stimulation (Figure. 4.7). The addition of exogenous carnitine also had no significant effect on the production of IL-6 (Figure 5.8). Evaluation of CCL20 secretion in normoxia showed that induction of additional secretion was donor dependent, and in those that did secrete additional CCL20, exogenous carnitine had little impact on secretion (Figure

5.8). In hypoxic conditions, additional secretion of CCL20 in response to RA-SF was also donor dependent. Remarkably, carnitine promoted a significant increase in the production of CCL20 in hypoxia (**Figure 5.8**) Exogenous carnitine not only enhanced the release of CCL20 in donors that showed additional CCL20 secretion, but it induced CCL20 secretion in donors that previously did not secrete additional CCL20 (**Figure 5.8**). These data support the results in the previous chapter, where exogenous carnitine also increased the secretion of CCL20 in response to LPS (**Figure 4.8**). Intriguingly, the level of CCL20 that was detected in some donors was below the level of CCL20 found in the RA-SF medium, indicating that the monocytes may have started to exhibit consumption /uptake of CCL20 via CCR6. Indeed, CCL20 has been reported to attract CCR6⁺ monocytes to RA joints (Ruth et al. 2003).

The second approach to interrogate carnitine metabolism in this context was by pre-treatment with ETO (50µM). In the same manner as with LPS stimulated monocytes in the previous chapter, monocytes were pre-treated with ETO for 1 hour, and were then stimulated with media containing RA-SF (10%). Despite this, ETO had no significant effect on the production of IL-6 or CCL20 in normoxia or hypoxia (**Figure 5.9**). As with the results from **Figure 5.8**, hypoxia did not enhance the production of IL-6 or CCL20 in a manner similar to that observed with LPS in **Chapter 4**. When comparing the level of cytokine and chemokine that is produced by monocytes in response to RA-SF (**Figures 5.8 & 5.9**) to the levels released in response to LPS (**Figure 4.7**), the levels are markedly reduced, especially with IL-6. These data indicated that synovial fluid from a rheumatoid arthritis patient, which possesses a variety of pro-inflammatory mediators, does not induce as strong an inflammatory response as a pure TLR4 stimulus (LPS). Nevertheless, in both LPS and RA-SF stimulated monocytes, carnitine supplementation aids the secretion of CCL20, especially in hypoxia. These results propose a role for FAO in inflammatory responses mediated by both TLR-4 signalling via LPS and by the complex stimulus of RA-SF.

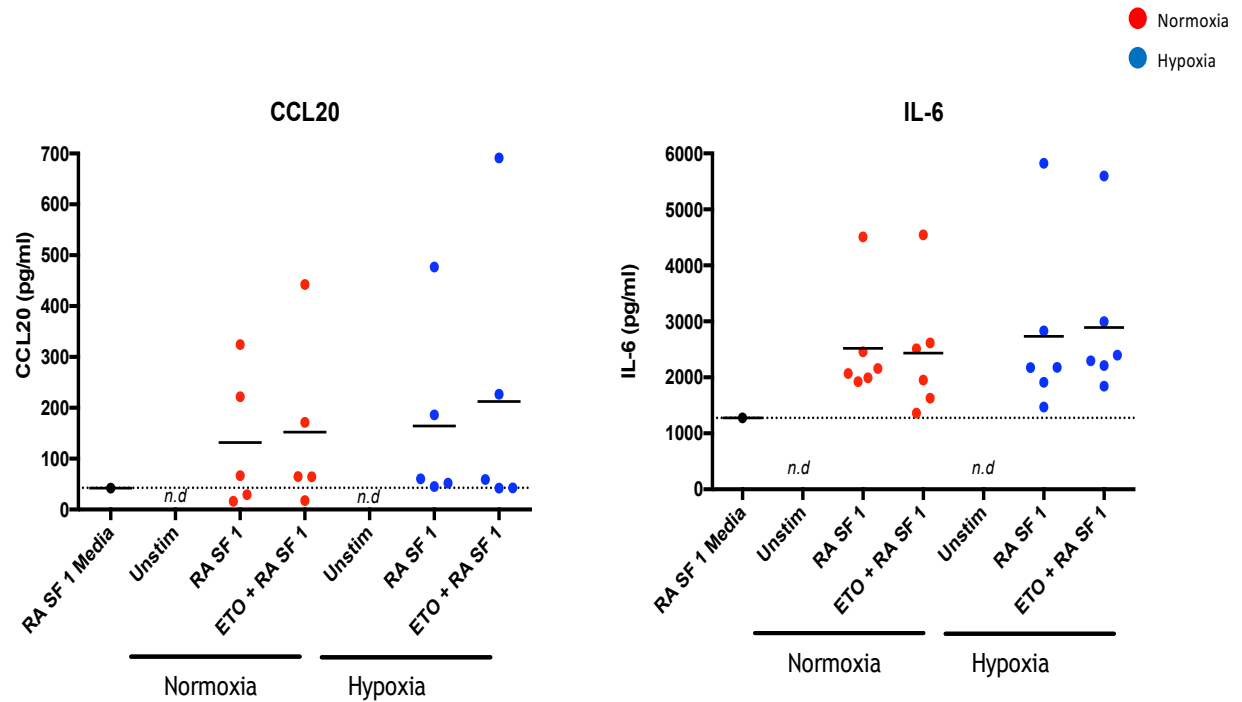


Figure 5.9 Hypoxia and ETO has no effect on CCL20 & IL-6 production in RA-SF treated monocytes. Monocytes were left unstimulated or were stimulated with RA-SF (10% in medium) for 16 hours in normoxia or hypoxia (1% O₂). In a separate condition, RA-SF treated monocytes were pre-treated for 1 hour with ETO (50 μ M). Supernatants were harvested and analysed by CCL20 and IL-6 ELISA. Dots indicative of separate healthy donors of monocytes with line showing the Mean. N = 5-6. n.d. = non-detectable.

5.2.3 Metabolic profiling and manipulation of intracellular carnitine in end polarised alveolar macrophages

Once blood monocytes are recruited to sites of inflammation in tissue, they often differentiate into tissue macrophages. Although carrying out experiments where isolated monocytes are differentiated experimentally *in vitro* in the presence of hypoxia and/or the presence of an inflammatory milieu are appealing. It was decided that in order to assess the metabolic effect on inflammatory function of macrophages, they would be isolated directly from human tissue. Joint tissue from RA patients were not available for this purpose. However, alveolar macrophages were readily accessible and were isolated directly from human lung tissue. It must be noted that human lung tissue originates from variable pathologies, such as transplant, COPD and cancer. Furthermore, the smoking status, age and gender are all variable in these patients, increasing variability in the overall study.

The metabolomics analyses from **Chapter 3** and in this chapter had identified that carnitine metabolites were altered in both hypoxia and in RA-SF compared to LPS and unstimulated cells. Therefore, this pathway was targeted specifically by mass spectrometry to assess how hypoxia and polarisation status of alveolar macrophages influences this metabolic pathway. This was achievable by measuring the abundance of a variety of carnitines against a set of known standards on the mass spectrometry platform (2.4.4). Alveolar macrophages were isolated, rested overnight and were either left untreated as 'M0', or were polarised to an M(LPS ± IFN γ) or M(IL-4) state (2.2.5). The intracellular metabolites were then harvested and the carnitine profile was analysed by mass spectrometry. In **Figure 5.10**, the name of each carnitine metabolite assessed is shown, with each having a corresponding shorthand name (C0-C16). This is based on the number of fatty acid acyl groups that have bound to free L-carnitine (C0). The results show that in untreated M0 macrophages, hypoxia reduced the level of C2, C4, C6 and C8 carnitine. However, these findings did not reach statistical significance (**Figure 5.10**). These observations resemble the findings in Chapter 3, where hypoxia reduced the level of carnitines in untreated monocytes (**Figure 3.8**). In comparison to M0 macrophages, LPS and IFN γ treatment did not appear to have a significant influence on the abundance of the carnitines, with the exception of C0 and C3, which did exhibit increases in specific donors. Furthermore, hypoxia again had a non-significant effect in M(LPS + IFN γ) macrophages, but donor specific decreases were observed in C4, C5 and C6 (**Figure 5.10**). Likewise, the polarisation conditions of M(IL-4) macrophages did not induce any noticeable changes in metabolites when compared with M0 or M(LPS + IFN γ) macrophages. However, hypoxia promoted some reduction in C2, C4, C6 and C8 abundance in certain donors (**Figure 5.10**). In summation, these data suggest that polarising macrophages *in vitro* to M(LPS + IFN γ) or M(IL-4) does not significantly alter the abundance of intracellular carnitines. Furthermore, hypoxia has little impact on carnitine abundance in polarised macrophages.

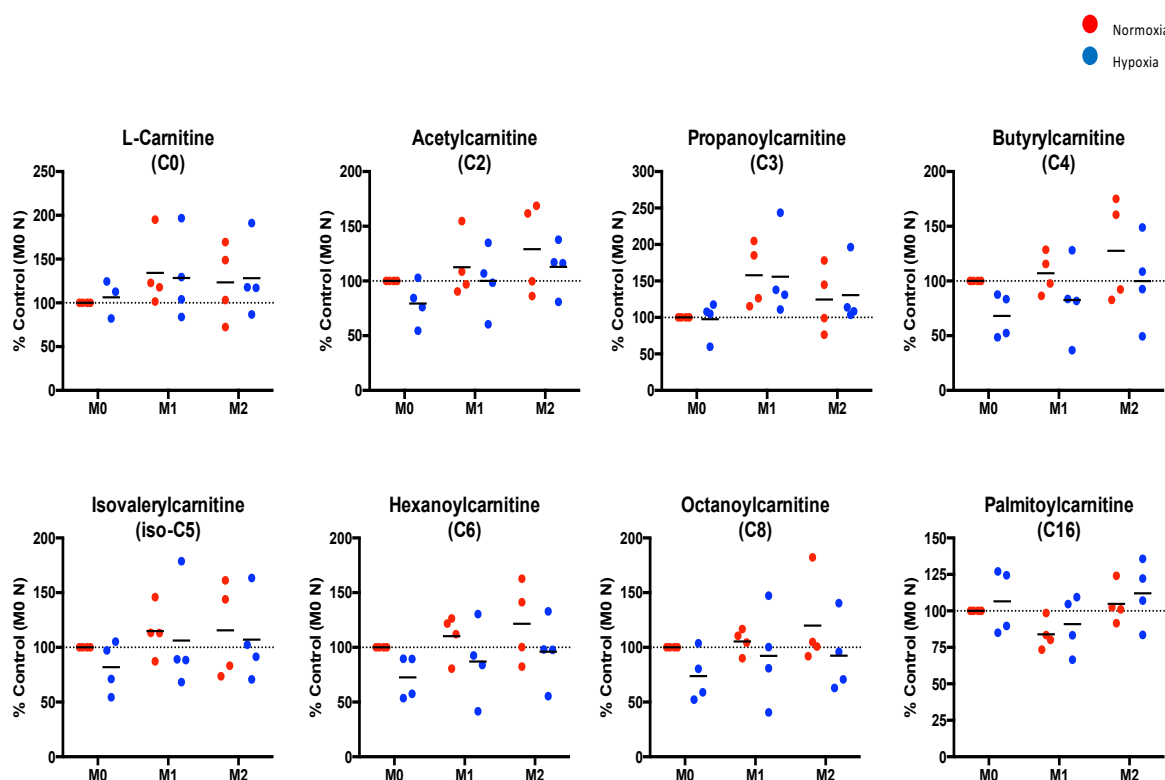


Figure 5.10 Endogenous carnitine abundance in polarised alveolar macrophages. Alveolar macrophages were left untreated (M0) or were polarised to M1 (M(LPS + IFN γ)) or M2 (M(IL-4)) states in normoxia or hypoxia (1% O₂) for 24 hours. Intracellular metabolites were extracted and carnitine metabolites were analysed by mass spectrometry. Dots are indicative of separate donors with line showing the Mean. N = 3-4.

Even though no detectable changes were observed in AM upon exposure to a hypoxic environment or classical stimuli, we sought to assess the impact of carnitine metabolism on the ability of polarised alveolar macrophages to secrete pro-inflammatory mediators. This was carried out by using the same two methods described in previous experiments above: carnitine supplementation and inhibition of the carnitine shuttle by pre-treatment with ETO. In this instance, alveolar macrophages were isolated, rested overnight and were either untreated as M0 or were polarised for 24 hours as M(LPS + IFN γ) or M(IL-4) in normoxic or hypoxic (1% O₂) conditions. The supernatants were harvested and were subject to ELISA or MSD assessment. M(LPS + IFN γ) macrophages were assessed for the pro-inflammatory cytokines and chemokines TNF α , IL-6, IL-1 β , IL-8 and CCL20. Supernatants from M(IL-4) macrophages were analysed for

CCL22, a classical chemokine secreted in these cells in response to IL-4. The results indicated that neither pre-treatment with ETO or supplementation with carnitine had any effect on the production of IL-6 or TNF α in M(LPS + IFN γ) macrophages in normoxia and hypoxia. (Figure 5.11). In addition, there were no consistent observations in regards to IL-1 β secretion under these conditions (Figure 5.11). A more consistent observation was made with IL-8, where ETO and exogenous carnitine, although to a lesser extent, reduced the level of IL-8 in all donors in hypoxic conditions (Figure 5.11). CCL20 showed significant alterations in LPS and RA-SF treated monocytes under hypoxic conditions, therefore this was assessed in the context of alveolar macrophages as well. Despite this, the two donors assessed showed inconsistent changes in CCL20 production across both treatments (Figure 5.11). The variable results from M(LPS + IFN γ) macrophages extended to M(IL-4) polarised cells. Indeed, when assessing CCL22 secretion, neither oxygen tension or carnitine manipulation yielded any conclusive findings. (Figure 5.11). These data suggest that when treated in the same way as healthy monocytes, alveolar macrophages may not possess the same level of sensitivity to metabolic manipulation. Nonetheless, these experiments would need to be repeated extensively due to the heterogeneous nature of patients.

● Normoxia
● Hypoxia

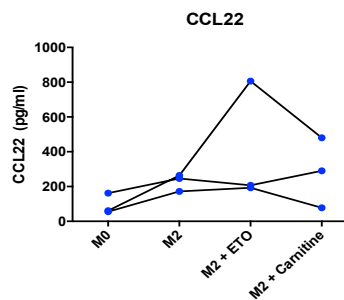
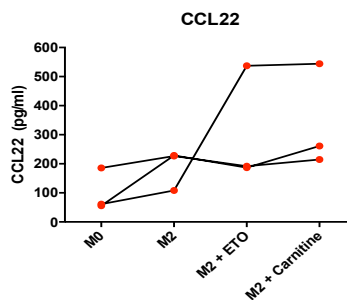
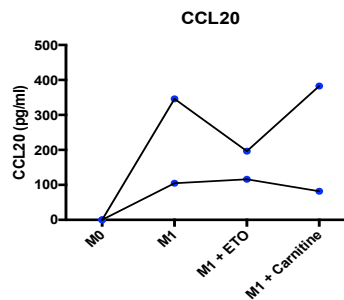
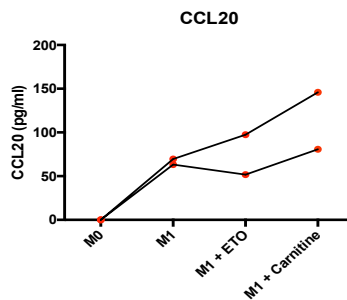
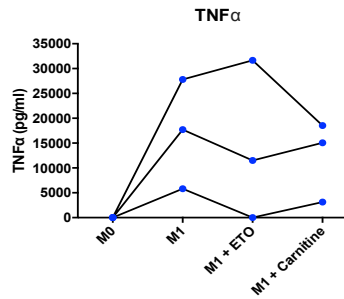
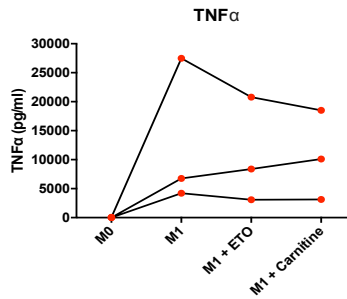
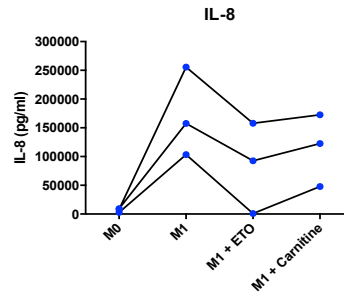
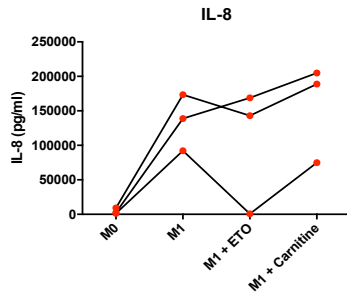
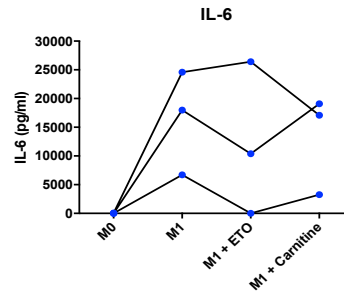
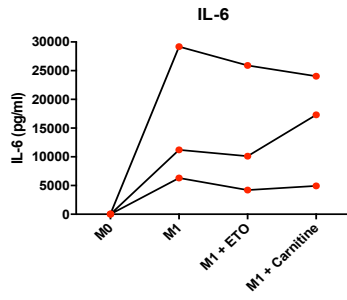
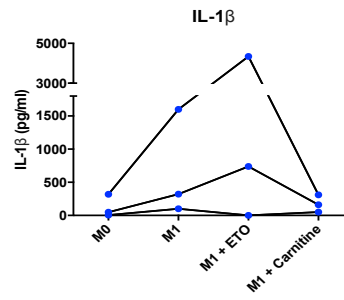
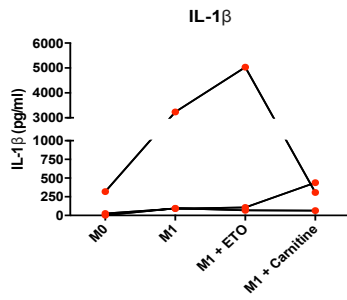


Figure 5.11 ETO and carnitine has no impact on the production of inflammatory mediators in alveolar macrophages. Alveolar macrophages were left untreated (M0) or were polarised to M1 or M2 states in normoxia or hypoxia (1% O₂) for 24 hours. For metabolic manipulation, macrophages were pre-treated with ETO (50µM) for 1 hour before polarisation or were supplemented with carnitine (10mM) simultaneously at time of polarisation. Supernatants were harvested and were analysed by MSD or ELISA. Dots representative of separate donors. N = 2-3.

In the previous experiment and in the studies in monocytes, the cells were stimulated, exposed to hypoxia and supplemented with carnitine simultaneously. In addition, the inhibitor, ETO, was typically added to the culture before subsequent stimulation for 1 hour. In a final preliminary experiment, alveolar macrophages were pre-exposed to hypoxia to assess if this could sensitise the cells to metabolic perturbation. To test this, untreated alveolar macrophages were cultured in normoxia or hypoxia for 3 hours. For treatment with ETO, the cells were pre-treated with the inhibitor for a further 1 hour before stimulation. The macrophages were then polarised for 24 hours to an M(LPS + IFN γ) phenotype under normoxia or hypoxia and the supernatants harvested for ELISA analysis. The data illustrates that neither hypoxia, ETO nor carnitine supplementation had any effect on IL-6 production (**Figure 5.12**). However, hypoxia induced a slight increase in the production of IL-1 β and CCL20 in M(LPS + IFN γ) macrophages. Moreover, pre-treatment with ETO increased IL-1 β in normoxic conditions. Supplementation of the cells with carnitine decreased the production of IL-1 β in both normoxia and hypoxia. In agreement with the previous work in monocytes, exogenous carnitine increased the production of CCL20 in hypoxia, albeit in only one donor (**Figure 5.12**). Caveats remain around the study size and the necessity for a pre-exposure to hypoxia to increase sensitivity to metabolic manipulation. However, these studies are one of the first to show that perturbation of alveolar macrophage metabolism can influence pro-inflammatory mediator release.

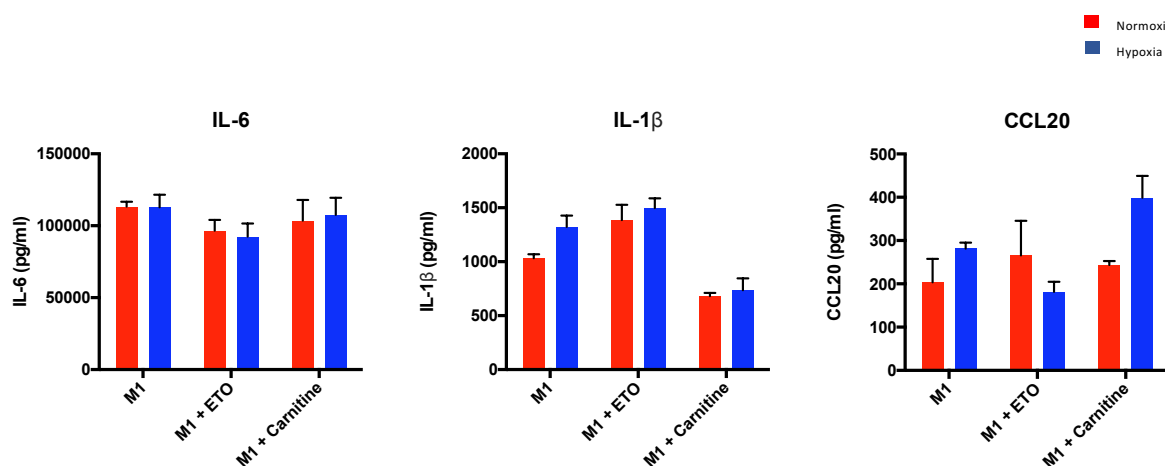


Figure 5.12 Pre-exposure of alveolar macrophages to hypoxia reveals differences in pro-inflammatory mediator release similar to that seen in monocytes. Untreated alveolar macrophages were incubated in normoxia or hypoxia (1% O₂) for 3 hours. For ETO (50 μ M) treatment, macrophages were pre-treated for a further 1 hour. Macrophages were then polarised to an M(LPS+IFN γ : termed M1) state for 24 hours. For carnitine (10mM) supplementation, the carnitine was added at the point of polarisation. The supernatants were harvested and analysed by ELISA. N = 1. Data shows the Mean \pm SD of 4 technical replicates.

5.3 Discussion

This chapter has set out to metabolically profile human monocytes under physiologically relevant *in vitro* conditions. By isolating primary human monocytes, exposing them to hypoxia and culturing the cells in the presence of synovial fluid spiked media, we aimed to capture a metabolic profile of monocytes recently recruited to a chronic disease state. The metabolomics analysis revealed that, in comparison to unstimulated cells, RA-SF promoted an accumulation of metabolites belonging to several pathways, including carnitines, creatinine biosynthesis and intermediates of purine degradation. In addition, RA-SF induced a divergent metabolic profile to that of LPS stimulation. Functional analysis indicated that RA-SF monocytes did not secrete inflammatory mediators to the levels of monocytes stimulated with LPS. However, carnitine supplementation increased CCL20 secretion in hypoxic conditions, a finding that was originally seen in LPS treated cells in **Chapter 4**. Since monocytes have the capacity to differentiate into macrophages in the tissue, the ability of alveolar macrophages to behave in a similar manner to hypoxia and carnitine manipulation was interrogated. Preliminary results suggest that aspects of cellular metabolism for the control of pro-inflammatory cascades are shared in

monocytes and macrophages under these conditions. However, this appeared to be dependent on the kinetics of hypoxic induction in the experimental setup.

One of the most striking observations in the metabolomic experiment was the increased abundance of metabolites in RA-SF treated cells in comparison to those untreated and treated with LPS. As opposed to unstimulated macrophages, stimulation with LPS induces a highly active metabolic programme which resembles the Warburg effect, by exhibiting increased glycolytic flux at the expense of mitochondrial metabolic cascades such as the TCA cycle and OXPHOS to generate ATP (Rodriguez-Prados et al. 2010; Tannahill et al. 2013). Furthermore, increased PPP has also been reported in these cells to boost nucleotide production for biosynthetic cascades (Freemerman et al. 2014; Haschemi et al. 2012). Therefore, the loss of metabolites observed in LPS stimulation when compared to RA-SF in this study may reflect monocytes undergoing a higher metabolic turnover and consumption of metabolites. Since metabolome analysis represents a snapshot of metabolites at the point of extraction, gene expression analysis of metabolic enzymes may reveal the full extent of metabolic activity within each pathway. In addition, when comparing the raw values of secretion of pro-inflammatory mediators in response to RA-SF, it was markedly reduced when compared to the levels of secretion in response to LPS. Thus, the metabolic profile obtained in RA-SF cells may be representative of a cell experiencing a phase of stasis, rendering the cell less inflammatory.

Alternative metabolic programmes and functional characteristics have been observed in human monocytes stimulated with different TLR ligands (Lachmandas et al. 2016). In the work by Lachmandas *et al* (2016), monocytes stimulated with LPS (TLR-4) and P3C (TLR-2) both increased their glycolytic machinery, however only P3C stimulated monocytes showed increased mitochondrial respiration. Furthermore, C-type lectin receptor stimulation has also been shown to promote glycolytic metabolism and the PPP in response to hyphae of *candida albicans*. Interestingly, the same study suggested that in addition to glycolysis and the PPP, *candida albicans* yeast induced OXPHOS and glutaminolysis to efficiently carry out an amplified inflammatory response (Domínguez-Andrés et al. 2017). The work presented in this chapter indicated that RA-SF induced a distinct metabolic programme in monocytes compared to

other inflammatory ligands such as LPS. This was emphasised by the notable accumulation of metabolites belonging to a number of pathways induced by RA-SF in comparison to LPS, including: carnitine metabolism; purine breakdown intermediates and creatinine biosynthesis. In addition to LPS, further work is warranted to assess the metabolome of monocytes in response to stimuli that may have been present in RA-SF. An obvious candidate being FcR stimulation via immune-complexes, known to be present in the RA synovial compartment (discussed in 1.2.1.3). Nevertheless, work to elucidate which inflammatory mechanisms are engaged in response to RA-SF could provide useful targets for alteration, however, given the heterogeneity amongst patients, this may vary. Given the robust accumulation of creatinine in RA-SF treated monocytes here, this could promote inflammatory or anti-inflammatory cascades that is shared amongst RA patients.

The literature surrounding monocytes cultured under RA-SF is limited, however, SF derived from RA patients has been shown to decrease receptor expression of Immunoglobulin-like transcript 4 (ILT4) and increase CD86 expression in monocytes (Chimenti et al. 2016). Furthermore, T cells produced significantly more TNF α and IFN γ when costimulated with monocytes cultured in the presence of RA-SF. In a separate study, synovial fluid monocytes showed higher surface expression of CD80, CD276 and HLA-DR compared to those in the peripheral blood of the same patients (Yoon et al. 2014). In addition, RA-SF (1:1 with culture medium) induced Activin-A, PHD3 and MMP-12 production in monocytes (Soler Palacios et al. 2015). These studies propose that RA-SF induces a pathogenic phenotype in monocytes, by showing a higher expression of costimulatory molecules and a lower expression of ILT4, which has been shown to be immunomodulatory in antigen presenting cells. The pathogenic phenotype induced by RA-SF is supported by the studies in this chapter, which showed that monocytes secrete the pro-inflammatory mediators, IL-6 and CCL20, in response to RA-SF. However, to the best of our knowledge, there has been no work which has evaluated the effect of RA-SF on the metabolomic set-point in human monocytes. The most robust alteration in monocytes cultured under RA-SF compared to unstimulated and LPS stimulated cells was the accumulation of creatinine. The importance of creatinine metabolites on myeloid cell function is not well understood, but creatinine and creatine supplementation of RAW 264.7

macrophages has been reported to reduce the expression of a variety of TLRs (Leland et al. 2011). Assessing the impact of creatinine and creatine supplementation on the inflammatory function of activated monocytes would be worth investigating in future studies. The accumulation of creatine/creatinine could limit the inflammatory response when the cells are exposed to RA-SF. This may support the concept that monocytes enter a period of stasis when they are subject to these conditions.

In addition, monocytes have been reported to exhibit lower levels of apoptosis in the presence of RA-SF (Chimenti et al. 2016). In support of this, conditioned medium from cultured RA synovial fibroblasts has been suggested to increase monocyte viability by up to 60% in co-culture systems. This was enhanced further when the synovial fibroblasts were stimulated with IL-1 β and TNF α , which are cytokines known to be present in the synovial milieu (Darrietort-Laffite et al. 2014). This research could indicate that the metabolic profile of RA-SF treated monocytes could resemble one for the preparation of longer-term survival. The accumulation of metabolites may be a necessary fuel for catabolic metabolism in monocytes to survive in this environment for the long term. Such characteristics have been reported in memory T cell populations (van der Windt & Pearce 2012), where fatty acid oxidation is thought to have a prominent role in their long term functioning. The metabolomics data suggest that carnitine metabolites are increased in RA-SF, which signals an increased utilisation of fatty acid metabolism. Interestingly, published work has revealed that CD14⁺ cells isolated from the SF of RA patients exhibit higher gene expression levels of CD36, an important surface receptor for fatty acid uptake (Soler Palacios et al. 2015). Taken together, stock piling of carnitine metabolites and the increased CD36 could lead to a dependence on fatty acid oxidation in this environment should they persist for longer periods of time.

The results showed that RA-SF induces the production of IL-6 and, in a donor specific fashion, CCL20. Although ETO had no impact on the production of either IL-6 or CCL20, exogenous carnitine increased the release of CCL20 in monocytes in hypoxic conditions. A familiar finding was made in LPS stimulated monocytes in the previous chapter. The mechanism of action of ETO is under some debate. While it has been reported to cause up to 90% inhibition of FAO at 10 μ M, higher

concentrations (250 μ M) are thought to be needed to influence cellular respiration (Namgaladze et al. 2014). In the studies presented here, 50 μ M was used, therefore further studies could be carried at higher concentrations to assess the impact of cellular respiration in this context. More specifically, this could be achieved with rotenone treatment, an inhibitor of the electron transport chain. Off target effects have also been reported in the use of this inhibitor (Vats et al. 2006). With this in mind, and given the differences in murine and human macrophage metabolism, genetic manipulation of human metabolic genes could specifically dissect the role of metabolic pathways in monocytes. This could be employed in BLaER1 monocytes, where Crispr/Cas9 gene editing has been successfully carried out for interrogation of the inflammasome pathway (Gaidt et al. 2016). Despite this, the findings witnessed with exogenous carnitine suggested a specific link between carnitines, FAO and CCL20 production. This appeared to be regardless of the original stimulus, be it through TLR4 (LPS) or through a variety of cytokines in the synovial environment. A human trial of patients with osteoarthritis has shown that carnitine supplements reduce serum IL-1 β and MMP1 in these individuals (Malek Mahdavi et al. 2016). Studies assessing the effect of carnitine supplements effect CCL20 levels (and other inflammatory mediators) in synovial fluid of RA patients could determine if the results presented here represent a biological phenomenon in RA. More work however is needed to assess the mechanism for this finding. Metabolites are now increasingly being implicated in the control of epigenetic modifications. For example, during FAO, acetyl-CoA has been reported to promote acetylation of histones in tumour cells (J. V. Lee et al. 2014). In addition, the NAD⁺-dependent histone deacetylase, SIRT1, has more recently been shown to reduce IL-9 production from Th9 cells by negatively regulating HIF-1 α and mTOR activity (Y. Wang et al. 2016). Therefore, FAO may have a role in the control of CCL20 production by inducing epigenetic alterations. However, the precise role of CCL20 in the context of rheumatoid arthritis needs further clarification. For instance, does it promote an imbalance between inflammatory cells (such as monocytes, Th1, Th17) and immunomodulatory cells (Tregs) in this environment?

As well as exhibiting effector function upon recruitment to the tissue, infiltrating blood monocytes have the ability to differentiate into tissue

macrophages. Due to the availability of obtaining alveolar macrophages, this population was interrogated to test if polarised macrophages displayed similar metabolic and functional characteristics compared to monocytes. As carnitine metabolites were altered in monocytes (**Chapter 3**), these metabolites were exclusively analysed. Compared to M0 macrophages, M(IL-4) macrophages polarisation alone did not significantly increase carnitine metabolites. This is rather at odds with the published work, where carnitine and fatty acid oxidation are greatly associated with murine M(IL-4) macrophages (Jha et al. 2015; S. C.-C. Huang et al. 2014). However, a proteomic study in human macrophages suggests that rather gluconeogenesis predominates when macrophages are polarised to an M(IL-4) state (Reales-Calderón et al. 2014). In support of this, human M(IL-4) macrophages have been reported to lack PGC-1 β , which is involved in the induction of FAO. In addition, ETO treatment in M(IL-4) macrophages did not alter M(IL-4) macrophage function, such as CCL18 production and MRC1 expression (Namgaladze & Brüne 2014). These studies strongly suggest that murine and human macrophages display distinct metabolic programmes and perhaps FAO does not have an essential role in cell functionality under this context. The work in this chapter did show that some donor M(IL-4) polarised alveolar macrophages exhibited an increase in carnitines. Therefore, the study may need to be increased to assess for biological significance. Interestingly, carnitine supplementation increased CCL20 production in M(LPS + IFN γ) polarised alveolar macrophages after pre-exposure to hypoxia (**Figure 5.12**). As with monocytes, these results suggested a role for FAO for the production of CCL20 in M(LPS + IFN γ) macrophages. On the other hand, the accumulation of carnitine metabolites alone could act as an intracellular danger signal for the production of CCL20, in a similar manner that has been reported for succinate and citrate in different contexts (Infantino et al. 2011; Tannahill et al. 2013). As macrophage phenotypes are now considered to be part of a broad spectrum (Xue et al. 2014), in future work it would be interesting to determine if this finding extends to other macrophage phenotypes.

This chapter is, to the best of our knowledge, one of the first to integrate the growing field of intracellular immunometabolism in monocytes in the context of chronic inflammatory disease. Here, the studies carried out in monocytes incorporated the response to RA-SF, show that at a metabolic level, they appear

divergent to those cultured with experimentally used ligands such as LPS. Notably, this work does reveals a novel link between FAO and CCL20 production that appears to be shared between monocytes stimulated with LPS, RA-SF and end differentiated alveolar macrophages. Progressing these studies in alveolar macrophages to assess their metabolic and functional response to bronchoalveolar lavage fluid from COPD patients remains an attractive proposition. It is of our belief that such experiments give a clearer indication of myeloid cell characteristics in a chronic inflammatory environment.

Chapter 6. General discussion

This body of work has set out to determine what impact the inflammatory disease microenvironment has on inflammatory mechanisms in human monocytes. One of the most characteristic features of such an environment, is the presence of hypoxia (Lund-Olesen 1970). Monocytes are capable of adapting to these conditions to survive and carry out effector function to drive inflammation, perhaps through mechanisms involving HIF-1 α , NF- κ B and/or mitochondrial complex II (Fangradt et al. 2012; Sharma et al. 2017). Nevertheless, we postulated that metabolic changes may drive any associated functional changes under hypoxic conditions.

In **Chapter 3**, a mass spectrometry based metabolomics approach was utilised to metabolically profile human monocytes under hypoxic conditions *in vitro*. An early time point of hypoxia exposure (4 hours) was chosen for metabolite extraction. This was a bid to mimic early metabolic changes monocytes would exhibit during recruitment from the blood to an affected tissue *in vivo*. Mass spectrometry analysis revealed that carnitine metabolites (for subsequent FAO) were decreased in human monocytes in comparison to cells cultured in normoxic conditions (**Figure 6.1**). The loss of carnitines resembled that of cancer cells, where HIF-1 α is thought to actively turn off FAO in these cells (D. Huang et al. 2014). Increases in glycolytic and purine metabolites further support the adoption of cancer cell like metabolism in hypoxic conditions (Guillaumond et al. 2013). This suggested that hypoxia severely shifts monocyte cellular metabolism towards glycolysis for their survival and functionality, fitting with published work (Roiniotis et al. 2009).

In order to ascertain how hypoxia influenced monocyte function, **Chapter 4** aimed to carry out a comprehensive analysis of functional characteristics. However, from the assays used, hypoxia did not induce any observable changes in untreated monocytes. Therefore, it was hypothesised that hypoxia may alter activated cells. To this aim, a classical TLR-4 stimulus, LPS, was used for this purpose. Strikingly, hypoxia significantly increased the production of pro-inflammatory mediators such as IL-1 β (**Figure 6.1**). This proposed that hypoxia in the inflammatory milieu can act as an extracellular danger signal. We did not detect any production of pro-inflammatory cytokines when monocytes were

exposed to hypoxia without LPS stimulation. This suggested that hypoxia may prime the cells at a metabolic level for an enhanced inflammatory response in response to specific stimuli.

Seminal immune-metabolic studies in LPS activated murine macrophages highlight the importance of glycolysis in production of IL-1 β (Tannahill et al. 2013). Therefore, the increased glycolytic flux observed both in hypoxia and in LPS activation may explain the synergistic increase in IL-1 β release. This supports the concept that hypoxia acts as a danger signal and primes monocytes metabolically (enhanced glycolysis) for a more robust inflammatory response after LPS stimulation. Hypoxia alone has previously been shown to increase CCL20 production in unstimulated monocytes (Bosco et al. 2006). Although this wasn't repeated in the work presented here, hypoxia did increase CCL20 release in LPS stimulated monocytes (**Figure 6.1**). This could reflect a role for metabolic pathways in the production of CCL20 in a similar manner to IL-1 β .

From these data, it was postulated that the metabolic changes induced by hypoxia may be an influencing factor in the increases in pro-inflammatory mediators. Therefore, studies to alter carnitine metabolites were exploited to determine its role, if any, in the production of these mediators. One method for this was to try and increase carnitine metabolism by supplementing the cell culture medium with exogenous carnitine, previously shown to be consumed by monocytes (Ingoglia et al. 2017). Interestingly, carnitine supplementation significantly increased CCL20 further in LPS activated monocytes, in both normoxia and hypoxia, suggesting a role for FAO in CCL20 production (**Figure 6.1**). However, no difference was observed in IL-1 β . In contrast, carnitine inhibition with ETO significantly increased the release of IL-1 β in activated monocytes in normoxia and hypoxia (**Figure 6.1**). However, an increase was only detected in CCL20 in normoxic conditions. The metabolic profile of monocytes cultured under ETO treatment was not analysed here. However, in order to generate sufficient acetyl-CoA for ATP generation through the TCA cycle, other sources may need to be relied upon, such as increased glycolysis (Schlaepfer et al. 2015). Such a shift could rationalise why IL-1 β production was increased under these circumstances (Tannahill et al. 2013). Taken together, pathways

such as glycolysis and FAO may work in conjunction for the suitable release of pro-inflammatory mediators.

Given the important role of glycolysis under these conditions, preliminary work was also carried out to assess the role of this pathway in this experimental set up. In a striking result, inhibition of glycolysis with 2-DG severely reduced the release of IL-6, IL-1 β and CCL20 in hypoxic conditions, although this study would need to be expanded. This highlights a seemingly vital role for glycolysis in pro-inflammatory function in hypoxic conditions. Since glycolysis is imperative for cell survival in hypoxic conditions too, this reduction could be attributed to cell death (Roiniotis et al. 2009).

Despite the hypoxic nature of inflammatory disease sites, alone it does not fully reflect the tissue environment, which contains a variety of PAMPS. Thus, **Chapter 5** set out to incorporate RA synovial fluid (RA-SF) to the *in vitro* hypoxic set up used in the previous chapters. In a similar approach to **Chapter 3**, monocytes were cultured in cell culture medium containing 10% RA-SF under normoxia and hypoxia and metabolically profiled by mass spectrometry. This profile was compared to the metabolic profile of untreated and LPS stimulated monocytes. Throughout the study, RA-SF monocytes showed an accumulation of metabolites (in comparison to untreated and LPS stimulated monocytes) belonging to several pathways, including carnitines, amino acids, nucleotides and energy metabolites such as ATP and NAD. The lack of abundance in metabolites from LPS treated monocytes may reflect a cell that is more energetically active than RA-SF monocytes with a constant metabolic turnover. The metabolite accumulation could suggest the monocyte is under a phase of stasis. Published work, however, does show that RA-SF monocytes express increased level of CD86, suggesting that RA-SF induces an inflammatory phenotype in these cells (Chimenti et al. 2016). Interestingly, hypoxia did not yield any significant changes in these metabolites. Thus metabolites which were not able to be putatively identified from this mass spectrometry analysis may be important.

Since carnitine metabolites were found to be altered in RA-SF monocytes, we examined if carnitine supplementation and/or inhibition changed the output of pro-inflammatory mediators under RA-SF treatment. In a similar finding to LPS

treated monocytes in **Chapter 3**, carnitine supplementation significantly increased the production of CCL20 in hypoxia (**Figure 6.1**). This may be as a result of similar processes as described for the findings in monocytes, where FAO and glycolysis may act together to regulate the release of cytokines and chemokines. Nevertheless, it shows that certain intracellular signalling processes may be shared between LPS stimulation and RA-SF treatment.

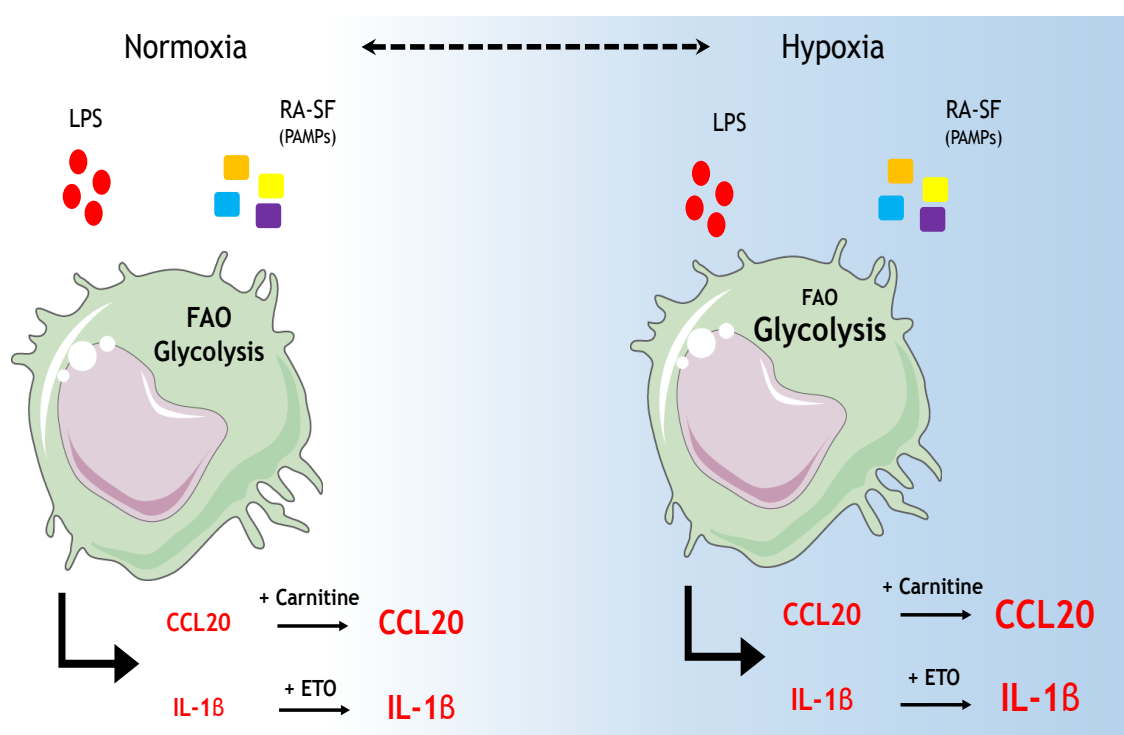


Figure 6.1 Hypoxia specific metabolism influences the release of pro-inflammatory mediators in monocytes. Compared to normoxia, hypoxia promotes the reduction of fatty acid oxidation (FAO) and increased glycolytic flux at metabolic level. In response to stimuli such as LPS or the plethora of PAMPs found in RA synovial fluid (RA-SF), monocytes show increased production of CCL20 and IL-1 β in hypoxia compared to normoxia. However, at both oxygen tensions, carnitine supplementation exacerbates CCL20 production whereas FAO inhibition with etomoxir (ETO) increases IL-1 β secretion further.

As well as carrying out effector function upon recruitment to the inflamed tissue, monocytes typically differentiate into macrophages. Therefore, the last section of **Chapter 5** analysed if the results of **Chapter 3** and **4** extended from monocytes into end differentiated macrophages. At the time of the study, alveolar macrophages (AM) from lung resection patients were available, and were chosen for this work. Targeted mass spectrometry for carnitines was

utilised to measure their abundance in M(LPS + IFN γ ; M1) and M(IL-4; M2) AM in normoxia and hypoxia. However, there were no statistically significant changes in carnitine abundance under any condition, suggesting the study would need to be extended to a larger cohort of patients. The apparent important role of FAO in M(IL-4) murine macrophages does not seem to translate into human macrophages, which questions the importance of this pathway under these polarisation conditions (Namgaladze & Brüne 2014; Nomura et al. 2016). Nevertheless, we tested the ability of polarised macrophages to secrete pro-inflammatory mediators in normoxia and hypoxia. Hypoxia increased the production of IL-1 β and CCL20 in M(LPS + IFN γ) polarised AM, however, this was only achieved if the macrophages were pre-exposed to hypoxia before stimulation and not simultaneously as seen in monocytes. This subtle difference could be explained in the seemingly different adaptation processes to hypoxia (Fangradt et al. 2012; Sharma et al. 2017). Moreover, exogenous carnitine further increases CCL20 production in M(LPS + IFN γ) AM, especially in hypoxia, in a similar finding to monocytes in **Chapter 4**. In addition, pre-treatment with ETO increased IL-1 β production in M1 AMs, highlighting that metabolic and functional characteristics may be shared between LPS treated monocytes and M(LPS + IFN γ) macrophages under hypoxic conditions.

6.1 Critical appraisal

With the benefit of hindsight, there are aspects to this body of work that may have been altered. From the outset, the oxygen tension defined as ‘hypoxia’ could have been more consistent. For instance, in **Chapter 3**, the viability of monocytes via an Annexin-V assay was assessed in 5% O₂ which was termed as hypoxia, but this study was not conducted at 1% O₂. This applies to the time-course experiment in **Chapter 4** with regard to CCL20 production in response to LPS. This experiment was carried out at 2.3% using the hypoxic incubator, but not at 1% O₂. Therefore, experiments to assess the effect of an oxygen gradient may have been more appropriate in these instances.

At a metabolic level, this study illustrated that hypoxia had reduced carnitine shuttling, and possibly FAO in human monocytes. Given that this metabolomics approach is not suitable for detecting lipids, more specific lipidomics platforms could have been utilised to assess FAO specifically. Further, preliminary

transcript data from Chapter 4 postulated that hypoxia attenuated CD36 expression, an important receptor for fatty acid uptake. However, only 1 donor was tested for CD36 receptor expression on the cell surface. Thus, additional studies are warranted to fully characterise its expression and functionality in a number of donors. These experiments also apply to the context of RA-SF and LPS, which were stimuli used throughout this thesis.

The metabolomic study in **Chapter 5** assessed monocyte metabolism in response to RA-SF, while LPS stimulation was utilised as a comparison. A more appropriate comparator stimulus with relevance to the RA milieu may have been used in this experiment, such as immune complex stimulation. This would have provided more detail in to how specific aspects of the RA environment can influence monocyte metabolism and function.

6.2 Future work

The work presented in this thesis has identified a novel link between intracellular metabolism (FAO and glycolysis) and the production of the pro-inflammatory mediators (IL-1 β and CCL20) in response to LPS and RA-SF in hypoxic conditions. However, precisely how metabolic pathways influence the release of these mediators in these instances remains elusive. Therefore, studies to describe a precise mechanism for this should be undertaken. For example, increased carnitine shuttling and FAO may increase the intracellular pool of acetyl-CoA which in turn may promote acetylation of histone residues, commonly associated with gene activation. Studies to assess acetylation (and activation status) around the CCL20 and IL-1 β promoter regions may describe how metabolism and mediator production are interlinked.

6.3 Conclusions

The work in this thesis has emphasised the importance of environmental factors in the functionality of myeloid cells in chronic inflammatory disease. Specific aspects of the tissue microenvironment such as hypoxia has been shown here to heavily influence the metabolic activities of monocytes, which in turn can promote inflammatory cascades in these conditions. This included the exacerbated secretion of IL-1 β and CCL20. Pharmacological manipulation of

altered metabolic pathways, such as carnitine shuttling, highlights their importance in regulating the release of pro-inflammatory mediators.

The metabolic and functional profiling of monocytes cultured under RA-SF stresses the diversity of this inflammatory milieu in comparison to classical stimuli such as LPS. Nevertheless, similarities in the regulation of CCL20 under LPS and RA-SF treatment may exist, as evident in its increased production after carnitine supplementation. Despite its difficulties, it is important to relate myeloid cell research further into the context of chronic inflammatory disease to gain a better understanding of inflammatory mechanisms.

Appendices

7.1 Metabolites that are significantly altered by hypoxia in comparison to normoxia in unstimulated monocytes (Unstim N vs H)

Metabolite	P value
sn_Glycerol_3_phosphate	0.004
4_Imidazolone_5_propanoate	0.006
R_Lactate	0.008

7.2 Metabolites that are significantly altered by hypoxia in comparison to normoxia in LPS stimulated monocytes (LPS N vs H)

Metabolite	P value
D_Glyceraldehyde_3_phosphate	0.001
N_Acetyl_D_glucosamine	0.002
Glycerophosphoglycerol	0.003
UDP_N_acetyl_D_glucosamine	0.003
Butyro_betaine	0.004
L_1_Pyrroline_3_hydroxy_5_carboxylate	0.007
Ecgonine	0.008
Leucyl_leucine	0.009
Thiamin	0.009

7.3 Metabolites that are significantly altered by hypoxia in comparison to normoxia in RA-SF treated monocytes (RA-SF N vs H)

Metabolite	P value
N_octanoyl_L_homoserine	0.001
1_Hydroxy_2_beta_D_glucosyloxy_9_10_anthraquinone	0.005
Hydroxybutyrylcarnitine	0.006
1H_Imidazole_4_ethanamine_2	0.006

7.4 Significantly altered metabolites in LPS stimulated cells in comparison to unstimulated monocytes in normoxia (Unstim vs LPS (N))

Metabolite	P value
PC_18_0_1_octadecanoyl_sn_glycero_3_phosphocholine	0.0001
DL_2_Aminooctanoicacid	0.0003
AMP	0.0003
UMP	0.001
D_Gluconic_acid	0.001
SP_methyl_13_0_13_0_2_0_methyl_3_13_13_dibromotrideca_1 E_12_dienyl_2H_azirine_2S_carboxylate	0.001
ADP	0.001
Asp_Gly_His	0.001
hydrogen_iodide	0.001
O_Butanoylcarnitine	0.002
Taurine	0.002
Hippurate	0.003
beta_Citryl_L_glutamic_acid	0.003
IMP	0.003
13_Hydroxylupanine	0.004
L_Aspartate	0.006
ATP	0.006
3_Dehydroxycarnitine	0.006
Ile_Pro	0.007
FA_amino_11_0_11_amino_undecanoic_acid	0.007
Hydroxybutyrylcarnitine	0.007
Hydroxymethylphosphonate	0.007
UDP	0.008
O_Acetylcarnitine	0.008
Citrate	0.008
Creatine	0.009

7.5 Significantly altered metabolites in RA-SF stimulated cells in comparison to unstimulated monocytes in normoxia (Unstim vs RA-SF (N))

Metabolite	P value
Guanosine	0.0005
ST_2_0_22S_25S_furospirost_5_en_3beta_26_diol	0.001
SP_Sphing_4_enine_1_phosphate	0.001
ST_hydrox_3alpha_7alpha_Dihydroxy_5beta_cholan_24_oic_Acid	0.003
Acetaminophenglucuronide	0.003
Lys_Val	0.003
4_Coumaryl_alcohol	0.003
1_8_Dihydroxy_3_methylnaphthalene	0.004
demethylsuberosin	0.004
Cholate	0.004
Val_Gly	0.005
SP_Sphinganine_1_phosphate	0.005
5_Acetylamino_6_amino_3_methyluracil	0.005
NAD_	0.007
Z_4_Hydroxyphenylacetaldehyde_oxime	0.007
N6_Methyl_L_lysine	0.008
Creatinine	0.009
Ethyl_R_3_hydroxyhexanoate	0.009

7.6 Significantly altered metabolites in LPS stimulated cells in comparison to unstimulated monocytes in hypoxia (Unstim vs LPS (H))

Metabolite	P value
Stachydrine	0.0001
Hydroxybutyrylcarnitine	0.0002
D_Galactosamine	0.0003
O_Butanoylcarnitine	0.0003
O_Acetylcarnitine	0.001
Methylmalonate	0.001
SP_methyl_13_0_13_0_2_0_methyl_3_13_13_dibromotrideca_1 E_12_dienyl_2H_azirine_2S_carboxylate	0.001
FA_hydroxy_10_0_N_3S_hydroxydecanoyl_L_serine	0.002
CAI_1	0.002
L_1_Pyrroline_3_hydroxy_5_carboxylate	0.002
Hippurate	0.003
Phenylacetic_acid	0.003
PC_18_0_1_octadecanoyl_sn_glycero_3_phosphocholine	0.003
Hypoxanthine	0.003
FA_amino_10_0_10_amino_decanoic_acid	0.004
Orthophosphate	0.004
O_Propanoylcarnitine	0.004
3_Butyrate	0.004
D_Glucose	0.005
4_4_Deoxy_alpha_D_gluc_4_enuronosyl_D_galacturonate	0.005
FA_8_0_octanoic_acid	0.005
Sulfate	0.006
trans_Hexadec_2_enoylecarnitine	0.006
FA_trihydroxy_18_1_9S_12S_13S_trihydroxy_10E_octadecenoic_ acid	0.006
Betaine	0.008
Harringtonine	0.008
Gly_His	0.008
Pyruvate	0.008
2_5_Dioxopentanoate	0.008

7.7 Significantly altered metabolites in RA-SF stimulated cells in comparison to unstimulated monocytes in hypoxia (Unstim vs RA-SF (H))

Metabolite	P value
Cholate	0.0001
2_Oxooctadecanoic_acid	0.0002
3_4_Hydroxyphenyl_lactate	0.0003
ST_2_0_22S_25S_furospirost_5_en_3beta_26_diol	0.001
Anthocyanin_3_O_beta_D_glucoside	0.001
D_Xylulose	0.001
N_acetyl_D_glucosaminitol	0.001
demethylsuberosin	0.002
O_Acetyl_L_homoserine	0.002
Acetaminophenglucuronide	0.002
1_8_Dihydroxy_3_methylnaphthalene	0.002
5_Acetylamino_6_amino_3_methyluracil	0.004
Phosphonate	0.004
Nalpha_Methylhistidine	0.004
Gly_His	0.004
Orthophosphate	0.005
ST_hydrox_3alpha_7alpha_Dihydroxy_5beta_cholan_24_oic_Acid	0.005
Ethyl_cinnamate	0.005
2_Hydroxyethanesulfonate	0.006
L_Rhamnose	0.007
FA_20_4_5Z_8Z_11Z_14Z_eicosatetraenoic_acid	0.008
Oxamate	0.008
Urate	0.008
NG_NG_Dimethyl_L_arginine	0.008
Val_Gly	0.008
1H_Imidazole_4_ethanamine_2	0.009

7.7 Significantly altered metabolites in RA-SF stimulated cells in comparison to LPS stimulated monocytes in normoxia (RA-SF vs LPS (N))

Metabolite	P value
Cholate	0.0001
ST_2_0_22S_25S_furospirost_5_en_3beta_26_diol	0.0001
ST_hydrox_3alpha_7alpha_Dihydroxy_5beta_cholan_24_oic_Acid	0.0001
Xanthine	0.0001
demethylsuberosin	0.0001
Val_Gly	0.0001
4_Imidazolone_5_propanoate	0.0001
Z_4_Hydroxyphenylacetaldehyde_oxime	0.0001
Acetaminophenglucuronide	0.0001
DL_2_Aminooctanoicacid	0.0001
1_8_Dihydroxy_3_methylnaphthalene	0.0001
Nalpha_Methylhistidine	0.0001
3_Dehydroxycarnitine	0.0001
5_Acetylamino_6_amino_3_methyluracil	0.0002
N5_Ethyl_L_glutamine	0.0002
Ecgonine	0.0003
2_Oxooctadecanoic_acid	0.0004
L_thiazolidine_4_carboxylate	0.0004
L_Citrulline	0.0005
Creatinine	0.0005
NG_NG_Dimethyl_L_arginine	0.0005
homomethionine	0.001
L_Rhamnose	0.001
4_Guanidinobutanoate	0.001
Ethyl_cinnamate	0.001
N_Acetyl_D_glucosamine	0.001
3_4_Hydroxyphenyl_lactate	0.001
Methylimidazoleacetic_acid	0.001
N6_Methyl_L_lysine	0.001
FA_amino_11_0_11_amino_undecanoic_acid	0.001
Urate	0.001
hydrogen_iodide	0.001
R_Lactate	0.002
Homocysteinesulfinicacid	0.002

7_8_diketopelargonate	0.002
Pirbuterol	0.002
Linamarin	0.002
Uncinatone	0.002
Creatine	0.002
S_glutathionyl_L_cysteine	0.002
1H_Imidazole_4_ethanamine_1	0.003
Leucyl_leucine	0.003
Hippurate	0.003
Anthocyanin_3_O_beta_D_glucoside	0.003
FA_oxo_14_0_3_oxo_tetradecanoic_acid	0.003
L_Arabinonate	0.003
O_Acetyl_L_homoserine	0.003
CAI_1	0.004
N_Ethylglycocycamine	0.004
L_Methionine_S_oxide	0.004
N_Acetyl_D_glucosamine_6_sulfate	0.004
S_Carnitine	0.004
L_Aspartate	0.004
O_Acetylcarnitine	0.004
ADP	0.005
N_acetyl_D_glucosaminitol	0.005
L_Carnitine	0.005
FA_hydroxy_10_0_N_3S_hydroxydecanoyl_L_serine	0.005
N_Formimino_L_glutamate	0.006
1H_Imidazole_4_ethanamine_2	0.006
L_Cysteate	0.007
FA_20_4_5Z_8Z_11Z_14Z_eicosatetraenoic_acid	0.007
5_6_Dihydrothymine	0.007
Athamantin	0.007
N6_N6_N6_Trimethyl_L_lysine	0.007
Pyruvate	0.008
N1_Methyl_2_pyridone_5_carboxamide	0.008
N6_Acetyl_L_lysine	0.008
R_2_Hydroxyglutarate	0.008
D_Gluconic_acid	0.009
Leu_Pro	0.009
Hydroxymethylphosphonate	0.009
Phosphodimethylethanolamine	0.009
2S_2_1_R_Carboxyethyl_amino_pentanoate	0.009

3_Butyrate	0.009
Cholate	0.009

List of References

- Akram, M., 2014. Citric acid cycle and role of its intermediates in metabolism. *Cell biochemistry and biophysics*, 68(3), pp.475-478.
- Alesci, S. et al., 2003. L-carnitine: A nutritional modulator of glucocorticoid receptor functions. *FASEB journal : official publication of the Federation of American Societies for Experimental Biology*, 17(11), pp.1553-1555.
- Anand, R.J. et al., 2007. Hypoxia causes an increase in phagocytosis by macrophages in a HIF-1 α -dependent manner. *Journal of Leukocyte Biology*, 82(5), pp.1257-1265.
- Arnold, L. et al., 2007. Inflammatory monocytes recruited after skeletal muscle injury switch into antiinflammatory macrophages to support myogenesis. *Journal of Experimental Medicine*, 204(5), pp.1057-1069.
- Auffray, C. et al., 2007. Monitoring of blood vessels and tissues by a population of monocytes with patrolling behavior. *Science*, 317(5838), pp.666-670.
- Bae, S. et al., 2012. α -Enolase expressed on the surfaces of monocytes and macrophages induces robust synovial inflammation in rheumatoid arthritis. *The Journal of Immunology*, 189(1), pp.365-372.
- Baggiolini, M., Imboden, P. & Detmers, P., 1992. Neutrophil activation and the effects of interleukin-8/neutrophil-activating peptide 1 (IL-8/NAP-1). *Cytokines*, 4, pp.1-17.
- Bain, C.C. et al., 2014. Constant replenishment from circulating monocytes maintains the macrophage pool in the intestine of adult mice. *Nature Immunology*, 15(10), pp.929-937.
- Barnes, P.J., 2016. Inflammatory mechanisms in patients with chronic obstructive pulmonary disease. *The Journal of allergy and clinical immunology*, 138(1), pp.16-27.
- Barnes, P.J., Shapiro, S.D. & Pauwels, R.A., 2003. Chronic obstructive pulmonary disease: molecular and cellular mechanisms. *The European respiratory journal*, 22(4), pp.672-688.
- Battaglia, F. et al., 2008. Hypoxia transcriptionally induces macrophage-inflammatory protein-3 α /CCL-20 in primary human mononuclear phagocytes through nuclear factor (NF)- κ B. *Journal of Leukocyte Biology*, 83(3), pp.648-662.
- Begovich, A.B. et al., 2004. A missense single-nucleotide polymorphism in a gene encoding a protein tyrosine phosphatase (PTPN22) is associated with rheumatoid arthritis. *American journal of human genetics*, 75(2), pp.330-337.
- Behrens, F. et al., 2007. Imbalance in distribution of functional autologous regulatory T cells in rheumatoid arthritis. *Ann Rheum Dis*, 66(9), pp.1151-1156.

- Belge, K.-U. et al., 2002. The proinflammatory CD14⁺CD16⁺DR⁺⁺ monocytes are a major source of TNF. *The Journal of Immunology*, 168(7), pp.3536-3542.
- Berenson, C.S. et al., 2013. Phagocytic dysfunction of human alveolar macrophages and severity of chronic obstructive pulmonary disease. *The Journal of infectious diseases*, 208(12), pp.2036-2045.
- Berra, E. et al., 2003. HIF prolyl-hydroxylase 2 is the key oxygen sensor setting low steady-state levels of HIF-1 α in normoxia. *The EMBO journal*, 22(16), pp.4082-4090.
- Berridge, M.V., Herst, P.M. & Tan, A.S., 2005. Tetrazolium dyes as tools in cell biology: new insights into their cellular reduction. *Biotechnology annual review*, 11, pp.127-152.
- Biernacki, W.A., Kharitonov, S.A. & Barnes, P.J., 2003. Increased leukotriene B₄ and 8-isoprostane in exhaled breath condensate of patients with exacerbations of COPD. *Thorax*, 58(4), pp.294-298.
- Blaser, H. et al., 2016. TNF and ROS Crosstalk in Inflammation. *Trends in Cell Biology*, 26(4), pp.249-261.
- Bosco, M.C. et al., 2006. Hypoxia Modifies the Transcriptome of Primary Human Monocytes: Modulation of Novel Immune-Related Genes and Identification Of CC-Chemokine Ligand 20 as a New Hypoxia-Inducible Gene. *The Journal of Immunology*, 177(3), pp.1941-1955.
- Brenner, D., Blaser, H. & Mak, T.W., 2015. Regulation of tumour necrosis factor signalling: live or let die. *Nature Reviews Immunology*, 15(6), pp.362-374.
- Burke, B. et al., 2003. Hypoxia-induced gene expression in human macrophages: implications for ischemic tissues and hypoxia-regulated gene therapy. *The American journal of pathology*, 163(4), pp.1233-1243.
- Burns, K., Martinon, F. & Tschopp, J., 2003. New insights into the mechanism of IL-1 β maturation. *Current opinion in immunology*, 15(1), pp.26-30.
- Calverley, P.M.A. et al., 2017. A randomised, placebo-controlled trial of anti-interleukin-1 receptor 1 monoclonal antibody MEDI8968 in chronic obstructive pulmonary disease. *Respiratory research*, 18(1), p.153.
- Caramori, G. et al., 2003. Nuclear localisation of p65 in sputum macrophages but not in sputum neutrophils during COPD exacerbations. *Thorax*, 58(4), pp.348-351.
- Carver, J.D. & Allan Walker, W., 1995. The role of nucleotides in human nutrition. *The Journal of Nutritional Biochemistry*, 6(2), pp.58-72.
- Cascão, R. et al., 2010. Neutrophils in rheumatoid arthritis: More than simple final effectors. *Autoimmunity reviews*, 9(8), pp.531-535.
- Cheng, S.C. et al., 2014. mTOR- and HIF-1 -mediated aerobic glycolysis as metabolic basis for trained immunity. *Science*, 345(6204), pp.1250684-1250684.

- Chimenti, M.S. et al., 2016. Synovial fluid from patients with rheumatoid arthritis modulates monocyte cell-surface phenotype. *J Int Med Res*, 44(1_suppl), pp.15-21.
- Coleman, M.M. et al., 2013. Alveolar macrophages contribute to respiratory tolerance by inducing FoxP3 expression in naive T cells. *American journal of respiratory cell and molecular biology*, 48(6), pp.773-780.
- Covarrubias, A.J. et al., 2016. Akt-mTORC1 signaling regulates Acly to integrate metabolic input to control of macrophage activation. *eLife*, 5, p.e11612.
- Cox, G., Crossley, J. & Xing, Z., 1995. Macrophage engulfment of apoptotic neutrophils contributes to the resolution of acute pulmonary inflammation in vivo. *American journal of respiratory cell and molecular biology*, 12(2), pp.232-237.
- Cramer, T. et al., 2003. HIF-1alpha is essential for myeloid cell-mediated inflammation. *Cell*, 112(5), pp.645-657.
- Crane, M.J. et al., 2014. The monocyte to macrophage transition in the murine sterile wound. J. Coers, ed. *PLoS ONE*, 9(1), p.e86660.
- Creek, D.J. et al., 2012. IDEOM: an Excel interface for analysis of LC-MS-based metabolomics data. *Bioinformatics (Oxford, England)*, 28(7), pp.1048-1049.
- Cros, J. et al., 2010. Human CD14dim monocytes patrol and sense nucleic acids and viruses via TLR7 and TLR8 receptors. *Immunity*, 33(3), pp.375-386.
- Culpitt, S.V. et al., 2003. Impaired inhibition by dexamethasone of cytokine release by alveolar macrophages from patients with chronic obstructive pulmonary disease. *American journal of respiratory and critical care medicine*, 167(1), pp.24-31.
- Darrietort-Laffite, C. et al., 2014. IL-1 β and TNF α promote monocyte viability through the induction of GM-CSF expression by rheumatoid arthritis synovial fibroblasts. *Mediators of inflammation*, 2014(1), pp.241840-10.
- Davies, L.C. et al., 2011. A quantifiable proliferative burst of tissue macrophages restores homeostatic macrophage populations after acute inflammation. *European journal of immunology*, 41(8), pp.2155-2164.
- del Fresno, C. et al., 2009. Potent Phagocytic Activity with Impaired Antigen Presentation Identifying Lipopolysaccharide-Tolerant Human Monocytes: Demonstration in Isolated Monocytes from Cystic Fibrosis Patients. *The Journal of Immunology*, 182(10), pp.6494-6507.
- Diehl, S.A. et al., 2008. STAT3-mediated up-regulation of BLIMP1 is coordinated with BCL6 down-regulation to control human plasma cell differentiation. *The Journal of Immunology*, 180(7), pp.4805-4815.
- Dinarello, C.A. & van der Meer, J.W.M., 2013. Treating inflammation by blocking interleukin-1 in humans. *Seminars in Immunology*, 25(6), pp.469-484.
- Domínguez-Andrés, J. et al., 2017. Rewiring monocyte glucose metabolism via C-

- type lectin signaling protects against disseminated candidiasis R. C. May, ed. *PLoS Pathogens*, 13(9), p.e1006632.
- Donnelly, L.E. & Barnes, P.J., 2012. Defective phagocytosis in airways disease. *Chest*, 141(4), pp.1055-1062.
- Dougados, M. et al., 2013. Adding tocilizumab or switching to tocilizumab monotherapy in methotrexate inadequate responders: 24-week symptomatic and structural results of a 2-year randomised controlled strategy trial in rheumatoid arthritis (ACT-RAY). *Ann Rheum Dis*, 72(1), pp.43-50.
- Dunay, I.R. et al., 2008. Gr1(+) inflammatory monocytes are required for mucosal resistance to the pathogen *Toxoplasma gondii*. *Immunity*, 29(2), pp.306-317.
- Eales, K.L., Hollinshead, K.E.R. & Tennant, D.A., 2016. Hypoxia and metabolic adaptation of cancer cells. *Oncogenesis*, 5(1), pp.e190 EP -.
- Eapen, M.S. et al., 2017. Abnormal M1/M2 macrophage phenotype profiles in the small airway wall and lumen in smokers and chronic obstructive pulmonary disease (COPD). *Scientific reports*, 7(1), p.13392.
- Ecker, J. et al., 2010. Induction of fatty acid synthesis is a key requirement for phagocytic differentiation of human monocytes. *Proceedings of the National Academy of Sciences of the United States of America*, 107(17), pp.7817-7822.
- Edwards, J.P. et al., 2006. Biochemical and functional characterization of three activated macrophage populations. *Journal of Leukocyte Biology*, 80(6), pp.1298-1307.
- England, H. et al., 2014. Release of interleukin-1 α or interleukin-1 β depends on mechanism of cell death. *The Journal of biological chemistry*, 289(23), pp.15942-15950.
- Epstein, A.C. et al., 2001. *C. elegans* EGL-9 and mammalian homologs define a family of dioxygenases that regulate HIF by prolyl hydroxylation. *Cell*, 107(1), pp.43-54.
- Fahy, J.V. & Dickey, B.F., 2010. Airway mucus function and dysfunction. *The New England journal of medicine*, 363(23), pp.2233-2247.
- Fangradt, M. et al., 2012. Human monocytes and macrophages differ in their mechanisms of adaptation to hypoxia. *Arthritis Research & Therapy*, 14(4), p.R181.
- Fearon, U. et al., 2016. Hypoxia, mitochondrial dysfunction and synovial invasiveness in rheumatoid arthritis. *Nature Reviews Rheumatology*, 12(7), pp.385-397.
- Feingold, K.R. et al., 2012. Mechanisms of triglyceride accumulation in activated macrophages. *Journal of Leukocyte Biology*, 92(4), pp.829-839.
- Fernandez, S. et al., 2004. Inhibition of IL-10 receptor function in alveolar

- macrophages by Toll-like receptor agonists. *The Journal of Immunology*, 172(4), pp.2613-2620.
- Filer, A., 2013. The fibroblast as a therapeutic target in rheumatoid arthritis. *Current opinion in pharmacology*, 13(3), pp.413-419.
- Firestein, G.S. & McInnes, I.B., 2017. Immunopathogenesis of Rheumatoid Arthritis. *Immunity*, 46(2), pp.183-196.
- Fleischmann, R. et al., 2012. Placebo-controlled trial of tofacitinib monotherapy in rheumatoid arthritis. *The New England journal of medicine*, 367(6), pp.495-507.
- Flytlie, H.A. et al., 2010. Expression of MDC/CCL22 and its receptor CCR4 in rheumatoid arthritis, psoriatic arthritis and osteoarthritis. *Cytokine*, 49(1), pp.24-29.
- Fortin, G. et al., 2009. L-carnitine, a diet component and organic cation transporter OCTN ligand, displays immunosuppressive properties and abrogates intestinal inflammation. *Clinical and experimental immunology*, 156(1), pp.161-171.
- Freemerman, A.J. et al., 2014. Metabolic Reprogramming of Macrophages: GLUCOSE TRANSPORTER 1 (GLUT1)-MEDIATED GLUCOSE METABOLISM DRIVES A PROINFLAMMATORY PHENOTYPE. *Journal of Biological Chemistry*, 289(11), pp.7884-7896.
- Gaidt, M.M. et al., 2016. Human Monocytes Engage an Alternative Inflammasome Pathway. *Immunity*, 44(4), pp.833-846.
- Galvan-Pena, S. & O'Neill, L.A.J., 2014. Metabolic reprogramming in macrophage polarization. *Frontiers in immunology*, 5, p.420.
- Gao, W. et al., 2015. Bronchial epithelial cells: The key effector cells in the pathogenesis of chronic obstructive pulmonary disease? *Respirology (Carlton, Vic.)*, 20(5), pp.722-729.
- Garaude, J. et al., 2016. Mitochondrial respiratory-chain adaptations in macrophages contribute to antibacterial host defense. *Nature Immunology*, 17(9), pp.1037-1045.
- Geissmann, F. et al., 2010. Development of Monocytes, Macrophages, and Dendritic Cells. *Science*, 327(5966), pp.656-661.
- Geissmann, F., Jung, S. & Littman, D.R., 2003. Blood Monocytes Consist of Two Principal Subsets with Distinct Migratory Properties. *Immunity*, 19(1), pp.71-82.
- Ginhoux, F. et al., 2010. Fate mapping analysis reveals that adult microglia derive from primitive macrophages. *Science*, 330(6005), pp.841-845.
- Godiska, R. et al., 1997. Human macrophage-derived chemokine (MDC), a novel chemoattractant for monocytes, monocyte-derived dendritic cells, and natural killer cells. *Journal of Experimental Medicine*, 185(9), pp.1595-1604.

- Gordon, S. & Martinez, F.O., 2010. Alternative activation of macrophages: mechanism and functions. *Immunity*, 32(5), pp.593-604.
- Gordon, S., Plüddemann, A. & Martinez Estrada, F., 2014. Macrophage heterogeneity in tissues: phenotypic diversity and functions. *Immunological reviews*, 262(1), pp.36-55.
- Grashoff, W.F. et al., 1997. Chronic obstructive pulmonary disease: role of bronchiolar mast cells and macrophages. *The American journal of pathology*, 151(6), pp.1785-1790.
- Griffith, J.W., Sokol, C.L. & Luster, A.D., 2014. Chemokines and chemokine receptors: positioning cells for host defense and immunity. *Annual review of immunology*, 32(1), pp.659-702.
- Grimshaw, M.J. & Balkwill, F.R., 2001. Inhibition of monocyte and macrophage chemotaxis by hypoxia and inflammation--a potential mechanism. *European journal of immunology*, 31(2), pp.480-489.
- Grumelli, S. et al., 2004. An immune basis for lung parenchymal destruction in chronic obstructive pulmonary disease and emphysema. P. J. Barnes, ed. *PLoS medicine*, 1(1), p.e8.
- Guillaumond, F. et al., 2013. Strengthened glycolysis under hypoxia supports tumor symbiosis and hexosamine biosynthesis in pancreatic adenocarcinoma. *Proceedings of the National Academy of Sciences of the United States of America*, 110(10), pp.3919-3924.
- Guilliams, M. et al., 2013. Alveolar macrophages develop from fetal monocytes that differentiate into long-lived cells in the first week of life via GM-CSF. *The Journal of experimental medicine*, 210(10), pp.1977-1992.
- Hall, C.J. et al., 2013. Immunoresponsive gene 1 augments bactericidal activity of macrophage-lineage cells by regulating β -oxidation-dependent mitochondrial ROS production. *Cell Metabolism*, 18(2), pp.265-278.
- Hall, D.A. et al., 1999. Signalling by CXC-chemokine receptors 1 and 2 expressed in CHO cells: a comparison of calcium mobilization, inhibition of adenylyl cyclase and stimulation of GTP γ S binding induced by IL-8 and GRO α . *British journal of pharmacology*, 126(3), pp.810-818.
- Hampel, U. et al., 2013. Chemokine and cytokine levels in osteoarthritis and rheumatoid arthritis synovial fluid. *Journal of immunological methods*, 396(1-2), pp.134-139.
- Harre, U. et al., 2012. Induction of osteoclastogenesis and bone loss by human autoantibodies against citrullinated vimentin. *The Journal of clinical investigation*, 122(5), pp.1791-1802.
- Haschemi, A. et al., 2012. The sedoheptulose kinase CARKL directs macrophage polarization through control of glucose metabolism. *Cell Metabolism*, 15(6), pp.813-826.
- Hashimoto, D. et al., 2013. Tissue-resident macrophages self-maintain locally

throughout adult life with minimal contribution from circulating monocytes. *Immunity*, 38(4), pp.792-804.

- Hashizume, M., Hayakawa, N. & Mihara, M., 2008. IL-6 trans-signalling directly induces RANKL on fibroblast-like synovial cells and is involved in RANKL induction by TNF-alpha and IL-17. *Rheumatology (Oxford, England)*, 47(11), pp.1635-1640.
- Haskó, G. & Pacher, P., 2012. Regulation of macrophage function by adenosine. *Arteriosclerosis, thrombosis, and vascular biology*, 32(4), pp.865-869.
- Haskó, G. et al., 2000. Inosine inhibits inflammatory cytokine production by a posttranscriptional mechanism and protects against endotoxin-induced shock. *The Journal of Immunology*, 164(2), pp.1013-1019.
- Heinrich, P.C. et al., 1998. Interleukin-6-type cytokine signalling through the gp130/Jak/STAT pathway. *The Biochemical journal*, 334 (Pt 2)(Pt 2), pp.297-314.
- Hettinger, J. et al., Origin of monocytes and macrophages in a committed progenitor. *Nature Immunology*, 14(8), pp.821-830.
- Hettinger, J. et al., 2013. Origin of monocytes and macrophages in a committed progenitor. *Nature Immunology*, 14(8), pp.821-830.
- Hirani, N. et al., 2001. The regulation of interleukin-8 by hypoxia in human macrophages--a potential role in the pathogenesis of the acute respiratory distress syndrome (ARDS). *Molecular medicine (Cambridge, Mass.)*, 7(10), pp.685-697.
- Hirota, K. et al., 2007. Preferential recruitment of CCR6-expressing Th17 cells to inflamed joints via CCL20 in rheumatoid arthritis and its animal model. *The Journal of experimental medicine*, 204(12), pp.2803-2812.
- Hmama, Z. et al., 1999. Monocyte adherence induced by lipopolysaccharide involves CD14, LFA-1, and cytohesin-1. Regulation by Rho and phosphatidylinositol 3-kinase. *Journal of Biological Chemistry*, 274(2), pp.1050-1057.
- Hodge, S. et al., 2003. Alveolar macrophages from subjects with chronic obstructive pulmonary disease are deficient in their ability to phagocytose apoptotic airway epithelial cells. *Immunology and cell biology*, 81(4), pp.289-296.
- Hodge, S. et al., 2011. Cigarette smoke-induced changes to alveolar macrophage phenotype and function are improved by treatment with procysteine. *American journal of respiratory cell and molecular biology*, 44(5), pp.673-681.
- Hoeffel, G. et al., 2012. Adult Langerhans cells derive predominantly from embryonic fetal liver monocytes with a minor contribution of yolk sac-derived macrophages. *The Journal of experimental medicine*, 209(6), pp.1167-1181.

- Hoeffel, G. et al., 2015. C-Myb(+) erythro-myeloid progenitor-derived fetal monocytes give rise to adult tissue-resident macrophages. *Immunity*, 42(4), pp.665-678.
- Hoidal, J.R., Schmeling, D. & Peterson, P.K., 1981. Phagocytosis, bacterial killing, and metabolism by purified human lung phagocytes. *The Journal of infectious diseases*, 144(1), pp.61-71.
- Houten, S.M. & Wanders, R.J.A., 2010. A general introduction to the biochemistry of mitochondrial fatty acid β -oxidation. *Journal of inherited metabolic disease*, 33(5), pp.469-477.
- Huang, D. et al., 2014. HIF-1-mediated suppression of acyl-CoA dehydrogenases and fatty acid oxidation is critical for cancer progression. *Cell reports*, 8(6), pp.1930-1942.
- Huang, S.C.-C. et al., 2014. Cell-intrinsic lysosomal lipolysis is essential for alternative activation of macrophages. *Nature Immunology*, 15(9), pp.846-855.
- Huang, S.C.-C. et al., 2016. Metabolic Reprogramming Mediated by the mTORC2-IRF4 Signaling Axis Is Essential for Macrophage Alternative Activation. *Immunity*, 45(4), pp.817-830.
- Hunter, C.A. & Jones, S.A., 2015. IL-6 as a keystone cytokine in health and disease. *Nature Immunology*, 16(5), pp.448-457.
- Hussell, T. & Bell, T.J., 2014. Alveolar macrophages: plasticity in a tissue-specific context. *Nature Reviews Immunology*, 14(2), pp.81-93.
- Ichinohe, T. et al., 2009. Inflammasome recognition of influenza virus is essential for adaptive immune responses. *The Journal of experimental medicine*, 206(1), pp.79-87.
- Imai, T. et al., 1999. Selective recruitment of CCR4-bearing Th2 cells toward antigen-presenting cells by the CC chemokines thymus and activation-regulated chemokine and macrophage-derived chemokine. *International immunology*, 11(1), pp.81-88.
- Infantino, V. et al., 2014. A key role of the mitochondrial citrate carrier (SLC25A1) in TNF α - and IFN γ -triggered inflammation. *Biochimica et biophysica acta*, 1839(11), pp.1217-1225.
- Infantino, V. et al., 2011. The mitochondrial citrate carrier: a new player in inflammation. *The Biochemical journal*, 438(3), pp.433-436.
- Ingoglia, F. et al., 2017. Human macrophage differentiation induces OCTN2-mediated L-carnitine transport through stimulation of mTOR-STAT3 axis. *Journal of Leukocyte Biology*, 101(3), pp.665-674.
- Ivan, M. et al., 2001. HIF α targeted for VHL-mediated destruction by proline hydroxylation: implications for O $_2$ sensing. *Science*, 292(5516), pp.464-468.
- Iwahashi, M. et al., 2004. Expression of Toll-like receptor 2 on CD16 $^+$ blood

- monocytes and synovial tissue macrophages in rheumatoid arthritis. *Arthritis & Rheumatism*, 50(5), pp.1457-1467.
- Jakubzick, C. et al., 2013. Minimal differentiation of classical monocytes as they survey steady-state tissues and transport antigen to lymph nodes. *Immunity*, 39(3), pp.599-610.
- Jawed, S., Gaffney, K. & Blake, D.R., 1997. Intra-articular pressure profile of the knee joint in a spectrum of inflammatory arthropathies. *Ann Rheum Dis*, 56(11), pp.686-689.
- Jenkins, S.J. et al., 2011. Local Macrophage Proliferation, Rather than Recruitment from the Blood, Is a Signature of TH2 Inflammation. *Science*, 332(6035), pp.1284-1288.
- Jha, A.K. et al., 2015. Network Integration of Parallel Metabolic and Transcriptional Data Reveals Metabolic Modules that Regulate Macrophage Polarization. *Immunity*, 42(3), pp.419-430.
- Jiang, H. et al., 2016. PFKFB3-Driven Macrophage Glycolytic Metabolism Is a Crucial Component of Innate Antiviral Defense. *Journal of immunology (Baltimore, Md. : 1950)*, 197(7), pp.2880-2890.
- Jiang, M. et al., 2013. Serum metabolic signatures of four types of human arthritis. *Journal of Proteome Research*, 12(8), pp.3769-3779.
- Jiang-Shieh, Y.-F. et al., 2010. Distribution and expression of CD200 in the rat respiratory system under normal and endotoxin-induced pathological conditions. *Journal of anatomy*, 216(3), pp.407-416.
- Johnson, A.R. et al., 2016. Metabolic reprogramming through fatty acid transport protein 1 (FATP1) regulates macrophage inflammatory potential and adipose inflammation. *Molecular metabolism*, 5(7), pp.506-526.
- Kallberg, H. et al., 2007. Gene-gene and gene-environment interactions involving HLA-DRB1, PTPN22, and smoking in two subsets of rheumatoid arthritis. *American journal of human genetics*, 80(5), pp.867-875.
- Kambayashi, S. et al., 2015. Hypoxia inducible factor 1 α expression and effects of its inhibitors in canine lymphoma. *The Journal of veterinary medical science*, 77(11), pp.1405-1412.
- Kapoor, S.R. et al., 2013. Metabolic Profiling Predicts Response to Anti-Tumor Necrosis Factor α Therapy in Patients With Rheumatoid Arthritis. *Arthritis & Rheumatism*, 65(6), pp.1448-1456.
- Kennedy, A. et al., 2010. Angiogenesis and blood vessel stability in inflammatory arthritis. *Arthritis & Rheumatism*, 62(3), pp.711-721.
- Kent, B.D., Mitchell, P.D. & McNicholas, W.T., 2011. Hypoxemia in patients with COPD: cause, effects, and disease progression. *International journal of chronic obstructive pulmonary disease*, 6, pp.199-208.
- Kim, S. et al., 2014. Global Metabolite Profiling of Synovial Fluid for the Specific

- Diagnosis of Rheumatoid Arthritis from Other Inflammatory Arthritis Y.-S. Bahn, ed. *PLoS ONE*, 9(6), p.e97501.
- Kinne, R.W., Stuhlmüller, B. & Burmester, G.-R., 2007. Cells of the synovium in rheumatoid arthritis. Macrophages. *Arthritis Research & Therapy*, 9(6), p.224.
- Koch, A.E. et al., 1995. Growth-related gene product alpha. A chemotactic cytokine for neutrophils in rheumatoid arthritis. *The Journal of Immunology*, 155(7), pp.3660-3666.
- Kochi, Y. et al., 2010. A regulatory variant in CCR6 is associated with rheumatoid arthritis susceptibility. *Nature genetics*, 42(6), pp.515-519.
- Komatsu, N. et al., 2014. Pathogenic conversion of Foxp3+ T cells into TH17 cells in autoimmune arthritis. *Nature Publishing Group*, 20(1), pp.62-68.
- Kong, Y.Y. et al., 1999. OPGL is a key regulator of osteoclastogenesis, lymphocyte development and lymph-node organogenesis. *Nature*, 397(6717), pp.315-323.
- Koning, N. et al., 2010. Expression of the inhibitory CD200 receptor is associated with alternative macrophage activation. *Journal of innate immunity*, 2(2), pp.195-200.
- Korb, A., Pavenstädt, H. & Pap, T., 2009. Cell death in rheumatoid arthritis. *Apoptosis : an international journal on programmed cell death*, 14(4), pp.447-454.
- Krishnamurthy, A. et al., 2016. Identification of a novel chemokine-dependent molecular mechanism underlying rheumatoid arthritis-associated autoantibody-mediated bone loss. *Ann Rheum Dis*, 75(4), pp.721-729.
- Krzysiek, R. et al., 2000. Regulation of CCR6 chemokine receptor expression and responsiveness to macrophage inflammatory protein-3alpha/CCL20 in human B cells. *Blood*, 96(7), pp.2338-2345.
- Kuhn, K.A. et al., 2006. Antibodies against citrullinated proteins enhance tissue injury in experimental autoimmune arthritis. *The Journal of clinical investigation*, 116(4), pp.961-973.
- Kurihara, T. et al., 1997. Defects in macrophage recruitment and host defense in mice lacking the CCR2 chemokine receptor. *Journal of Experimental Medicine*, 186(10), pp.1757-1762.
- Kzhyshkowska, J., Neyen, C. & Gordon, S., 2012. Role of macrophage scavenger receptors in atherosclerosis. *Immunobiology*, 217(5), pp.492-502.
- Lachmandas, E. et al., 2016. Microbial stimulation of different Toll-like receptor signalling pathways induces diverse metabolic programmes in human monocytes. 2(3), p.nmicrobiol2016246.
- Lally, F. et al., 2005. A novel mechanism of neutrophil recruitment in a coculture model of the rheumatoid synovium. *Arthritis & Rheumatism*,

52(11), pp.3460-3469.

- Lamkanfi, M. & Dixit, V.M., 2014. Mechanisms and functions of inflammasomes. *Cell*, 157(5), pp.1013-1022.
- Lampropoulou, V. et al., 2016. Itaconate Links Inhibition of Succinate Dehydrogenase with Macrophage Metabolic Remodeling and Regulation of Inflammation. *Cell Metabolism*, 24(1), pp.158-166.
- Lange, P., 2009. Chronic obstructive pulmonary disease and risk of infection. *Pneumonologia i alergologia polska*, 77(3), pp.284-288.
- Lavin, Y. et al., 2014. Tissue-resident macrophage enhancer landscapes are shaped by the local microenvironment. *Cell*, 159(6), pp.1312-1326.
- Lee, J.V. et al., 2014. Akt-dependent metabolic reprogramming regulates tumor cell histone acetylation. *Cell Metabolism*, 20(2), pp.306-319.
- Leland, K.M., McDonald, T.L. & Drescher, K.M., 2011. Effect of creatine, creatinine, and creatine ethyl ester on TLR expression in macrophages. *International immunopharmacology*, 11(9), pp.1341-1347.
- Liao, F. et al., 1999. CC-chemokine receptor 6 is expressed on diverse memory subsets of T cells and determines responsiveness to macrophage inflammatory protein 3 alpha. *The Journal of Immunology*, 162(1), pp.186-194.
- Lim, H.W. et al., 2008. Human Th17 cells share major trafficking receptors with both polarized effector T cells and FOXP3+ regulatory T cells. *The Journal of Immunology*, 180(1), pp.122-129.
- Lipscomb, M.F. et al., 1986. Human alveolar macrophages: HLA-DR-positive macrophages that are poor stimulators of a primary mixed leukocyte reaction. *The Journal of Immunology*, 136(2), pp.497-504.
- Lisignoli, G. et al., 2007. CCL20 chemokine induces both osteoblast proliferation and osteoclast differentiation: Increased levels of CCL20 are expressed in subchondral bone tissue of rheumatoid arthritis patients. *Journal of cellular physiology*, 210(3), pp.798-806.
- Lisignoli, G. et al., 2009. CCL20/CCR6 chemokine/receptor expression in bone tissue from osteoarthritis and rheumatoid arthritis patients: different response of osteoblasts in the two groups. *Journal of cellular physiology*, 221(1), pp.154-160.
- Littlewood-Evans, A. et al., 2016. GPR91 senses extracellular succinate released from inflammatory macrophages and exacerbates rheumatoid arthritis. *The Journal of experimental medicine*, 213(9), pp.1655-1662.
- Livak, K.J. & Schmittgen, T.D., 2001. Analysis of relative gene expression data using real-time quantitative PCR and the 2(-Delta Delta C(T)) Method. *Methods (San Diego, Calif.)*, 25(4), pp.402-408.
- Losa García, J.E. et al., 1999. Evaluation of inflammatory cytokine secretion by

- human alveolar macrophages. *Mediators of inflammation*, 8(1), pp.43-51.
- Lozano, R. et al., 2012. Global and regional mortality from 235 causes of death for 20 age groups in 1990 and 2010: a systematic analysis for the Global Burden of Disease Study 2010. *Lancet (London, England)*, 380(9859), pp.2095-2128.
- Lukacs, N.W. et al., 1995. TNF-alpha mediates recruitment of neutrophils and eosinophils during airway inflammation. *The Journal of Immunology*, 154(10), pp.5411-5417.
- Lund-Olesen, K., 1970. Oxygen tension in synovial fluids. *Arthritis & Rheumatism*, 13(6), pp.769-776.
- Lyons, C.R. et al., 1986. Inability of human alveolar macrophages to stimulate resting T cells correlates with decreased antigen-specific T cell-macrophage binding. *The Journal of Immunology*, 137(4), pp.1173-1180.
- Mahdi, H. et al., 2009. Specific interaction between genotype, smoking and autoimmunity to citrullinated alpha-enolase in the etiology of rheumatoid arthritis. *Nature genetics*, 41(12), pp.1319-1324.
- Mailer, R.K.W. et al., 2015. IL-1 β promotes Th17 differentiation by inducing alternative splicing of FOXP3. *Scientific reports*, 5, p.14674.
- Malandrino, M.I. et al., 2015. Enhanced fatty acid oxidation in adipocytes and macrophages reduces lipid-induced triglyceride accumulation and inflammation. *American journal of physiology. Endocrinology and metabolism*, 308(9), pp.E756-69.
- Malaviya, R., Laskin, J.D. & Laskin, D.L., 2017. Anti-TNF α therapy in inflammatory lung diseases. *Pharmacology & therapeutics*, 180, pp.90-98.
- Malek Mahdavi, A., Mahdavi, R. & Kolahi, S., 2016. Effects of l-Carnitine Supplementation on Serum Inflammatory Factors and Matrix Metalloproteinase Enzymes in Females with Knee Osteoarthritis: A Randomized, Double-Blind, Placebo-Controlled Pilot Study. *Journal of the American College of Nutrition*, 35(7), pp.597-603.
- Mantovani, A. et al., 2013. Macrophage plasticity and polarization in tissue repair and remodelling. E. S. White & A. R. Mantovani, eds. *The Journal of pathology*, 229(2), pp.176-185.
- Mantovani, A. et al., 2004. The chemokine system in diverse forms of macrophage activation and polarization. *Trends in immunology*, 25(12), pp.677-686.
- Manzo, A. et al., 2005. Systematic microanatomical analysis of CXCL13 and CCL21 in situ production and progressive lymphoid organization in rheumatoid synovitis. *European journal of immunology*, 35(5), pp.1347-1359.
- Maus, U.A. et al., 2002. Role of resident alveolar macrophages in leukocyte traffic into the alveolar air space of intact mice. *American journal of physiology. Lung cellular and molecular physiology*, 282(6), pp.L1245-52.

- McInnes, I.B. & Schett, G., 2011. The pathogenesis of rheumatoid arthritis. *The New England journal of medicine*, 365(23), pp.2205-2219.
- McKeown, S.R., 2014. Defining normoxia, physoxia and hypoxia in tumours-implications for treatment response. *The British journal of radiology*, 87(1035), p.20130676.
- Melnicoff, M.J. et al., 1988. Maintenance of peritoneal macrophages in the steady state. *Journal of Leukocyte Biology*, 44(5), pp.367-375.
- Michelucci, A. et al., 2013. Immune-responsive gene 1 protein links metabolism to immunity by catalyzing itaconic acid production. *Proceedings of the National Academy of Sciences of the United States of America*, 110(19), pp.7820-7825.
- Milkiewicz, M., Pugh, C.W. & Egginton, S., 2004. Inhibition of endogenous HIF inactivation induces angiogenesis in ischaemic skeletal muscles of mice. *The Journal of physiology*, 560(Pt 1), pp.21-26.
- Miller, E.J. et al., 1992. Elevated levels of NAP-1/interleukin-8 are present in the airspaces of patients with the adult respiratory distress syndrome and are associated with increased mortality. *The American review of respiratory disease*, 146(2), pp.427-432.
- Millet, P. et al., 2016. GAPDH Binding to TNF- α mRNA Contributes to Posttranscriptional Repression in Monocytes: A Novel Mechanism of Communication between Inflammation and Metabolism. *Journal of immunology (Baltimore, Md. : 1950)*, 196(6), pp.2541-2551.
- Mills, C.D. et al., 2000. M-1/M-2 Macrophages and the Th1/Th2 Paradigm. *The Journal of Immunology*, 164(12), pp.6166-6173.
- Mills, E.L. et al., 2016. Succinate Dehydrogenase Supports Metabolic Repurposing of Mitochondria to Drive Inflammatory Macrophages. *Cell*, 167(2), pp.457-470.e13.
- Misharin, A.V. et al., 2014. Nonclassical Ly6C(-) monocytes drive the development of inflammatory arthritis in mice. *Cell reports*, 9(2), pp.591-604.
- Mitani, A. et al., 2016. Restoration of Corticosteroid Sensitivity in Chronic Obstructive Pulmonary Disease by Inhibition of Mammalian Target of Rapamycin. *American journal of respiratory and critical care medicine*, 193(2), pp.143-153.
- Mole, D.R. et al., 2009. Genome-wide association of hypoxia-inducible factor (HIF)-1 α and HIF-2 α DNA binding with expression profiling of hypoxia-inducible transcripts. *Journal of Biological Chemistry*, 284(25), pp.16767-16775.
- Monsó, E. et al., 1998. [The impact of bronchial colonization in the quality of life of patients with chronic, stable bronchitis]. *Medicina clinica*, 111(15), pp.561-564.

- Moon, J.-S. et al., 2015. UCP2-induced fatty acid synthase promotes NLRP3 inflammasome activation during sepsis. *The Journal of clinical investigation*, 125(2), pp.665-680.
- Morris, D.G. et al., 2003. Loss of integrin alpha(v)beta6-mediated TGF-beta activation causes Mmp12-dependent emphysema. *Nature*, 422(6928), pp.169-173.
- Mosser, D.M., 2003. The many faces of macrophage activation. *Journal of Leukocyte Biology*, 73(2), pp.209-212.
- Möttönen, M. et al., 2005. CD4+ CD25+ T cells with the phenotypic and functional characteristics of regulatory T cells are enriched in the synovial fluid of patients with rheumatoid arthritis. *Clinical and experimental immunology*, 140(2), pp.360-367.
- Murphy, C. & Newsholme, P., 1998. Importance of glutamine metabolism in murine macrophages and human monocytes to L-arginine biosynthesis and rates of nitrite or urea production. *Clinical science (London, England : 1979)*, 95(4), pp.397-407.
- Murray, P.J. et al., 2014. Macrophage activation and polarization: nomenclature and experimental guidelines. *Immunity*, 41(1), pp.14-20.
- Nadkarni, S., Mauri, C. & Ehrenstein, M.R., 2007. Anti-TNF-alpha therapy induces a distinct regulatory T cell population in patients with rheumatoid arthritis via TGF-beta. *Journal of Experimental Medicine*, 204(1), pp.33-39.
- Namgaladze, D. & Brüne, B., 2014. Fatty acid oxidation is dispensable for human macrophage IL-4-induced polarization. *Biochimica et biophysica acta*, 1841(9), pp.1329-1335.
- Namgaladze, D. et al., 2014. Inhibition of macrophage fatty acid β -oxidation exacerbates palmitate-induced inflammatory and endoplasmic reticulum stress responses. *Diabetologia*, 57(5), pp.1067-1077.
- Netea, M.G. et al., 2015. Inflammasome-independent regulation of IL-1-family cytokines. *Annual review of immunology*, 33(1), pp.49-77.
- Newman, S.L. & Tucci, M.A., 1990. Regulation of human monocyte/macrophage function by extracellular matrix. Adherence of monocytes to collagen matrices enhances phagocytosis of opsonized bacteria by activation of complement receptors and enhancement of Fc receptor function. *The Journal of clinical investigation*, 86(3), pp.703-714.
- Ng, C.T. et al., 2010. Synovial tissue hypoxia and inflammation in vivo. *Ann Rheum Dis*, 69(7), pp.1389-1395.
- Nigrovic, P.A. & Lee, D.M., 2007. Synovial mast cells: role in acute and chronic arthritis. *Immunological reviews*, 217(1), pp.19-37.
- Nomura, M. et al., 2016. Fatty acid oxidation in macrophage polarization. *Nature Immunology*, 17(3), pp.216-217.

- Nurieva, R.I. et al., 2009. Bcl6 mediates the development of T follicular helper cells. *Science*, 325(5943), pp.1001-1005.
- O'Neill, L.A.J., 2015. A Broken Krebs Cycle in Macrophages. *Immunity*, 42(3), pp.393-394.
- Ohata, J. et al., 2005. Fibroblast-like synoviocytes of mesenchymal origin express functional B cell-activating factor of the TNF family in response to proinflammatory cytokines. *The Journal of Immunology*, 174(2), pp.864-870.
- Oliver, K.M. et al., 2009. Hypoxia activates NF-kappaB-dependent gene expression through the canonical signaling pathway. *Antioxidants & redox signaling*, 11(9), pp.2057-2064.
- Palsson-McDermott, E.M. et al., 2015. Pyruvate kinase M2 regulates Hif-1 α activity and IL-1 β induction and is a critical determinant of the warburg effect in LPS-activated macrophages. *Cell Metabolism*, 21(1), pp.65-80.
- Panina-Bordignon, P. et al., 2001. The C-C chemokine receptors CCR4 and CCR8 identify airway T cells of allergen-challenged atopic asthmatics. *The Journal of clinical investigation*, 107(11), pp.1357-1364.
- Park, Y.M., 2014. CD36, a scavenger receptor implicated in atherosclerosis. *Experimental & molecular medicine*, 46(6), p.e99.
- Patel, A.A. et al., 2017. The fate and lifespan of human monocyte subsets in steady state and systemic inflammation. *The Journal of experimental medicine*, 214(7), pp.1913-1923.
- Patra, K.C. & Hay, N., 2014. The pentose phosphate pathway and cancer. *Trends in Biochemical Sciences*, 39(8), pp.347-354.
- Pedley, A.M. & Benkovic, S.J., 2017. A New View into the Regulation of Purine Metabolism: The Purinosome. *Trends in Biochemical Sciences*, 42(2), pp.141-154.
- Pelletier, M. et al., 2010. Evidence for a cross-talk between human neutrophils and Th17 cells. *Blood*, 115(2), pp.335-343.
- Penatti, A. et al., 2017. Differences in serum and synovial CD4⁺ T cells and cytokine profiles to stratify patients with inflammatory osteoarthritis and rheumatoid arthritis. *Arthritis Research & Therapy*, 19(1), p.103.
- Persoons, J.H. et al., 1996. Alveolar macrophages autoregulate IL-1 and IL-6 production by endogenous nitric oxide. *American journal of respiratory cell and molecular biology*, 14(3), pp.272-278.
- Pène, J. et al., 2008. Chronically inflamed human tissues are infiltrated by highly differentiated Th17 lymphocytes. *The Journal of Immunology*, 180(11), pp.7423-7430.
- Piguet, P.F. et al., 1990. Requirement of tumour necrosis factor for development of silica-induced pulmonary fibrosis. *Nature*, 344(6263), pp.245-247.

- Piret, J.-P. et al., 2002. CoCl₂, a chemical inducer of hypoxia-inducible factor-1, and hypoxia reduce apoptotic cell death in hepatoma cell line HepG2. *Annals of the New York Academy of Sciences*, 973, pp.443-447.
- Présumey, J. et al., 2013. Nicotinamide phosphoribosyltransferase/visfatin expression by inflammatory monocytes mediates arthritis pathogenesis. *Ann Rheum Dis*, 72(10), pp.1717-1724.
- Raggi, F. et al., 2014. Identification of CD300a as a new hypoxia-inducible gene and a regulator of CCL20 and VEGF production by human monocytes and macrophages. *Innate immunity*, 20(7), pp.721-734.
- Raupach, B. et al., 2006. Caspase-1-mediated activation of interleukin-1beta (IL-1beta) and IL-18 contributes to innate immune defenses against *Salmonella enterica* serovar Typhimurium infection. *Infection and immunity*, 74(8), pp.4922-4926.
- Reales-Calderón, J.A. et al., 2014. Proteomic characterization of human proinflammatory M1 and anti-inflammatory M2 macrophages and their response to *Candida albicans*. *PROTEOMICS*, 14(12), pp.1503-1518.
- Richens, T.R. et al., 2009. Cigarette smoke impairs clearance of apoptotic cells through oxidant-dependent activation of RhoA. *American journal of respiratory and critical care medicine*, 179(11), pp.1011-1021.
- Rider, P. et al., 2011. IL-1 α and IL-1 β recruit different myeloid cells and promote different stages of sterile inflammation. *Journal of immunology (Baltimore, Md. : 1950)*, 187(9), pp.4835-4843.
- Roberts, C.A., Dickinson, A.K. & Taams, L.S., 2015. The Interplay Between Monocytes/Macrophages and CD4(+) T Cell Subsets in Rheumatoid Arthritis. *Frontiers in immunology*, 6(3), p.571.
- Rodriguez-Prados, J.C. et al., 2010. Substrate Fate in Activated Macrophages: A Comparison between Innate, Classic, and Alternative Activation. *The Journal of Immunology*, 185(1), pp.605-614.
- Roiniotis, J. et al., 2009. Hypoxia Prolongs Monocyte/Macrophage Survival and Enhanced Glycolysis Is Associated with Their Maturation under Aerobic Conditions. *The Journal of Immunology*, 182(12), pp.7974-7981.
- Rossol, M. et al., 2012. The CD14(bright) CD16+ monocyte subset is expanded in rheumatoid arthritis and promotes expansion of the Th17 cell population. *Arthritis & Rheumatism*, 64(3), pp.671-677.
- Rubbert-Roth, A. et al., 2017. TNF inhibitors in rheumatoid arthritis and spondyloarthritis: Are they the same? *Autoimmunity reviews*.
- Ruiz-Garcia, A. et al., 2011. Cooperation of adenosine with macrophage Toll-4 receptor agonists leads to increased glycolytic flux through the enhanced expression of PFKFB3 gene. *Journal of Biological Chemistry*, 286(22), pp.19247-19258.
- Russell, R.E.K., Culpitt, S.V., et al., 2002. Release and activity of matrix

- metalloproteinase-9 and tissue inhibitor of metalloproteinase-1 by alveolar macrophages from patients with chronic obstructive pulmonary disease. *American journal of respiratory cell and molecular biology*, 26(5), pp.602-609.
- Russell, R.E.K., Thorley, A., et al., 2002. Alveolar macrophage-mediated elastolysis: roles of matrix metalloproteinases, cysteine, and serine proteases. *American journal of physiology. Lung cellular and molecular physiology*, 283(4), pp.L867-73.
- Ruth, J.H. et al., 2003. Role of macrophage inflammatory protein-3alpha and its ligand CCR6 in rheumatoid arthritis. *Laboratory investigation; a journal of technical methods and pathology*, 83(4), pp.579-588.
- Saeed, S. et al., 2014. Epigenetic programming of monocyte-to-macrophage differentiation and trained innate immunity. *Science*, 345(6204), pp.1251086-1251086.
- Saetta, M. et al., 1993. Activated T-lymphocytes and macrophages in bronchial mucosa of subjects with chronic bronchitis. *The American review of respiratory disease*, 147(2), pp.301-306.
- Saetta, M. et al., 1998. CD8+ T-lymphocytes in peripheral airways of smokers with chronic obstructive pulmonary disease. *American journal of respiratory and critical care medicine*, 157(3 Pt 1), pp.822-826.
- Safi, W. et al., 2016. Differentiation of human CD14+ monocytes: an experimental investigation of the optimal culture medium and evidence of a lack of differentiation along the endothelial line. *Experimental & molecular medicine*, 48(4), pp.e227-e227.
- Sakaguchi, S. et al., 2003. SKG mice, a new genetic model of rheumatoid arthritis. *Arthritis Research & Therapy*, 5(Suppl 3), pp.10-10.
- Salazar-Mather, T.P., Orange, J.S. & Biron, C.A., 1998. Early Murine Cytomegalovirus (MCMV) Infection Induces Liver Natural Killer (NK) Cell Inflammation and Protection Through Macrophage Inflammatory Protein 1 α (MIP-1 α)-dependent Pathways. *Journal of Experimental Medicine*, 187(1), pp.1-14.
- Sasaki, M. et al., 2000. Differential regulation of metalloproteinase production, proliferation and chemotaxis of human lung fibroblasts by PDGF, interleukin-1beta and TNF-alpha. *Mediators of inflammation*, 9(3-4), pp.155-160.
- Sawyer, R.T., Strausbauch, P.H. & Volkman, A., 1982. Resident macrophage proliferation in mice depleted of blood monocytes by strontium-89. *Laboratory investigation; a journal of technical methods and pathology*, 46(2), pp.165-170.
- Schett, G. & Gravallesse, E., 2012. Bone erosion in rheumatoid arthritis: mechanisms, diagnosis and treatment. *Nature Reviews Rheumatology*, 8(11), pp.656-664.
- Schioppa, T. et al., 2003. Regulation of the chemokine receptor CXCR4 by

- hypoxia. *Journal of Experimental Medicine*, 198(9), pp.1391-1402.
- Schittenhelm, L., Hilkens, C.M. & Morrison, V.L., 2017. B2 Integrins As Regulators of Dendritic Cell, Monocyte, and Macrophage Function. *Frontiers in immunology*, 8, p.1866.
- Schlaepfer, I.R. et al., 2015. Inhibition of Lipid Oxidation Increases Glucose Metabolism and Enhances 2-Deoxy-2-[18F]Fluoro-d-Glucose Uptake in Prostate Cancer Mouse Xenografts. *Molecular Imaging and Biology*, 17(4), pp.529-538.
- Schulz, C. et al., 2012. A lineage of myeloid cells independent of Myb and hematopoietic stem cells. *Science*, 336(6077), pp.86-90.
- Semba, H. et al., 2016. HIF-1 α -PDK1 axis-induced active glycolysis plays an essential role in macrophage migratory capacity. *Nature Communications*, 7, p.11635.
- Semenza, G.L., 2009. Regulation of cancer cell metabolism by hypoxia-inducible factor 1. *Seminars in cancer biology*, 19(1), pp.12-16.
- Semenza, G.L. & Wang, G.L., 1992. A nuclear factor induced by hypoxia via de novo protein synthesis binds to the human erythropoietin gene enhancer at a site required for transcriptional activation. *Molecular and cellular biology*, 12(12), pp.5447-5454.
- Seok, J. et al., 2013. Genomic responses in mouse models poorly mimic human inflammatory diseases. *Proceedings of the National Academy of Sciences of the United States of America*, 110(9), pp.3507-3512.
- Serbina, N.V. & Pamer, E.G., 2006. Monocyte emigration from bone marrow during bacterial infection requires signals mediated by chemokine receptor CCR2. *Nature Immunology*, 7(3), pp.311-317.
- Serbina, N.V. et al., 2003. TNF/iNOS-producing dendritic cells mediate innate immune defense against bacterial infection. *Immunity*, 19(1), pp.59-70.
- Seyler, T.M. et al., 2005. BlyS and APRIL in rheumatoid arthritis. *The Journal of clinical investigation*, 115(11), pp.3083-3092.
- Shao, M.X.G., Nakanaga, T. & Nadel, J.A., 2004. Cigarette smoke induces MUC5AC mucin overproduction via tumor necrosis factor-alpha-converting enzyme in human airway epithelial (NCI-H292) cells. *American journal of physiology. Lung cellular and molecular physiology*, 287(2), pp.L420-7.
- Sharma, S. et al., 2017. Mitochondrial complex II regulates a distinct oxygen sensing mechanism in monocytes. *Human molecular genetics*, 26(7), pp.1328-1339.
- Shi, C. & Pamer, E.G., 2011. Monocyte recruitment during infection and inflammation. *Nature Reviews Immunology*, 11(11), pp.nri3070-774.
- Shigeyama, Y. et al., 2000. Expression of osteoclast differentiation factor in rheumatoid arthritis. *Arthritis & Rheumatism*, 43(11), pp.2523-2530.

- Smolen, J.S. et al., 2018. Rheumatoid arthritis. *Nature Reviews Disease Primers*, 4, pp.18001.
- Snodgrass, R.G. et al., 2016. Hypoxia Potentiates Palmitate-induced Pro-inflammatory Activation of Primary Human Macrophages. *The Journal of biological chemistry*, 291(1), pp.413-424.
- Sokolove, J. et al., 2011. Immune complexes containing citrullinated fibrinogen costimulate macrophages via Toll-like receptor 4 and Fc γ receptor. *Arthritis & Rheumatism*, 63(1), pp.53-62.
- Soler Palacios, B. et al., 2015. Macrophages from the synovium of active rheumatoid arthritis exhibit an activin A-dependent pro-inflammatory profile. *The Journal of pathology*, 235(3), pp.515-526.
- Staples, K.J. et al., 2011. Monocyte-derived macrophages matured under prolonged hypoxia transcriptionally up-regulate HIF-1 α mRNA. *Immunobiology*, 216(7), pp.832-839.
- Stein, M. et al., 1992. Interleukin 4 potently enhances murine macrophage mannose receptor activity: a marker of alternative immunologic macrophage activation. *Journal of Experimental Medicine*, 176(1), pp.287-292.
- Strehl, C. et al., 2014. Hypoxia: how does the monocyte-macrophage system respond to changes in oxygen availability? *Journal of Leukocyte Biology*, 95(2), pp.233-241.
- Sullivan, D.E. et al., 2005. Tumor necrosis factor-alpha induces transforming growth factor-beta1 expression in lung fibroblasts through the extracellular signal-regulated kinase pathway. *American journal of respiratory cell and molecular biology*, 32(4), pp.342-349.
- Suzuki, T. et al., 2007. Differential regulation of caspase-1 activation, pyroptosis, and autophagy via Ipaf and ASC in Shigella-infected macrophages. *PLoS Pathogens*, 3(8), p.e111.
- Symmons, D.P. et al., 1997. Blood transfusion, smoking, and obesity as risk factors for the development of rheumatoid arthritis: results from a primary care-based incident case-control study in Norfolk, England. *Arthritis & Rheumatism*, 40(11), pp.1955-1961.
- Takami, M., Terry, V. & Petruzzelli, L., 2002. Signaling pathways involved in IL-8-dependent activation of adhesion through Mac-1. *The Journal of Immunology*, 168(9), pp.4559-4566.
- Takao, K. & Miyakawa, T., 2015. Genomic responses in mouse models greatly mimic human inflammatory diseases. *Proceedings of the National Academy of Sciences of the United States of America*, 112(4), pp.1167-1172.
- Takayanagi, H., 2007. Osteoimmunology: shared mechanisms and crosstalk between the immune and bone systems. *Nature Reviews Immunology*, 7(4), pp.292-304.
- Tamoutounour, S. et al., 2013. Origins and functional specialization of

- macrophages and of conventional and monocyte-derived dendritic cells in mouse skin. *Immunity*, 39(5), pp.925-938.
- Tan, Z. et al., 2015. Pyruvate dehydrogenase kinase 1 participates in macrophage polarization via regulating glucose metabolism. *Journal of immunology (Baltimore, Md. : 1950)*, 194(12), pp.6082-6089.
- Tanida, S. et al., 2009. CCL20 produced in the cytokine network of rheumatoid arthritis recruits CCR6+ mononuclear cells and enhances the production of IL-6. *Cytokine*, 47(2), pp.112-118.
- Tannahill, G.M. et al., 2013. Succinate is a danger signal that induces IL-1 β via HIF-1 α . *Nature*, 496(7444), pp.238-242.
- Tatar, Z. et al., 2016. Variations in the metabolome in response to disease activity of rheumatoid arthritis. *BMC musculoskeletal disorders*, 17(1), p.353.
- Tondravi, M.M. et al., 1997. Osteopetrosis in mice lacking haematopoietic transcription factor PU.1. *Nature*, 386(6620), pp.81-84.
- Traves, S.L. et al., 2004. Specific CXC but not CC chemokines cause elevated monocyte migration in COPD: a role for CXCR2. *Journal of Leukocyte Biology*, 76(2), pp.441-450.
- Tso, C., Rye, K.-A. & Barter, P., 2012. Phenotypic and functional changes in blood monocytes following adherence to endothelium. P. Madeddu, ed. *PLoS ONE*, 7(5), p.e37091.
- Turner, L. et al., 1999. Hypoxia inhibits macrophage migration. *European journal of immunology*, 29(7), pp.2280-2287.
- Turner, M.D. et al., 2014. Cytokines and chemokines: At the crossroads of cell signalling and inflammatory disease. *Biochimica et biophysica acta*, 1843(11), pp.2563-2582.
- Van den Bossche, J., O'Neill, L.A. & Menon, D., 2017. Macrophage Immunometabolism: Where Are We (Going)? *Trends in immunology*, 38(6), pp.395-406.
- van der Windt, G.J.W. & Pearce, E.L., 2012. Metabolic switching and fuel choice during T-cell differentiation and memory development. *Immunological reviews*, 249(1), pp.27-42.
- van der Woude, D. et al., 2010. Epitope spreading of the anti-citrullinated protein antibody response occurs before disease onset and is associated with the disease course of early arthritis. *Ann Rheum Dis*, 69(8), pp.1554-1561.
- van Furth, R. & Cohn, Z.A., 1968. The origin and kinetics of mononuclear phagocytes. *Journal of Experimental Medicine*, 128(3), pp.415-435.
- van Furth, R. et al., 1972. The mononuclear phagocyte system: a new classification of macrophages, monocytes, and their precursor cells. *Bulletin of the World Health Organization*, 46(6), pp.845-852.

- Vats, D. et al., 2006. Oxidative metabolism and PGC-1 β attenuate macrophage-mediated inflammation. *Cell Metabolism*, 4(1), pp.13-24.
- Vlahos, R. & Bozinovski, S., 2014. Role of alveolar macrophages in chronic obstructive pulmonary disease. *Frontiers in immunology*, 5, p.435.
- Vlahos, R. et al., 2012. Glucocorticosteroids differentially regulate MMP-9 and neutrophil elastase in COPD. D. Hartl, ed. *PLoS ONE*, 7(3), p.e33277.
- Volpe, E. et al., 2008. A critical function for transforming growth factor- β , interleukin 23 and proinflammatory cytokines in driving and modulating human T(H)-17 responses. *Nature Immunology*, 9(6), pp.650-657.
- Wallace, C. & Keast, D., 1992. Glutamine and macrophage function. *Metabolism: clinical and experimental*, 41(9), pp.1016-1020.
- Wang, Y. et al., 2016. Histone Deacetylase SIRT1 Negatively Regulates the Differentiation of Interleukin-9-Producing CD4(+) T Cells. *Immunity*, 44(6), pp.1337-1349.
- Wen, H. et al., 2011. Fatty acid-induced NLRP3-ASC inflammasome activation interferes with insulin signaling. *Nature Immunology*, 12(5), pp.408-415.
- Weyand, C.M. et al., 1992. The influence of HLA-DRB1 genes on disease severity in rheumatoid arthritis. *Annals of internal medicine*, 117(10), pp.801-806.
- Wiktor-Jedrzejczak, W. & Gordon, S., 1996. Cytokine regulation of the macrophage (M ϕ) system studied using the colony stimulating factor-1-deficient op/op mouse. *Physiological reviews*, 76(4), pp.927-947.
- Wilson, K.P. et al., 1994. Structure and mechanism of interleukin-1 β converting enzyme. *Nature*, 370(6487), pp.270-275.
- Wolf, A.J. et al., 2016. Hexokinase Is an Innate Immune Receptor for the Detection of Bacterial Peptidoglycan. *Cell*, 166(3), pp.624-636.
- Wu, M., Fang, H. & Hwang, S.T., 2001. Cutting edge: CCR4 mediates antigen-primed T cell binding to activated dendritic cells. *The Journal of Immunology*, 167(9), pp.4791-4795.
- Xie, M. et al., 2016. PKM2-dependent glycolysis promotes NLRP3 and AIM2 inflammasome activation. *Nature Communications*, 7, p.13280.
- Xue, J. et al., 2014. Transcriptome-based network analysis reveals a spectrum model of human macrophage activation. *Immunity*, 40(2), pp.274-288.
- Yamazaki, T. et al., 2008. CCR6 regulates the migration of inflammatory and regulatory T cells. *Journal of immunology (Baltimore, Md. : 1950)*, 181(12), pp.8391-8401.
- Yang, Z. et al., 2016. Restoring oxidant signaling suppresses proarthritogenic T cell effector functions in rheumatoid arthritis. *Science translational medicine*, 8(331), p.331ra38.
- Yoon, B.R. et al., 2014. Functional phenotype of synovial monocytes modulating

inflammatory T-cell responses in rheumatoid arthritis (RA). *PLoS ONE*, 9(10), p.e109775.

Zheng, H. et al., 1995. Resistance to fever induction and impaired acute-phase response in interleukin-1 beta-deficient mice. *Immunity*, 3(1), pp.9-19.

Ziegler-Heitbrock, L. et al., 2010. Nomenclature of monocytes and dendritic cells in blood. *Blood*, 116(16), pp.e74-80.